

Quantifying the Effects of Humeral Elevation Angle, Plane of Elevation,
and Motion Phase on 3D Shoulder Kinematics during Dynamic Humeral
Movement in Multiple Vertical Planes

by

Bryan Picco

A thesis

presented to the University of Waterloo

in fulfillment of the

thesis requirement for the degree of

Master of Science

in

Kinesiology

Waterloo, Ontario, Canada, 2012

©Bryan Picco 2012

AUTHOR'S DECLARATION

I hereby declare that I am the sole author of this thesis. This is a true copy of the thesis, including any required final revisions, as accepted by my examiners.

I understand that my thesis may be made electronically available to the public.

ABSTRACT

A thorough understanding of typical shoulder motion is desirable for both clinicians and shoulder researchers. With this knowledge, comparisons between normal and special populations (e.g. athletic, working, elderly, injured) are enabled and injury mechanisms for heightened or diminished performance may be identified. The purpose of this study was to generate a robust quantification of typical shoulder kinematic profiles during dynamic humeral elevation in six vertical movement planes, and to determine the influence of humeral movement plane, movement phase, gender, and humeral elevation angle on typical scapulothoracic (ST), glenohumeral (GH), acromioclavicular (AC), and sternoclavicular (SC) kinematics.

Upper limb kinematic data were collected on 15 males and 14 females as they elevated and lowered their right humerus in six vertical movement planes with elbows fully extended. A total of 60 shoulder kinematic profiles were generated for both raising and lowering motion phases. Trial-to-trial repeatability of the measured rotations, as indicated by intra-class correlation coefficient was found to be moderate (0.658) to high (0.999). Overall, as the humerus was elevated, scapulothoracic (ST) upward rotation, ST posterior tilt, sternoclavicular (SC) elevation, SC retraction, acromioclavicular (AC) elevation and glenohumeral (GH) elevation all increased. However, ST protraction/retraction, GH internal/external rotation, GH anterior/posterior plane of elevation, and AC protraction/retraction responses were less consistent.

There was a main effect of humeral movement plane and elevation angle ($p < 0.001$) identified for all measured joint rotations. A significant phase main effect was not found for right glenohumeral +anterior/-posterior plane of elevation (GAP), glenohumeral +medial/-lateral

elevation (GLE), and acromioclavicular protraction/retraction (APR). At least one significant interaction of the main effects, including that of gender, was present for all rotations.

The typical shoulder kinematic profiles provided in this investigation is the largest to date of its kind obtained using skin-mounted shoulder tracking techniques. Clinical scientists will find the profiles useful because they provide motion trends that can be compared to profiles from other segments of the population, including patients with specific shoulder injuries. This work supports the more ambitious future clinical goal of being able to identify people who are at risk for developing shoulder pathologies in clinical settings in a non-invasive manner.

ACKNOWLEDGEMENTS

I would first like to thank my advisor Dr. Clark Dickerson for his constant guidance and instruction throughout my Masters studies. I would also like to thank my committee members Drs. Jack Callaghan and Richard Well for their thoughtful recommendations throughout this project. A special thanks is extended to Dr. Steve Fischer who, along with Dr, Dickerson, mentored me early in my research career. In addition, I would like to acknowledge Tyler Allen, Elora Brenneman, and Alan Cudlip who each assisted with this project's data collection and reduction.

To all my officemates on the first and third floors of Burt Matthews Hall, your friendship was vital to me persevering through the many emotional ups and downs that we all experience as graduate students. Finally, I would like to show a great deal of gratitude to my parents Bill and Nina and my brother Vince for their constant encouragement throughout my 7.5 years at the University of Waterloo. Likewise, endless thanks to my girlfriend Tara Travaglini for her daily emotional support in all matters of life.

TABLE OF CONTENTS

| | |
|---|------------|
| LIST OF FIGURES | ix |
| LIST OF TABLES | xiv |
| 1. INTRODUCTION | 1 |
| 1.1 <i>Shoulder motion description</i> | <i>1</i> |
| 1.2 <i>Inconsistencies in past shoulder motion research.....</i> | <i>3</i> |
| 1.3 <i>Normative shoulder kinematic data applications.....</i> | <i>4</i> |
| 1.4 <i>Purpose.....</i> | <i>5</i> |
| 1.5 <i>Hypotheses</i> | <i>6</i> |
| 2. REVIEW OF RELEVANT LITERATURE | 8 |
| 2.1 <i>Shoulder joint motion capture and description.....</i> | <i>8</i> |
| 2.1.1 <i>Shoulder motion capture</i> | <i>8</i> |
| 2.1.2 <i>Euler Angles.....</i> | <i>13</i> |
| 2.1.3 <i>Euler Angle Limitations.....</i> | <i>13</i> |
| 2.1.4 <i>Standardization of shoulder kinematic descriptions</i> | <i>15</i> |
| 2.1.5 <i>Normal shoulder joints' ranges of motion</i> | <i>19</i> |
| 2.2 <i>Determinants of shoulder kinematics.....</i> | <i>22</i> |
| 2.2.1 <i>External force.....</i> | <i>22</i> |
| 2.2.2 <i>Humeral elevation velocity.....</i> | <i>23</i> |
| 2.2.3 <i>Plane of elevation.....</i> | <i>23</i> |
| 2.2.4 <i>Injury.....</i> | <i>24</i> |
| 2.3 <i>Clinical implications of scapular motion.....</i> | <i>24</i> |
| 2.3.1 <i>Links between shoulder pathology and shoulder motion</i> | <i>25</i> |
| 3. RESEARCH METHODS..... | 27 |
| 3.1 <i>Participants</i> | <i>27</i> |
| 3.2 <i>Experimental variables</i> | <i>28</i> |
| 3.3 <i>Equipment.....</i> | <i>29</i> |
| 3.3.1 <i>Motion tracking.....</i> | <i>29</i> |
| 3.3.2 <i>Digitizing stylus</i> | <i>30</i> |
| 3.3.3 <i>Acromion marker cluster</i> | <i>31</i> |

| | | |
|-----------|--|------------|
| 3.4 | <i>Experimental protocol</i> | 32 |
| 3.4.1 | Collection volume calibration..... | 32 |
| 3.4.2 | Collection protocol..... | 33 |
| 3.5 | <i>Data analysis</i> | 34 |
| 3.5.1 | Kinematics | 35 |
| 3.5.3 | Joint rotation descriptions | 39 |
| 3.6 | <i>Statistical analysis</i> | 43 |
| 3.6.1 | Intra-class correlation coefficient (ICC) | 43 |
| 3.6.2 | Kinematic profiles..... | 43 |
| 3.6.3 | Variability summary | 43 |
| 3.6.4 | Analysis of variance (ANOVA)..... | 44 |
| 4. | RESULTS | 45 |
| 5.1 | <i>Intra-class Correlation Coefficients</i> | 45 |
| 4.2 | <i>Descriptive Statistics and motion profiles</i> | 47 |
| 4.2.1 | Scapulothoracic Kinematics..... | 47 |
| 4.2.2 | Glenohumeral Kinematics | 52 |
| 4.2.3 | Acromioclavicular Kinematics | 57 |
| 4.2.4 | Sternoclavicular Kinematics | 60 |
| 4.3 | <i>Analysis of Variance (ANOVA)</i> | 63 |
| 4.3.1 | Scapulothoracic Kinematics..... | 63 |
| 4.3.2 | Glenohumeral Kinematics | 79 |
| 4.3.3 | Acromioclavicular Kinematics | 93 |
| 4.3.4 | Sternoclavicular Kinematics | 104 |
| 4.4 | <i>Variability Summary</i> | 115 |
| 5. | DISCUSSION | 117 |
| 5.1 | <i>Addressing the Hypotheses</i> | 117 |
| 5.2 | <i>Kinematic profiles - Comparison to the literature</i> | 120 |
| 5.2.1 | Scapular Kinematics | 121 |
| 5.2.2 | Glenohumeral kinematics | 124 |
| 5.2.4 | Sternoclavicular kinematics | 126 |
| 5.3 | <i>Kinematic profile application example</i> | 127 |

| | | |
|-----------|---|------------|
| 5.4 | <i>The utility of kinematic profiles for identifying pathological shoulder motion</i> | 130 |
| 5.5 | <i>Kinematic profile variability</i> | 132 |
| 5.6 | <i>Intra-class correlation coefficient interpretation</i> | 135 |
| 5.7 | <i>Statistical Interpretations</i> | 136 |
| 5.7.1 | Plane and elevation angle effects on shoulder kinematics | 136 |
| 5.7.2 | Gender effects on shoulder kinematics | 139 |
| 5.7.3 | Movement phase effects on shoulder kinematics | 141 |
| 5.8 | <i>Study Limitations</i> | 144 |
| 5.9 | <i>Future Research Directions</i> | 146 |
| 5.10 | <i>Clinical applications of findings</i> | 148 |
| 6. | CONCLUSIONS | 151 |
| | REFERENCES | 153 |
| | APPENDIX A: Link segment and local coordinate system descriptions | 164 |
| | APPENDIX B: Decomposition and rotational transformation matrices | 169 |
| | APPENDIX C: Descriptive statistics and intra-class correlation | 171 |
| | APPENDIX D: Kinematic profiles for the lowering phase | 174 |
| | APPENDIX E: Kinematic profiles' average standard deviation by elevation angle | 184 |
| | APPENDIX F: Analysis of variance (anova) summaries | 185 |

LIST OF FIGURES

| | |
|--|----|
| Figure 1: Adjustable scapula locator..... | 11 |
| Figure 2: Scapula tracker fixed to the mid-portion of the scapula spine and posterior lateral acromion.... | 11 |
| Figure 3: Acromion marker cluster attached to acromion | 12 |
| Figure 5: Humerus coordinate system and example of GH joint motion..... | 17 |
| Figure 6: Clavicle coordinate system and example of SC joint motion..... | 17 |
| Figure 7: Scapula coordinate system and example of AC joint motion..... | 18 |
| Figure 8: Plot of 3D scapulothoracic motion relative to humeral elevation angle..... | 21 |
| Figure 9: Plot showing a significant effect of external load on scapular lateral rotation at 35° and 45° of arm elevation..... | 22 |
| Figure 10: A visual representation of sub-acromial impingement of the supraspinatus tendon and sub-acromial bursa..... | 26 |
| Figure 11: Sub-acromial impingement tests | 28 |
| Figure 12: Digitizing stylus with orthogonal coordinate system. | 31 |
| Figure 13: Acromion marker cluster secured to participant’s posterior lateral acromion with tape..... | 32 |
| Figure 14: Palpating the inferior angle of the scapula with the digitizing stylus..... | 33 |
| Figure 15: Examples of recorded elevation motions..... | 34 |
| Figure 16: Graphical user interface used to determine participant cut-off frequencies using residual analysis..... | 36 |
| Figure 17: Example thoracohumeral elevation profile used to identify when the humerus was within 10E to 120E humeral elevation | 38 |
| Figure 18: Scapulothoracic tilt profile and range of tilt occurring between 10E and 120E humeral elevation..... | 38 |
| Figure 19: Profiles of the three scapulothoracic tilt measures and their computed average displayed relative to humeral elevation angle | 39 |
| Figure 20: Graphical user interface used to screen outputted joint kinematics for abnormalities | 42 |
| Figure 21: Mean scapular +protraction/-retraction kinematic profiles, with +/- one standard deviation, for the six tested vertical planes – raising phase..... | 48 |
| Figure 22: Mean scapulothoracic +medial/-lateral rotation kinematic profiles, with +/- one standard deviation, for the six tested vertical planes – raising phase | 49 |
| Figure 23: Mean scapulothoracic +posterior/-anterior tilt kinematic profiles, with +/- one standard deviation, for the six tested vertical planes – raising phase | 51 |
| Figure 24: Mean glenohumeral +anterior/-posterior elevation plane kinematic profiles, with +/- one standard deviation, for the six tested vertical planes – raising phase..... | 53 |
| Figure 25: Mean glenohumeral -elevation kinematic profiles, with +/- one standard deviation, for the six tested vertical planes – raising phase | 54 |
| Figure 26: Mean glenohumeral –internal/+external rotation kinematic profiles, with +/- one standard deviation, for the six tested vertical planes – raising phase | 56 |
| Figure 27: Mean acromioclavicular +protraction/-retraction kinematic profiles, with +/- one standard deviation, for the six tested vertical planes – raising phase. | 58 |
| Figure 28: Mean acromioclavicular –elevation/+depression kinematic profiles, with +/- one standard deviation, for the six tested vertical planes – raising phase. | 59 |

| | |
|---|----|
| Figure 29: Mean sternoclavicular +protraction/-retraction kinematic profiles, with +/- one standard deviation, for the six tested vertical planes – raising phase | 61 |
| Figure 30: Mean sternoclavicular –elevation/+depression kinematic profiles, with +/- one standard deviation, for the six tested vertical planes – raising phase. | 62 |
| Figure 31: Interaction effects of humeral movement plane and elevation angle on least squares mean (LSM) right scapulothoracic +protraction/-retraction..... | 64 |
| Figure 32: Interaction effects of humeral elevation phase and elevation angle on LSM right scapulothoracic +protraction/-retraction. | 66 |
| Figure 33: Interaction effects of sex and humeral elevation angle on LSM right +protraction/retraction.. | 66 |
| Figure 34: Interaction effects of humeral elevation phase and movement plane on LSM right +protraction/-retraction | 67 |
| Figure 35: Interaction effects of sex and humeral movement plane on LSM +protraction/-retraction..... | 68 |
| Figure 36: Interaction effects of sex and humeral elevation phase on LSM right +protraction/-retraction | 68 |
| Figure 37: Interaction effects of humeral movement plane and elevation angle on LSM right scapulothoracic +medial/-lateral rotation..... | 70 |
| Figure 38: Interaction effects of humeral elevation phase and elevation angle on LSM right scapulothoracic +medial/-lateral rotation..... | 71 |
| Figure 39: Interaction effects of sex and humeral elevation angle on LSM right scapulothoracic +medial/-lateral rotation | 71 |
| Figure 40: Interaction effects of humeral elevation phase and movement plane on LSM right scapulothoracic +medial/-lateral rotation..... | 72 |
| Figure 41: Interaction effects of sex and humeral movement plane on LSM right scapulothoracic +medial/-lateral rotation..... | 72 |
| Figure 42: Interaction effects of sex and humeral elevation phase on LSM right scapulothoracic +medial/-lateral rotation | 73 |
| Figure 43: Interaction effects of humeral movement plane and elevation angle on LSM right scapulothoracic +posterior/-anterior tilt..... | 74 |
| Figure 44: Interaction effects of humeral elevation phase and elevation angle on LSM right scapulothoracic +posterior/-anterior tilt..... | 76 |
| Figure 45: Interaction effects of sex and humeral elevation angle on LSM right scapulothoracic +posterior/-anterior tilt..... | 76 |
| Figure 46: Interaction effects of humeral elevation phase and movement plane on LSM right scapulothoracic +posterior/-anterior tilt..... | 77 |
| Figure 47: Interaction effects of sex and humeral movement plane on LSM right scapulothoracic +posterior/-anterior tilt..... | 78 |
| Figure 48: Interaction effects of sex and humeral elevation phase on LSM right scapulothoracic +posterior/-anterior tilt..... | 78 |
| Figure 49: Effects of humeral movement plane and elevation angle on LSM right glenohumeral +anterior/-posterior rotation..... | 80 |
| Figure 50: Effects of humeral elevation phase and elevation angle on LSM right glenohumeral +anterior/-posterior rotation..... | 82 |
| Figure 51: Effects of sex and humeral elevation angle on LSM right glenohumeral +anterior/-posterior rotation | 82 |

| | |
|--|-----|
| Figure 52: Effects of humeral elevation phase and movement plane on LSM right glenohumeral +anterior/-posterior rotation..... | 83 |
| Figure 53: Effects of sex and humeral movement plane on LSM right glenohumeral +anterior/-posterior rotation..... | 83 |
| Figure 54: Effects of sex and humeral elevation phase on LSM right glenohumeral +anterior/-posterior rotation..... | 84 |
| Figure 55: Effects of humeral movement plane and elevation on LSM right glenohumeral elevation..... | 85 |
| Figure 56: Effects of humeral elevation phase and elevation angle on LSM glenohumeral elevation..... | 86 |
| Figure 57: Effects of sex and humeral elevation angle on LSM right glenohumeral elevation..... | 86 |
| Figure 58: Effects of humeral elevation phase and movement plane on LSM glenohumeral elevation..... | 87 |
| Figure 59: Effects of sex and humeral movement plane on LSM right glenohumeral elevation..... | 87 |
| Figure 60: Effects of sex and humeral elevation phase on LSM right glenohumeral elevation..... | 88 |
| Figure 61: Effects of humeral movement plane and elevation angle on LSM right glenohumeral internal (+)/external (-) rotation..... | 89 |
| Figure 62: Effects of humeral elevation phase and elevation angle on LSM right glenohumeral +internal/+external rotation..... | 91 |
| Figure 63: Effects of sex and humeral elevation angle on LSM right glenohumeral +internal/+external rotation..... | 91 |
| Figure 64: Effects of humeral elevation phase and movement plane on LSM right GH +internal/+external rotation..... | 92 |
| Figure 65: Effects of sex and humeral movement plane on LSM right glenohumeral +internal/+external rotation..... | 92 |
| Figure 66: Effects of sex and humeral elevation phase on LSM right glenohumeral +internal/+external rotation..... | 93 |
| Figure 67: Effects of humeral movement plane and elevation angle on LSM right acromioclavicular -depression /+elevation..... | 95 |
| Figure 68: Effects of humeral elevation phase and elevation angle on LSM right acromioclavicular – elevation/+depression..... | 97 |
| Figure 69: Effects of sex and humeral elevation angle on LSM right acromioclavicular – elevation/+depression..... | 97 |
| Figure 70: Effects of humeral elevation phase and movement plane on LSM right acromioclavicular – elevation/+depression..... | 98 |
| Figure 71: Effects of sex and humeral movement plane on LSM right acromioclavicular – elevation/+depression..... | 98 |
| Figure 72: Effects of sex and humeral elevation phase on LSM right acromioclavicular – elevation/+depression..... | 99 |
| Figure 73: Effects of humeral movement plane and elevation angle on LSM right acromioclavicular +protraction/-retraction..... | 100 |
| Figure 74: Effects of humeral elevation phase and elevation angle on LSM right acromioclavicular +protraction/-retraction..... | 101 |
| Figure 75: Effects of sex and humeral elevation angle on LSM right acromioclavicular +protraction/-retraction..... | 101 |
| Figure 76: Effects of humeral elevation phase and movement plane on LSM right acromioclavicular +protraction/-retraction..... | 102 |

| | |
|--|-----|
| Figure 77: Effects of sex and humeral movement plane on LSM right acromioclavicular +protraction/-retraction | 102 |
| Figure 78: Effects of sex and humeral elevation phase on LSM right acromioclavicular +protraction/-retraction | 103 |
| Figure 79: Effects of humeral movement plane and elevation angle on LSM right sternoclavicular +protraction/-retraction | 105 |
| Figure 80: Effects of humeral elevation phase and elevation angle on LSM right sternoclavicular +protraction/-retraction | 107 |
| Figure 81: Effects of sex and humeral elevation angle on LSM right sternoclavicular +protraction/-retraction | 107 |
| Figure 82: Effects of humeral elevation phase and movement plane on LSM right sternoclavicular +protraction/-retraction | 108 |
| Figure 83: Effects of sex and humeral movement plane on LSM right sternoclavicular +protraction/-retraction | 108 |
| Figure 84: Effects of sex and humeral elevation phase on LSM right sternoclavicular +protraction/-retraction | 109 |
| Figure 85: Effects of humeral movement plane and elevation angle on LSM right sternoclavicular -depression/+elevation | 110 |
| Figure 86: Effects of humeral elevation phase and elevation angle on LSM right sternoclavicular -depression/+elevation | 112 |
| Figure 87: Effects of sex and humeral elevation angle on LSM right sternoclavicular -depression/+elevation | 112 |
| Figure 88: Effects of humeral elevation phase and movement plane on LSM right sternoclavicular -depression/+elevation | 113 |
| Figure 89: Effects of sex and humeral movement plane on LSM right sternoclavicular -depression/+elevation | 113 |
| Figure 90: Effects of sex and humeral elevation phase on LSM right sternoclavicular -depression/+elevation | 114 |
| Figure 91: Total and individual joint rotation variation (standard deviation) at all measured humeral elevation angles averaged across planes | 115 |
| Figure 92: Total and individual joint rotation variation (standard deviation) for all measured humeral elevation angles averaged within planes | 116 |
| Figure 93: Comparison of ST protraction observed during humeral elevation (raising phase) in the scapular plane with select kinematic profiles available in the literature..... | 128 |
| Figure 94: Comparison of ST upward rotation observed during humeral elevation (raising phase) in the scapular plane with select kinematic profiles available in the literature..... | 129 |
| | |
| Figure A1: Orthogonal thorax system with the origin at the supersternal notch (SSN) at A. Y_t is directed perpendicular to the plane created by XP, SSN, C7, and T8 directed forward..... | 165 |
| Figure A2: Orthogonal clavicle system with the origin at the sternoclavicular joint at point A. Y_c is directed perpendicular to the plane created by Z_t and X_c directed forward | 165 |
| Figure A3: Orthogonal scapula system with the origin at the acromion angle AA at point A. Y_s is directed perpendicular to the plane created by the AA, inferior angle (IA) at C, and scapular spine root (SR) at C directed forward | 166 |

| | |
|--|-----|
| Figure A4: Orthogonal humerus system with the origin at the glenohumeral joint (GH) at point A. Y_h is directed perpendicular to the plane created by the medial epicondyle (ME), lateral epicondyle (LE), and GH directed forward | 166 |
| Figure A5: Orthogonal acromion marker cluster (AMC) coordinate system | 168 |
| Figure A6: Orthogonal digitizing stylus system with the origin at STY4. S_d is perpendicular to the plane created by STY1, STY2, STY3, and STY4 directed forward..... | 168 |
| Figure D1: Mean scapulothoracic +protraction/-retraction kinematic profiles, with +/- one standard deviation, for the six tested vertical planes – lowering phase..... | 174 |
| Figure D2: Mean scapulothoracic +medial/-lateral rotation kinematic profiles, with +/- one standard deviation, for the six tested vertical planes – lowering phase..... | 175 |
| Figure D3: Mean scapulothoracic +positive/-retraction kinematic profiles, with +/- one standard deviation, for the six tested vertical planes – lowering phase..... | 176 |
| Figure D4: Mean glenohumeral +anterior/-posterior elevation plane kinematic profiles, with +/- one standard deviation, for the six tested vertical planes – lowering phase | 177 |
| Figure D5: Mean glenohumeral -elevation kinematic profiles, with +/- one standard deviation, for the six tested vertical planes – lowering phase..... | 178 |
| Figure D6: Mean glenohumeral +internal/-external rotation kinematic profiles, with +/- one standard deviation, for the six tested vertical planes – lowering phase..... | 179 |
| Figure D7: Mean acromioclavicular +protraction/-retraction kinematic profiles, with +/- one standard deviation, for the six tested vertical planes – lowering phase..... | 180 |
| Figure D8: Mean acromioclavicular -elevation/+depression kinematic profiles, with +/- one standard deviation, for the six tested vertical planes – lowering phase..... | 181 |
| Figure D9: Mean sternoclavicular +protraction/-retraction kinematic profiles, with +/- one standard deviation, for the six tested vertical planes – lowering phase..... | 182 |
| Figure D10: Mean sternoclavicular -elevation/+depression kinematic profiles, with +/- one standard deviation, for the six tested vertical planes – lowering phase..... | 183 |

LIST OF TABLES

| | |
|---|-----|
| Table 1: Shoulder joints' range of motion | 20 |
| Table 2: Study participants' anthropometrics | 27 |
| Table 3: Anatomical locations and acronyms of reflective markers | 30 |
| Table 4: Cluster markers labels and descriptions..... | 30 |
| Table 5: Overall ICCs for each rotation. Each mean ICC represents the average within-rotation mean ICCs displayed in Table C6 | 46 |
| Table 6: Interaction effects of movement plane and humeral elevation angle on least squares mean (LSM) scapulothoracic +protraction/-retraction. | 65 |
| Table 7: Interaction effects of sex and humeral elevation angle on least squares mean (LSM) scapulothoracic +protraction/-retraction | 67 |
| Table 8: Interaction effects of movement plane and humeral elevation angle on least squares mean (LSM) scapulothoracic +posterior/-anterior tilt..... | 75 |
| Table 9: Interaction effects of sex and humeral elevation angle on least squares mean (LSM) scapulothoracic +postanuserior/-anterior tilt. | 77 |
| Table 10: Interaction effects of movement plane and humeral elevation angle on least squares mean (LSM) glenohumeral +anterior/-posterior movement plane..... | 81 |
| Table 11: Interaction effects of movement plane and humeral elevation angle on least squares mean (LSM) glenohumeral +internal/-external rotation..... | 90 |
| Table 12: Interaction effects of movement plane and humeral elevation angle on least squares mean (LSM) acromioclavicular elevation. | 96 |
| Table 13: Interaction effects of sex and humeral movement plane on least squares mean (LSM) acromioclavicular +protraction/-retraction. | 103 |
| Table 14: Interaction effects of movement plane and humeral elevation angle on least squares mean (LSM) sternoclavicular +protraction/-retraction..... | 106 |
| Table 15: Interaction effects of movement plane and humeral elevation angle on least squares mean (LSM) sternoclavicular +depression/-elevation..... | 111 |
| | |
| Table A1: Link segment definitions anatomical landmarks | 164 |
| Table A2: Segment-based orthogonal coordinate system definitions..... | 164 |
| Table A3: Marker cluster orthogonal coordinate system definitions | 167 |
| Table A4: Joint coordinate system (JCS) definitions of the SC and AC joints; ST and TH segments..... | 167 |
| Table C1: Three-dimensional scapulothoracic kinematics descriptive statistics for the examined humeral elevation planes organized by elevation phase | 171 |
| Table C2: Scapulothoracic rhythm for the examined humeral elevation planes organized by elevation phase | 171 |
| Table C3: Three-dimensional glenohumeral kinematics descriptive statistics for the examined humeral elevation planes organized by elevation phase | 172 |
| Table C4: Two-dimensional acromioclavicular kinematics descriptive statistics for the examined humeral elevation planes organized by elevation phase | 172 |
| Table C5: Two-dimensional sternoclavicular kinematics descriptive statistics for the examined humeral elevation planes organized by elevation phase | 173 |

| | |
|--|-----|
| Table C6: Mean intra-class correlation coefficients (ICCs) of all measured joint rotations for each plane of humeral elevation. ICCs are sorted from largest to smallest | 173 |
| Table E: Standard deviation measurements used in Figure 91 and 92..... | 184 |
| Table F1: Scapulothoracic protract/retraction ANOVA summary table..... | 185 |
| Table F2: Scapulothoracic medial/lateral rotation ANOVA summary table. | 185 |
| Table F3: Scapulothoracic posterior/anterior tilt ANOVA summary table. | 185 |
| Table F4: Glenohumeral anterior/posterior plane ANOVA summary table. | 186 |
| Table F5: Glenohumeral elevation ANOVA summary table..... | 186 |
| Table F6: Glenohumeral internal/external rotation ANOVA summary table..... | 186 |
| Table F7: Acromioclavicular protraction/retraction ANOVA summary table. | 187 |
| Table F8: Acromioclavicular elevation ANOVA summary table..... | 187 |
| Table F9: Sternoclavicular protraction/retraction ANOVA summary table. | 187 |
| Table F10: Sternoclavicular elevation ANOVA summary table. | 188 |

1. INTRODUCTION

1.1 Shoulder motion description

Accurately describing human shoulder motion has been a goal of shoulder researchers and clinicians for some time. Inman et al. (1944) first described the geometric characteristics and scapulothoracic motion during humeral abduction and flexion, as well as describing the muscular contribution to these motions. The results of this study provided fundamental insight into scapular motion that is still relevant today, including that normal glenohumeral joint motion relies not only on the interaction of the humerus and scapula at the glenohumeral joint, but also on the interactions of the sternoclavicular and acromioclavicular joints and scapulothoracic gliding (Inman et al., 1944). They concluded, in abduction, that the ratio between glenohumeral and scapulothoracic rotation was 2:1. This general finding has guided clinicians in shoulder assessments. Unfortunately, the scapulothoracic results of this classic study were limited to 2-dimensional roentgenographic analysis on a single subject and objective information on other joint involvement was limited (Inman et al., 1944; Hogfers et al., 1995; de Groot et al, 1998; Borstad and Ludewig, 2002). Moreover, the researchers themselves admitted that the ratio was inconsistent below 30° of humeral elevation. This notion was confirmed by subsequent researchers who found ratios between 4:1 (Poppen and Walker, 1976) and 7:1 (Doody et al., 1970) at humeral elevation angles below 30° in the “scapular plane”, (approximately 40° anterior to the frontal plane). In addition, inter-subject variability of this ratio increases at higher elevation angles (Ludewig et al., 2009). Modern work on glenohumeral and scapular motion has expanded on the topic in terms of the planes assessed (Karduna et al., 2001; McClure et al., 2006; Bourne et al., 2007; Ludewig et al., 2009), comparisons of healthy and injured individuals (McClure et al., 2004; Fayad et al., 2008; Braman et al., 2009), and static and dynamic three-

dimensional kinematic analysis, (static – de Groot et al., 1998; Meskers et al., 2000; dynamic – Karduna et al., 2001; Ludewig et al., 2009).

Controlled shoulder motion is a coordinated effort involving several moving irregular shaped bones and joints, which makes scapular kinematic measurement difficult. The shoulder is essentially a closed chain linkage, composed of the sternum, clavicle, scapula, humerus and thorax, and the joints that connect them, including the gliding of the scapula over the thorax (Happee and van der Helm, 1995). Therefore, the clavicle and thorax constrain scapular motion creating an interdependency of the sternoclavicular (SC) and acromioclavicular (AC) articulations during any scapular movement. This has important modeling implications. In order to successfully model three-dimensional (3D) shoulder kinematics, one must consider the rotations and translations about these joints along with the glenohumeral (GH) and scapulothoracic (ST) joints (Happee and Van der Helm, 1995).

Several shoulder motion capture techniques exist, each with their own benefits and limitations. Traditional methods of measurement of these articulations included skin-mounted goniometry (Doody et al., 1965), and roentgenographic projection (Inman et al., 1944; de Groot et al., 1998). The accuracies of these methods are debatable, and analysis is often planar with limited applicability. Transcortical bone pins (Karduna et al., 2000, 2001; Ludewig et al., 2009; McClure et al., 2006) may provide more robust information with reduced skin artifact; however the invasiveness of these techniques limits the sample size of these studies. More recently, skin-mounted electromagnetic (de Groot et al., 1998; Meskers et al., 1998; Borstad et al., 2002) and infrared motion capture (van Andel et al., 2009) technologies have been presented as reliable and acceptable methods to measure 3D scapular kinematics while the humerus remains below 120° of elevation. Above this angle, soft tissue overlying the acromion reduces the accuracy of these

techniques. Reliable and accurate skin-mounted kinematic techniques would be advantageous because they would allow for dynamic motion capture and analysis on large sample sizes.

1.2 Inconsistencies in past shoulder motion research

Comparing results of studies investigating glenohumeral and scapular kinematics must be done with caution due to several confounding factors which affect scapular motion. 3D rotations of the scapula depend on humeral elevation angle, plane of elevation (Ludewig et al., 2009; McClure et al., 2006), external shoulder load (Kon et al., 2008; McQuade and Smidt, 1998; Meskers et al., 1998), humeral elevation velocity (de Groot et al., 1998; Johnson et al., 2001), and rotation sequence used to calculate segment rotation (Karduna et al., 2000) among other factors. Also, the variability of shoulder motion across individuals is very high, emphasizing the need to have a high participant sample size in shoulder kinematic studies. Since most scapular kinematic studies are limited in the number of humeral elevation planes tested (typically less than three), understanding 3D scapular position during diverse glenohumeral and scapular motions requires combining the results of several studies with differing methodological approaches. Therefore, clinicians and upper limb researchers would benefit from having a robust collection of shoulder kinematic profiles collected on a large sample of participants.

Although experimental protocols differ between prior studies, there have been attempts to standardize data collection techniques. Standardized definitions of bony landmarks used to define upper limb segment coordinate systems and to describe joint rotations have been suggested by the International Society of Biomechanics (Wu et al., 2005). This is vital when using Euler angles to describe scapular rotation because the resulting angles are sequence dependent (and non-commutative). Moreover, researchers have attempted to control for the humeral orientation in that the majority of upper limb studies. The most common approach is to

limit analyses to vertical planar humeral motions, particularly in the scapular plane. Although controlling for plane is beneficial, narrowing focus to one motion plane limits what can be learned about typical shoulder motion. Interesting information on typical shoulder motion may be gained by investigating other planes, and injured shoulders could potentially show different joint motion in vertical planes other than the scapular plane.

1.3 Normative shoulder kinematic data applications

Possessing normative typical shoulder kinematic data would make the identification of pathological shoulder motion easier for clinicians. These data would provide a single source for clinicians to contrast results from a clinical assessment against. If an individual or individuals motion trends are deviant relative to typical normative kinematic data, these trends could be classified as atypical. Early identification of atypical shoulder motion would allow for the prescription of clinical interventions such as postural correction or corrective exercises to prevent shoulder injury from occurring (McClure et al., 2006). Moreover, tracking a patient's shoulder kinematic profiles during a prolonged rehabilitation program can serve as a means to monitor recovery towards an uninjured state (McClure et al., 2004).

Understanding what factors affect healthy dynamic shoulder motion will justify current clinical assessment approaches and assist with assessment design. For example, a common approach applied by therapists during a shoulder assessment is to track scapular motion visually during humeral elevation and lowering (Borstad & Ludewig, 2002). If obvious kinematic changes occur between motion phases, clinicians consider these differences as abnormal or “dyskinetic” (Kibler & McMullen, 2003). Therefore, discovering no meaningful effects of motion phase on scapular kinematics for a typical population would justify this approach. In addition, finding scapular kinematic differences during humeral elevation in one plane (e.g.

frontal plane) compared to elevation in another (e.g. sagittal plane) would suggest pathological motion if typical normative data shows no effect of plane. Finally, discovering kinematic changes at specific elevation angles might indicate atypical motion if the typical population does not display similar changes. For instance, a reduction in posterior tilt and upward scapular rotation is often hypothesized to occur in populations suffering with rotator cuff pathologies (Ludewig & Cook, 2000; McClure et al., 2004).

Understanding how an uninjured shoulder moves may also provide insight into potential injury mechanisms. Contrasting scapular kinematic profiles of an injured population against a robust collection of healthy scapular kinematics should show incidences where the profiles deviate from each other. The direction of this deviance might explain a contributing cause of the injury. For example, if injured profiles of scapular tilt and upward rotation become less posterior and less upward compared to a healthy population, this would hint at a reduction of sub-acromial space. This trend is often suggested to occur in populations suffering from sub-acromial impingement syndrome (Lukasiewicz et al, 1999).

1.4 Purpose

The purposes of this investigation were to produce a comprehensive description of typical shoulder kinematics during dynamic humeral elevation in six vertical movement planes, and to identify which factors contribute to typical shoulder motion. Results of this study will offer clinical researchers normative typical upper limb kinematic profiles that will assist with the identification of pathological shoulder motion. Specifically, the following questions are asked:

- Do significant changes in 3D shoulder rotations occur as the humerus is elevated in planes other than the scapula plane?

- Do gender and motion phase (i.e. raising or lowering the humerus) influence typical shoulder motion?
- Are certain shoulder kinematic outcomes more influenced by vertical humeral movement plane or by humeral elevation level
- If shoulder kinematic changes occur due to the modification of movement plane, elevation angle, motion phase, or gender, do these changes contribute to or diminish the possibility of becoming injured?
- How does the variability of shoulder joint rotations change as the humerus is elevated?
- Does humerus elevation in certain vertical movement planes produce more reliable upper limb kinematic measures than others?

Current shoulder kinematic data is incomplete due to limited scope of previous studies or inadequate measurement techniques. A common ambition of many clinical researchers is to be able to reliably classify atypical shoulder motion as a means to identify individuals at risk of developing some upper extremity disorder. In order to successfully do this, what is known about typical shoulder motion and its determinants must be expanded. The results of this study will help build on what is known about typical shoulder motion, as the research questions address several of the limitations of current work on the 3D scapular kinematics outlined previously. Finally, recording shoulder kinematic data on a single population sample will limit the errors associated with making comparisons across studies

1.5 Hypotheses

This investigation will quantify scapular kinematics in multi-planar humeral motion and demonstrate the dependency of shoulder muscular activation on the same humeral motion. The specific hypotheses of this investigation were:

- 1) As vertical humeral movement plane is changed progressively across the body, dynamic shoulder rotations occurring about a vertical axis (i.e. scapulothoracic protraction, acromioclavicular protraction, sternoclavicular protraction) and axial shoulder rotations (i.e. glenohumeral internal rotation, glenohumeral anterior plane of elevation) will increase more than shoulder rotations occurring about a horizontal axis (i.e. scapulothoracic lateral rotation, scapulothoracic posterior/anterior tilt, glenohumeral elevation, acromioclavicular elevation, sternoclavicular elevation).
- 2) As humeral elevation angle increases, dynamic shoulder rotations occurring about a horizontal axis will increase more than those rotations occurring about a vertical axis.
- 3) Intra-subject trial-to-trial reliability, indicated by intra-class correlation coefficients (ICC), of shoulder (i.e. scapulothoracic, glenohumeral, acromioclavicular, and sternoclavicular) kinematics will be high.
- 4) 3D scapular kinematics inter-subject variability, indicated by standard deviation, will be highest below 30° of humeral elevation for all thoracohumeral elevation planes
- 5) There will be no effect of gender on shoulder kinematics.
- 6) Lowering the humerus will produce significantly different shoulder kinematics than elevation.

2. REVIEW OF RELEVANT LITERATURE

2.1 Shoulder joint motion capture and description

Positioning the humerus in three-dimensional (3D) space can be accomplished by means of countless orientations of SC, AC, GH, and ST joints thereby making joint description challenging. The following sub-sections outline the methods used to collect shoulder kinematics and describe upper limb joint motion and inter-connecting segments orientations.

2.1.1 Shoulder motion capture

The earliest method of assessing upper limb motion was by means of hand-held goniometers. Their published use dates back to the early 1920's and are still used in clinical settings (Hewitt, 1928; Bovens et al., 1990). The device can also be used to reliably position the humerus in desired elevation angles or planes. The technique is useful in rehabilitation settings due to quick and easy measurement outcomes and high intra-tester reliability with experience use (Youdas et al., 1994). However, 3D scapular kinematics cannot be deduced with a single hand-held goniometer. Bovens et al (1990) found that the error of measurement when using a goniometer is as high as 10° for several upper limb joint measurements.

With researchers' strong desire to collect accurate GH and ST kinematic data, advanced imaging techniques have been utilized as early as the 1940's. Inman et al's (1944) oft cited description of the "spino-humeral" angle in sagittal plane flexion and frontal plane abduction, better known today as scapulothoracic rhythm, was captured using 2-dimensional roentgenography. Modern studies continue to use 2-dimensional projections (Bagg and Forrest, 1988; de Groot et al., 1998), but cannot accurately capture shoulder kinematics because upper limb motions are not planar or static (de Groot et al., 1998). The advent of cine film in the 1950's allowed for the capture of passive skin based surface markers during dynamic motions (Taylor

and Blascke, 1951; Engen and Spencer, 1968; Dvir, 1978; Langrana, 1981). Unfortunately, data processing of cine film is laborious and skin based surface markers were prone to skin artifact error. Motion capture systems using active markers such as light-emitting diodes (Anglin and Wyss, 2000; van Andel et al., 2008), or passive optical technology (Picco et al., 2010) have also been applied recently.

Most recently, there has been increased use of electromagnetic motion tracking systems consisting of a transmitter containing three energized orthogonal coils that emit electromagnetic fields detected by skin-mounted sensors' orthogonal fields. This technique allows for the calculation of the 6 degree of freedom position and orientation of skin mounted receivers relative to a transmitter. However, the accuracy of this system is greatly affected by any object that interferes with magnetic fields (e.g. metals, computer monitors, and mains) the distance between the transmitter and receivers (Nixon et al., 1998) and must be carefully calibrated.

Of the upper limb segments, 3D scapular kinematics are the most challenging to collect with current motion capture technologies due to skin motion artifact and movement of bones subcutaneously. Bone pins inserted directly into the scapula are frequently cited as a gold standard for scapular kinematic collection (Ludewig et al., 2009). However, due to its invasiveness and limited access to those qualified to insert the pins, it is difficult to collect data on a large sample population using the pins. This has led to the development of several scapula tracking techniques that allow for the scapula to be either directly measured over the skin; or by means of reconstructing the scapula with a rigid marker cluster. Accuracy of these methods is often assessed by means of bone pins. The more commonly used techniques are as follows:

Palpator (van der Helm and Pronk, 1995): The positions of 11 anatomical landmarks are recorded manually with a palpator whose endpoint location is calculated using potentiometers.

Rotations of the scapula are described relative to the torso reference system located at the jugular notch. Drawbacks to this technique are that only static recordings are possible due to the time required for each posture measurement. Each posture took approximately 2.5 minutes to manually record increasing fatigue potential. The accuracy of this system was assessed by the repeatability of locating the landmarks with the palpator and was deemed acceptable. Measurement error was found to be comparable with other contemporary techniques at the time.

Scapula locator (Meskers et al., 1998): Two rigid pieces of plastic are connected in the middle similar to a lowercase “t” (Figure 1). At the end of the rigid pieces are three movable rods that can be positioned over the acromion angle (AA), root of the scapular spine (RS), and inferior scapula angle (IA). A reference system is created on the locator with an electromagnetic sensor or marker cluster. The orientations of the three rods relative to the locator reference system are measured with a digitizer, allowing for a scapula reference system to be reconstructed for every measured frame. The orientation of this reference system is used to decompose Euler angles and describe scapula orientation. Similar to the palpator, the locator’s applicability is limited to measuring static postures. However, the measurement of each posture is reduced compared to the 2.5 minutes noted by van der Helm and Pronk (1995), as orientations of the humerus, clavicle, and torso area reconstructed each frame from electromagnetic sensors with embedded reference systems. Locator accuracy was assessed in a similar fashion as the palpator and orientation results were found to be comparable to van der Helm and Pronk’s *palpator* (1995), with some differences being attributable to methodological differences.

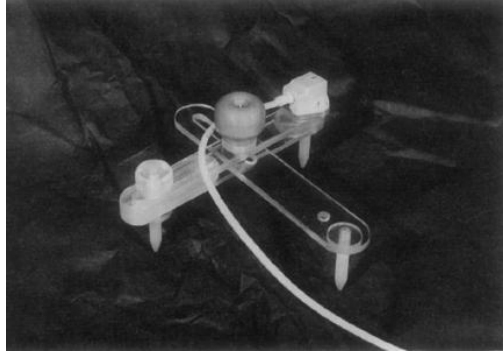


Figure 1: Adjustable scapula locator (Meskers et al., 1998)

Scapula tracker (Karduna et al., 2001): An electromagnetic receiver is mounted to an adjustable “base” that conforms to the mid-portion of the scapula spine. An adjustable “arm” extends from the base and at its end is a footpad secured to the posterior lateral acromion (Figure 2). Both the base and the footpad are secured to the skin overlying the scapula with Velcro. Scapula anatomical landmark locations relative to the reference system embedded in the receiver are determined with a digitizer and reconstructed for subsequent tracked motions. The advantage of this technique is that it can record dynamic scapula motion. Also, the scapula tracker has been validated with bone pins for humeral elevation angles less than 120°

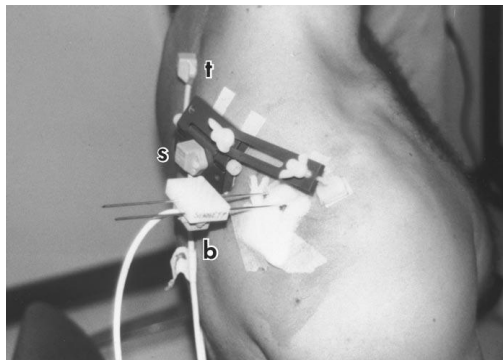


Figure 2: Scapula tracker fixed to the mid-portion of the scapula spine and posterior lateral acromion (Karduna et al., 2001)

Acromion marker cluster (McQuade and Smidt, 1998; Karduna et al., 2001; van Andel et al., 2008): Either an electromagnetic receiver or marker cluster is fixed to the posterior-lateral

acromion proximal to the deltoid attachment (Figure 3). Similar to the tracker method, relevant anatomical landmark locations relative to the cluster are captured in a calibration frame and are reconstructed in subsequent frames. The majority of recent studies recording scapular motions use a version of the acromion marker cluster (AMC). The major difference between studies centers on the materials used to construct the acromion reference system (e.g. active or passive infra red markers, electromagnetic sensors). This technique has also been validated using bone pins for humeral elevations under 120° (Karduna et al., 2001).

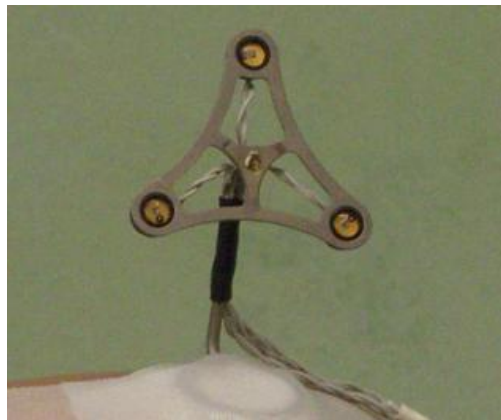


Figure 3: Acromion marker cluster (AMC) attached to acromion (van Andel et al., 2008)

Measuring clavicle rotations with surface markers is also challenging due to skin motion artifact and methods to correct this error have been attempted. The most accurate way to measure clavicle motion and minimize this error is with a coordinate system fixed to a bone pin inserted into the clavicle (Inman et al., 1944; Karduna et al., 2009). However, because of the invasiveness of this technique and the difficulties in measuring axial rotation with surface markers, sternoclavicular (SC) and acromioclavicular (AC) joint motion is often ignored in many upper limb kinematic analyses. At best, clavicle protraction/retraction and elevation/depression angles are used to describe the translation of the scapula (Anglin and Wyss, 2000; Karduna et al., 2001; McClure et al., 2001; 2004).

A new technique that attempts to track 3D clavicle rotation with a coordinate system fixed to the skin overlying the clavicle has been proposed by Szucs et al., (2010). In their study, clavicle kinematics was measured simultaneously with a skin-based coordinate system and a bone-fixed system on six cadaver shoulders. Corrective regression equations using thoracohumeral (TH) elevation angle and recorded rotations were generated that correct elevation angle and axial rotation. Limitations to this technique are obvious including the use of cadavers and limited number of specimens. However, the regression equations generated offer the only available method to define an orthogonal clavicle coordinate system that is crucial in describing 3D clavicle rotations in accordance to ISB standards (Wu et al., 2005).

2.1.2 Euler Angles

Commonplace in upper limb kinematic analysis is the use of Euler angles to describe 3D joint rotations. Euler angles allow for the orientation of one segment to be described relative to another segment or system of interest. Between the two segments is some articulation where these rotations are assumed to take place. To apply this technique to a desired joint, body segment coordinate systems of the segments proximal and distal to the articulation are first constructed using appropriate anatomical landmarks. Then, the orientation of the distal segment's coordinate system is described relative to the proximal segment's coordinate system using three rotations (i.e. "Euler angles") of its system. Depending on the order of rotations chosen, the descriptive Euler angles can be used to describe clinically relevant joint rotations (Wu et al., 2005), as well as joint dynamics if desired (Vaughan et al., 1999).

2.1.3 Euler Angle Limitations

The magnitudes of the Euler angles calculated depend on the order of rotation because the rotations are not cumulative (Hill et al., 2007). Depending on the order of rotations about the

distal segment axes, the resulting Euler angles will be different. For some investigators, this notion is seen as a drawback to the technique (Woitring, 1994). When Karduna et al (2000) altered rotation sequences differences in joint rotations were as large as 50° . An often cited clinical example illustrating this limitation is “Codman’s Paradox” (Figure 4), where the humerus is flexed 90° in the sagittal plane, then abducted 90° in the transverse plane, then adducted 90° in the frontal plane (Codman, 1934). The position of the humerus is “paradoxically” externally rotated 90° .

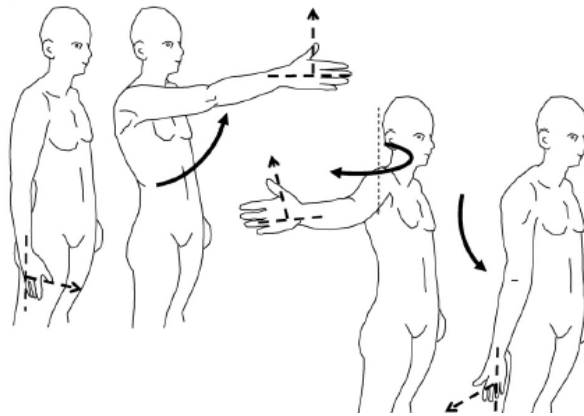


Figure 4: Visual representation of Codman’s Paradox (Hill et al., 2008)

A second drawback of using Euler angles to describe joint motion is that one must assume that there is no joint translation. Neglecting to account for intersegmental translation when modeling shoulder articulations will result in descriptions unrepresentative of clinical reality. For example, due to the degree of freedom constraints of Euler notation, the glenohumeral joint is often modeled as a pure ball and socket joint with no linear translation between the glenoid fossa and humeral head. However, it is known that as the humerus is elevated, the GH center of rotation is not fixed, and that the humeral head, slides and rolls along the glenoid fossa (Paletta et al. 1997; Yamaguchi et al., 2000). Attempts have been made to account for both ST rotations and translations at the AC joint. Karduna et al (2001) and McClure

et al (2006) have modeled the ST joint motion with 3 degrees of rotational freedom and 2 degrees of translational freedom. Translation was limited 2 degrees of freedom (elevation/depression; protraction/retraction) due to the rigidity of the clavicle.

A final drawback associated with the use of Euler angles is the potential for Gimbal lock. Gimbal lock occurs when the sequence of rotation used to describe a segment's orientation causes axes to become coincident (Hill et al., 2008). A system that once had 3 DOF becomes an indeterminate 2 DOF system. For example, in a shoulder abducted to 90°, the axial rotation axis of the humerus would coincide with the flexion axis of the GH joint. If the first Euler angle of the sequence is flexion, the system would be indeterminate (Rab et al., 2002). If the experimental design does not guard against Gimbal lock, erroneous shoulder kinematic measurements will result.

2.1.4 Standardization of shoulder kinematic descriptions

The widespread use of Euler angles in shoulder kinematic studies has resulted in the establishment of standardized protocols for reporting shoulder kinematic data. Standardization prevents comparisons of rotations deduced from different rotation sequences. The Standardization and Terminology Committee of International Society of Biomechanics (ISB) proposed definitions of joint coordinate systems and rotations for each segment and articulation of the upper limb (Wu et al., 2005). The definitions are outlined in a way similar to that of Grood and Suntay's "Joint Coordinate System (JCS)" of the knee (Grood and Suntay, 1983). A "Body-fixed" axis is identified in each segment whose relative motions are being analyzed. The two segments share a common "floating" axis that is perpendicular to the body fixed axes. In their description, the rotations of the distal segment are described with respect to the proximal segment, using rotations about the body fixed and floating axes. The orientations of the axes are

defined to allow for clinically relevant joint rotation to be determined. A summary of all upper limb anatomical landmarks and JCS defined by the International Society of Biomechanics are provided by Wu et al. (2005).

When interpreting the results from past studies, consideration to the methods used is important when interpreting results. Studies specifically measuring scapular kinematics have also been performed utilizing methods pre-existing ISB standards with the abovementioned techniques (van der Helm et al., 1995; Karduna et al., 2001; McClure et al., 2006). In the following section, all joint motions are summarized using the joint coordinate systems defined International Society of Biomechanics guidelines unless otherwise stated (Wu et al., 2005).

Glenohumeral (GH) joint: The GH joint is typically modeled as a perfect ball-and-socket joint with 3 degrees of rotational freedom. The sequence of the three rotations is (Figure 5):

- 1) Plane of elevation measured about an axis fixed to the scapula coincident with the y-axis of the scapula
- 2) elevation about the humeral fixed axis coincident with the x-axis of the humerus coordinate systems
- 3) axial (internal/external rotation) about the y-axis of the humerus

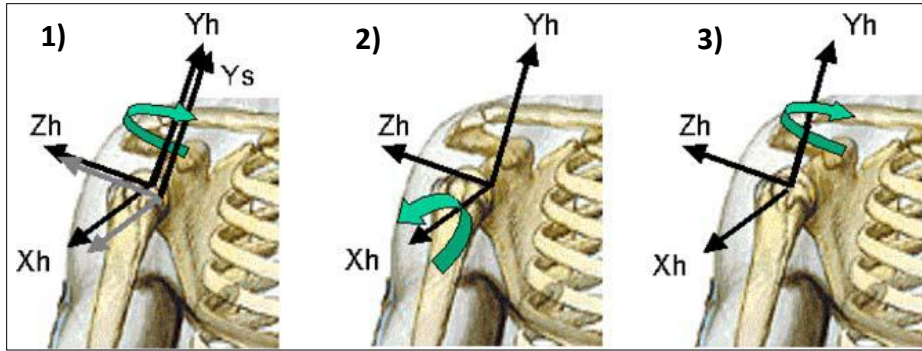


Figure 5: Humerus coordinate system and example of GH joint motion. Lowercase h refers to the humeral local coordinate system; lowercase s refers to the scapula coordinate system. 1) Glenohumeral plane of elevation; 2) Thoracohumeral elevation; 3) Humeral axial rotation (Wu et al., 2005)

Sternoclavicular (SC) joint: The sequence of rotations defined for the three SC joint are (Figure 6):

- 1) Clavicle retraction/protraction about the fixed thorax axis coincident with the y-axis of the thorax coordinate system
- 2) Clavicle elevation/depression about a common axis perpendicular to the fixed axes of the thorax and clavicle coincident
- 3) Axial rotation about the fixed clavicle axis coincident with the z-axis of the clavicle coordinate system

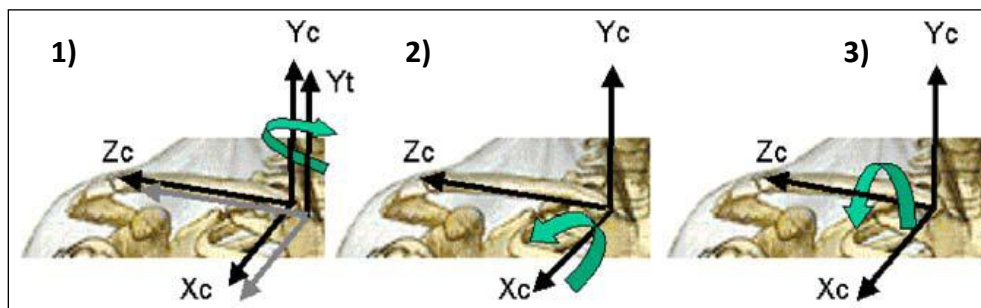


Figure 6: Clavicle coordinate system and example of SC joint motion. Lowercase c refers to the clavicle local system; lowercase t refers to the thorax system. 1) SC protraction/ retraction; 2) SC depression/elevation; 3) Clavicle axial rotation (Wu et al., 2005)

Acromioclavicular (AC) joint: The sequence of rotations defined for the AC joint is

(Figure 7):

- 1) Scapula retraction/protraction relative to the clavicle fixed axis coincident with the y-axis of the clavicle
- 2) Scapula lateral/medial rotation about the common axis perpendicular to the clavicle and scapula fixed axis
- 3) Anterior/posterior scapula tilt about the scapula fixed axis coincident with the z-axis of the scapula coordinate system.

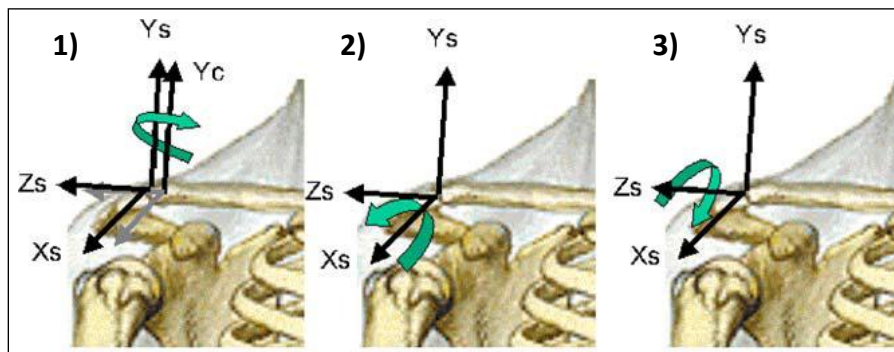


Figure 7: Scapula coordinate system and example of AC joint motion. Lowercase s refers to the scapula local coordinate system; lowercase c refers to the clavicle coordinate system. 1) AC protraction/retraction; 2) AC lateral/medial rotation; 3) AC anterior/posterior tilt (Wu et al., 2005)

Scapulothoracic (ST) joint: The ST joint is often modeled as a segment with 3 degrees of rotational freedom about the thorax local coordinate system. It is important to note that the ST joint is not a true joint as it has no fixed axis of rotation. Rather, motion descriptions for this joint describe segment rotation not joint rotation (Hill et al., 2007). ST joint motion is typically documented relative to humeral-thoracic elevation. The ratio between ST joint motion and humeral elevation is called “rhythm.” The sequence of rotation describing scapula motion at the ST joint is:

1. Scapula retraction/protraction about fixed thorax axis

2. Scapula lateral/medial rotation about the common axis perpendicular to the fixed axis of the thorax and scapula
3. Scapula anterior/posterior tilt about the scapula fixed axis

2.1.5 Normal shoulder joints' ranges of motion

Shoulder joint motion ranges are typically presented relative to humeral elevation angle. Since the majority of methods used to collect scapular rotational kinematics are valid for less than 120° of humeral elevation, most joint ranges presented in the literature are only valid sub-maximally. Table 1 indicates the average resting position and end range of motion at 120° humeral elevation for each shoulder joint (Ludewig et al., 2009). End ranges were averaged across each plane to give an indication of general shoulder motion. For instance, from the table, one can see that ST joint upward rotation increases nearly 44° on average (from 5.4° to 50°) during humeral elevation. An example plot of ST joint motion is demonstrated in Figure 8. For additional plots of shoulder motion, the reader is referred to Ludewig et al (2009).

Table 1: Shoulder joints' range of motion: Initial = resting anatomical position; End = 120° humeral elevation in the respective plane anatomical position. ¹All angles are measured relative to the torso with the exception of the acromioclavicular and glenohumeral joints and are averaged across frontal and scapular plane abduction and sagittal plane flexion

| Joint | *Mean initial position (°) | ¹Average end position (°) |
|-------------------------------------|-----------------------------------|---|
| Sternoclavicular joint (SC) | | |
| Retraction | 19.2 (SE 2) | 39 |
| Elevation | 5.9 (SE 1) | 17 |
| Posterior rotation | 0.1 (SE 0) | 31 |
| Scapulothoracic joint (ST) | | |
| Internal rotation | 41.1 (SE 2) | 35 |
| Upward rotation | 5.4 (SE 1) | 50 |
| Anterior tilting | 13.5 (SE 2) | -8 |
| Acromioclavicular joint (AC) | | |
| Internal rotation | 60 (SE 2) | 65 |
| Upward rotation | 2.5 (SE 1) | 16 |
| Anterior tilting | 8.4 (SE 2) | -15 |
| Glenohumeral joint (GH) | | |
| Elevation | 0.8 (SE 1) | 85 |
| Plane of elevation | 3.1 (SE 2) | - |
| External rotation | 14.1 (SE 4) | 51 |

It is well established that there is high between-subject variability in shoulder kinematic measures. For example, recorded ratios between GH and ST rotation vary between 2:1 (Inman et al., 1944) to 7:1 (Doody et al., 1970). In addition, between-subject scapula protraction/retraction recorded during elevation is most variable of the three scapulothoracic measures (McClure et al., 2004; Ludewig et al., 2009). As the humerus is elevated, it is known that the scapula consistently rotates upward, and tilts posteriorly. However, whether the scapula protracts or retracts appears to depend on the individual. Within-subject kinematic measures are more precise, although accuracy is difficult to determine. Typical trial-to-trial intra-class correlation coefficients of measured joint rotations are typically above 0.94, signifying that rotation measurements were repeatable (Bourne et al., 2007; Ludewig et al., 2009). Scapulothoracic rotation root mean square

differences between trials range from 1.1° (Bourne et al., 2007) to 5.4° (de Groot & Valstar, 1998)

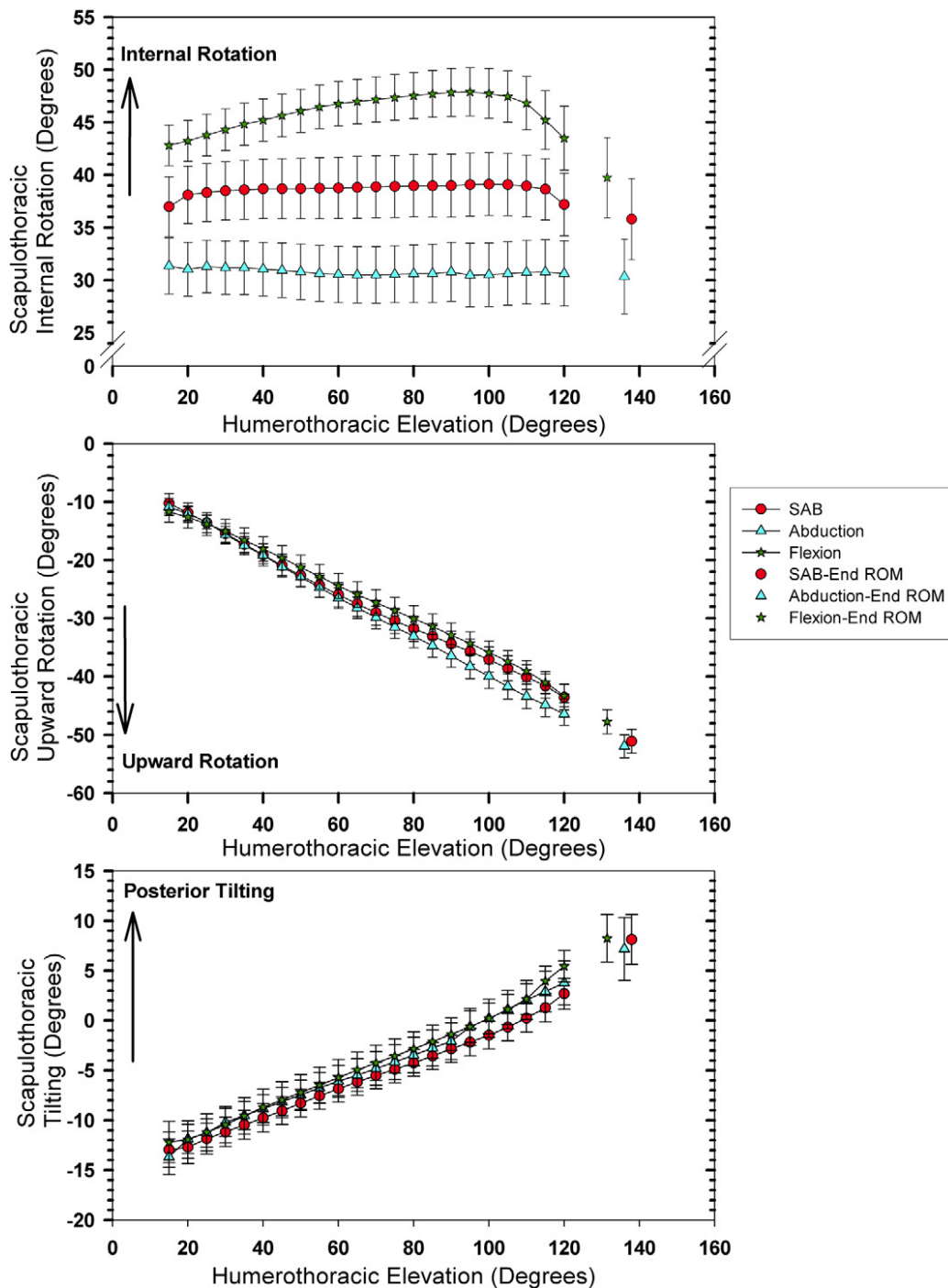


Figure 8: Plot of 3D scapulothoracic motion relative to humeral elevation angle (from Ludewig et al., 2009)

2.2 Determinants of shoulder kinematics

2.2.1 External force

Scapular kinematics are dependent on the weight held in the hand, although the magnitude of the affect is difficult to conclude. McQuade and Smidt (1998) used the acromion marker cluster method (via an electromagnetic receiver) to quantify external arm resistance's effects on scapula lateral rotation in scapular plane abduction. Three loads were tested: passive abduction, zero external load, and maximal resisted arm elevation applied using a Cybex isokenetic dynamometer. The ratio of scapula lateral rotation to thoracohumeral elevation was not consistent between conditions. Important to note, however, is that the largest relative changes were seen at near maximum humeral elevation angles and beyond the range that the cluster method has been validated. Pascoal et al (2000) attempted address the narrow scope of McQuade and Smidt's investigation. They utilized moderate external loads (0-4kg) and tested different planes of humeral elevation (frontal and sagittal). They also found that the affect of load was not consistent for all planes tested and all rotations calculated. Unfortunately, the direction of the affect is unclear and interactions between elevation angle and external load were not accounted for. Kon et al (2008) found significant affects of arm load on lateral scapular rotation at scapulothoracic elevation angles between 35° and 45° only (Figure 9).

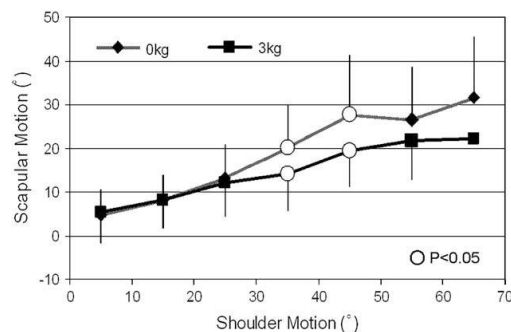


Figure 9: Plot showing a significant effect of external load on scapular lateral rotation at 35° and 45° of arm elevation (Kon et al., 2008)

2.2.2 Humeral elevation velocity

Recent evidence suggests that the velocity of humeral elevation will affect scapular kinematics. de Groot et al (1998) found a significant effect of scapular plane humeral elevation velocity of planar scapular kinematics, but concluded that the differences were negligibly small. However, the fidelity of de Groot et al's findings is speculative, as scapular orientation was calculated with a 2-dimensional x-ray video system. Later work comparing dynamic and static scapular orientation during scapular plane abduction showed that scapular lateral rotation measurements were significantly different, although the techniques used to assess motion were not the same as de Groot et al. (Johnson et al, 2001). Later work by Fayad et al (2006) investigating sagittal plane flexion and frontal plane abduction found less scapula lateral rotation in dynamic measurements. Reasons used to explain the differences between static and dynamic measures are speculative and generally lack rigorous evaluation.

2.2.3 Plane of elevation

The plane of humeral elevation often dictates shoulder joint orientations. Ludewig et al. (2009) directly tracked clavicle, humerus, and scapula movements with electromagnetic sensors fixed to bone pins during humeral elevation in frontal, sagittal, and scapular planes. These planes have been investigated before, but rarely are all three evaluated in the same investigation. This allows for comparisons of SC, AC, GH, and ST joint motions across the same population sample. For example, in each elevation plane, transverse-plane joint rotations showed the largest changes in magnitude for each plane. In flexion, the clavicle was more protracted, the scapula was more internally rotated, and the humerus was more internally rotated than in abduction. Detailed descriptions of the significant joint rotation differences across planes are numerous and described by Ludewig et al (2009).

Scapular kinematics observed during arm eccentric humeral lowering show subtle yet significant differences compared to concentric arm elevations. Ludewig et al (2009) verbally described small differences between lowering and raising the humerus, although these differences were not presented graphically nor tabulated. Borstad and McClure (2002) did not find any significant changes in scapular kinematics between raising and lowering the humerus in the scapular plane below 80°. However, at higher abduction angles, greater posterior scapular tilting was evident. McClure et al (2001) observed similar scapular joint rotations patterns for both raising and lowering the humerus, although joint rotation description differences between the two actions reached 5° or more.

2.2.4 Injury

A connection between shoulder kinematics and shoulder pathology has been made. Unfortunately, whether the altered kinematics pre-exist an injury or are caused by an injury is unknown. The links between injury and kinematic outcome are discussed in section 2.4.1 “Links between shoulder pathology and shoulder motion”

2.3 Clinical implications of scapular motion

Shoulder pathology occurrence has been linked to scapular kinematics and relative muscle activity. This deduction comes from comparing kinematics and EMG profiles of an injury symptom-free population sample to an affected population. Comparisons do not always yield consistent results and whether or not the aberrations are compensatory or causal is often speculative. Although causation cannot be confidently determined, the link between altered kinematics and muscle activity to shoulder pathologies, such as rotator cuff disorders or glenohumeral instability, is interesting and warrants further research. Future references to

“normal” kinematics and muscle activity refer to kinematics of a non-symptomatic, pain-free, typical population sample.

2.3.1 Links between shoulder pathology and shoulder motion

Shoulder pathology is often associated with abnormal scapular kinematics. Shoulder disorders linked to deviations in scapular kinematics include rotator cuff disorders (Cools et al., 2003; Phadke et al., 2009), GH joint instability (Matias and Pascoal, 2006), and adhesive capsulitis (Fayad et al., 2008). The rotator cuff disorder sub-acromial impingement syndrome (SAIS) has received the most attention in kinematic studies due to its high prevalence in working populations (Cook et al., 1996; Hagberg and Wegman, 1987; Herberts et al., 1984). First described by Neer (1972) SAIS is a consequence of mechanical compression of the rotator cuff muscles (particularly the supraspinatus tendon) and sub-acromial bursa against the undersurface of the acromion process (Figure 10). Scapular lateral rotation and posterior tilt present in normal populations are said to occur to increase the sub-acromial space as the humerus elevates and thus decrease mechanical compression on the rotator cuff (Cools et al., 2003). Any significant increase in this rotation in patients with SAIS is assumed to be compensatory. If a causative link between the shoulder pathology and scapular kinematics is made, clinicians can design interventions that prevent future injury by correcting the kinematics.

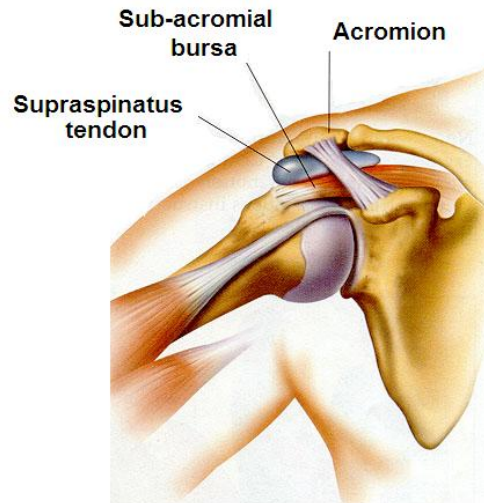


Figure 10: A visual representation of sub-acromial impingement of the supraspinatus tendon and sub-acromial bursa

Unfortunately, the kinematic changes correlated with SAIS are not consistent. McClure et al. (2006) found increased scapular lateral rotation and clavicle elevation during humeral flexion and greater posterior scapular tilt and clavicle retraction in scapular plane humeral abduction in patients with SAIS. On the contrary, Endo et al, (2001) found less lateral scapular rotation and posterior tilt in symptomatic subjects. Ludewig et al (2000) investigated the affect of elevation angle on lateral rotation and saw an initial decrease in symptomatic subjects at angles below 60° and then a compensatory increase as the humerus was positioned above 90°. Explanations for these discrepancies are likely associated with methodological differences. Ludewig et al (2000) tested special population (injured construction workers) and tracked scapular motion utilizing the acromion marker cluster method (McQuade and Smidt, 1998), while McClure et al (2006) utilized the scapula tracker (Karduna et al., 2001). Furthermore, Endo et al (2001) used planar radiographic projections to calculate angles, while both McClure et al (2006) and Ludewig et al (2000) described motion with 3D Euler rotations. Also, interactions between plane of humeral elevation and humeral elevation angle cloud interpretations.

3. RESEARCH METHODS

Data collection occurred in sessions lasting approximately one and a half hours in the Digital Industrial Ergonomics and Shoulder Evaluation Laboratory at the University of Waterloo. Participants raised and lowered their right arm in six different vertical planes with posture recorded with passive reflective markers. Each motion was repeated twice.

3.1 Participants

Twenty-nine (15 males; 14 females) right-hand dominant participants sampled from the University of Waterloo student population volunteered to participate in this investigation. (Participant anthropometrics are provided in Table 2). Exclusion criteria for study participation included a history of shoulder instability, positive Neer (Neer, 1983) and Hawkins-Kennedy (Hawkins and Abrams, 1987) tests for shoulder impingement, painful arc of motion between 60° and 120° (Kessel and Watson, 1977) (Figure 11), or allergies to rubbing alcohol and skin adhesives. The study received clearance from the Office of Research Ethics and participants provided informed consent.

Table 2: Study participants' anthropometrics

| Gender | Age (years) | Stature (cm) | Mass (Kg) |
|---------------|--------------------|---------------------|------------------|
| Male | 23.4 (+1.5) | 180.2(+6.4) | 82.9(+10.0) |
| Female | 22.8(+3.0) | 167.0(+7.6) | 61.4(+12.7) |



Figure 11: Sub-acromial impingement tests: 1) Painful arc of motion (Hawkins and Abrams, 1987); 2) Hawkins-Kennedy test; 3) Neer test (Park et al., 2005)

3.2 Experimental variables

Upper limb motion data was collected dynamically during each trial. Each trial was repeated twice. Four independent variables were tested with differing levels of each variable:

- 1) Shoulder elevation plane (6): 0°, 30°, 40° (i.e. scapular plane), 60°, 90°, 120°
- 2) Thoracohumeral elevation angle (23): 5 degree increments between 10° and 120°, measured dynamically
- 3) Motion phase (2): Raising, lowering
- 4) Gender (2): Male, female

The shoulder elevation plane was measured relative to the approximate glenohumeral (GH) joint center. The 0° plane was parallel with the frontal plane while the 120° plane was directed 30° medial to the sagittal plane. Elevation planes were measured externally with a goniometry about a vertical axis coincident with the vertical z-axis of the thorax coordinate system at the GH joint (Wu et al., 2005). Thoracohumeral (TH) elevation angle was measured with kinematic data after data collection and defined as the rotation about an axis coincident with the forward pointing y-axis of the humerus at the GH joint (See Table A2 and Figures A1-A4 in Appendix A for descriptions of segment coordinate systems). In subsequent sections, values referring to humeral elevation increments will be identified with an “E” after the increment and

elevation plane will be denoted using a “P.” For example, “60E” refers to 60° of humeral elevation, while “60P” refers to the 60° movement plane.

Each participant had 2- seconds to raise their humerus past 120° starting from the anatomical position and 2 seconds lower the humerus to the initial position with the aid of a metronome. Dependent variables were scapulothoracic (ST) +protraction/-retraction, ST +medial/-lateral rotation, ST +posterior/-anterior tilt, glenohumeral (GH) +anterior/-posterior plane of elevation, GH -elevation, GH –internal/+external rotation, sternoclavicular (SC) -elevation, SC +protraction/-retraction, acromioclavicular (AC) -elevation, and AC +protraction/-retraction.

3.3 Equipment

3.3.1 Motion tracking

Three-dimensional thorax, clavicle, scapula, and humerus motion were tracked using eight VICON MX20 infrared cameras. The cameras tracked the position of ten passive reflective markers secured to the skin over anatomical landmarks outlined in Table 3. Ten additional markers constituting rigid marker clusters of the humerus, acromion marker cluster, and digitizing stylus tracked (Table 4, Table A3 in Appendix A). Captured kinematic data was recorded using the VICON Nexus 1.4 software (VICON Motion Systems, Oxford, UK) at a 50 Hz sampling rate.

Table 3: Anatomical locations and acronyms of reflective markers

| Marker label | Description |
|---------------------|---------------------------------------|
| C7 | 7th cervical vertebra spinous process |
| RA | Right acromion |
| AC | Right AC joint |
| SC | Right SC joint |
| LA | Left acromion |
| SSN | Suprasternal notch |
| XP | Xyphoid process |
| T8 | 8th thoracic vertebra spinous process |
| ME | Medial humeral epicondyle |
| LE | Lateral humeral epicondyle |

Table 4: Cluster markers labels and descriptions

| Marker label | Description |
|------------------------------|-------------------------|
| AMC1 AMC2 AMC3 | Acromion Marker Cluster |
| HUM1 HUM2 HUM3 | Humerus triad |
| STY1 STY2 STY3 STY4 | Stylus markers |

3.3.2 Digitizing stylus

A digitizing stylus was manufactured from a rigid plate with a defined point (diameter = 2.0 mm) secured at one end. Four reflective markers (diameter = 9.0 mm) were secured to the plate surface with double sided tape to create the stylus coordinate system (Figure 13). The tip was at an orientation represented by the vector [7.0, 134.0, 25.5] mm measured in the local stylus coordinate system from the origin at STY4 (Figure 12). The stylus allowed for scapular anatomical landmark positions to be captured in a static calibration frame.

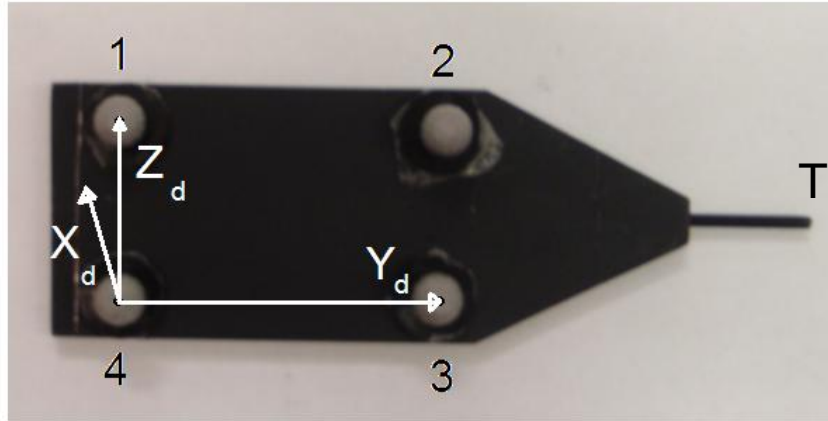


Figure 12: Digitizing stylus with orthogonal coordinate system. X_d is perpendicular to the plane created by STY1, STY2, STY3, and STY4 directed forward. “T” is the tip of the stylus

3.3.3 Acromion marker cluster

The acromion marker cluster (AMC) method (McQuade and Smidt, 1998; van Andel et al., 2008) was used in an effort to reduce skin motion artifact during scapular motion capture. The method has been validated for humeral elevation angles less than 120° . The AMC used consisted of a triangular cluster of three reflective markers (inter-marker distance 30 mm) fixed to a rigid plate secured to a metal “L”-bracket. The base of the bracket is positioned over the flat portion of the posterior lateral-acromion and secured with tape (Figure 13). The cluster was converted to a local coordinate system so that scapular landmarks could be measured relative to a calibration frame (Table A3 and Figure A5 in Appendix A). The scapular landmarks were then recreated in each frame for subsequent trials rather than being directly captured using skin mounted markers.

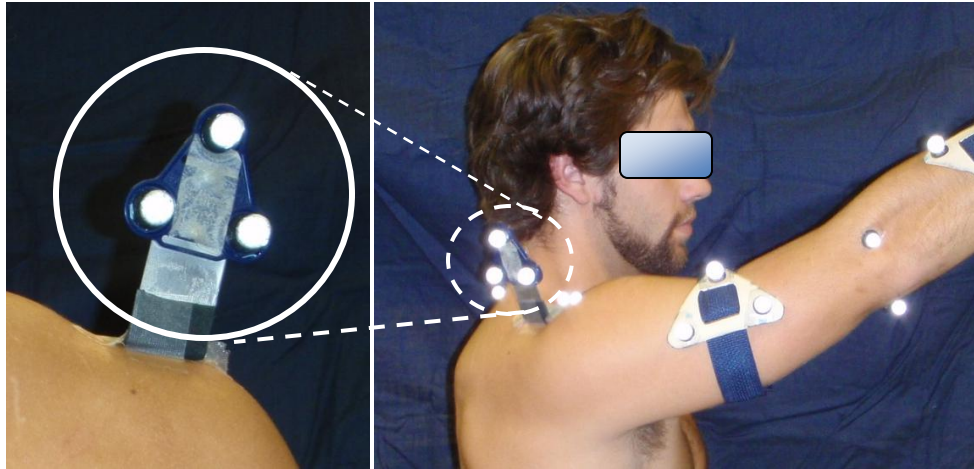


Figure 13: Acromion marker cluster secured to participant's posterior lateral acromion with tape

3.4 Experimental protocol

3.4.1 Collection volume calibration

The 8 VICON cameras were aimed, focused and calibrated prior to motion data collection and participant instrumentation. First, the calibration wand provided by VICON was placed in the center of the anticipated motion capture volume and each camera was aimed and focused to ensure that any reflective marker passing through the volume was visible by all cameras. Any aberrant reflective noise seen by cameras was manually masked. Next, the VICON cameras were calibrated allowing the system to define the capture volume and the relative orientation of the cameras. To calibrate, the calibration wand was waved through the collection volume, allowing each camera to record the wand position. The calibration was deemed acceptable if the root mean square difference of the markers recorded locations and real locations were less than 0.20 mm for each camera. Finally, the global coordinate system origin was defined as a point on the ground so that all participant marker positions were positive. The global positive x- y- and z-axes were directed right, forward and up in relation to the body, respectively.

3.4.2 Collection protocol

Reflective markers were secured to the participant's skin overlying the 10 anatomical landmarks outlined in Table 3. Rigid plates containing 3 markers each were fixed in place over the mid-humerus. Finally, the acromion marker cluster (AMC) was fixed to the posterior lateral acromion with adhesive tape. Three static anatomical calibration trials were then performed with the participant seated with feet shoulder width apart in anatomical position, allowing for the acromion angle (AA), acromion inferior angle (IA), and the root of the scapula spine (RS) locations to be palpated and recorded with the digitizing stylus (Figure 14). Foot alignment was indicated on the floor with tape. The calibration allowed for the global position of all anatomical and clustered markers to be known.

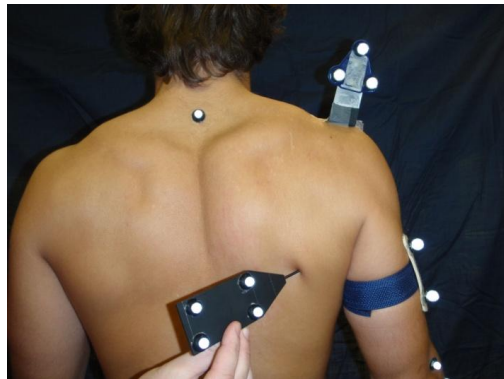


Figure 14: Palpating the inferior angle (AA) of the scapula with the digitizing stylus

Participants remained seated with feet shoulder-width apart and pointed forward as the researcher identified the six movement planes. To do so, the upper limb was positioned in the desired humeral elevation plane with the arm fully extended, elevated to 90° and thumb pointing upward, using a goniometer located at the approximate GH joint center. The arm position for subsequent humeral elevation trials was constrained with a tall narrow rod as to guide the participant's humeral motion and prevent line-of-sight obstructions with the infrared cameras. The rod positions for the respective elevation planes were marked with tape on the floor. A

second rod was placed behind the participant. He or she was asked to maintain contact with this rod during all trials. To reinforce this rod's position, it was taped to the participant's back. If the participant side flexed his or her torso during humeral elevation, the rod visibly swayed and the trial was repeated.

Participants performed the seated humeral elevation trials in the outlined planes three times in a random order for a total of 18 upper limb movements. Anatomical position with the thumb pointed in the direction of the movement plane represented the initial and final positions for all trials. On the investigator's cue, the participant raised the arm maintaining an extended elbow to a sub-maximal elevation angle beyond 120E along the specific elevation plane and then lowered it back on plane to the anatomical position (Figure 15). For movement within the 120P, the elbow was bent at lower elevation as to prevent collisions with the thigh (Figure 16). Each raise-lower cycle was performed to a metronome and completed in 4 seconds.

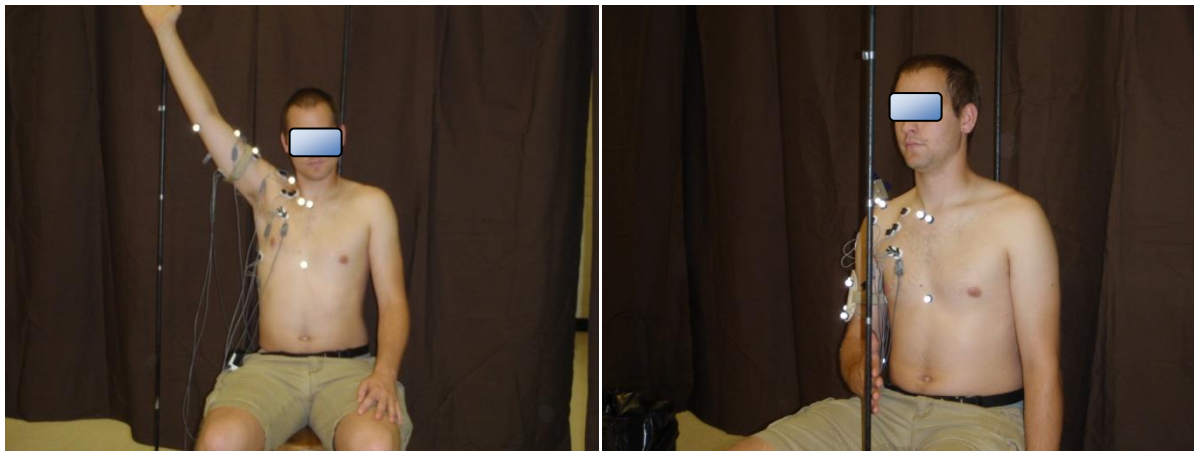


Figure 15: Examples of recorded elevation motions. LEFT: 0P sub-maximal elevation. RIGHT: starting position of the 120P humeral elevation

3.5 Data analysis

Upper limb kinematic data was processed using custom-built scripts written in MATLAB software version R2009b (Mathworks Inc., MA, USA). Link segments were deduced from

filtered marker data and segment coordinate systems created. Analyses of variance were performed using JMP® 8.0.2.2 statistical software (SAS Institute Inc., NC, USA) while intra-class correlation coefficients were calculated using SPSS Statistics v19.0 (IBM, NY, USA).

3.5.1 Kinematics

All raw kinematic data were low pass filtered with a cut-off frequency specific to each participant as determined by residual analysis (Figure 16) (Winter, 2009). One cut-off frequency per participant was chosen in a conservative matter (2.0 – 6.5 Hz cut-off range). Segment length and orthogonal coordinate systems were constructed using definitions provided by Wu et al (2005) (Tables A1, A2, A3, and Figures A1-A4 in Appendix A). The scapula landmarks acromion angle (AA), inferior angle (IA), and scapular spine root (RS) were measured using the digitizing stylus in three calibration trials with the participant in anatomical position (i.e. one calibration per digitized landmark) and used to define the scapula plane. The global three-dimensional position of the stylus tip and anatomical landmarks it palpates were calculated with (from Meskers, 1998):

$$\begin{bmatrix} s_x \\ s_y \\ s_z \end{bmatrix} = \begin{bmatrix} o_{sx} \\ o_{sy} \\ o_{sz} \end{bmatrix} + [R]_{cluster}^{GLOBAL} \cdot \begin{bmatrix} v_{Cx} \\ v_{Cy} \\ v_{Cz} \end{bmatrix} \quad (1.0)$$

Where s_x , s_y , and s_z is the position vector of the stylus tip in the global system; o_{sx} , o_{sy} , and o_{sz} is the position vector of the origin of the stylus coordinate system in the global system; v_{Cx} , v_{Cy} , and v_{Cz} are the position coordinates of the vector between the stylus tip and the origin of the stylus coordinate system; $[R]$ is the cluster to global rotational matrix as described in Appendix B.

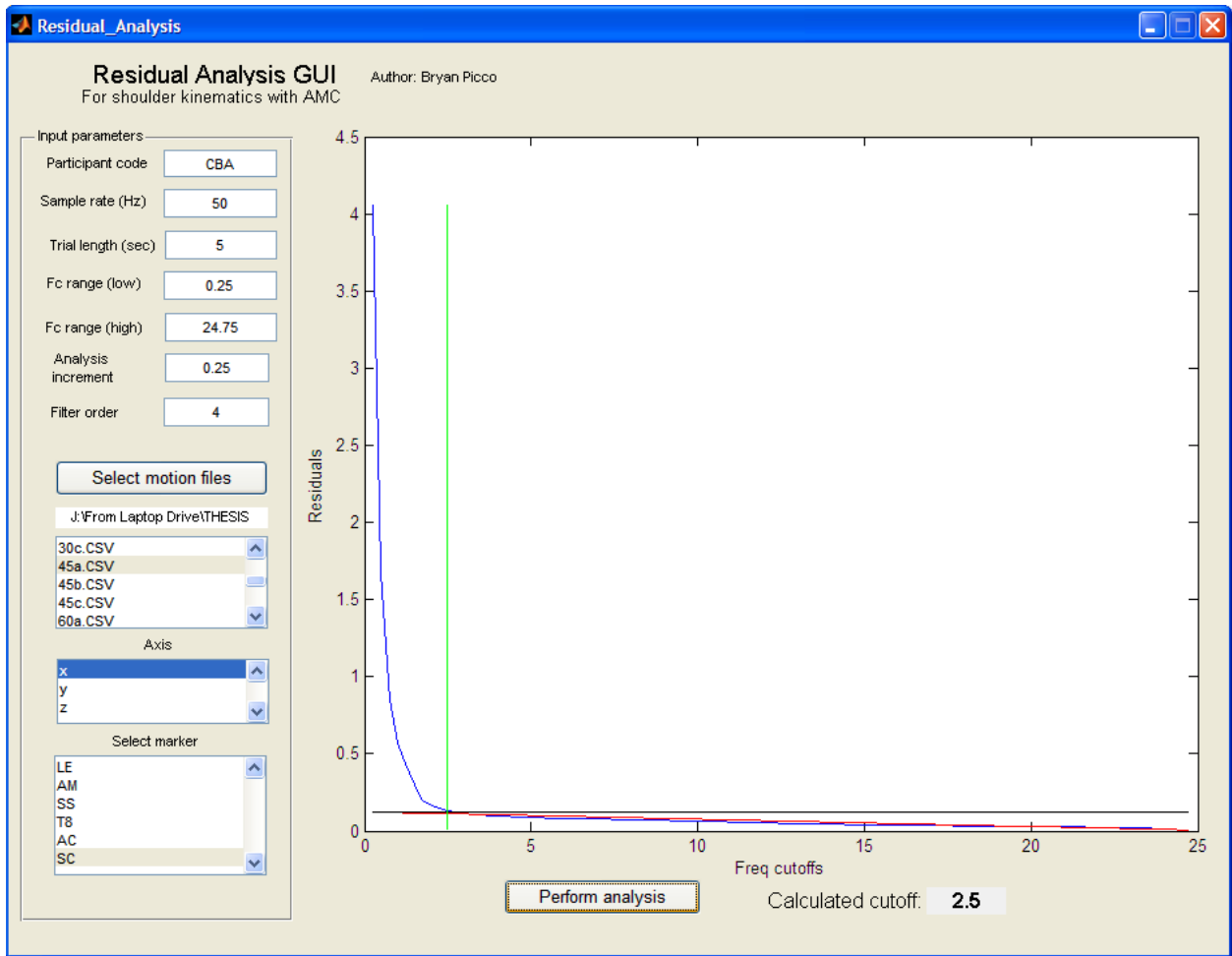


Figure 16: Graphical user interface used to determine participant cut-off frequencies using residual analysis (Winter, 2009)

Static calibration trials were performed to determine the position of the scapular landmarks relative to the acromion marker cluster (ACM) coordinate system and allowed for the scapular plane to be reconstructed in every subsequent recorded frame. The vectors between the digitized AA, IA, RS landmarks and the ACM were calculated by (from Meskers, 1998):

$$\begin{bmatrix} v_{bx} \\ v_{by} \\ v_{bz} \end{bmatrix} = [R]_{cluster}^{GLOBAL} \cdot \begin{bmatrix} b_x - o_{bx} \\ b_y - o_{by} \\ b_z - o_{bz} \end{bmatrix} \quad (2.0)$$

Where v_{bx} , v_{by} , and v_{bz} are the coordinates of the vector between the AMC system and a scapular landmark (AA, IA, or RS); b_x , b_y , and b_z are the global coordinates of the position vector the scapular landmark; o_{sx} , o_{sy} , and o_{sz} are the global coordinates of the position vector of the origin of the AMC system; [R] is the cluster to global rotational matrix as described in Appendix B.

Upper limb joint angle amplitudes were reported at 5° increments of humeral elevation and lowering, beginning and ending at 10° of elevation. Due to the dynamic nature of the task, there was a continuous stream of kinematic data collected throughout the trial and there was no guarantee that the incremental elevation angle outcomes would be explicitly recorded. To correct for this, joint rotational data were averaged across $\pm 1.5^\circ$ of the targeted humeral elevation angle. For example, an elevation trial may produce a continuous stream of thoracohumeral angles of 59.4°, 59.7°, 60.1°, 60.6°, 60.9°, and no angle at exactly 60E. To account for this, all recorded joint rotations at humeral elevation angles between 58.5° and 61.5° were averaged to generate one value for 60E elevation.

Figures 17 through 19 provide an example of the process used to obtain relevant kinematic data for one joint rotation (scapulothoracic tilt) during movement within one plane (OP) repeated twice. First, the relevant humeral elevation angle range had to be identified. Figure 17 demonstrates the complete thoracohumeral elevation range (interrupted line) and the relevant humeral raising range between 10E and 120E (solid line). The frames in which this relevant range occurs were noted. Next, the angle magnitudes occurring over these frames were recorded (Figure 18). This was done for all three trials and the resulting angle profiles were averaged to provide one joint rotation measure for one movement plane (Figure 19).

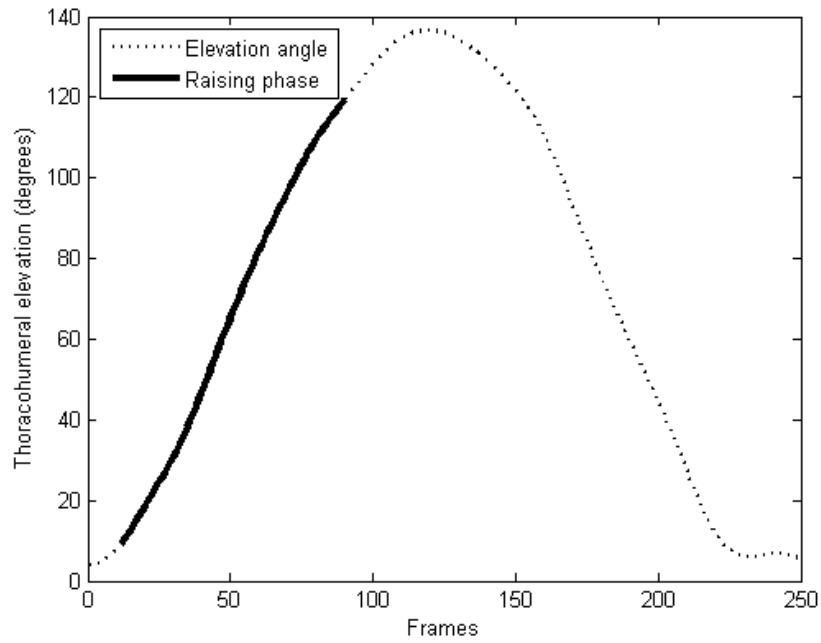


Figure 17: Example thoracohumeral elevation profile (dashed line) used to identify when the humerus was within 10E to 120E humeral elevation (solid line)

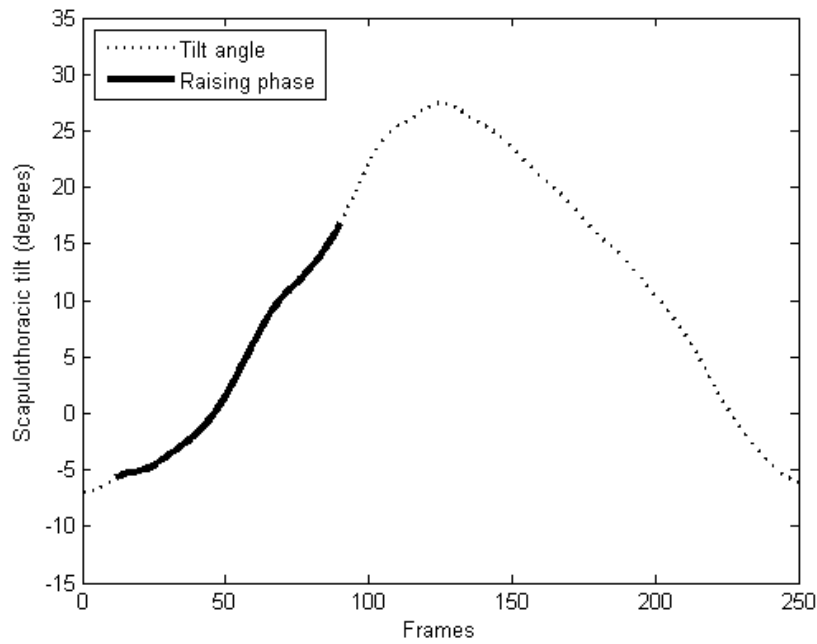


Figure 18: Scapulothoracic tilt profile (dashed line) and range of tilt occurring between 10E and 120E humeral elevation (solid line)

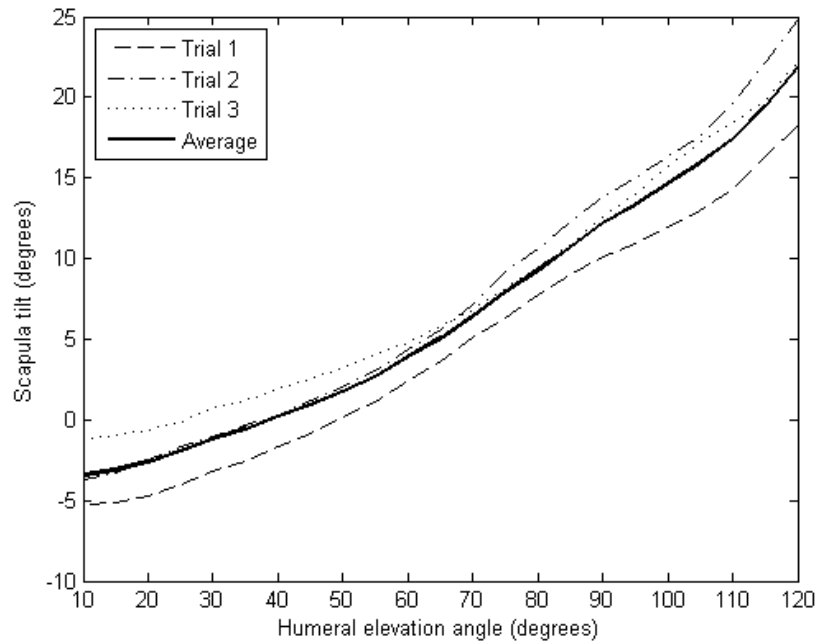


Figure 19: Tracings of the three scapulothoracic tilt measures (interrupted lines) and their computed average (solid line) displayed relative to humeral elevation angle

3.5.3 Joint rotation descriptions

Grood and Suntay’s “Joint Coordinate System” (JCS) method (1983) for describing upper limb joint motion was applied to analyze the SC joint ST interaction and Euler decomposition were used to describe GH joint rotations in adherence to ISB standards found in Wu et al (2005). However, for the SC joint, only clavicle elevation/depression and protraction/retraction were recorded because clavicle axial rotation could not be measured. AC joint descriptions did not adhere to ISB guidelines for the same reason. The JCS method was developed to give clinically relevant meaning to three-dimensional joint rotation descriptions. System axes from the proximal and distal segment are defined as “body-fixed” axes and a common perpendicular to these axes is called the “floating” axis. As a result, the floating axis is constantly altered as the distal segment rotates relative to the proximal segment (Robertson et al.,

2004). Joint rotations were measured as angular projection of the floating axis or an axis from the distal segment on to an axis from the proximal segment. For the ST joint:

$$\alpha = 90 - \cos^{-1}|FA \bullet J| \quad (3.1)$$

$$\beta = -90 - \cos^{-1}|i \bullet K| \quad (3.2)$$

$$\gamma = 90 - \cos^{-1}|FA \bullet j| \quad (3.3)$$

Where α , β , and γ are the angles of scapula protraction(+ve)/retraction(-ve), medial(+ve)/ lateral (-ve) (i.e. upward) rotation, posterior(+ve)/anterior(-ve) tilt respectively; J is an axis at the joint coincident with the positive thorax y-axis. i is an axis at the joint coincident with the positive scapula x-axis; K is an axis coincident with the positive thorax z-axis; FA is the floating axis normal to the body fixed axes (thorax z-axis and scapula x-axis).

For the SC joint, γ could not be calculated accurately because j (clavicle forward-pointing y-axis) is created using the normal to the torso's vertical z-axis and the clavicle laterally directed x-axis. Since the torso's vertical axis was stationary, j could not be accurately determined. However, α and β were calculated using Equations 3.1 and 3.2. They represented clavicle protraction(+ve)/retraction(-ve) and depression(+ve)/ elevation(-ve) respectively. J is an axis at the joint coincident with the positive thorax y-axis; i is an axis at the joint coincident with the positive clavicle x-axis; K is an axis at the joint coincident with the positive thorax z-axis; FA is the floating axis normal to the body fixed axes (thorax z-axis and clavicle x-axis)

Further difficulties were present for AC joint motion calculations because no vertical clavicle z-axis was discernible. As a result, an attempt was made to modify the AC joint description described in Wu et al. (2005). The FA used for AC joint rotation in the current study was created using the normal to the long axis of the clavicle pointed towards the thorax and the scapular vertical z-axis. This allowed for α (acromion protraction(+ve)/retraction(-ve)) and β (acromion depression(+ve)/ elevation(-ve)) to be calculated using equations 3.1 and 3.2. J

represents the scapula's forward pointing y-axis, i represents the long axis of the clavicle pointing towards the torso, and K represents the vertical z-axis of the scapula.

GH joint descriptions were based on a Z-Y-Z Euler rotation sequence (Wu et al., 2005):

$$\begin{bmatrix} s_x \\ s_y \\ s_z \end{bmatrix} = (R_z(\gamma_h) \cdot R_y(\beta_h) \cdot R_z(\alpha_h)) \cdot \begin{bmatrix} h_x \\ h_y \\ h_z \end{bmatrix} \quad (4.0)$$

where α_h , β_h , and γ_h are the GH plane of elevation about the scapula z-axis, GH elevation about the humerus y-axis, and axial rotation about humerus z-axis respectively. Decomposition and rotational transformation matrices for equation 4.0 are found in Appendix B. A graphical user interface (Figure 20) was created in Matlab to view outputted ST and GH angle measurements to ensure that neither system became indeterminate and entered Gimbal Lock.

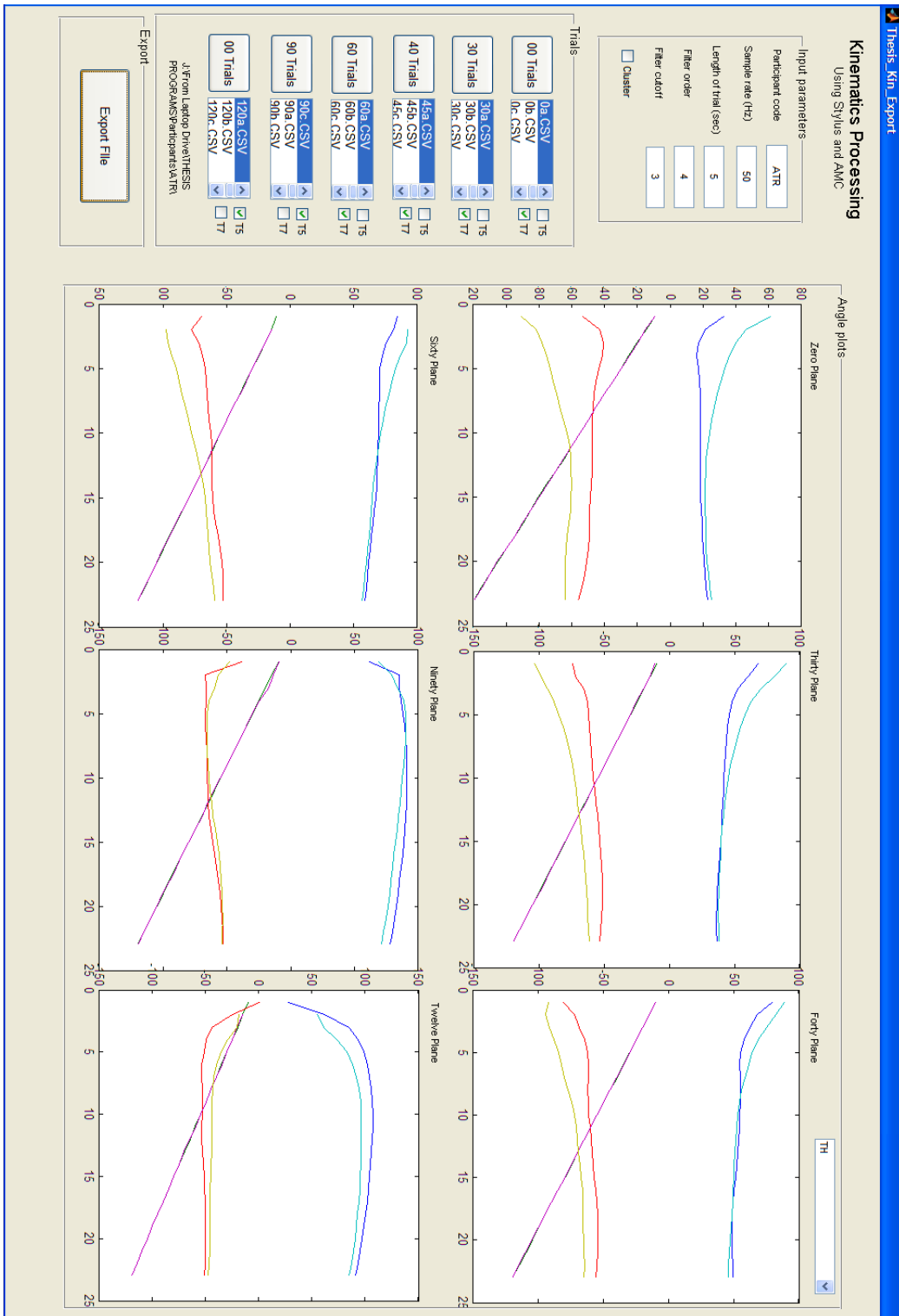


Figure 20: Graphical user interface used to screen outputted joint kinematics for potential abnormalities.

3.6 *Statistical analysis*

3.6.1 *Intra-class correlation coefficient (ICC)*

Intra-class correlation coefficient (ICC – Type 3,1) was used to determine trial-to- trial consistency (Shrout & Fleiss, 1979; Weir, 2005) of each participant’s joint motions. This resulted in a collection of ten ICCs (i.e. one for every measured rotation) per measured movement plane for a total of 60 ICCs per participant. These data were then averaged across participants in two ways. First ICCs were averaged across plane and across individuals to produce ten overall joint rotational ICCs. The second method had ICCs averaged within plane and then across individuals to produce one ICC per plane. Absolute maximum and minimum recorded ICCs were determined, along with variability indicated by (standard deviation)

3.6.2 *Kinematic profiles*

All joint three-dimensional rotations were presented graphically relative to humeral elevation angle at 5° increments with variability provided. Between each increment, linear interpolation was performed. Standard deviation was chosen over standard error because the demonstration of high kinematic variability was to be emphasized. Presenting standard error would have given the perception that the profiles were more reliable, due to the higher sample size. Sixty plots were generated for each motion phase (ten joint rotations x six movement planes). Profiles included both male and female data.

3.6.3 *Variability summary*

Joint rotation variability at every increment of humeral elevation (indicated by standard deviation from the kinematic profiles) was averaged across each movement plane and presented in a stacked bar graph. This gave the reader an indication of how the variation of certain joint rotations changed over the range of humeral elevation measured. A second stacked bar graph of

the joint rotational variability averaged within each plane was provided to give an overall indication of which movement plane resulted in the highest joint motion variability.

3.6.4 Analysis of variance (ANOVA)

Ten separate 4-way mixed model analysis of variance (ANOVA) were used to test the effects of the independent variables (plane of elevation, elevation angle, motion phase of and gender) on the ten measured joint. To allow for independent comparisons of humeral motion, only eight levels of humeral elevation were tested: 15E, 30E, 45E, 60E, 75E, 90E, 105E, and 120E. Statistical significance was considered at $\alpha = 0.05$. When interaction effects were present, Tukey HSD was used post hoc to compare individual factor means.

4. RESULTS

Participant trial-to-trial movement consistency was found to be moderate to high and significant movement plane, humeral elevation angle, phase, and their interactions effects were present for the majority of averaged joint rotations. Repeatability of the joint motion ranges between 0.658 and 0.999 when rotational ICCs are averaged across tested movement planes. When ICCs are averaged within movement planes, repeatability ranged between 0.822 and 0.852. Observable changes in kinematic profiles due to humeral elevation angle and movement plane are more prominent than changes due to elevation phase. Glenohumeral elevation displays largest overall range of motion (73.32° , 120P, raising phase). The smallest range of motion is seen in scapular posterior/anterior tilt (2.44° , 30P, raising phase). Significant main effects of humeral movement plane, elevation angle, elevation phase are seen for the majority of measured joint rotations; at least one main effect interaction is seen for all measured joint rotations. Finally, most cumulative kinematic variability is evident at lower humeral elevation angles.

5.1 Intra-class Correlation Coefficients

Mean three-dimension upper limb joint rotation ICCs varied from moderate (0.597) to high (0.999). Mean, maximum and minimum ICCs for the measured rotations organized by tested movement plane are presented in Table C6 in Appendix C. Each mean in Table C6 is an average across all participants and both movement phases while each maximum and minimum are individual values. Glenohumeral elevation, glenohumeral internal/external rotation, humeral elevation, clavicle elevation/depression, and scapular protraction/retraction all had ICCs of greater than 0.90 regardless of movement plane. Glenohumeral movement plane, acromioclavicular protraction/retraction, and humeral internal/external rotation had ICCs of less

than 0.80 regardless of movement plane. Individual ICCs ranged between 0.000 (acromioclavicular elevation – 120 plane) to 0.999 (multiple rotation-plane combinations).

Similar results to the mean ICCs for the measured rotations are seen when these means are averaged across humeral movement plane; however, there is little difference between overall joint rotation ICCs within each humeral movement plane. Glenohumeral elevation, glenohumeral internal/external rotation, humeral elevation, clavicle elevation/depression, and scapular protraction/retraction ICCs remain greater than 0.90 (see Table 5). However, when rotations are averaged across humeral movement plane, glenohumeral movement plane, acromioclavicular protraction/retraction, and humeral internal/external rotation had ICCs of less than 0.70. When all rotations are averaged within a humeral movement plane, there is little difference between resultant ICCs (see Table 6).

Table 5: Overall ICCs for each rotation. Each mean ICC represents the average within-rotation mean ICCs displayed in Table C6

| Rotation | Mean ICC | STD |
|-----------------|-----------------|------------|
| GLE | 0.999 | 0.004 |
| CED | 0.959 | 0.046 |
| GIE | 0.924 | 0.059 |
| SPR | 0.935 | 0.049 |
| SPA | 0.918 | 0.071 |
| CPR | 0.814 | 0.019 |
| AED | 0.808 | 0.042 |
| SML | 0.744 | 0.019 |
| APR | 0.693 | 0.043 |
| GAP | 0.658 | 0.021 |

Table 6: Overall ICCs for each plane of humeral elevation. Each mean ICC represents the average within-plane mean ICCs displayed in Table C6

| Plane | Mean ICC | STD |
|--------------|-----------------|------------|
| 0° | 0.828 | 0.139 |
| 30° | 0.830 | 0.149 |
| Scapular | 0.838 | 0.147 |
| 60° | 0.825 | 0.130 |
| 90° | 0.852 | 0.108 |
| 120° | 0.822 | 0.114 |

4.2 Descriptive Statistics and motion profiles

4.2.1 Scapulothoracic Kinematics

There was a tendency for the scapula to protract as the humerus is elevated; however at high humeral elevation angles there was a small scapula protraction reduction relative to the thorax. At rest (10° elevation angle), the participants' scapula was protracted. Range of motion (ROM) was marginal for the movement planes from 0P through to 60P, with a maximum range of 4.14° for these respective planes. Protraction ROM increased more substantially for the remaining movement planes, with a maximum 18.87° ROM seen in the 120P. Movement phase had very little effect on ROM. Scapulothoracic kinematics descriptive statistics are seen in Table C1 in Appendix C. Scapulothoracic +protraction/-retraction (SPR) motion profiles with variability for the raising phase are shown in Figure 21 below while the lowering phase profiles can be found in Figure D1 in Appendix D.

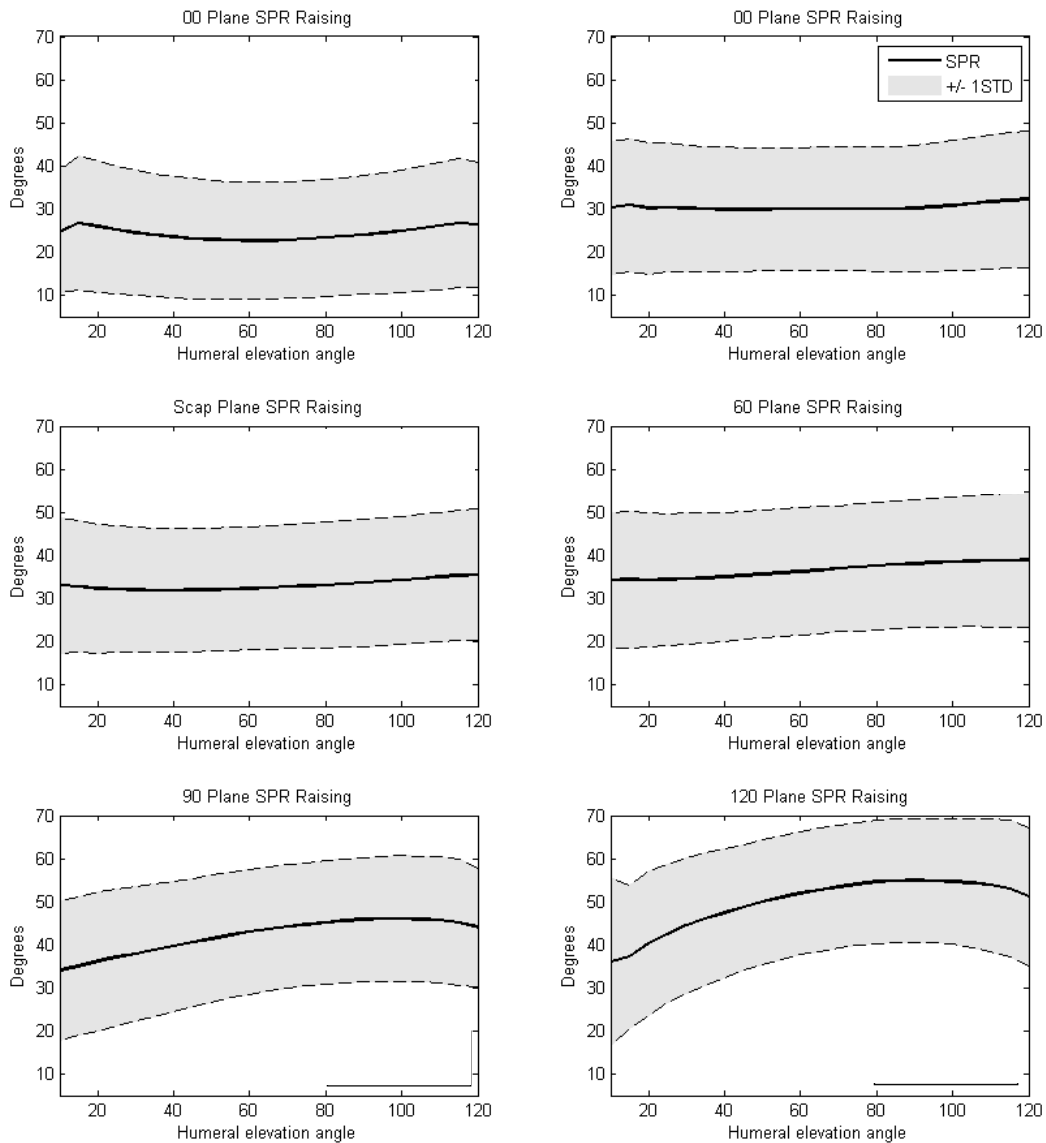


Figure 21: Mean scapular +protraction/-retraction (SPR) kinematic profiles, with +/- one standard deviation, for the six tested vertical planes – raising phase

As the humerus elevated, the scapula laterally rotated upwards. Overall scapulothoracic rhythm was -3.13 (SD 0.37) and -3.33 (SD 0.52) for raising and lowering phases respectively (a complete list of the scapulothoracic rhythm organized by plane can be found in Table C2 in Appendix C). Scapula lateral rotation ROM decreased marginally as the movement plane changes from the 0P plane across to the 120P plane (36.71° to 32.70° respectively), and phase

changes were subtle. Scapulothoracic +medial/-lateral (SML) rotation motion profiles for the raising phase are shown in Figure 22 below while the lowering phase profiles are seen in Figure D2 in Appendix D.

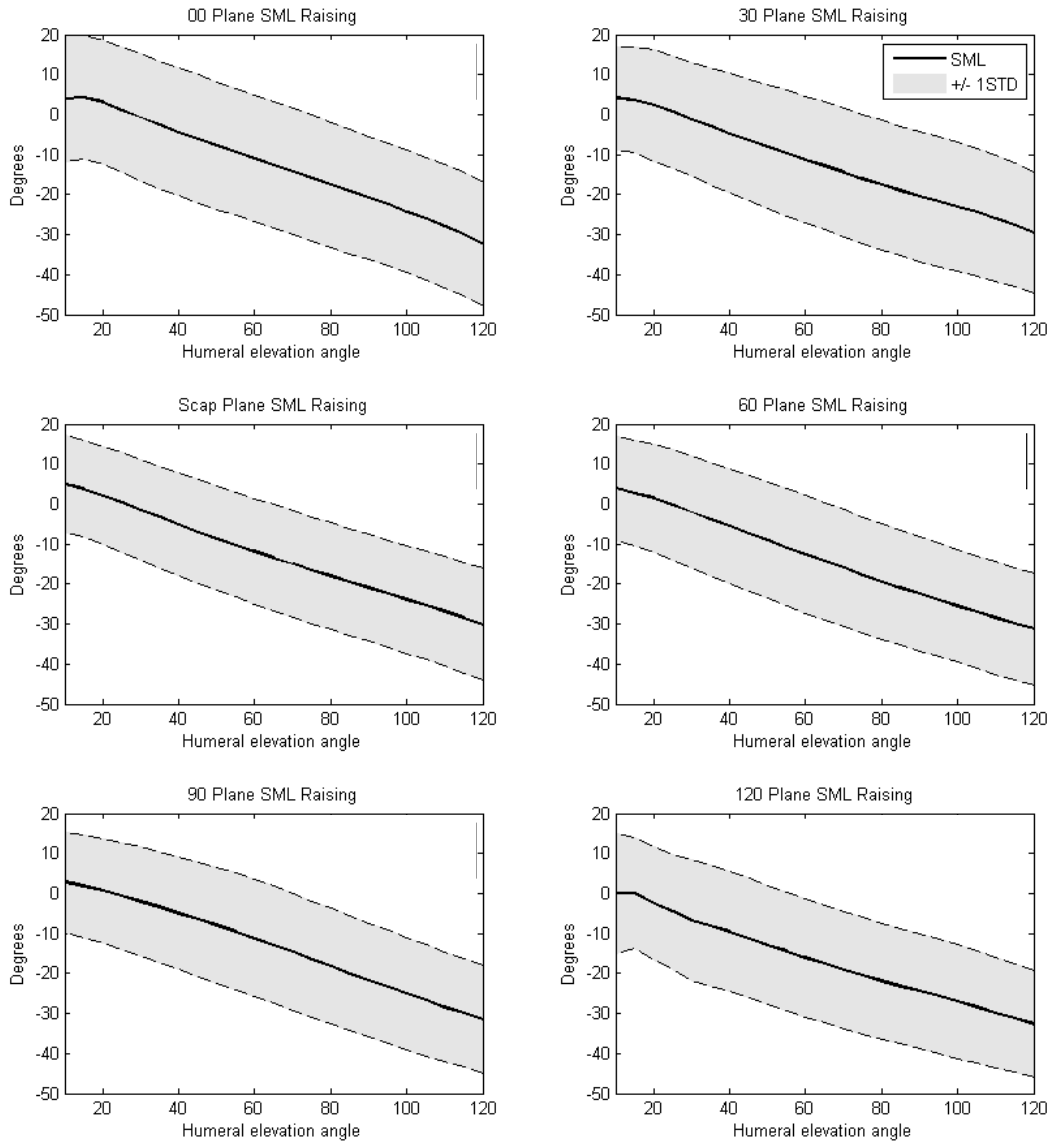


Figure 22: Mean scapulothoracic +medial/-lateral rotation (SML) kinematic profiles, with +/- one standard deviation, for the six tested vertical planes – raising phase

The scapula tilted posteriorly relative to the thorax as the humerus elevated in all tested movement planes. At rest, the scapula tended to be anteriorly titled. Tilting ROM increases as the movement plane changes from the 0P across to the 120P (7.62° to 11.92° respectively). Also, there is a small reduction in tilting ROM during lowering phases compared to the raising phase in the 0P, 30P, and SCAP. An increase in the ROM for the remaining movement planes was found. Scapulothoracic +posterior/-anterior tilt motion profiles for the raising phase are shown in Figure 23 below while the lowering phase profiles are seen in Figure D3 in Appendix D.

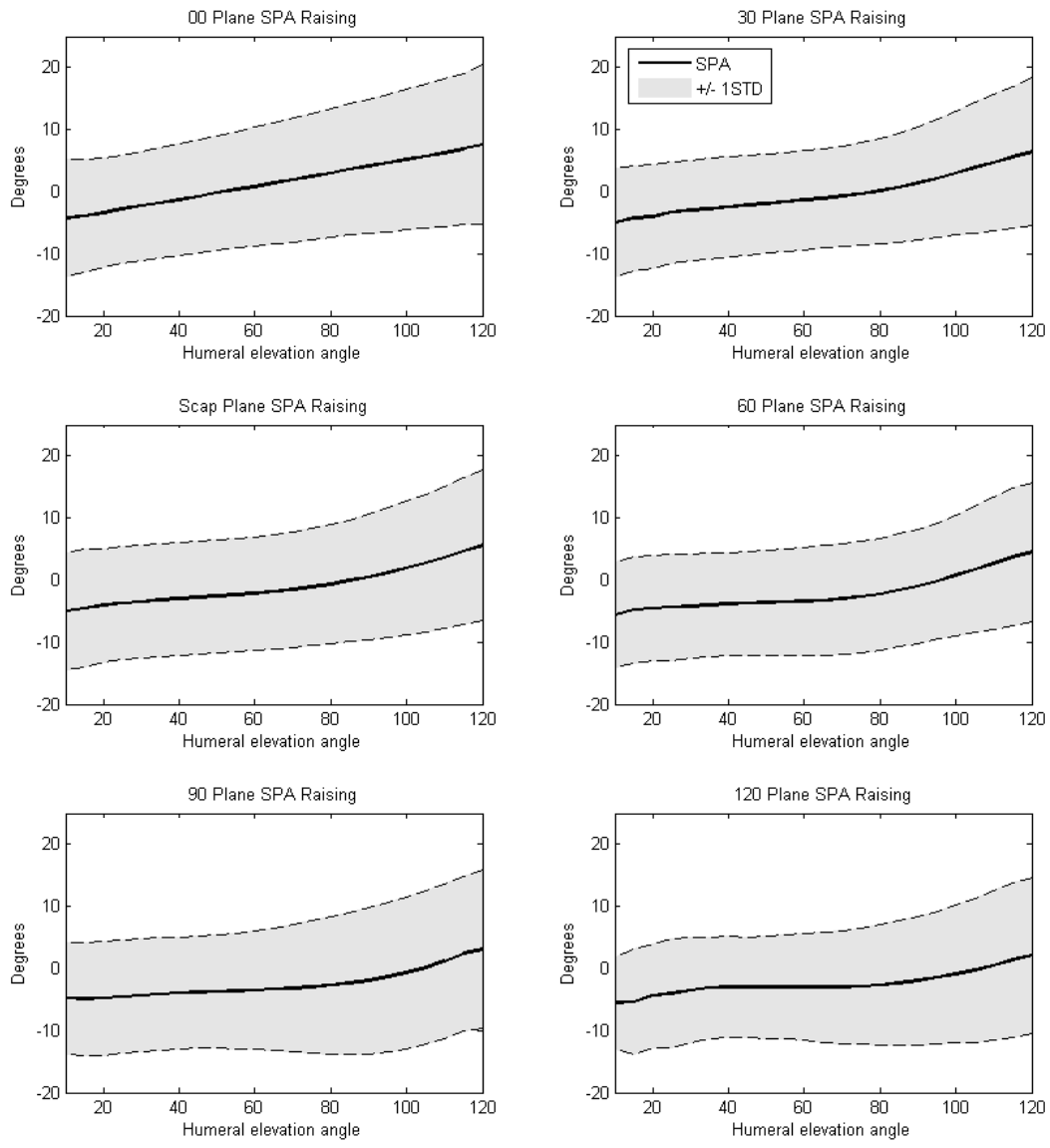


Figure 23: Mean scapulothoracic +posterior/-anterior (SPA) tilt kinematic profiles, with +/- one standard deviation, for the six tested vertical planes – raising phase

4.2.2 *Glenohumeral Kinematics*

Glenohumeral motion plane (GAP) profiles and ROM were influenced by the plane of humeral elevation. At elevation angles below 60°, there are no consistent trends across movement planes. However, as the humerus moves elevates to the end of the movement (for the raising phase; start of the movement for the lowering phase), GAP tended to return to the magnitude observed at the start of the movement for the raising phase (i.e. end of movement for lowering phase). Glenohumeral plane ROM increased substantially movement plane was modified from 0P across to 120P (18.07° to 35.16° respectively). The lowering phase produced glenohumeral plane reductions for movement planes past the SCAP. Glenohumeral kinematics descriptive statistics are seen in Table C3 in Appendix C. Glenohumeral +anterior/-posterior plane motion profiles with variability for the raising phase are shown in Figure 24 below while the lowering phase profiles are seen in Figure D4 in Appendix D.

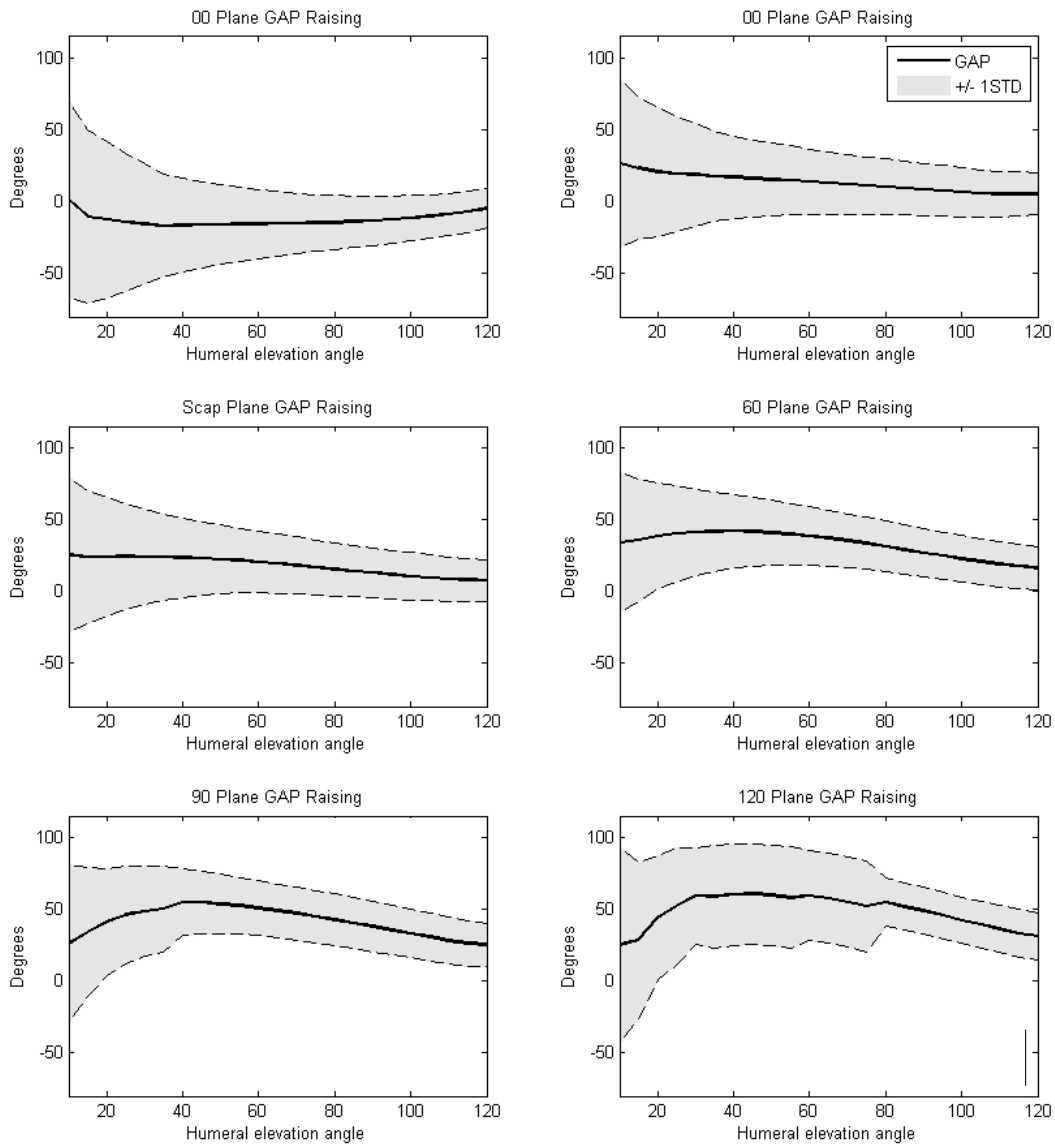


Figure 24: Mean glenohumeral +anterior/-posterior elevation plane (GAP) kinematic profiles, with +/- one standard deviation, for the six tested vertical planes – raising phase

There was a direct linear relationship between glenohumeral and humeral elevation angles. Glenohumeral elevation (GLE) ROM varied between 68.33° and 73.32° across humeral movement planes, with no specific trends between them. The phase of humeral motion did not affect glenohumeral elevation in a consistent matter. Glenohumeral -elevation motion profiles

with variability for the raising phase are shown in Figure 25 below while the lowering phase profiles are seen in Figure D5 in Appendix D.

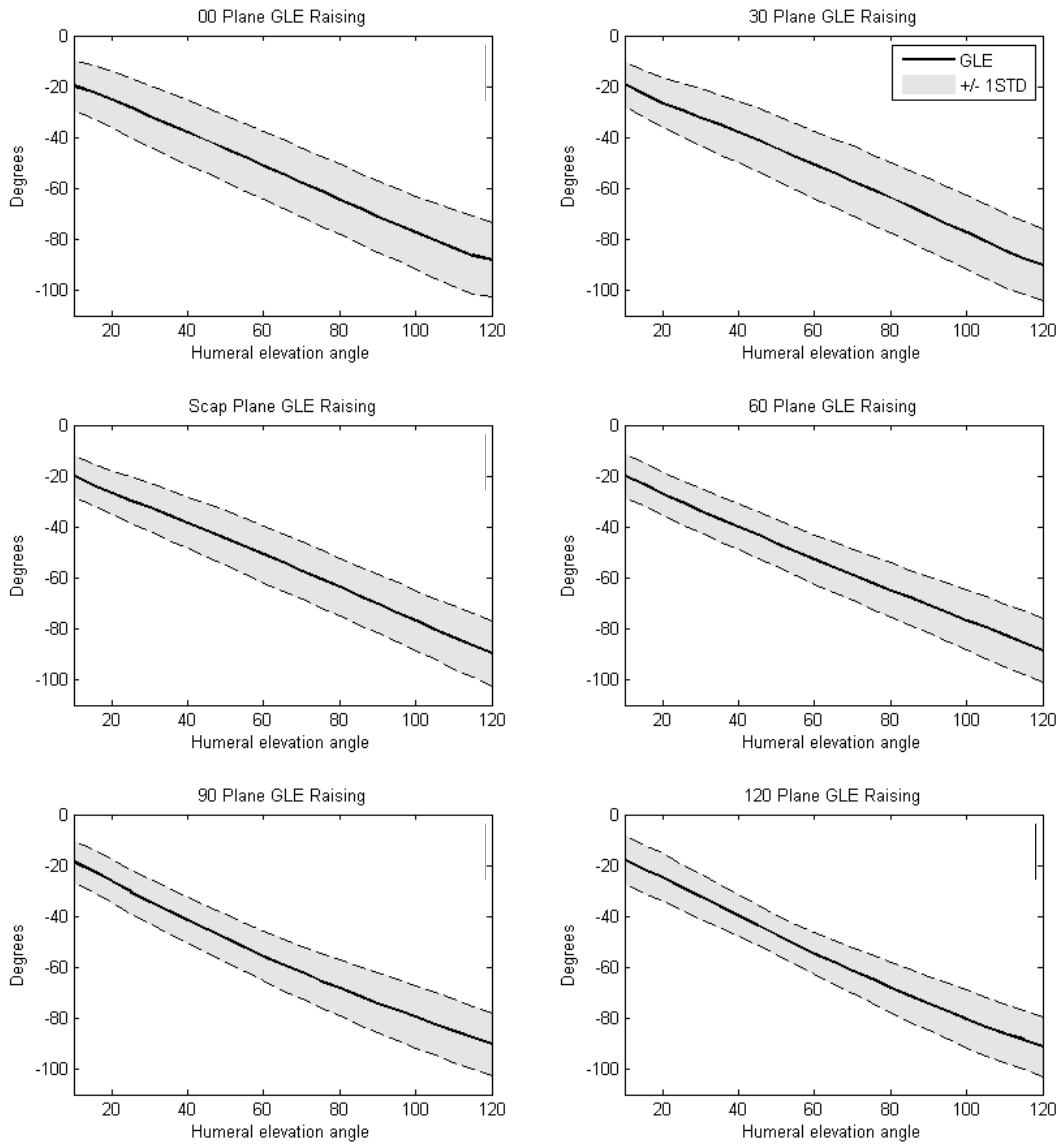


Figure 25: Mean glenohumeral -elevation (GLE) kinematic profiles, with +/- one standard deviation, for the six tested vertical planes – raising phase

Both plane of humeral elevation and motion phase influenced the glenohumeral internal/external rotation motion profiles. Glenohumeral external rotation ROM increased as movement plane was modified from the 0 plane across to the 120 plane for both phases of motion (10.01° to 37.06° for the raising phase; 6.94° to 43.56° for the lowering phase). Generally, as the humerus was at 60° of elevation or below for both phases, the humerus externally rotated on the glenoid. At humeral elevation angles above 60°, the humerus generally internally rotated. Also, as humeral movement plane was varied from 0P to 120 P, the humerus was progressively more internally rotated at the start of the recorded humeral motion. Glenohumeral +internal/-external rotation motion profiles with variability for the raising phase are shown in Figure 26 below while the lowering phase profiles are seen in Figure D6 in Appendix D.

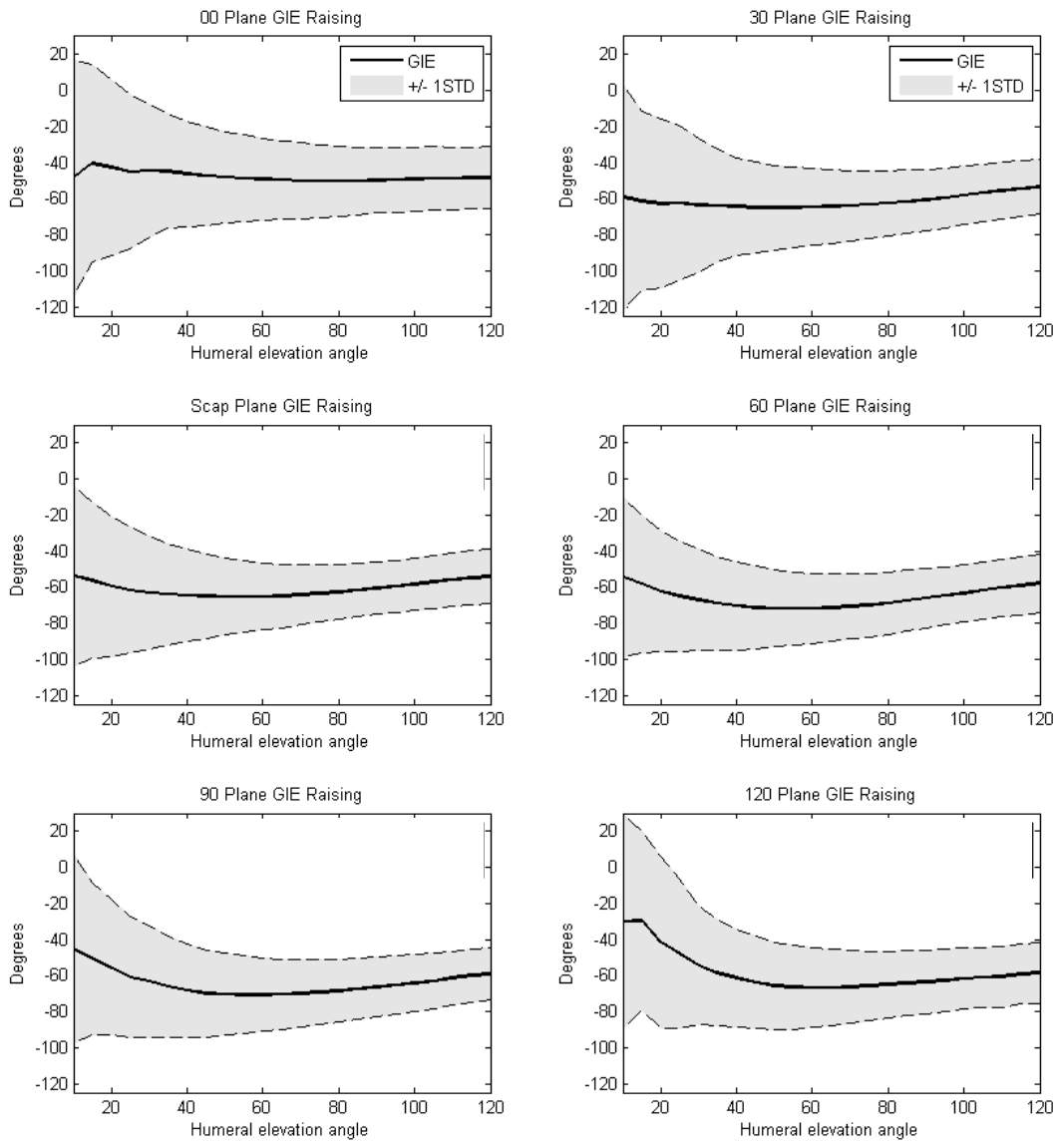


Figure 26: Mean glenohumeral -internal/+external rotation (GIE) kinematic profiles, with +/- one standard deviation, for the six tested vertical planes – raising phase

4.2.3 *Acromioclavicular Kinematics*

As the humerus elevated in the examined movement planes, the acromion first retracts relative to the clavicle at elevation angles approximately below 40° and then protracts for the remainder of the motion. For all tested humeral elevation angles and planes, the acromion was protracted. For the raising phase, the total ROM increased within the tested planes as participants movement planes progressed in order from 0P to 120P (6.38° to 12.98° respectively). More acromioclavicular retraction accounted for this increase in ROM. For the lowering phase, this trend of increasing ROM stopped at 90P (6.29° to 10.86°). Acromioclavicular kinematics descriptive statistics are seen in Table C4 in Appendix C. Acromioclavicular +protraction/-retraction motion profiles with variability for the raising phase are shown in Figure 27 below while the lowering phase profiles are seen in Figure D7 in Appendix D.

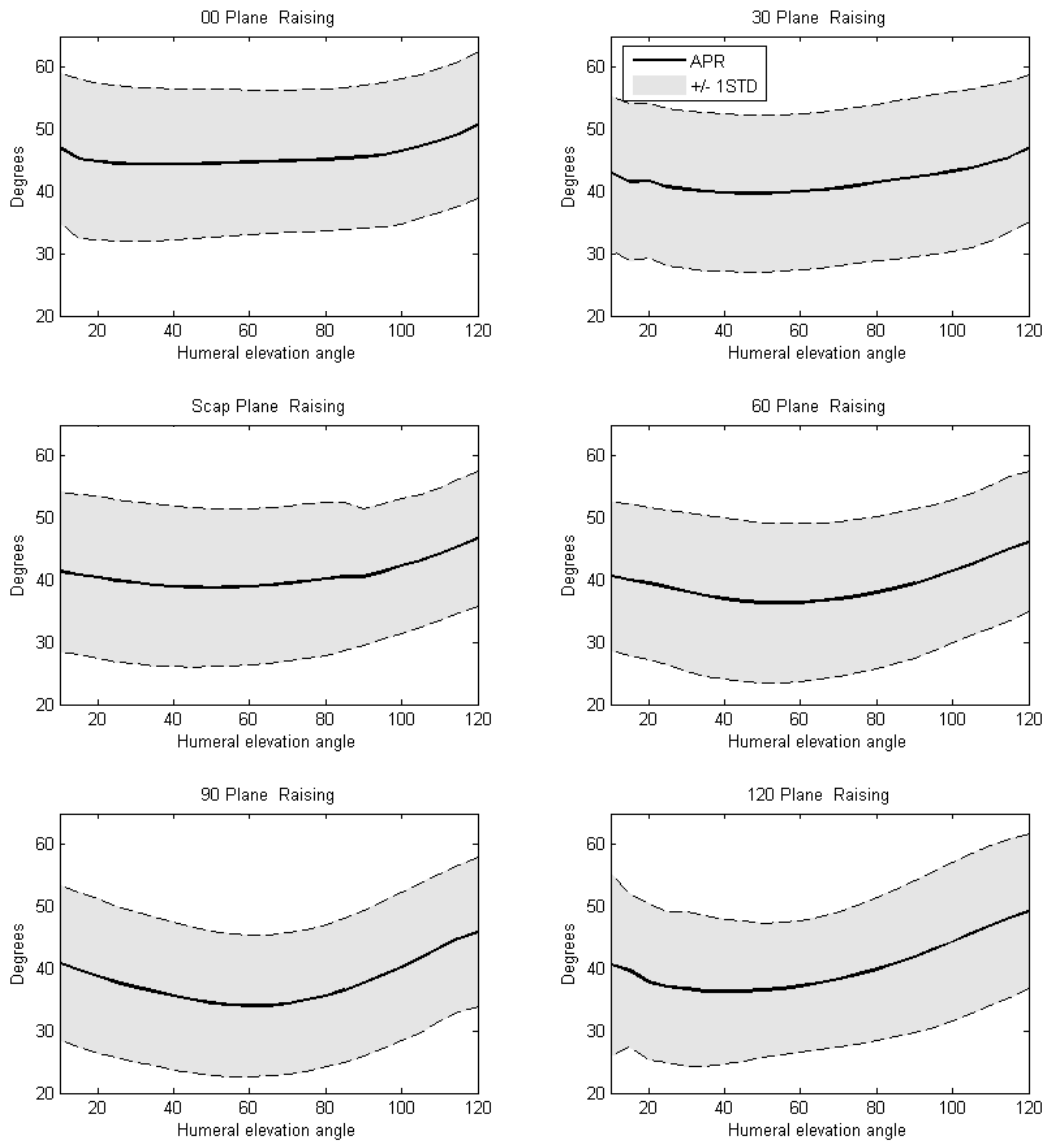


Figure 27: Mean acromioclavicular +protraction/-retraction (APR) kinematic profiles, with +/- one standard deviation, for the six tested vertical planes – raising phase.

Overall, the acromion elevated relative to the clavicle as the humerus elevated within the tested movement planes. Most acromion elevation occurred above 60° degrees of humeral elevation. As humeral movement planes progressed from abduction (0P) to 120P, ROM increased (12.26° to 21.13°). Acromioclavicular +elevation/-depression motion profiles with

variability for the raising phase are shown in Figure 28 below while the lowering phase profiles are seen in Figure D8 in Appendix D.

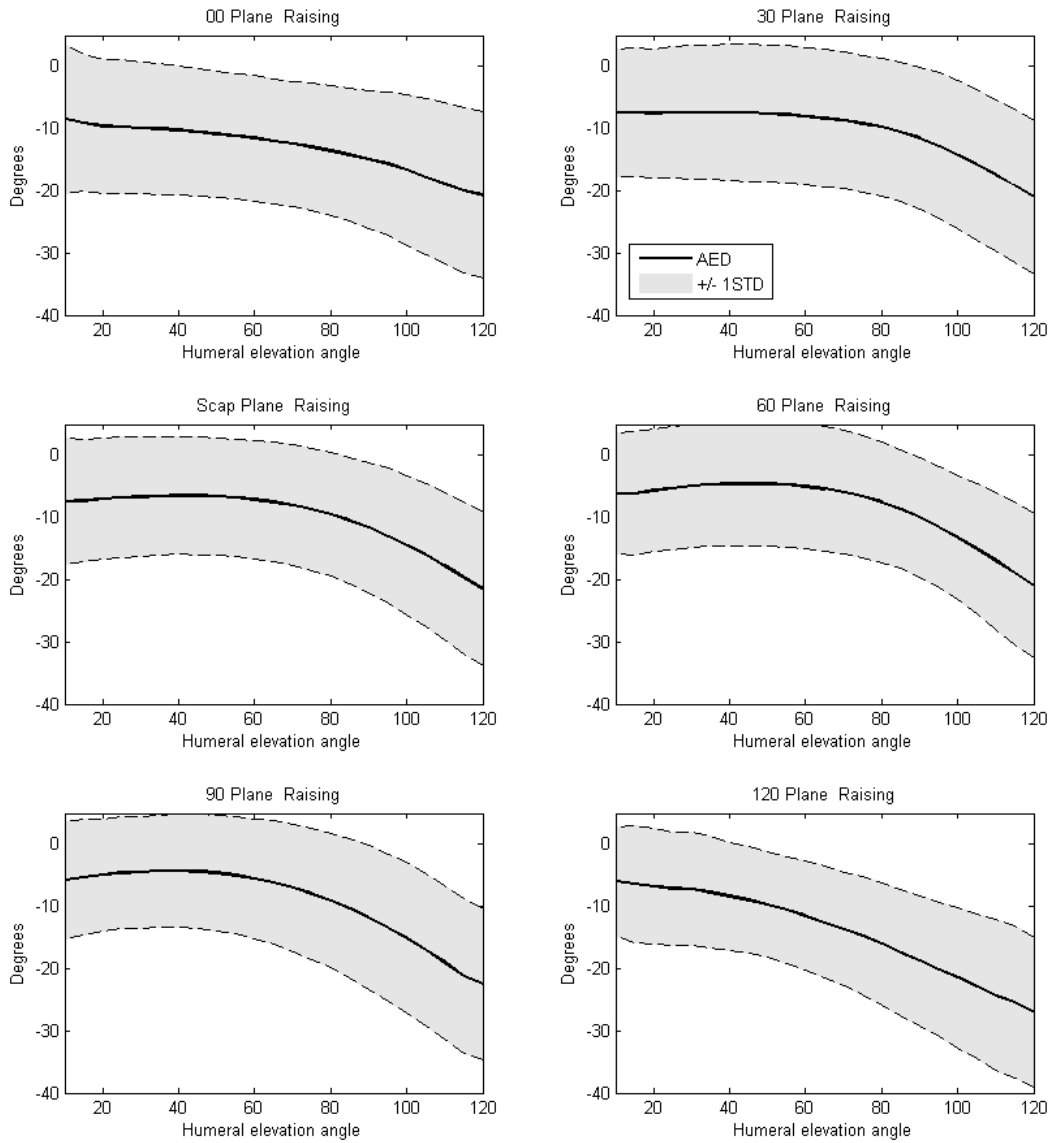


Figure 28: Mean acromioclavicular –elevation/+depression (AED) kinematic profiles, with +/- one standard deviation, for the six tested vertical planes – raising phase.

4.2.4 *Sternoclavicular Kinematics*

As the humerus was elevated, the clavicle retracted relative to the sternum in all examined planes except the 120P where protraction occurred at lower elevation angles. These motion trends also existed for the lowering phase in a reversing trend. ROM changes due to humeral movement plane changes were marginal for both phases of motion (1.37° maximal difference for the raising phase; 1.4° maximal difference for the lowering phase). There was a subtle decrease in ROM in the lowering phase across all tested movement planes. Sternoclavicular +protraction/-retraction motion profiles with variability for the raising phase are shown in Figure 29 below while the lowering phase profiles are seen in Figure D9 in Appendix D. Sternoclavicular kinematics descriptive statistics are seen in Table C5 in Appendix C.

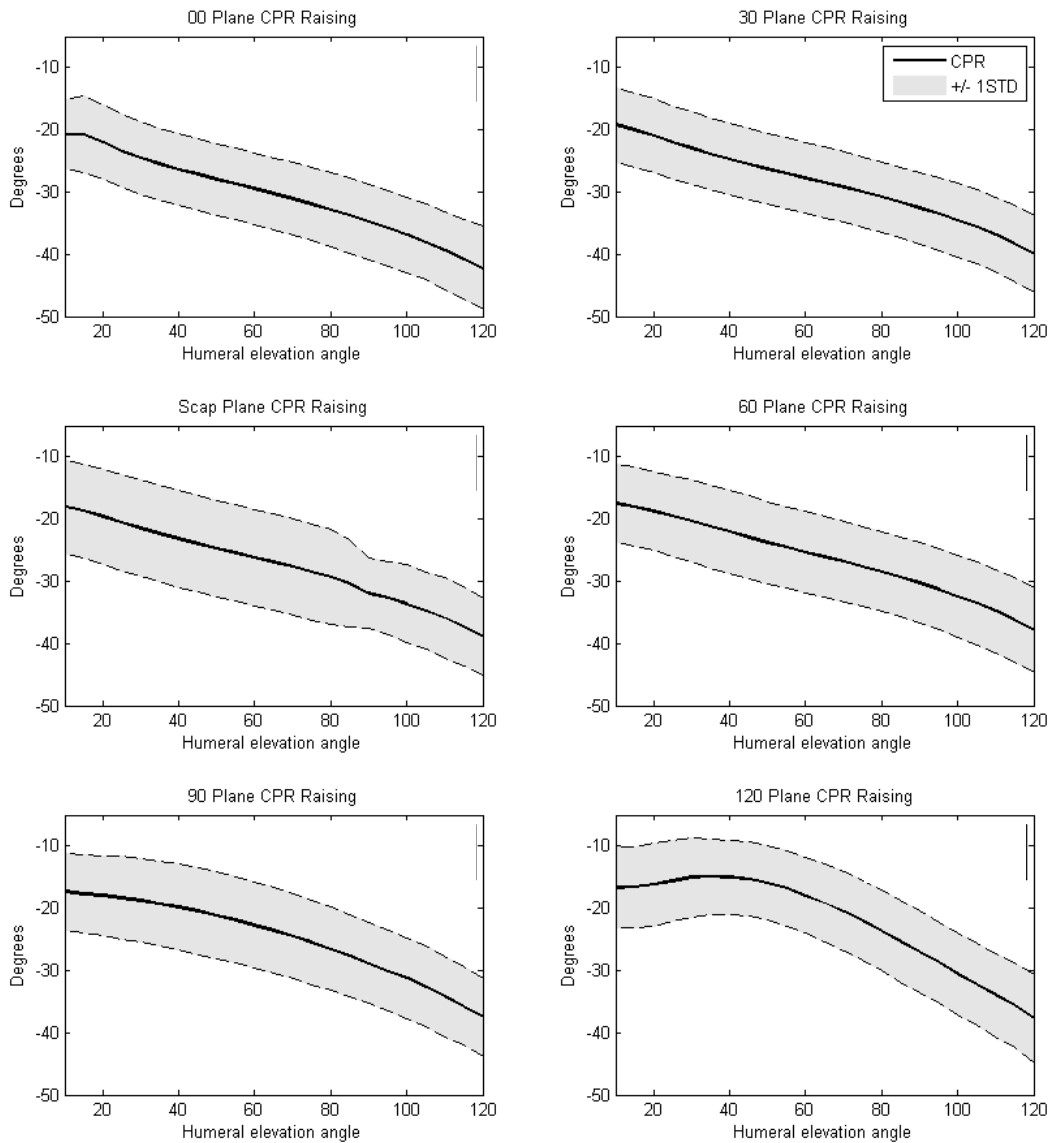


Figure 29: Mean sternoclavicular +protraction/-retraction (CPR) kinematic profiles, with +/- one standard deviation, for the six tested vertical planes – raising phase

Overall, the clavicle was elevated relative to the sternum when the humerus was elevated away from the torso for both motion phases. However, this relationship was less direct during the lowering phase, as evident by comparing the motion profiles for each phase in Figures 28 and D9 in Appendix D. ROM for 30P, SCAP, 60P, and 90P were very similar for both phases as indicated in Table C5 in Appendix C (0.62° maximal difference for the raising phase within

these movement planes; 0.76° maximal difference for the lowering phase). Sternoclavicular -elevation/+depression motion profiles with variability for the raising phase are shown in Figure 30 below while the lowering phase profiles are seen in Figure D10 in Appendix D.

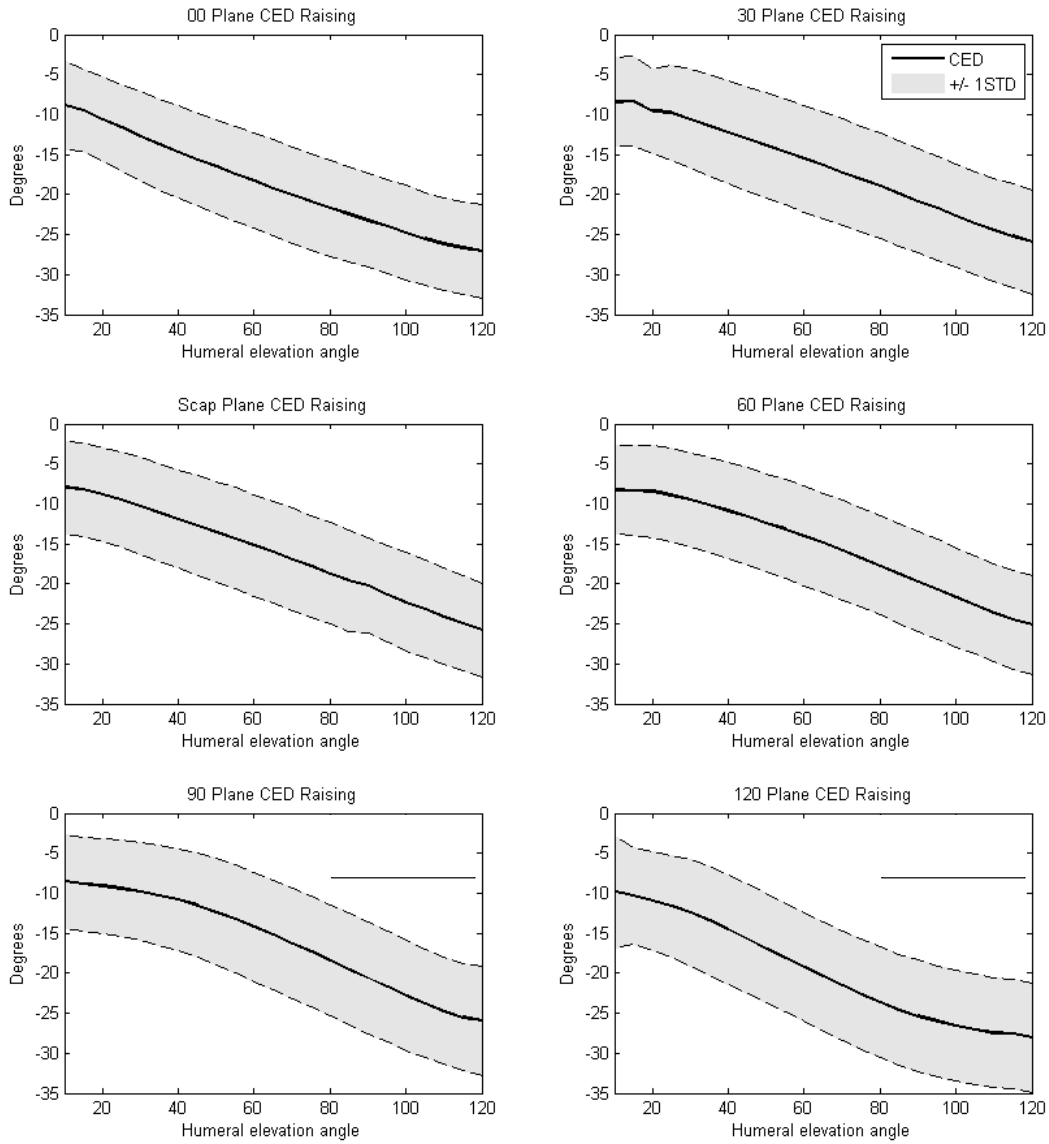


Figure 30: Mean sternoclavicular -elevation/+depression (CED) kinematic profiles, with +/- one standard deviation, for the six tested vertical planes – raising phase.

4.3 Analysis of Variance (ANOVA)

4.3.1 Scapulothoracic Kinematics

There was a main effect of humeral movement plane ($p < 0.0001$), angle ($p < 0.0001$), and phase ($p < 0.0001$) on right scapulothoracic +protraction/-retraction (SPR), +medial/-lateral rotation (SML), and +posterior/-anterior tilt (SPA). An interaction effect of sex and plane was present for all three ST rotations ($p < 0.0355$, $p = 0.0001$, and $p = 0.0001$ for SPR, SML, and SPA respectively). Sex-elevation angle and movement plane-elevation angle interaction effects occurred for SPR ($p < 0.0001$; $p < 0.0001$) and SPA ($p < 0.0001$; $p < 0.0001$). An interaction effect of sex and phase was present for SPR ($p = 0.0277$) and SML rotations ($p < 0.0001$). Finally, a plane-phase interaction existed for SPA ($p < 0.0001$) and SML ($p = 0.0012$). A summary of the main effects and interactions with F-statistics and p -values for scapulothoracic kinematics is provided in Tables F1 through F3 in Appendix F.

As movement plane was modified progressively across the body from 0P to 120P, overall least square mean (LSM) scapular protraction (SPR) increased significantly for each plane (23.93° for 0P to 48.72° for 120P). As humeral elevation angle increased, scapular protraction increased. Higher humeral elevation angles 90E, 105E, and 120E displayed statistically the same amount of protraction (36.94° , 37.52° and 37.75° respectively), while 15E had significantly lower scapular protraction (32.21°) than all other elevation angles. Additionally, the raising phase displayed significantly more scapular protraction (36.15°) than the lowering phase (34.66°). Plots of interaction effects indicating the results of post-hoc Tukey HSD for scapulothoracic kinematics are provided in Figures 31 through 36 below, with the exception SPR sex-humeral elevation and movement plane-elevation angle interactions. These interactions are displayed in Tables 5 and 6.

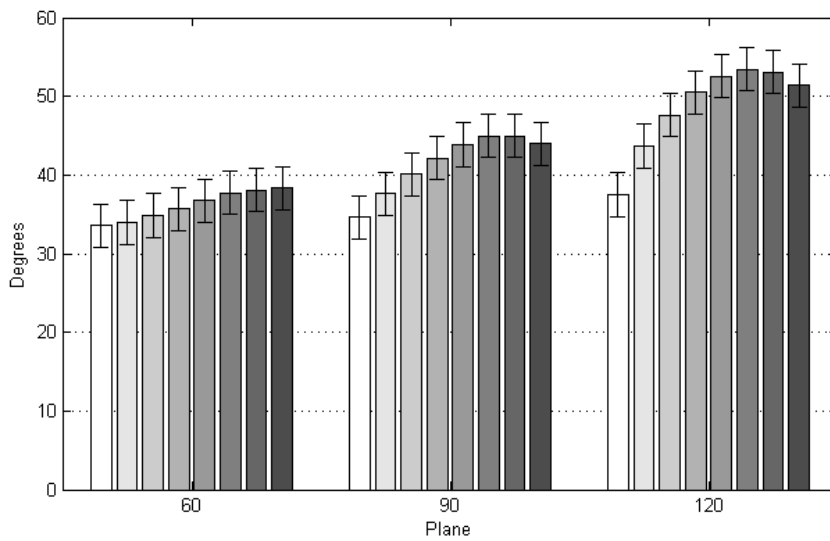
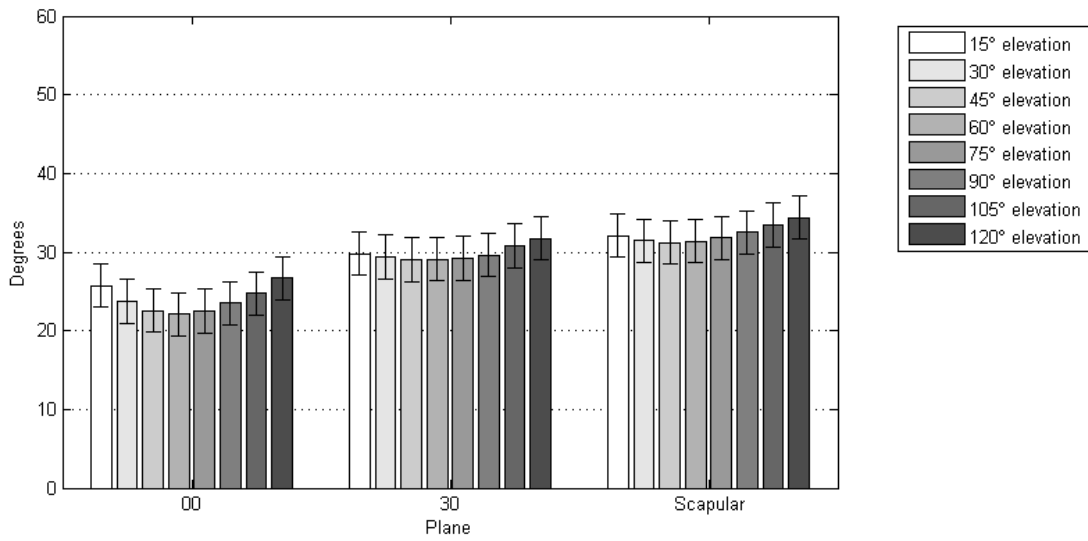


Figure 31: Interaction effects of humeral movement plane and elevation angle on least squares mean (LSM) right scapulothoracic +protraction/-retraction (SPR)

Table 6: Interaction effects of movement plane and humeral elevation angle on least squares mean (LSM) scapulothoracic +protraction/-retraction. For plane, 1 = 0° plane; 2 = 30° plane; 3 = scapular plane; 4 = 60° plane; 5 = 90° plane; 6 = 120° plane. Levels not connected by same letter are significantly different (*p*-value: 0.05)

| Level | LSM |
|-------|---------------------|
| 6,90 | A 53.42 |
| 6,105 | A 53.06 |
| 6,75 | A 52.57 |
| 6,120 | A 51.36 |
| 6,60 | A B 50.52 |
| 6,45 | B C 47.63 |
| 5,105 | C D 44.99 |
| 5,90 | C D 44.94 |
| 5,120 | D 43.99 |
| 5,75 | D 43.87 |
| 6,30 | D 43.68 |
| 5,60 | D E 42.16 |
| 5,45 | E F 40.07 |
| 4,120 | F G 38.33 |
| 4,105 | F G 38.11 |
| 4,90 | F G H 37.70 |
| 5,30 | F G H 37.64 |
| 6,15 | F G H I 37.51 |
| 4,75 | G H I J 36.73 |
| 4,60 | G H I J K 35.65 |
| 4,45 | H I J K L 34.83 |
| 5,15 | H I J K L M 34.60 |
| 3,120 | I J K L M N 34.40 |
| 4,30 | J K L M N O 33.99 |
| 4,15 | K L M N O P 33.57 |
| 3,105 | K L M N O P 33.43 |
| 3,90 | L M N O P Q 32.51 |
| 3,15 | L M N O P Q R 32.09 |
| 3,75 | L M N O P Q R 31.81 |
| 2,120 | M N O P Q R 31.73 |
| 3,30 | N O P Q R 31.42 |
| 3,60 | N O P Q R 31.41 |
| 3,45 | O P Q R 31.18 |
| 2,105 | P Q R 30.80 |
| 2,15 | Q R S 29.77 |
| 2,90 | Q R S 29.58 |
| 2,30 | R S 29.37 |
| 2,75 | R S 29.21 |
| 2,60 | R S 29.10 |
| 2,45 | R S 29.03 |
| 1,120 | S T 26.66 |
| 1,15 | T U 25.71 |
| 1,105 | T U V 24.74 |
| 1,30 | T U V 23.73 |
| 1,90 | U V 23.49 |
| 1,45 | V 22.53 |
| 1,75 | V 22.52 |
| 1,60 | V 22.08 |

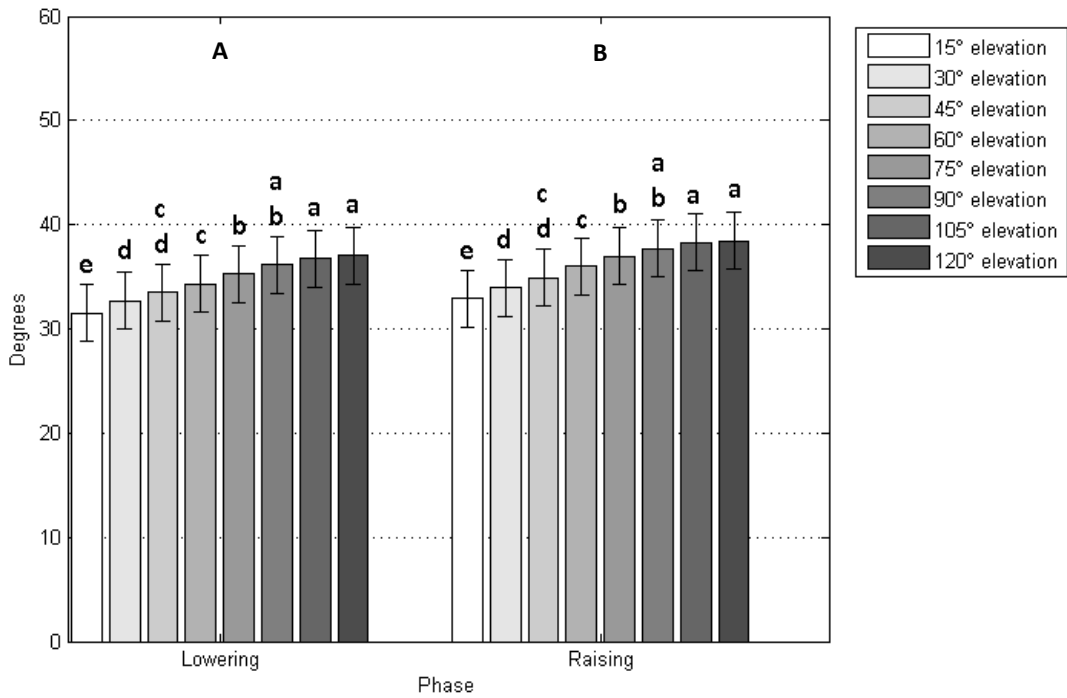


Figure 32: Interaction effects of humeral elevation phase and elevation angle on LSM right scapulothoracic +protraction/-retraction (SPR). Levels not connected by same letter are significantly different (p-value: 0.05)

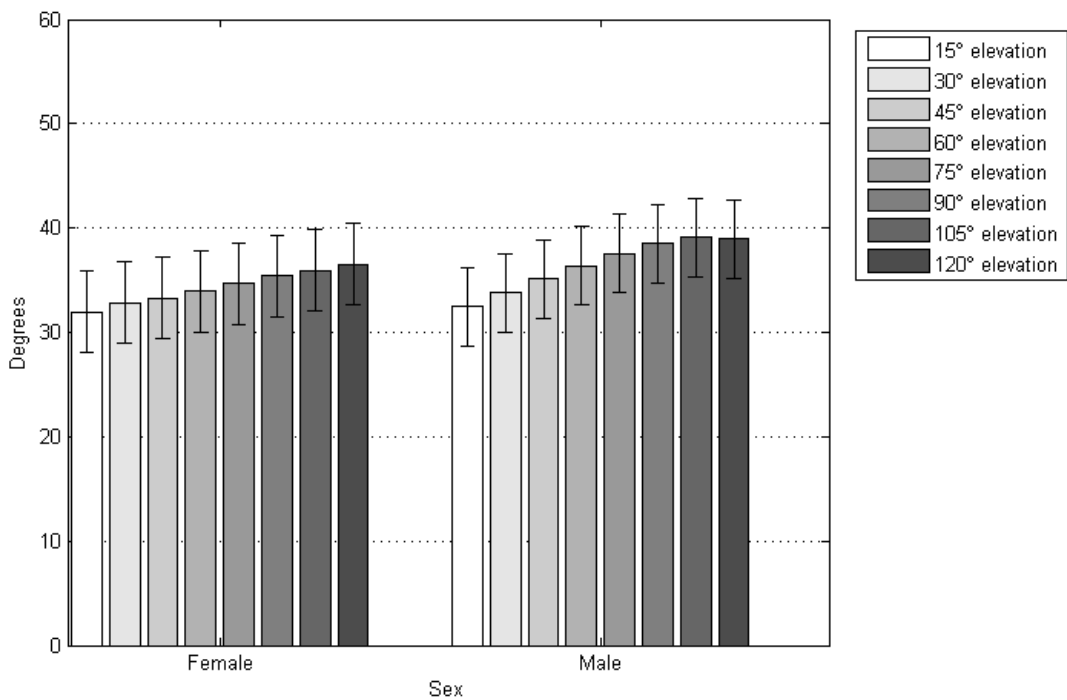


Figure 33: Interaction effects of sex and humeral elevation angle on LSM right +protraction/-retraction (SPR). Levels not connected by same letter are significantly different (p-value: 0.05)

Table 7: Interaction effects of sex and humeral elevation angle on least squares mean (LSM) scapulothoracic +protraction/-retraction (SPR). For sex, 1 = female; 2 = male. Levels not connected by same letter are significantly different (p-value: 0.05)

| Level | | LSM |
|-------|-----------------------|-------|
| 2,105 | A B C M | 39.08 |
| 2,120 | A B C M | 38.95 |
| 2,90 | A B C M | 38.49 |
| 2,75 | A B C D F M | 37.56 |
| 1,120 | A D E G H | 36.55 |
| 2,60 | D E F I | 36.35 |
| 1,105 | A B D E F G H I J | 35.97 |
| 1,90 | A B C D E F G H I J K | 35.39 |
| 2,45 | E G I J K L | 35.12 |
| 1,75 | B C F I J K L | 34.68 |
| 1,60 | C K L M N | 33.95 |
| 2,30 | G H J K L N O | 33.80 |
| 1,45 | L M N O | 33.30 |
| 1,30 | M N O | 32.80 |
| 2,15 | H N O | 32.47 |
| 1,15 | O | 31.95 |

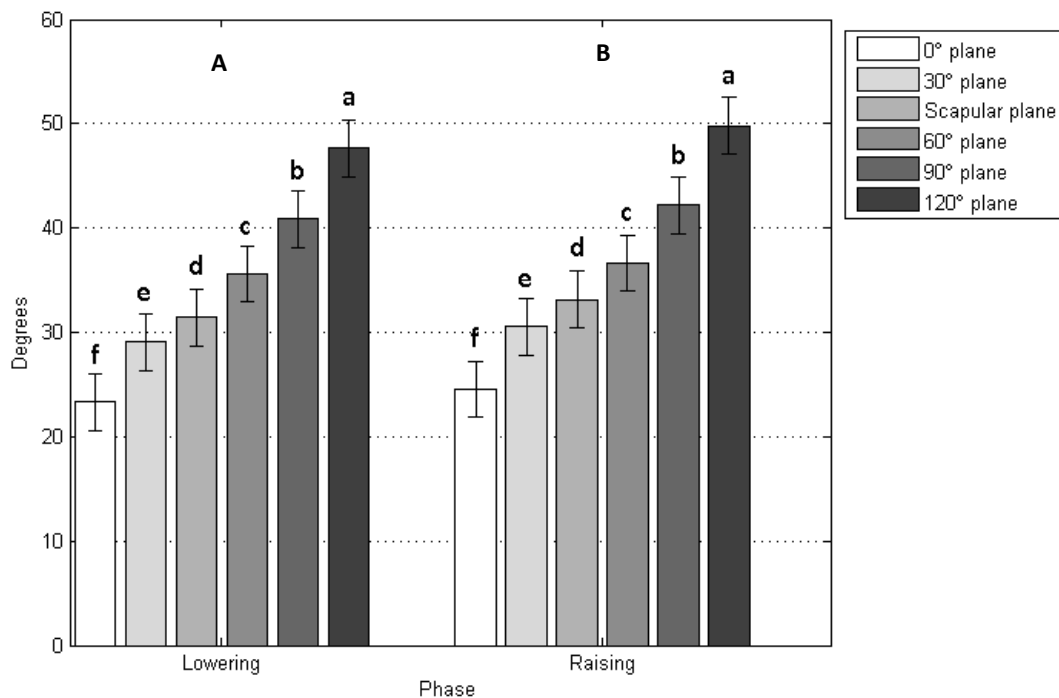


Figure 34: Interaction effects of humeral elevation phase and movement plane on LSM right +protraction/-retraction (SPR). Levels not connected by same letter are significantly different (p-value: 0.05)

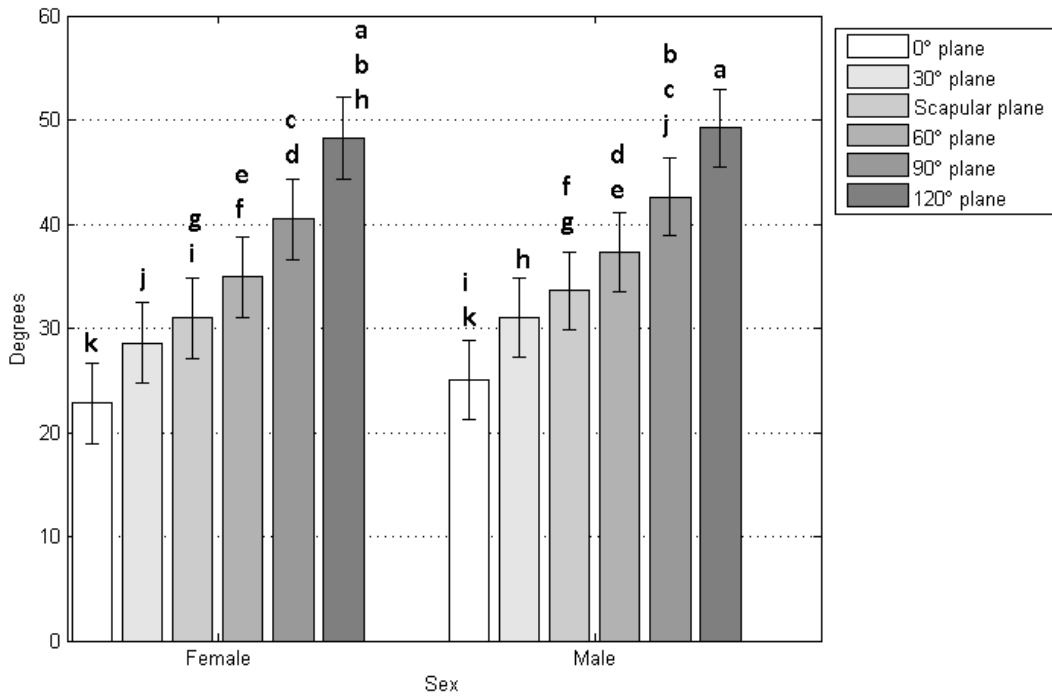


Figure 35: Interaction effects of sex and humeral movement plane on LSM right +protraction/-retraction (SPR). Levels not connected by same letter are significantly different (p-value: 0.05)

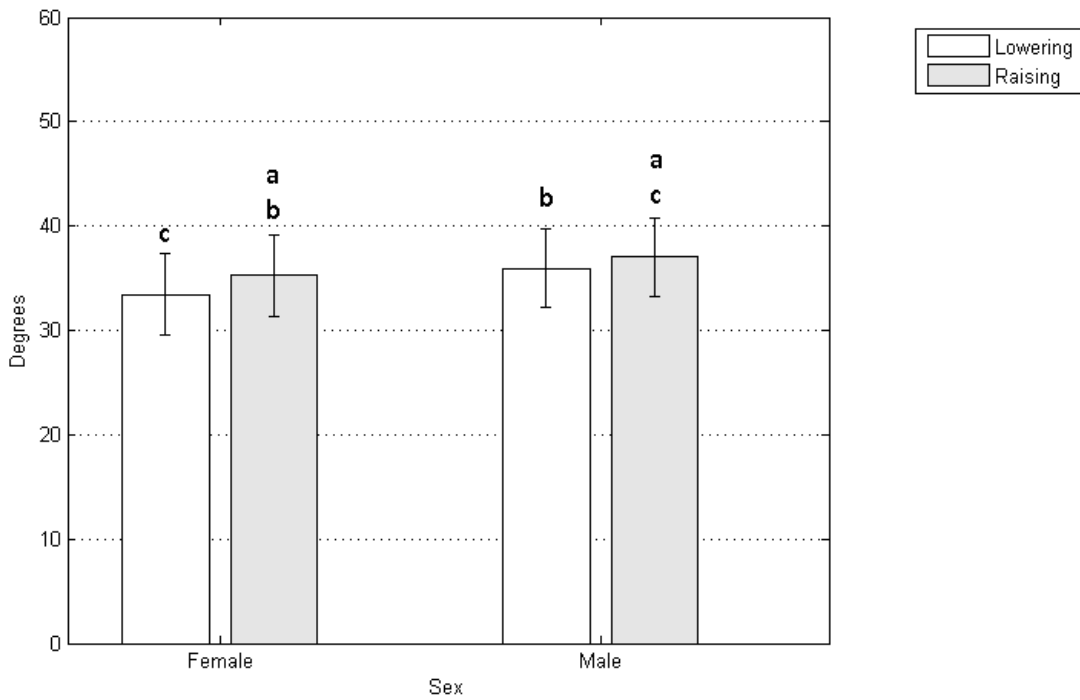


Figure 36: Interaction effects of sex and humeral elevation phase on LSM right +protraction/-retraction (SPR). Levels not connected by same letter are significantly different (p-value: 0.05)

There were no significant difference in scapula +medial/-lateral (SML) rotation for the movement planes between 0P (-14.26°) and 60P (-14.26°), while 120P had significantly lower higher lateral scapular rotation than all other planes (-18.15°). Moreover, each increasing humeral elevation increment produced progressively greater scapular lateral rotation (2.01° at 15E; -31.01° at 120E). Also, the lowering phase demonstrated more scapular lateral rotation (-15.12°) than the raising phase (-14.49°). Plots of interaction effects indicating the results of post-hoc Tukey HSD for SML kinematics are provided in Figures 37 through 42 below.

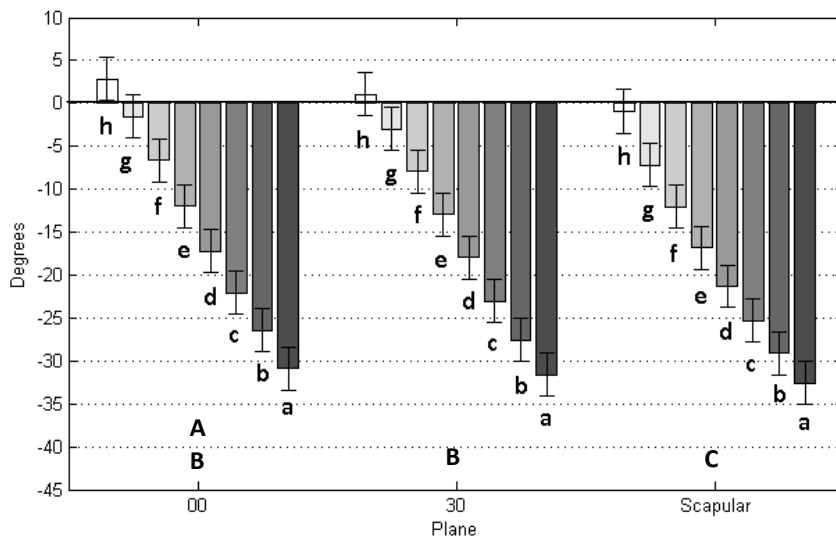
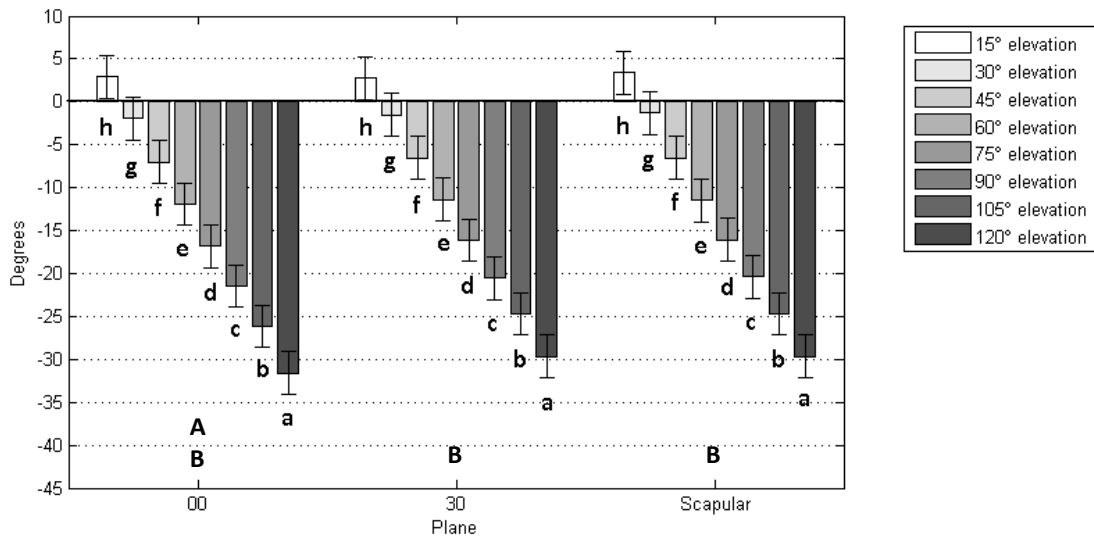


Figure 37: Interaction effects of humeral movement plane and elevation angle on LSM right scapulothoracic +medial/-lateral rotation (SML). Levels not connected by same letter are significantly different (p-value: 0.05)

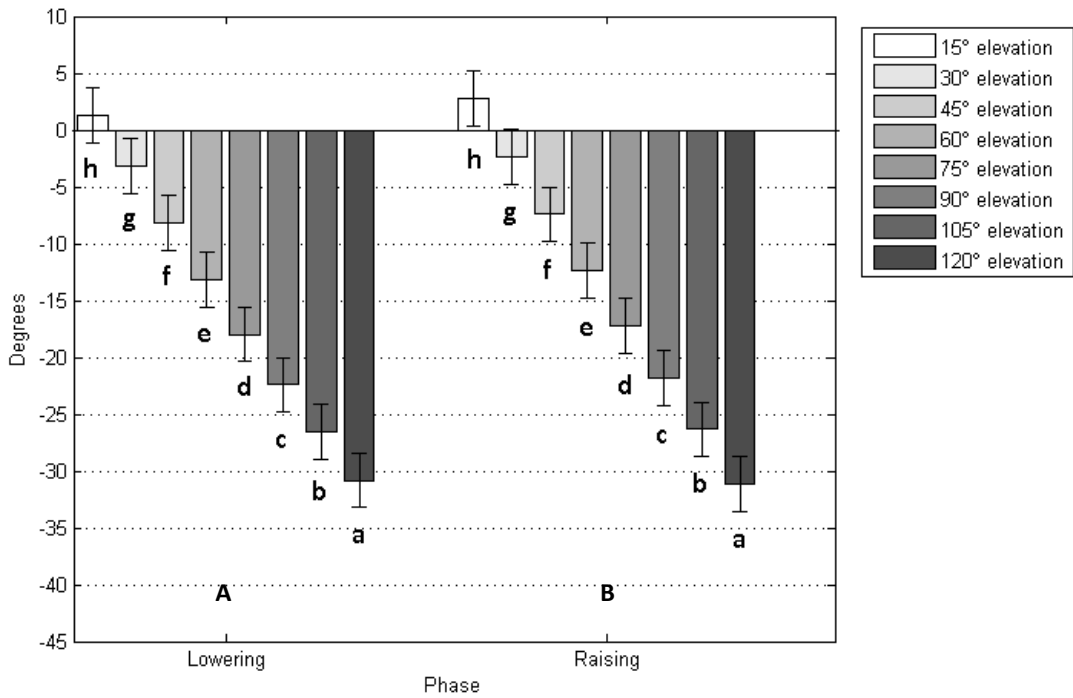


Figure 38: Interaction effects of humeral elevation phase and elevation angle on LSM right scapulothoracic +medial/-lateral rotation (SML). Levels not connected by same letter are significantly different (p -value: 0.05)

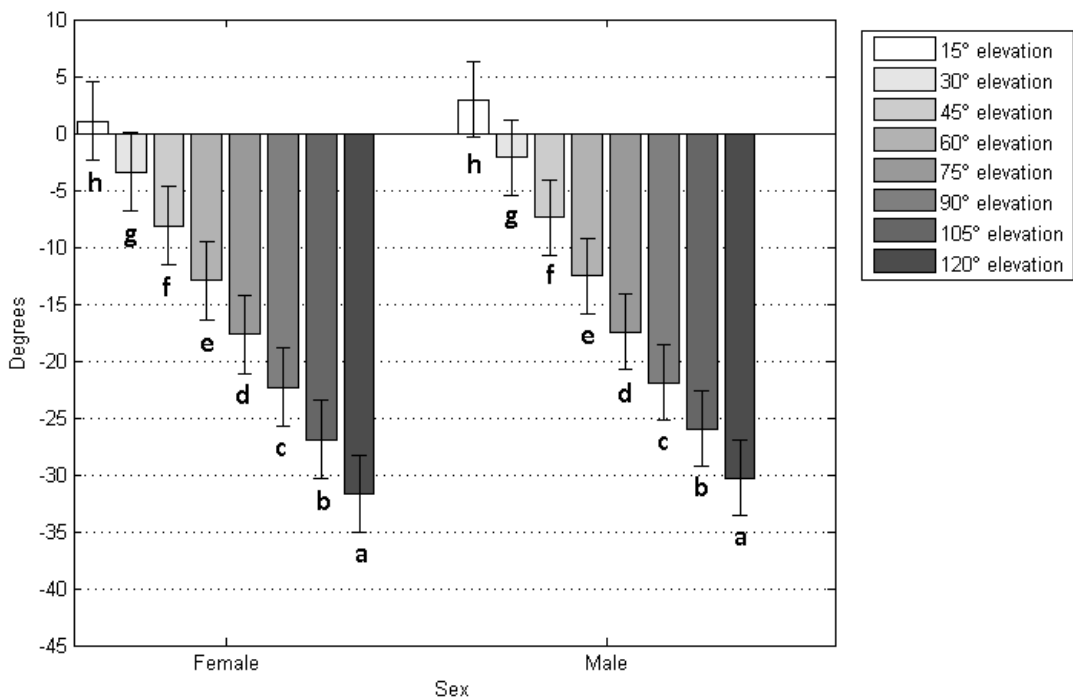


Figure 39: Interaction effects of sex and humeral elevation angle on LSM right scapulothoracic +medial/-lateral rotation (SML). Levels not connected by same letter are significantly different (p -value: 0.05)

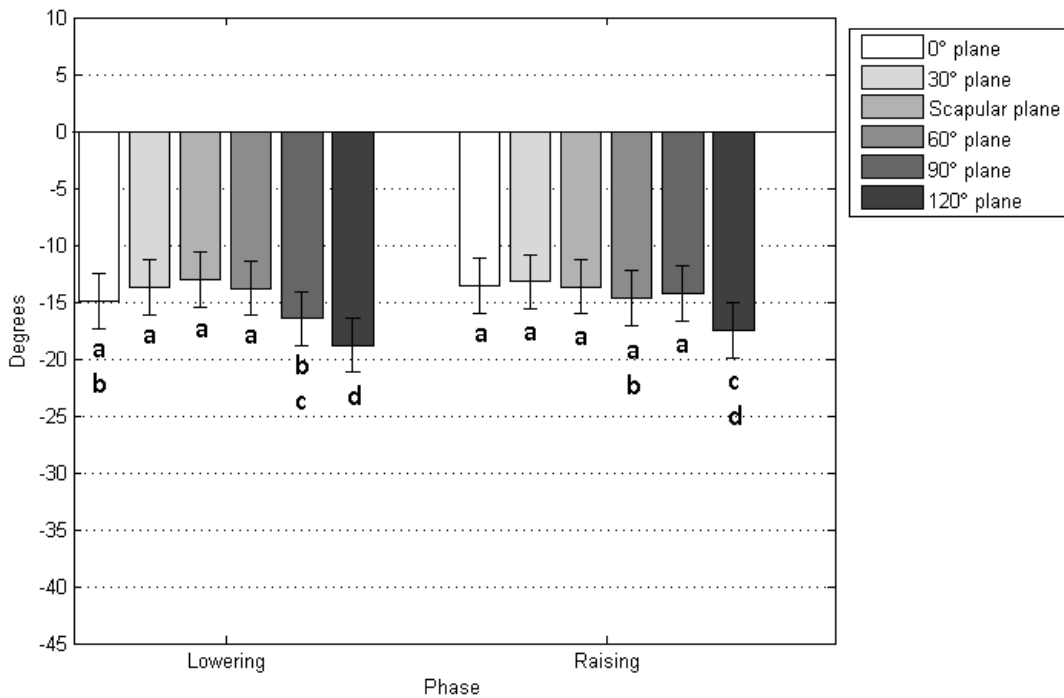


Figure 40: Interaction effects of humeral elevation phase and movement plane on LSM right scapulothoracic +medial/-lateral rotation (SML). Levels not connected by same letter are significantly different (p -value: 0.05)

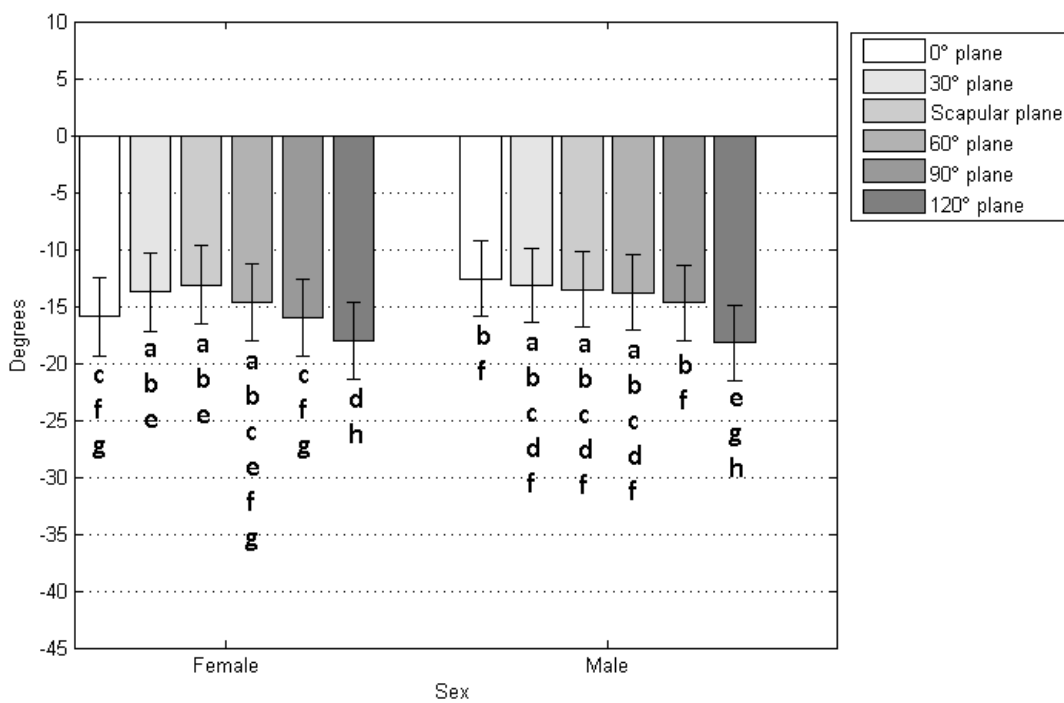


Figure 41: Interaction effects of sex and humeral movement plane on LSM right scapulothoracic +medial/-lateral rotation (SML). Levels not connected by same letter are significantly different (p -value: 0.05)

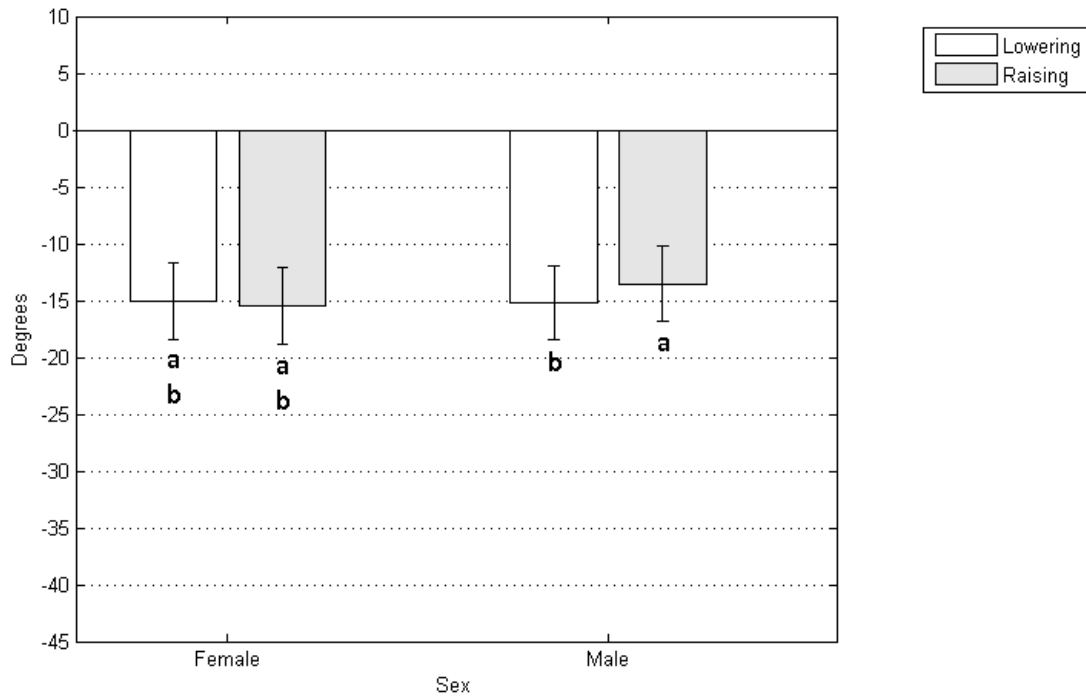


Figure 42: Interaction effects of sex and humeral elevation phase on LSM right scapulothoracic +medial/-lateral rotation (SML). Levels not connected by same letter are significantly different (p-value: 0.05)

For scapulothoracic +posterior/-anterior tilt, (SPA), more scapular posterior tilt occurred as movement plane was modified from 0P through all movement planes to 120P. 0P resulted in significantly more scapula posterior tilt than all other planes (2.99°), while planes 90P (-2.14°) and 120P (-2.77°) resulted in significantly more anterior tilt than any other planes. In addition, there was a direct relationship between humerus elevation angle and scapular posterior tilt. 15E displayed the most scapular anterior tilt (-4.51°), while 120E displayed the most posterior scapular tilt (4.99°). Finally, the lowering phase displayed significantly less anterior tilting (-0.13°) than the raising phase (-0.88°). Plots of interaction effects indicating the results of post-hoc Tukey HSD for ST kinematics are provided in Figures 43 through 48 below, with the exception of SPA of sex-humeral elevation and movement plane-elevation angle interactions. These interactions are displayed in Tables 8 and 9.

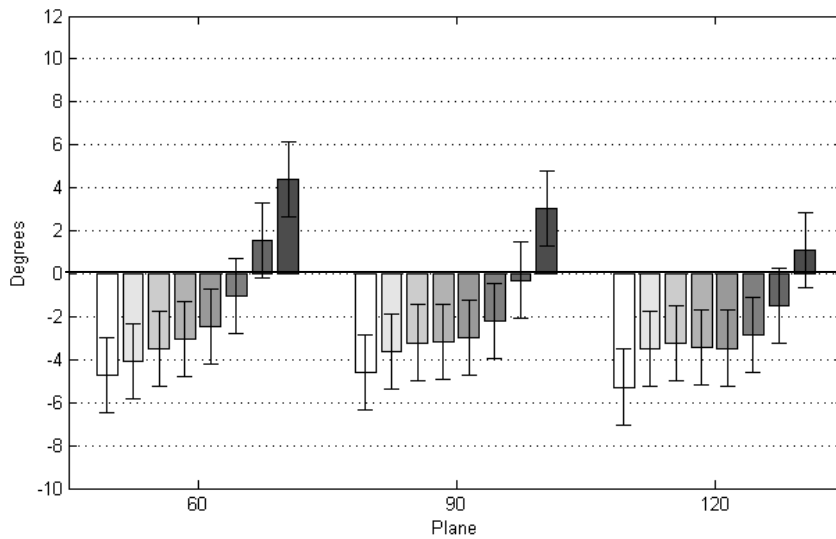
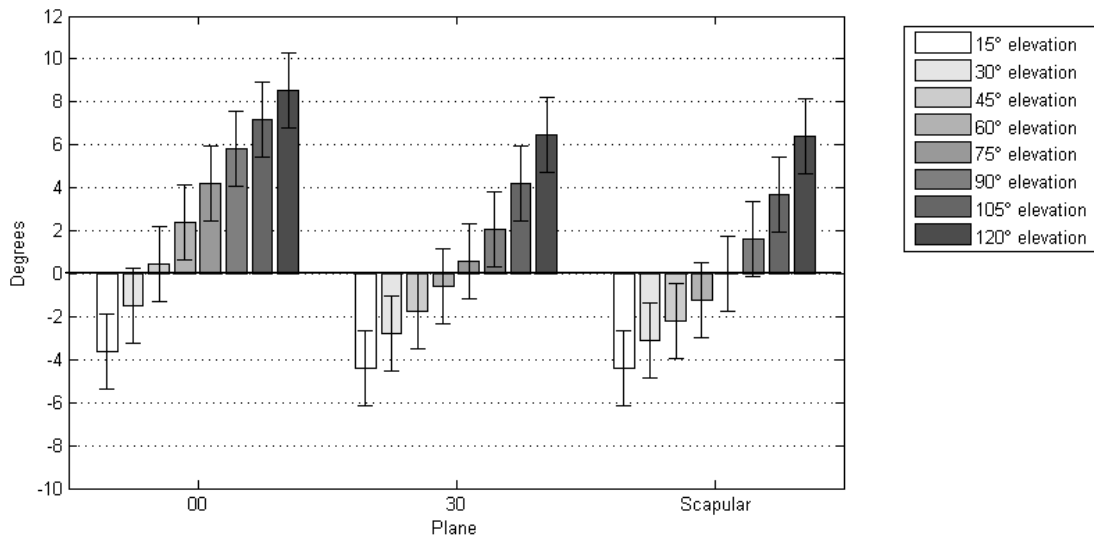


Figure 43: Interaction effects of humeral movement plane and elevation angle on LSM right scapulothoracic +posterior/-anterior tilt (SPA)

Table 8: Interaction effects of movement plane and humeral elevation angle on least squares mean (LSM) scapulothoracic +posterior/-anterior tilt (SPA). Levels not connected by same letter are significantly different (*p*-value: 0.05)

| Level | LSM |
|-------|---------------------------|
| 1,120 | A 8.56 |
| 1,105 | A B 7.18 |
| 2,120 | A B C 6.45 |
| 3,120 | A B C 6.42 |
| 1,90 | A B C D 5.84 |
| 4,120 | B C D E 4.37 |
| 1,75 | B C D E 4.22 |
| 2,105 | B C D E 4.19 |
| 3,105 | C D E F 3.71 |
| 5,120 | C D E F G 3.02 |
| 1,60 | D E F G H 2.40 |
| 2,90 | E F G H I 2.07 |
| 3,90 | E F G H I J 1.60 |
| 4,105 | E F G H I J 1.52 |
| 6,120 | E F G H I J K 1.10 |
| 2,75 | F G H I J K L 0.57 |
| 1,45 | F G H I J K L M 0.44 |
| 3,75 | G H I J K L M N -0.01 |
| 5,105 | G H I J K L M N O -0.30 |
| 2,60 | H I J K L M N O -0.58 |
| 4,90 | I J K L M N O P -1.05 |
| 3,60 | I J K L M N O P Q -1.21 |
| 6,105 | J K L M N O P Q R -1.48 |
| 1,30 | J K L M N O P Q R S -1.49 |
| 2,45 | J K L M N O P Q R S -1.74 |
| 5,90 | K L M N O P Q R S -2.21 |
| 3,45 | K L M N O P Q R S -2.22 |
| 4,75 | L M N O P Q R S -2.47 |
| 2,30 | L M N O P Q R S -2.79 |
| 6,90 | L M N O P Q R S -2.83 |
| 5,75 | M N O P Q R S -2.98 |
| 4,60 | N O P Q R S -3.04 |
| 3,30 | N O P Q R S -3.12 |
| 5,60 | N O P Q R S -3.20 |
| 5,45 | N O P Q R S -3.21 |
| 6,45 | N O P Q R S -3.23 |
| 6,60 | N O P Q R S -3.43 |
| 6,75 | O P Q R S -3.47 |
| 6,30 | O P Q R S -3.49 |
| 4,45 | O P Q R S -3.50 |
| 1,15 | O P Q R S -3.64 |
| 5,30 | O P Q R S -3.65 |
| 4,30 | P Q R S -4.10 |
| 2,15 | P Q R S -4.38 |
| 3,15 | P Q R S -4.40 |
| 5,15 | Q R S -4.60 |
| 4,15 | R S -4.75 |
| 6,15 | S -5.29 |

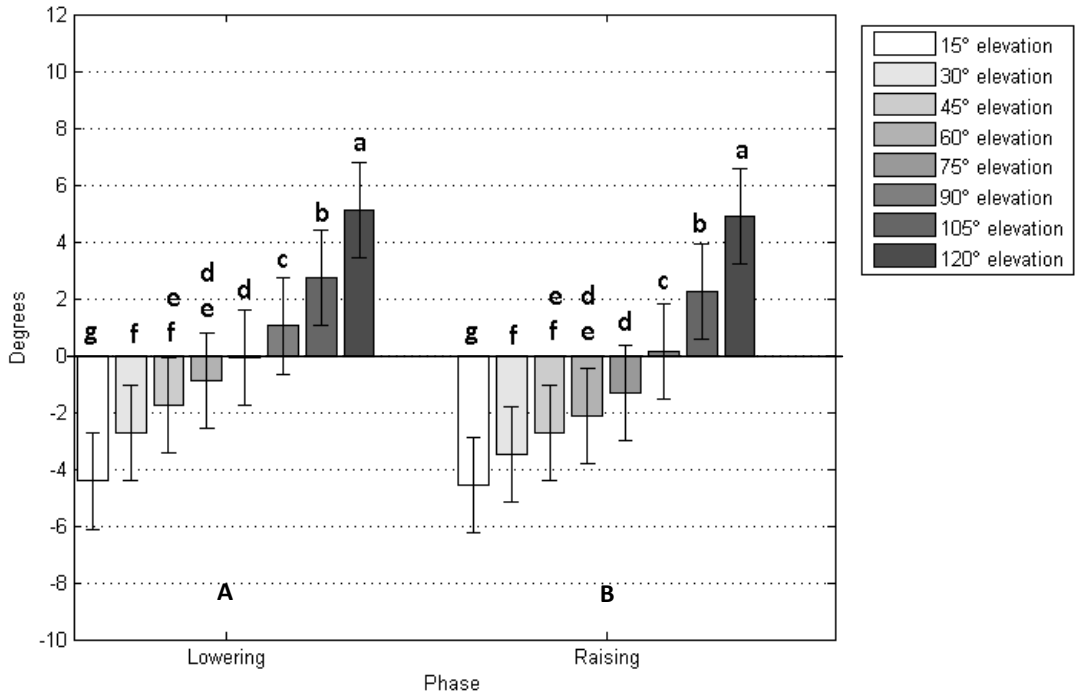


Figure 44: Interaction effects of humeral elevation phase and elevation angle on LSM right scapulothoracic +posterior/-anterior tilt (SPA). Levels not connected by same letter are significantly different (p-value: 0.05)

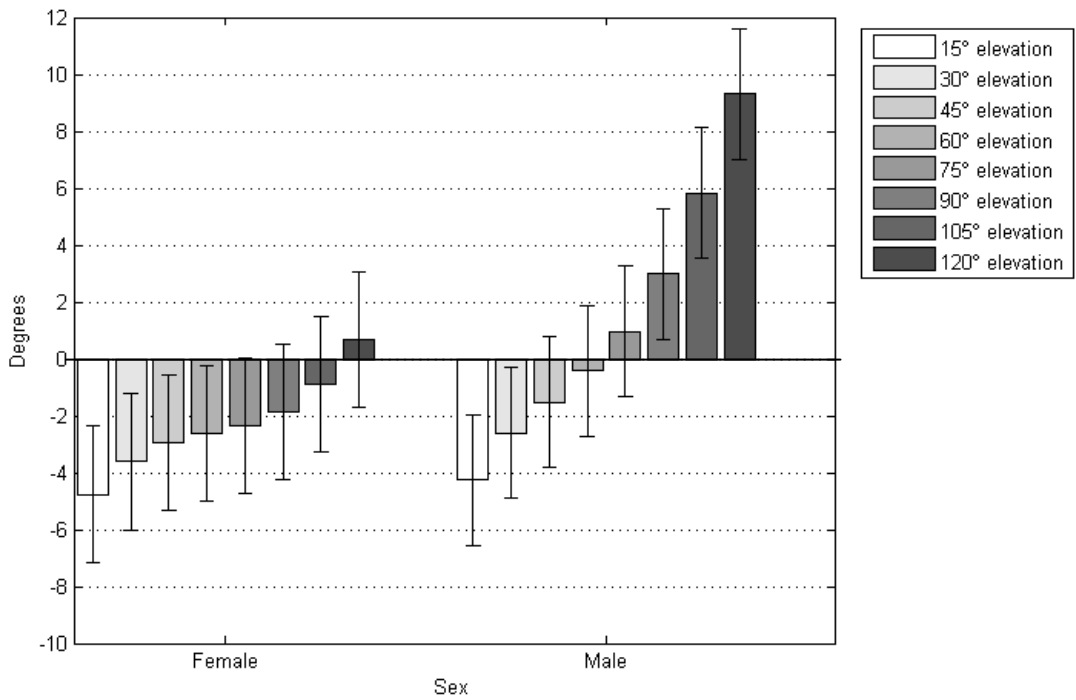


Figure 45: Interaction effects of sex and humeral elevation angle on LSM right scapulothoracic +posterior/-anterior tilt (SPA).

Table 9: Interaction effects of sex and humeral elevation angle on least squares mean (LSM) scapulothoracic +posterior/-anterior tilt. Levels not connected by same letter are significantly different (p -value: 0.05)

| Level | | | | | | | | | | | LSM | | | | |
|-------|---|---|---|---|---|---|---|---|---|---|------|-------|-------|-------|-------|
| 2,120 | A | | | | | | | | | J | 9.30 | | | | |
| 2,105 | B | | | | | | | | L | | 5.82 | | | | |
| 2,90 | C | | | | | | | | | | 2.99 | | | | |
| 2,75 | | | | | D | F | | | | | | 0.96 | | | |
| 1,120 | A | B | C | D | E | F | G | | | | 0.68 | | | | |
| 2,60 | | | | | D | E | F | H | | | | -0.42 | | | |
| 1,105 | A | B | C | D | E | F | G | H | I | | | -0.88 | | | |
| 2,45 | | | | | E | G | | H | I | K | | -1.52 | | | |
| 1,90 | | | | | | F | H | | I | J | K | M | -1.84 | | |
| 1,75 | | | | | | F | H | | I | J | K | L | M | N | -2.33 |
| 2,30 | | | | | | | G | I | | K | M | N | O | -2.60 | |
| 1,60 | | | | | | F | H | | I | J | K | L | M | N | -2.60 |
| 1,45 | | | | | | | | J | | K | L | M | N | -2.97 | |
| 1,30 | | | | | | | | | L | N | O | -3.62 | | | |
| 2,15 | | | | | | | | | | M | N | O | -4.26 | | |
| 1,15 | | | | | | | | | | | O | -4.76 | | | |

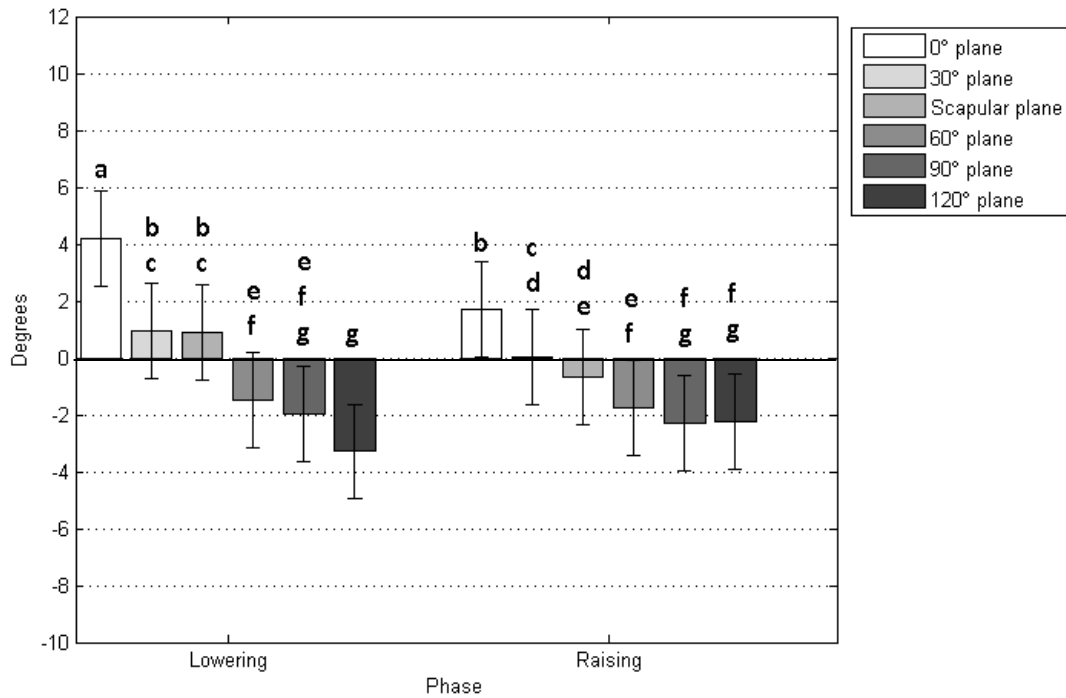


Figure 46: Interaction effects of humeral elevation phase and movement plane on LSM right scapulothoracic +posterior/-anterior tilt (SPA). Levels not connected by same letter are significantly different (p -value: 0.05)

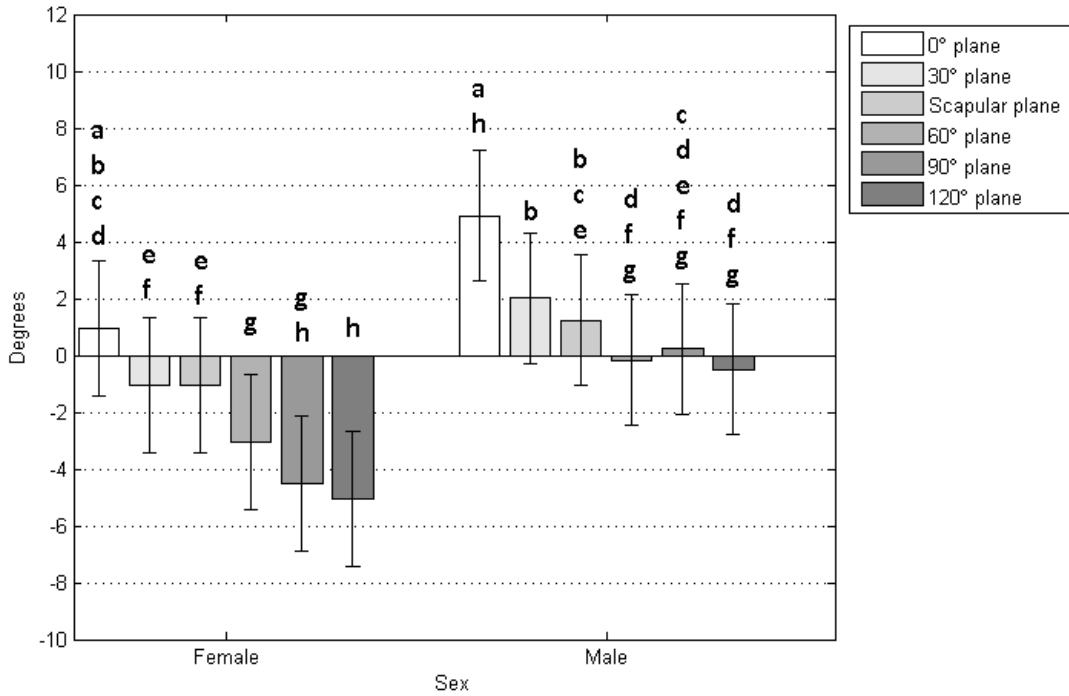


Figure 47: Interaction effects of sex and humeral movement plane on LSM right scapulothoracic +posterior/- anterior tilt (SPA). Levels not connected by same letter are significantly different (p-value: 0.05)

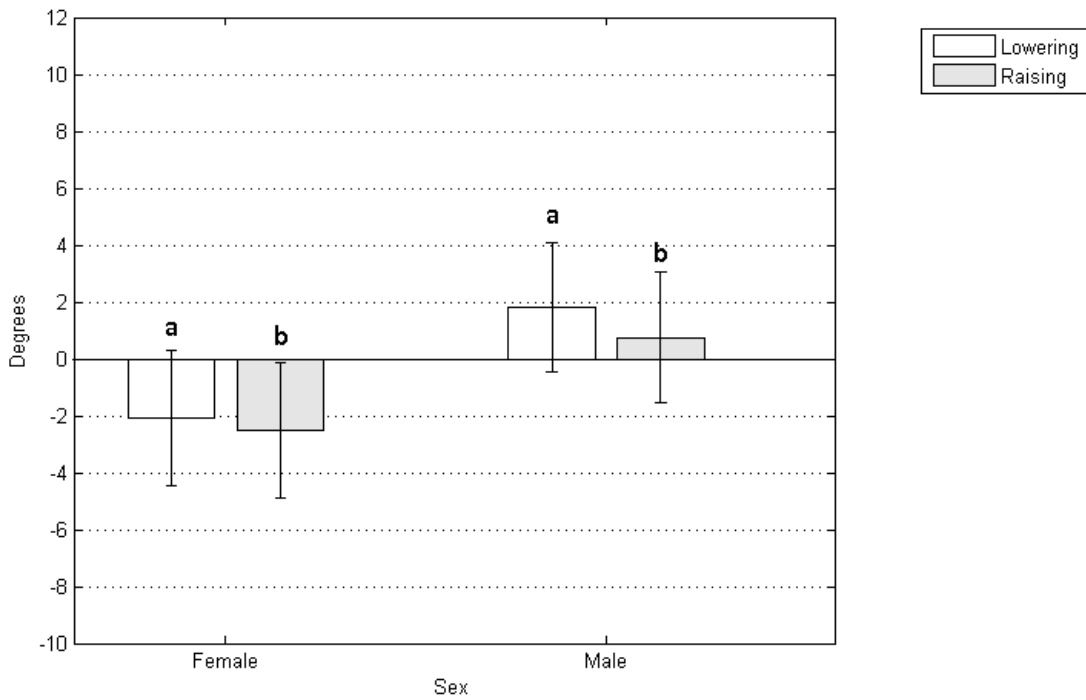


Figure 48: Interaction effects of sex and humeral elevation phase on LSM right scapulothoracic +posterior/- anterior tilt (SPA). Levels not connected by same letter are significantly different (p-value: 0.05)

4.3.2 Glenohumeral Kinematics

There was a main effect of humeral movement plane ($p < 0.0001$) and angle ($p < 0.0001$) on right glenohumeral (GH) +anterior/-posterior plane of elevation (GAP), +medial/-lateral elevation (GLE), and +internal/-external rotation (GIE). There was also a movement phase effect ($p = 0.0008$) on GIE. A movement plane-elevation angle interaction effect occurred for GAP ($p < 0.0001$) and GIE ($p < 0.0001$). Additionally, sex-movement plane ($p < 0.0001$), sex-elevation angle ($p < 0.0001$), and sex-movement phase ($p = 0.0024$) interactions were present for GLE. A summary of the main effects and interactions with F-statistics and p -values for GH kinematics is provided in Tables F4 through F6 in Append F.

As movement plane progressively changed across the body from 0P to 120P, overall LSM GH plane significantly increased anteriorly (23.93° for 0P through to 48.72° for 120P). GAP at 15E (23.19°) was statistically the same as 75E (24.64°) and 90E (21.08°). GAP at 30E (28.88°) was statistically the same as 45E (29.95°), 60E (28.23) and 75E (24.64). Plots of interaction effects indicating the results of post-hoc Tukey HSD for GAP kinematics are provided in Figures 49 through 54 below, with the exception GAP movement plane-elevation angle interactions. These interactions are displayed in Tables 10.

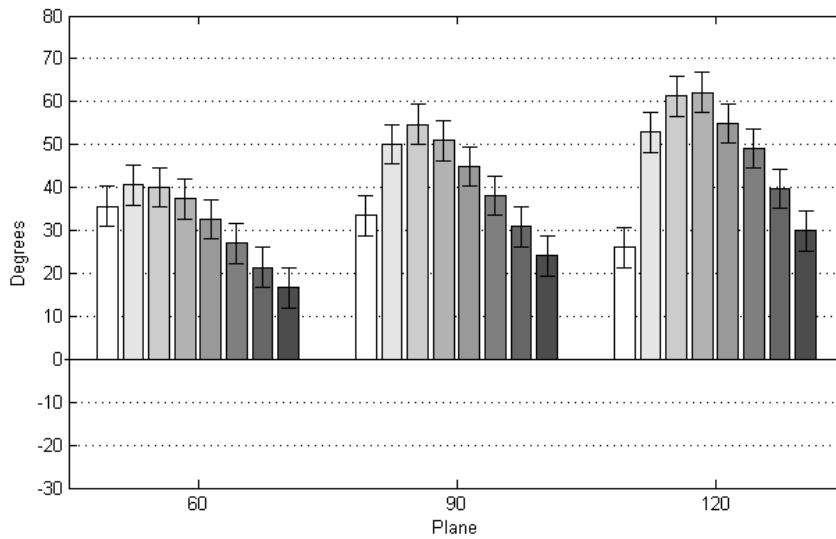
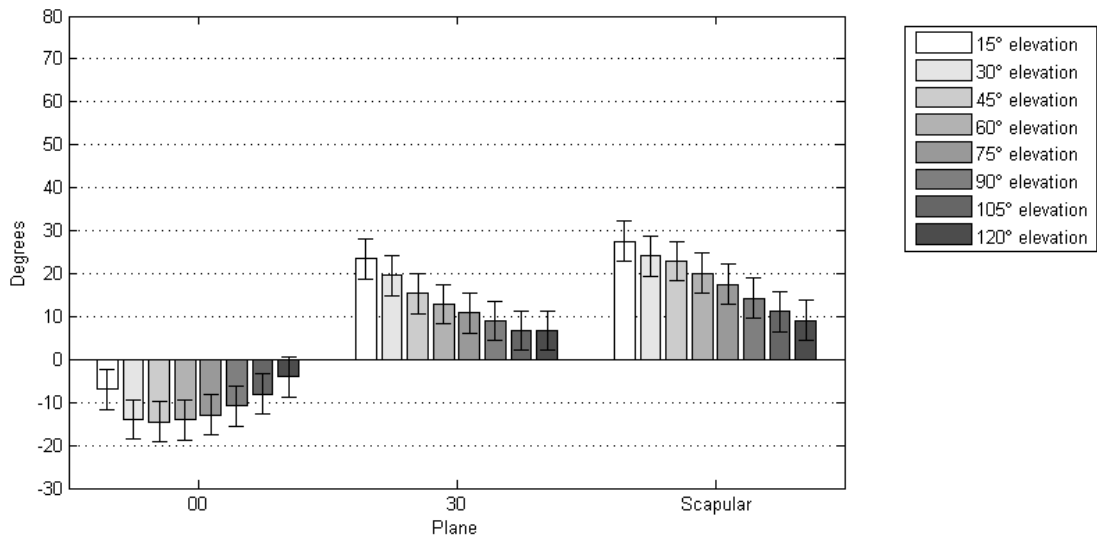


Figure 49: Effects of humeral movement plane and elevation angle on LSM right glenohumeral +anterior/-posterior rotation (GAP)

Table 10: Interaction effects of movement plane and humeral elevation angle on least squares mean (LSM) glenohumeral +anterior/-posterior movement plane. Levels not connected by same letter are significantly different (*p*-value: 0.05)

| Level | LSM |
|-------|---------------------------|
| 6,60 | A 62.19 |
| 6,45 | A 61.25 |
| 6,75 | A B 54.93 |
| 5,45 | A B C 54.66 |
| 6,30 | A B C D 52.87 |
| 5,60 | A B C D E 50.93 |
| 5,30 | A B C D E F 50.11 |
| 6,90 | A B C D E F 49.06 |
| 5,75 | B C D E F G 44.87 |
| 4,30 | B C D E F G H 40.63 |
| 4,45 | C D E F G H 40.02 |
| 6,105 | D E F G H 39.77 |
| 5,90 | D E F G H I 38.05 |
| 4,60 | E F G H I J 37.34 |
| 4,15 | F G H I J K 35.62 |
| 5,15 | G H I J K L 33.43 |
| 4,75 | G H I J K L 32.58 |
| 5,105 | G H I J K L M 30.88 |
| 6,120 | H I J K L M N 29.91 |
| 3,15 | H I J K L M N O 27.56 |
| 4,90 | H I J K L M N O 26.99 |
| 6,15 | H I J K L M N O P 26.00 |
| 3,30 | I J K L M N O P 24.14 |
| 5,120 | I J K L M N O P Q 24.04 |
| 2,15 | I J K L M N O P Q R 23.44 |
| 3,45 | J K L M N O P Q R 22.94 |
| 4,105 | K L M N O P Q R S 21.34 |
| 3,60 | L M N O P Q R S 20.13 |
| 2,30 | L M N O P Q R S 19.52 |
| 3,75 | M N O P Q R S 17.54 |
| 4,120 | M N O P Q R S 16.61 |
| 2,45 | N O P Q R S 15.40 |
| 3,90 | O P Q R S 14.26 |
| 2,60 | O P Q R S 12.91 |
| 3,105 | P Q R S 11.15 |
| 2,75 | P Q R S T 10.80 |
| 3,120 | Q R S T 9.14 |
| 2,90 | R S T 8.99 |
| 2,105 | S T U 6.76 |
| 2,120 | S T U 6.71 |
| 1,120 | T U V -4.11 |
| 1,15 | U V -6.92 |
| 1,105 | U V -8.00 |
| 1,90 | V -10.90 |
| 1,75 | V -12.86 |
| 1,30 | V -13.99 |
| 1,60 | V -14.10 |
| 1,45 | V -14.56 |

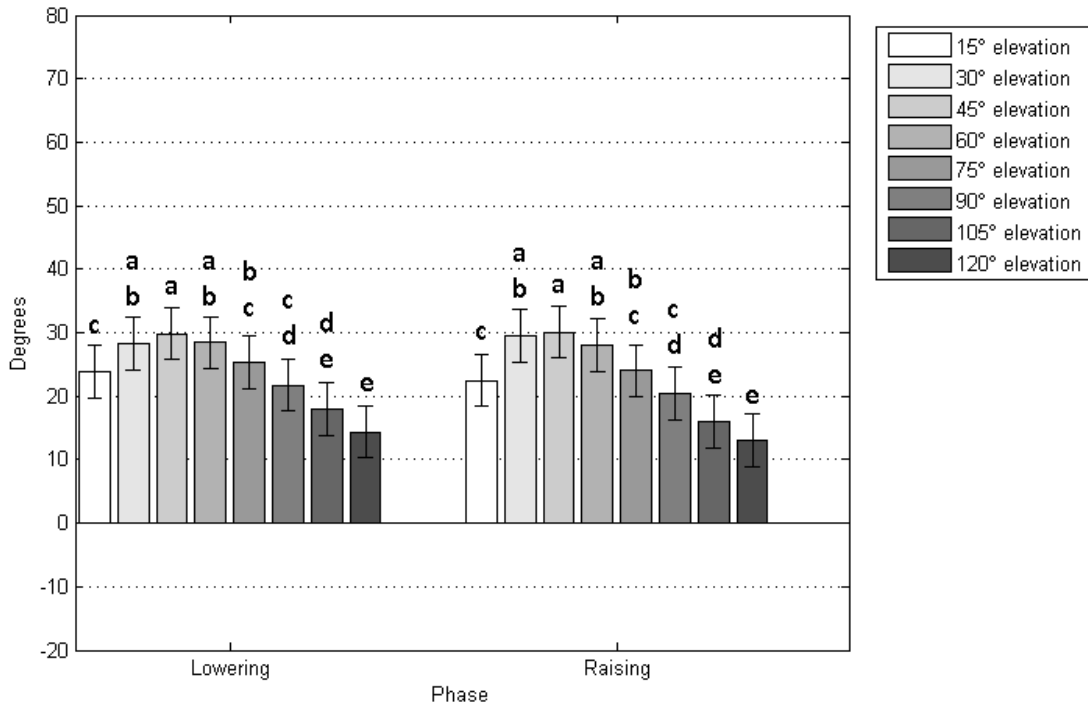


Figure 50: Effects of humeral elevation phase and elevation angle on LSM right glenohumeral +anterior/-posterior rotation (GAP). Levels not connected by same letter are significantly different (p-value: 0.05)

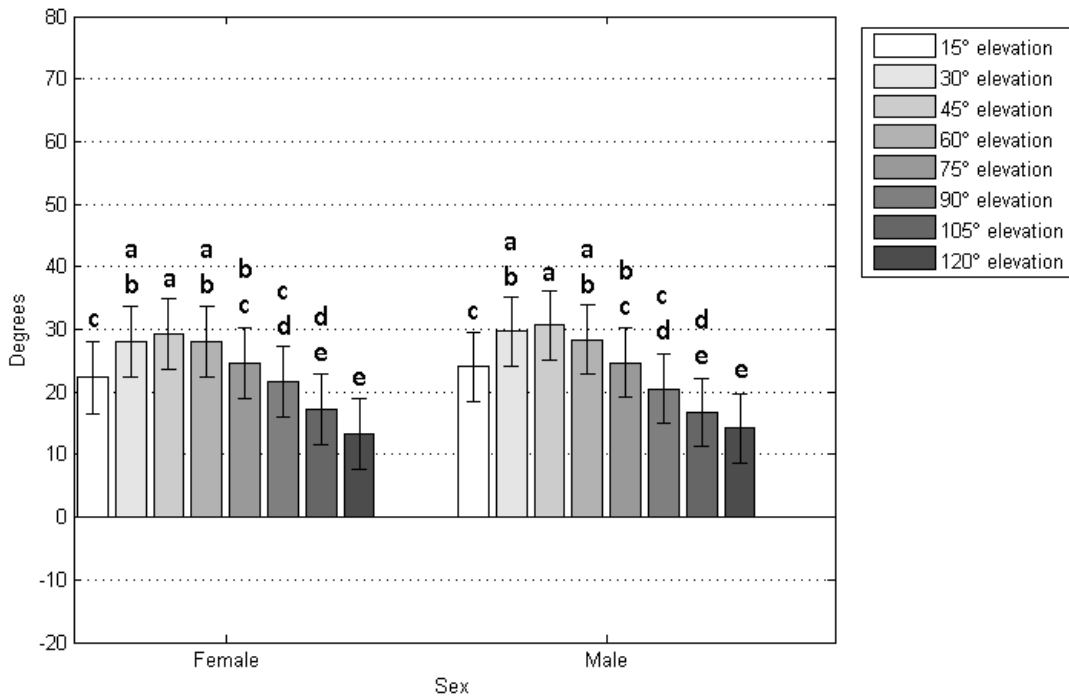


Figure 51: Effects of sex and humeral elevation angle on LSM right glenohumeral +anterior/-posterior rotation (GAP). Levels not connected by same letter are significantly different (p-value: 0.05)

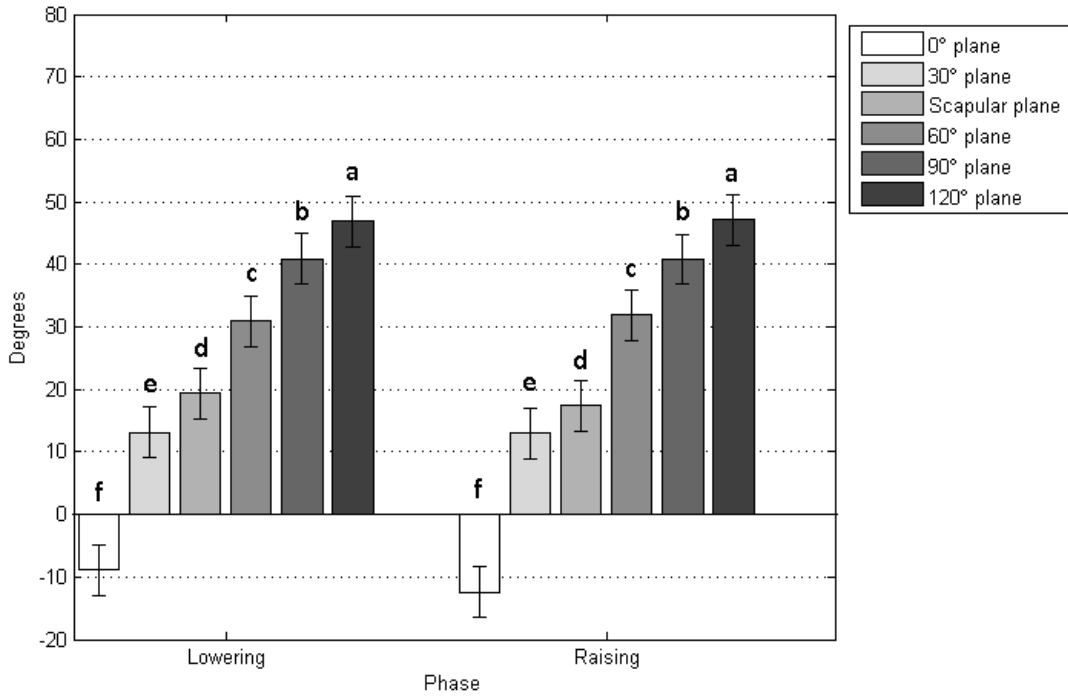


Figure 52: Effects of humeral elevation phase and movement plane on LSM right glenohumeral +anterior/-posterior rotation (GAP). Levels not connected by same letter are significantly different (p-value: 0.05)

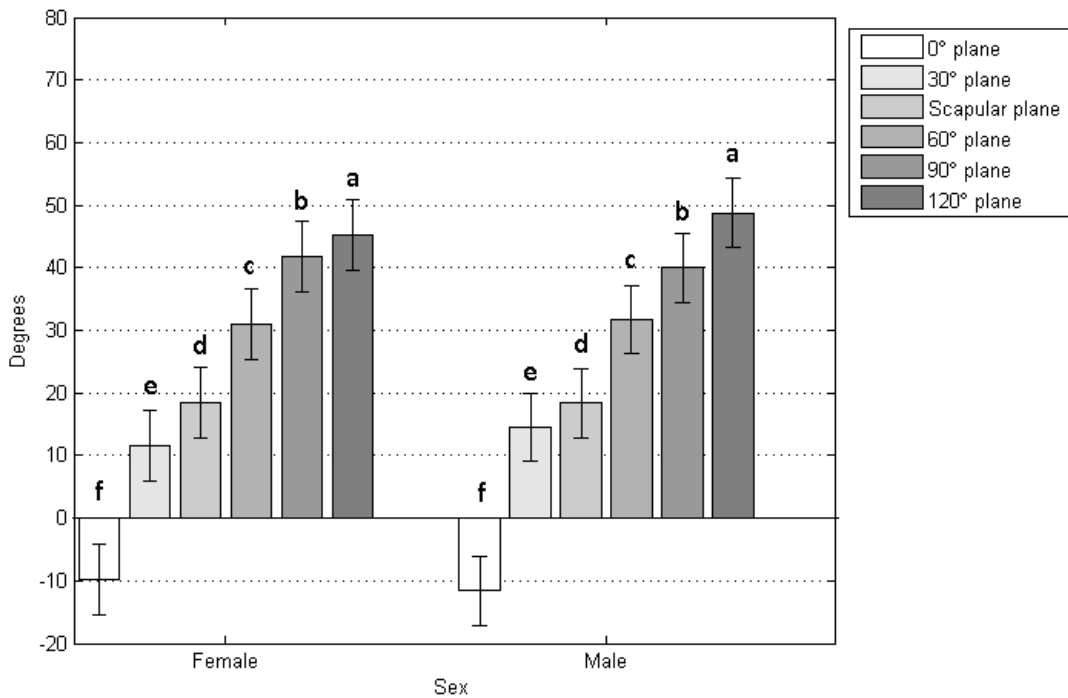


Figure 53: Effects of sex and humeral movement plane on LSM right glenohumeral +anterior/-posterior rotation (GAP). Levels not connected by same letter are significantly different (p-value: 0.05)

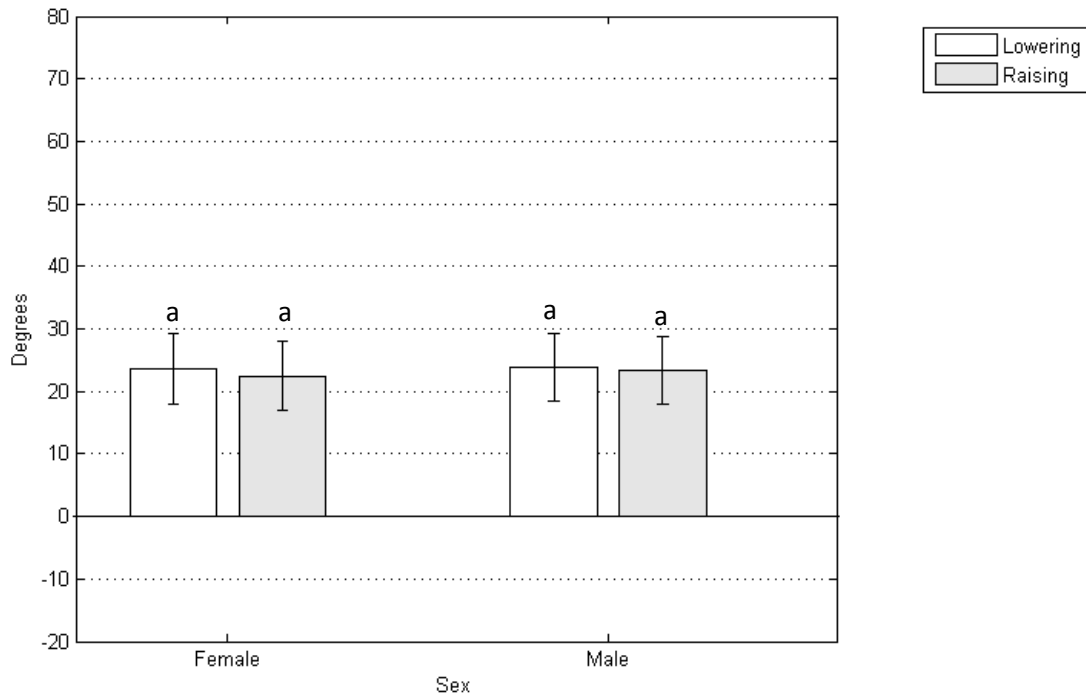


Figure 54: Effects of sex and humeral elevation phase on LSM right glenohumeral +anterior/-posterior rotation (GAP). Levels not connected by same letter are significantly different (p-value: 0.05)

For glenohumeral (GH +lowering/-elevation (GLE), GH elevation increased as movement plane changed across the body. Although some differences were significant, magnitude of changes were small. A maximum significant difference of -3.07° GLE occurred between 0P (-55.18°) and 120P (-58.25°). 30P, SCAP, and 60P were statistically the same. Finally, there were no significant GLE differences between 60P, 90P and 120P. Each increasing humeral elevation increment produced progressively greater glenohumeral elevation (-22.22° at 15E; -89.99° at 120E). Plots of interaction effects indicating the results of post-hoc Tukey HSD for GLE kinematics are provided in Figures 55 through 60.

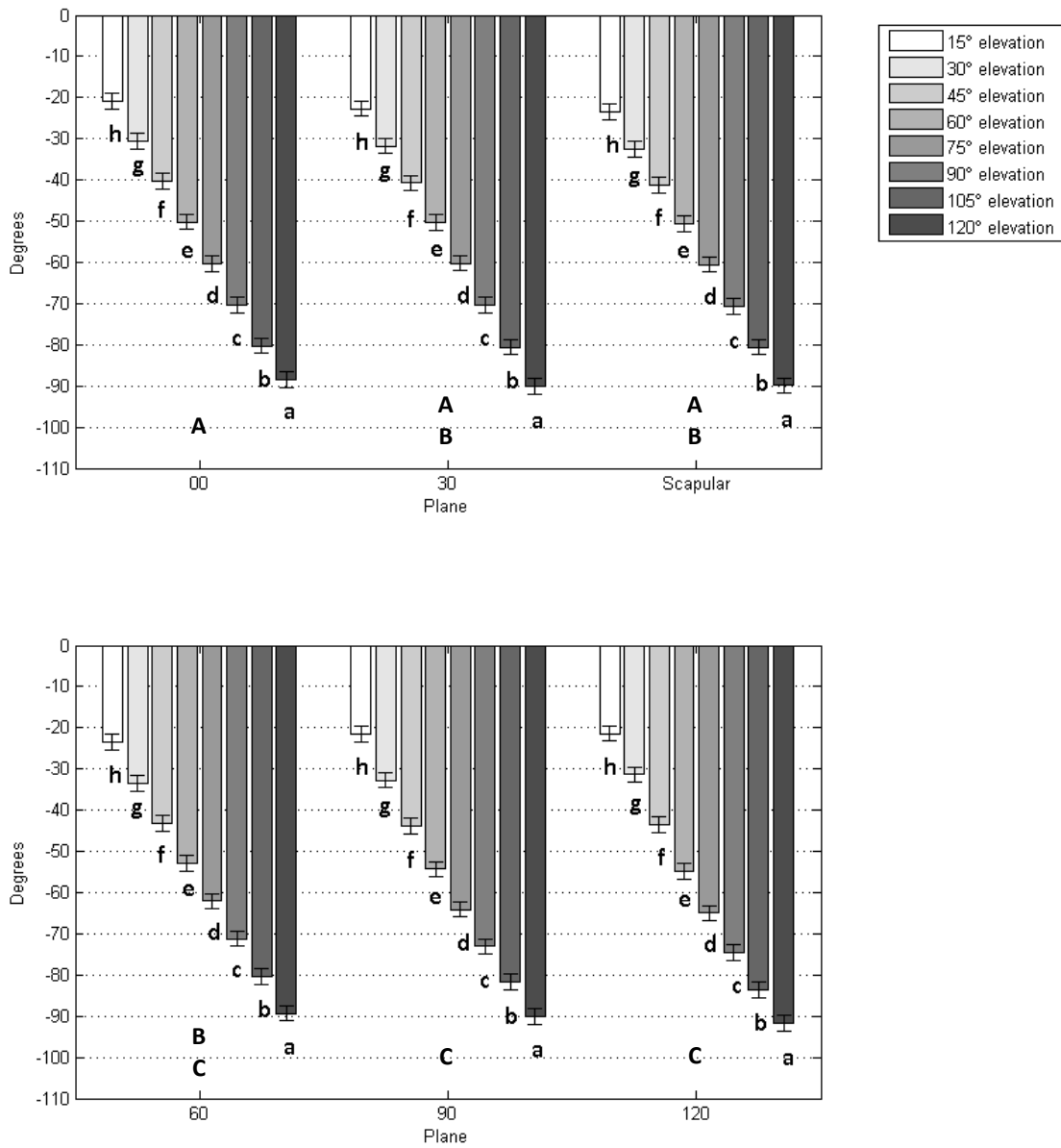


Figure 55: Effects of humeral movement plane and elevation angle on LSM right glenohumeral elevation (-) (GLE). Levels not connected by same letter are significantly different (p-value: 0.05)

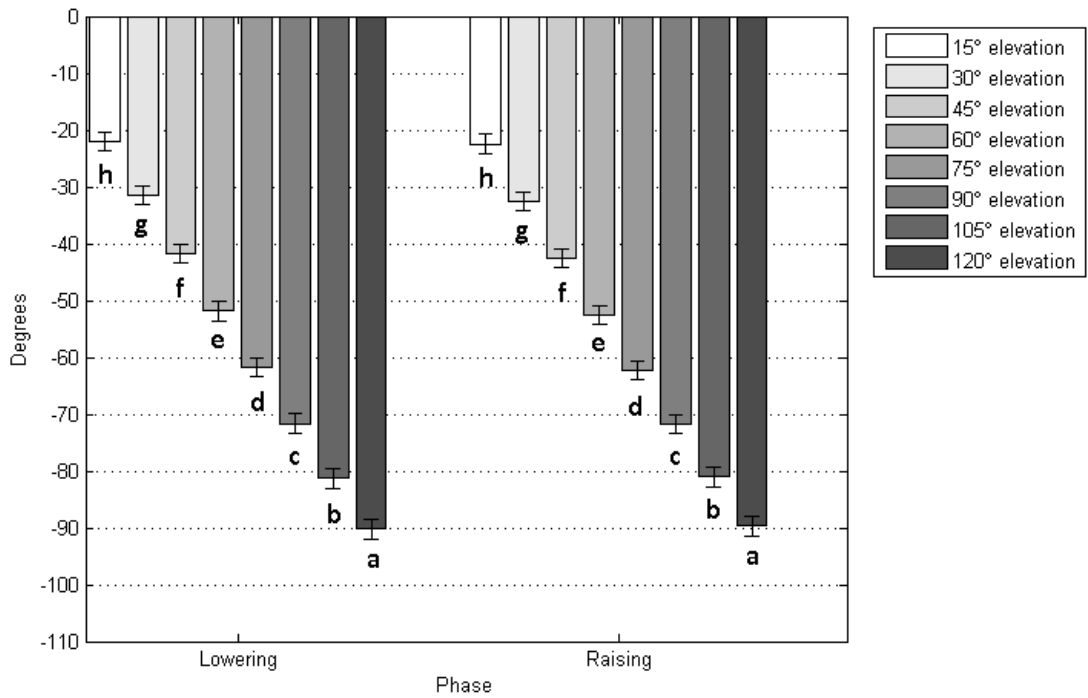


Figure 56: Effects of humeral elevation phase and elevation angle on LSM right glenohumeral elevation (-) (GLE). Levels not connected by same letter are significantly different (p-value: 0.05)

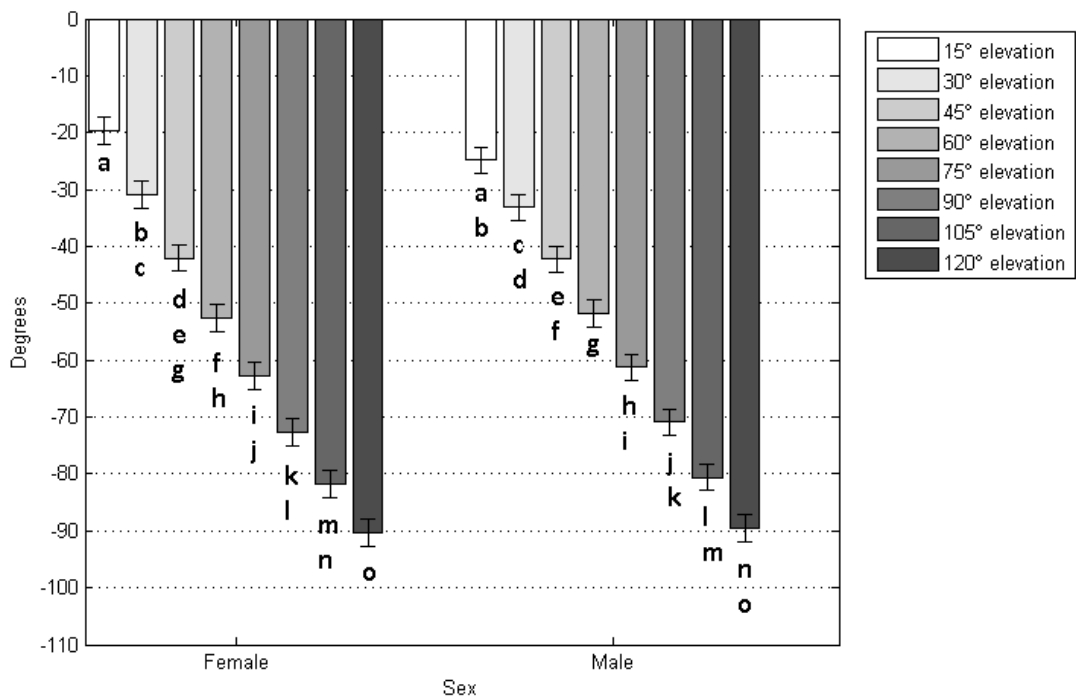


Figure 57: Effects of sex and humeral elevation angle on LSM right glenohumeral elevation (-) (GLE). Levels not connected by same letter are significantly different (p-value: 0.05)

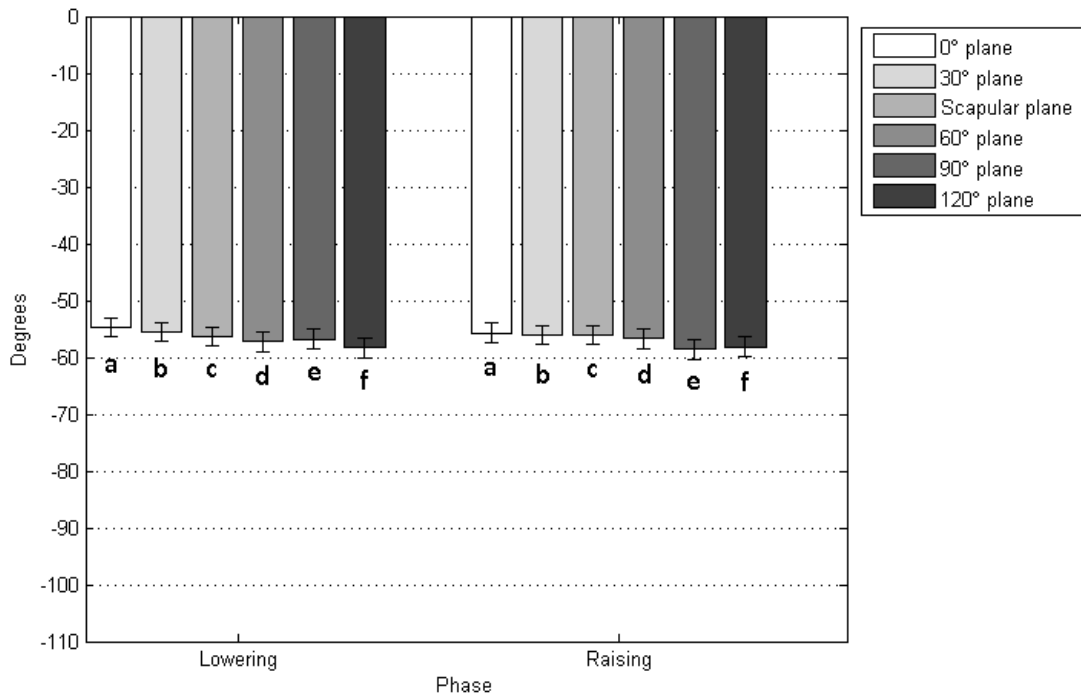


Figure 58: Effects of humeral elevation phase and movement plane on LSM right glenohumeral elevation (-) (GLE). Levels not connected by same letter are significantly different (p-value: 0.05)

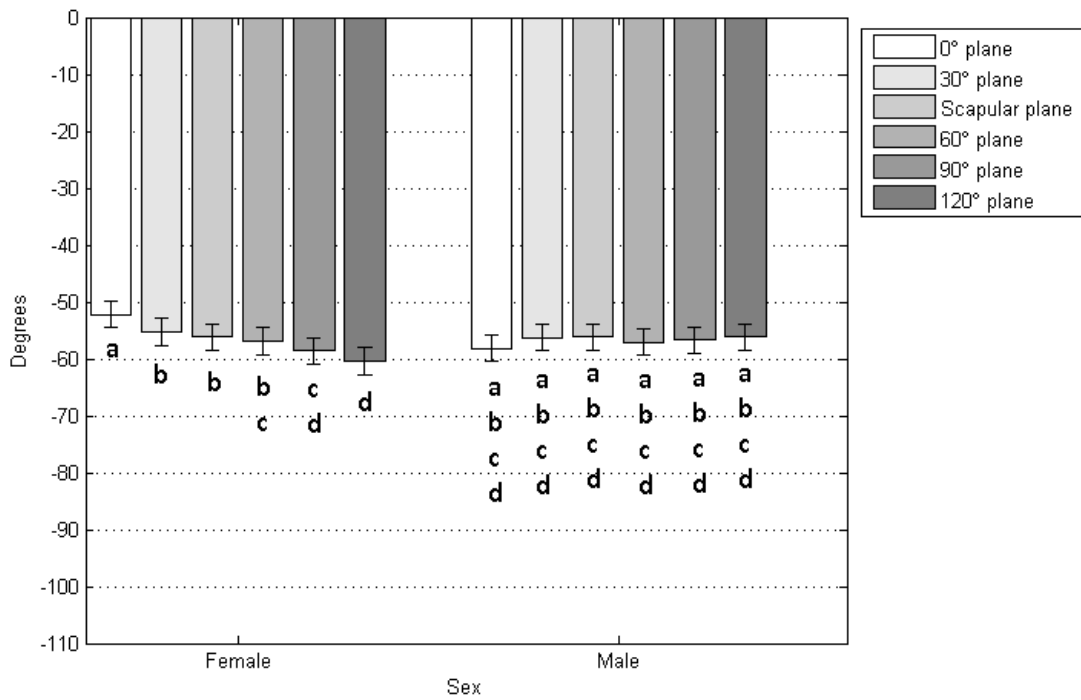


Figure 59: Effects of sex and humeral movement plane on LSM right glenohumeral elevation (-) (GLE). Levels not connected by same letter are significantly different (p-value: 0.05)

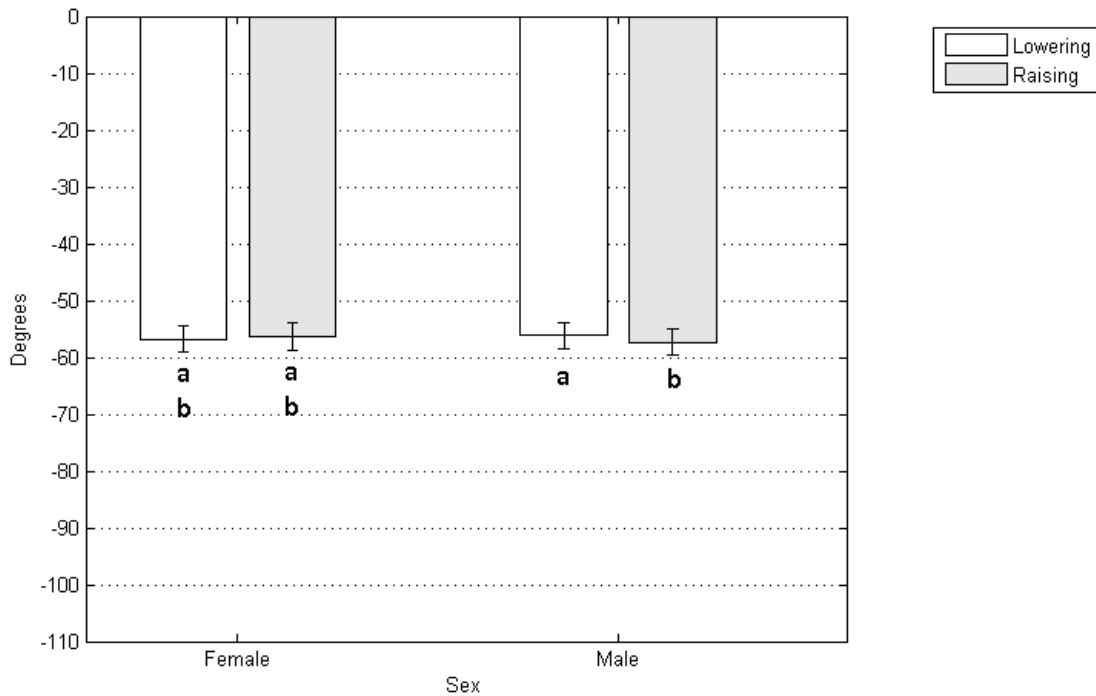


Figure 60: Effects of sex and humeral elevation phase on LSM right glenohumeral elevation (-) (GLE). Levels not connected by same letter are significantly different (p-value: 0.05)

Changing the movement plane 30P through to 90P did not significantly change the resulting glenohumeral (GH) +internal/-external rotation (GIE) (-62.50° through -65.65° respectively). 0P had significantly less external GH rotation than all other planes (-50.17°). There was no significant difference in measured external rotation between 30E (-62.26°) and 90E (-61.69°). 15E and 120E had the least external rotation (-52.59° and -54.97° respectively) and were statistically the same. Lastly, the raising phase demonstrated significantly less GH external rotation than the lowering phase (-59.46° and -61.91° respectively). Plots of interaction effects indicating the results of post-hoc Tukey HSD for GIE kinematics are provided in Figures 61 through 66 below, with the exception GIE movement plane-elevation angle interactions.

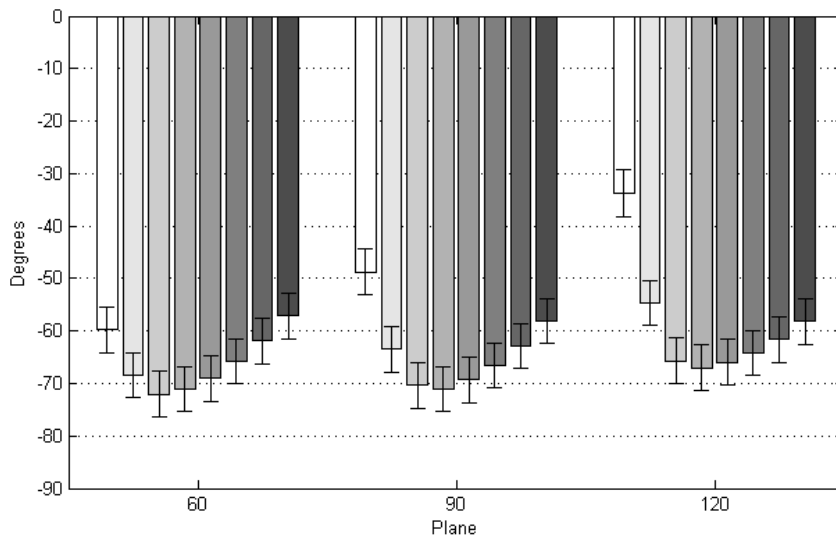
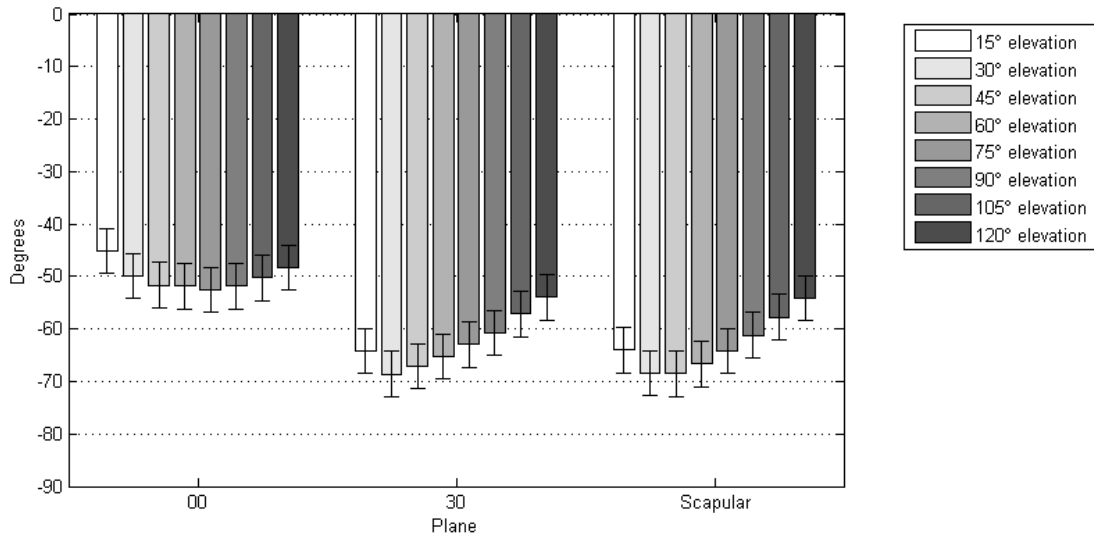


Figure 61: Effects of humeral movement plane and elevation angle on LSM right glenohumeral internal (+)/external (-) rotation (GIE).

Table 11: Interaction effects of movement plane and humeral elevation angle on least squares mean (LSM) glenohumeral +internal/-external rotation. Levels not connected by same letter are significantly different (*p*-value: 0.05)

| Level | LSM |
|-------|--------------------------------|
| 6,15 | A -33.80 |
| 1,15 | A B -45.09 |
| 1,120 | A B C -48.28 |
| 5,15 | B C D -48.74 |
| 1,30 | B C D E -49.88 |
| 1,105 | B C D E F -50.26 |
| 1,45 | B C D E F G -51.62 |
| 1,60 | B C D E F G H -51.85 |
| 1,90 | B C D E F G H -51.86 |
| 1,75 | B C D E F G H I -52.55 |
| 2,120 | B C D E F G H I J -53.98 |
| 3,120 | B C D E F G H I J -54.13 |
| 6,30 | B C D E F G H I J K -54.71 |
| 2,105 | B C D E F G H I J K L -57.13 |
| 4,120 | B C D E F G H I J K L -57.16 |
| 3,105 | B C D E F G H I J K L -57.71 |
| 5,120 | B C D E F G H I J K L M -58.09 |
| 6,120 | B C D E F G H I J K L M -58.18 |
| 4,15 | C D E F G H I J K L M -59.76 |
| 2,90 | C D E F G H I J K L M -60.69 |
| 3,90 | C D E F G H I J K L M -61.16 |
| 6,105 | C D E F G H I J K L M -61.67 |
| 4,105 | C D E F G H I J K L M -61.90 |
| 5,105 | D E F G H I J K L M -62.81 |
| 2,75 | E F G H I J K L M -63.00 |
| 5,30 | E F G H I J K L M -63.52 |
| 3,15 | E F G H I J K L M -64.00 |
| 6,90 | F G H I J K L M -64.13 |
| 2,15 | F G H I J K L M -64.14 |
| 3,75 | F G H I J K L M -64.20 |
| 2,60 | G H I J K L M -65.30 |
| 6,45 | G H I J K L M -65.69 |
| 4,90 | G H I J K L M -65.77 |
| 6,75 | H I J K L M -65.95 |
| 5,90 | I J K L M -66.54 |
| 3,60 | I J K L M -66.68 |
| 6,60 | J K L M -67.01 |
| 2,45 | J K L M -67.16 |
| 3,30 | K L M -68.41 |
| 4,30 | K L M -68.45 |
| 3,45 | K L M -68.53 |
| 2,30 | K L M -68.59 |
| 4,75 | L M -69.04 |
| 5,75 | L M -69.30 |
| 5,45 | L M -70.38 |
| 5,60 | L M -71.05 |
| 4,60 | L M -71.05 |
| 4,45 | M -72.06 |

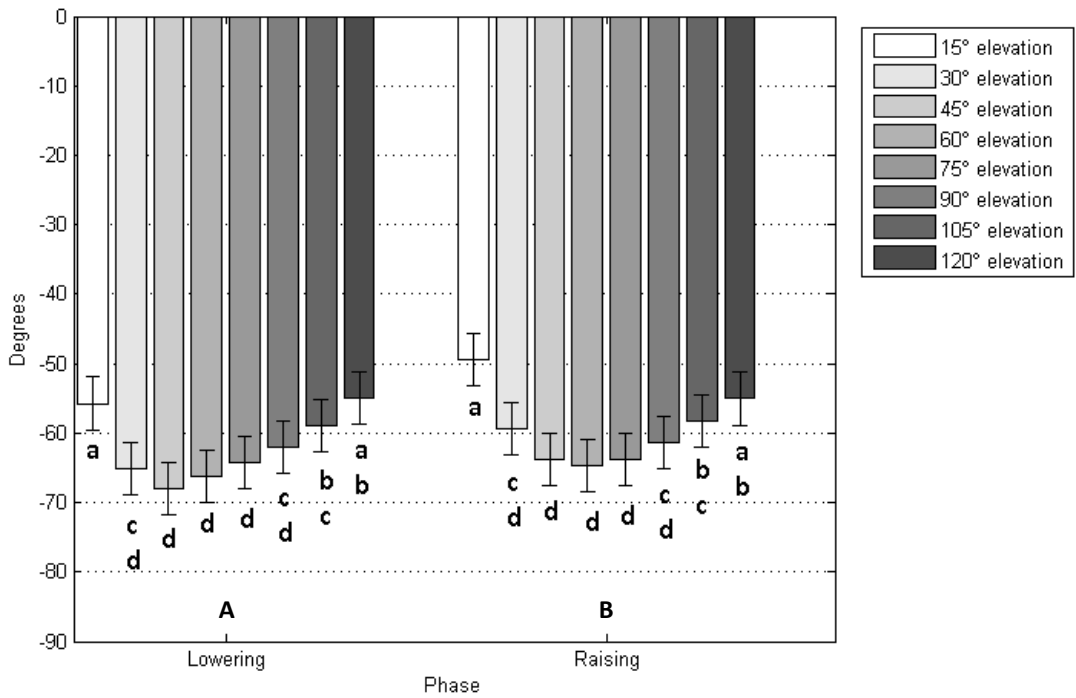


Figure 62: Effects of humeral elevation phase and elevation angle on LSM right glenohumeral +internal/+external rotation (GIE). Levels not connected by same letter are significantly different (p-value: 0.05)

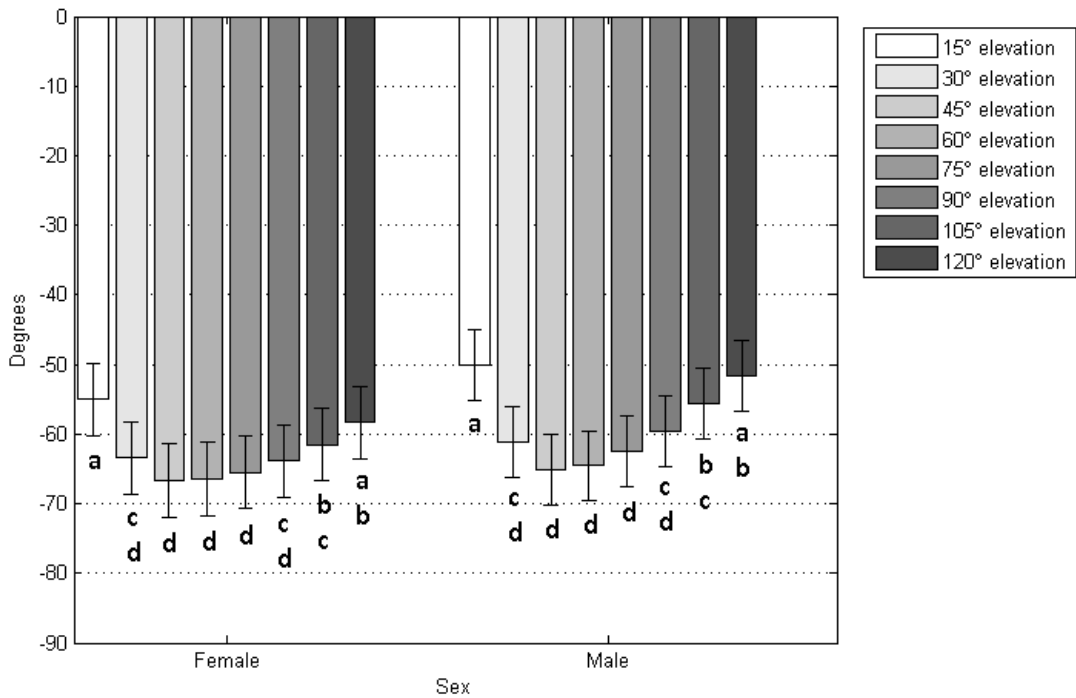


Figure 63: Effects of sex and humeral elevation angle on LSM right glenohumeral +internal/+external rotation (GIE). Levels not connected by same letter are significantly different (p-value: 0.05)

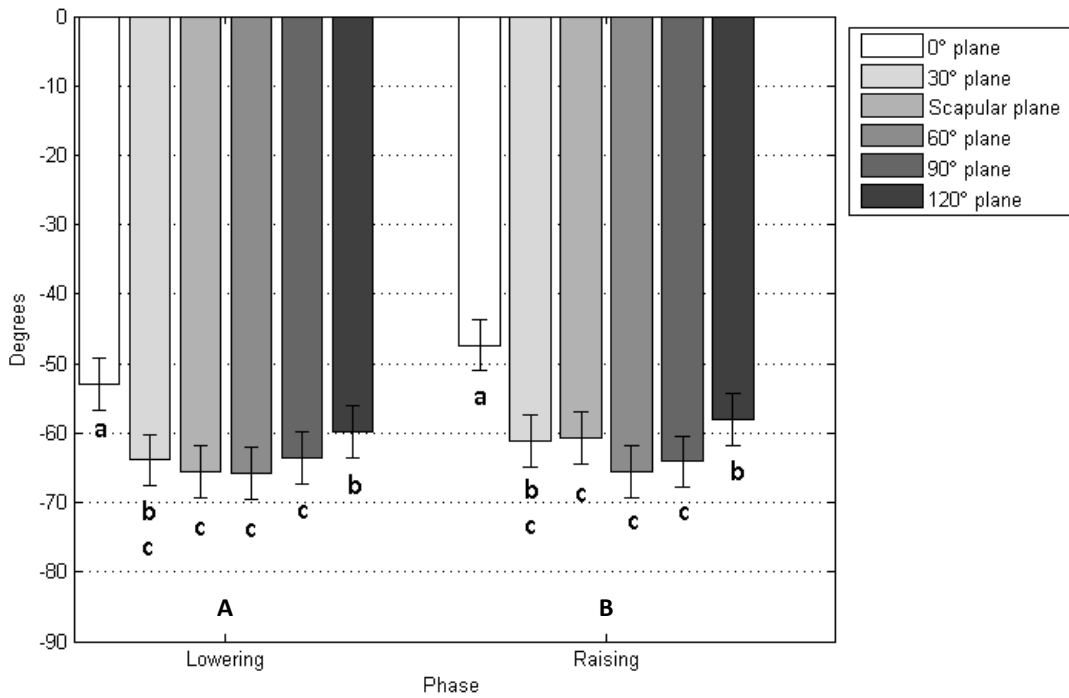


Figure 64: Effects of humeral elevation phase and movement plane on LSM right GH +internal/+external rotation (GIE). Levels not connected by same letter are significantly different (p-value: 0.05)

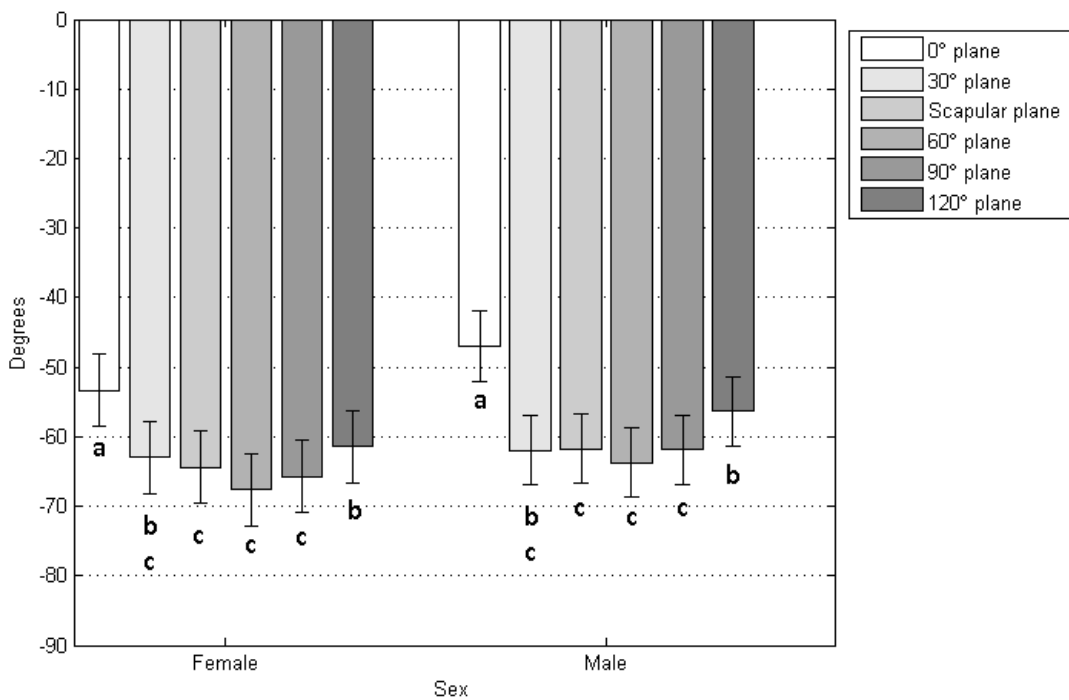


Figure 65: Effects of sex and humeral movement plane on LSM right glenohumeral +internal/+external rotation (GIE). Levels not connected by same letter are significantly different (p-value: 0.05)

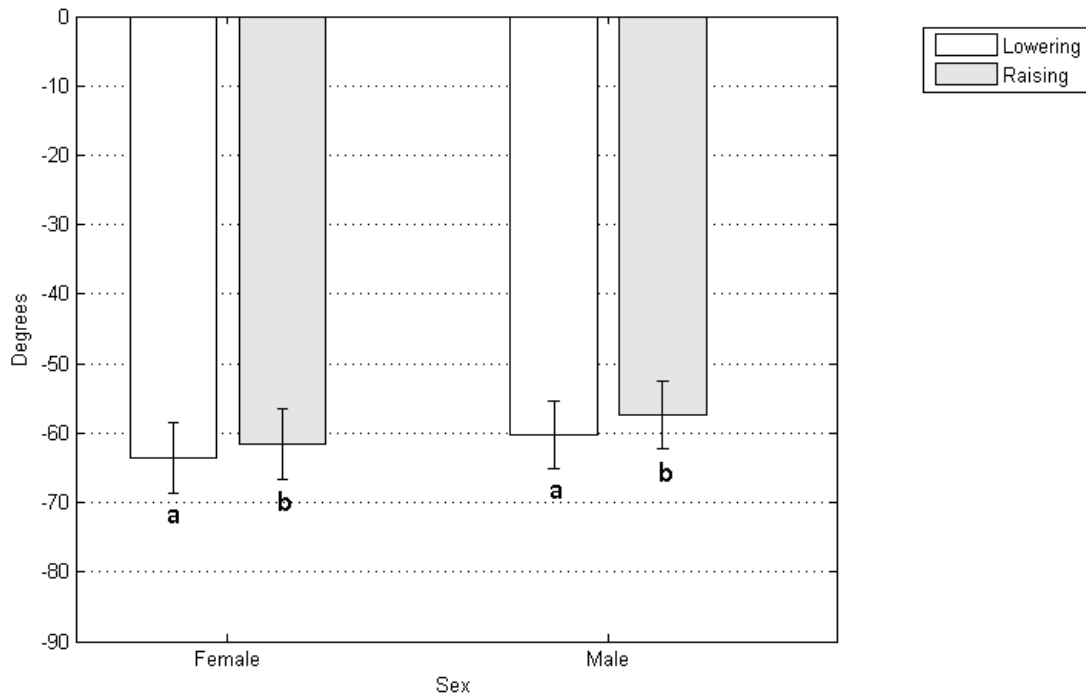


Figure 66: Effects of sex and humeral elevation phase on LSM right glenohumeral +internal/+external rotation (GIE). Levels not connected by same letter are significantly different (p-value: 0.05)

4.3.3 Acromioclavicular Kinematics

There was a main effect of humeral movement plane ($p < 0.0001$) and angle ($p < 0.0001$) on right acromioclavicular (AC) +protraction/-retraction (APR) and +depression/-elevation (AED). There was also an elevation phase effect on AED ($p < 0.0001$). A sex-plane interaction effect existed for both APR ($p = 0.0004$) and AED ($p < 0.0001$); however, sex-elevation angle ($p < 0.0001$), movement plane-angle ($p < 0.0001$), and elevation angle-phase ($p = 0.0002$) interactions existed only for APR. A summary of the main effects and interactions with F-statistics and p -values for AC kinematics is provided in Tables F7 in Appendix F8.

Humeral elevation within 60P resulted in significantly less AC elevation than any other plane (10.18°) while 30P, SCAP and 90P produced statistically identical AC elevation results (11.59° , 11.40° and 11.06 respectively). The most elevation was seen in the 120P (15.32°).

Increasing humeral elevation increments from 60E to 120E displayed significant increases in AC elevation (9.56° of elevation for 60E and 22.20° for 120E), while 15E, 30E and 45E were statistically the same and resulted in the lowest AC elevation (7.44°, 7.59° and 8.19° of elevation respectively). Finally, the lowering phase resulted in significantly less AC elevation (13.24°) than the raising phase (11.40°). Plots of interaction effects indicating the results of post-hoc Tukey HSD for acromioclavicular –elevation/+depression (AED) kinematics are provided in Figures 67 through 72, with the exception of AED movement plane-elevation angle interactions which are presented in Table 12.

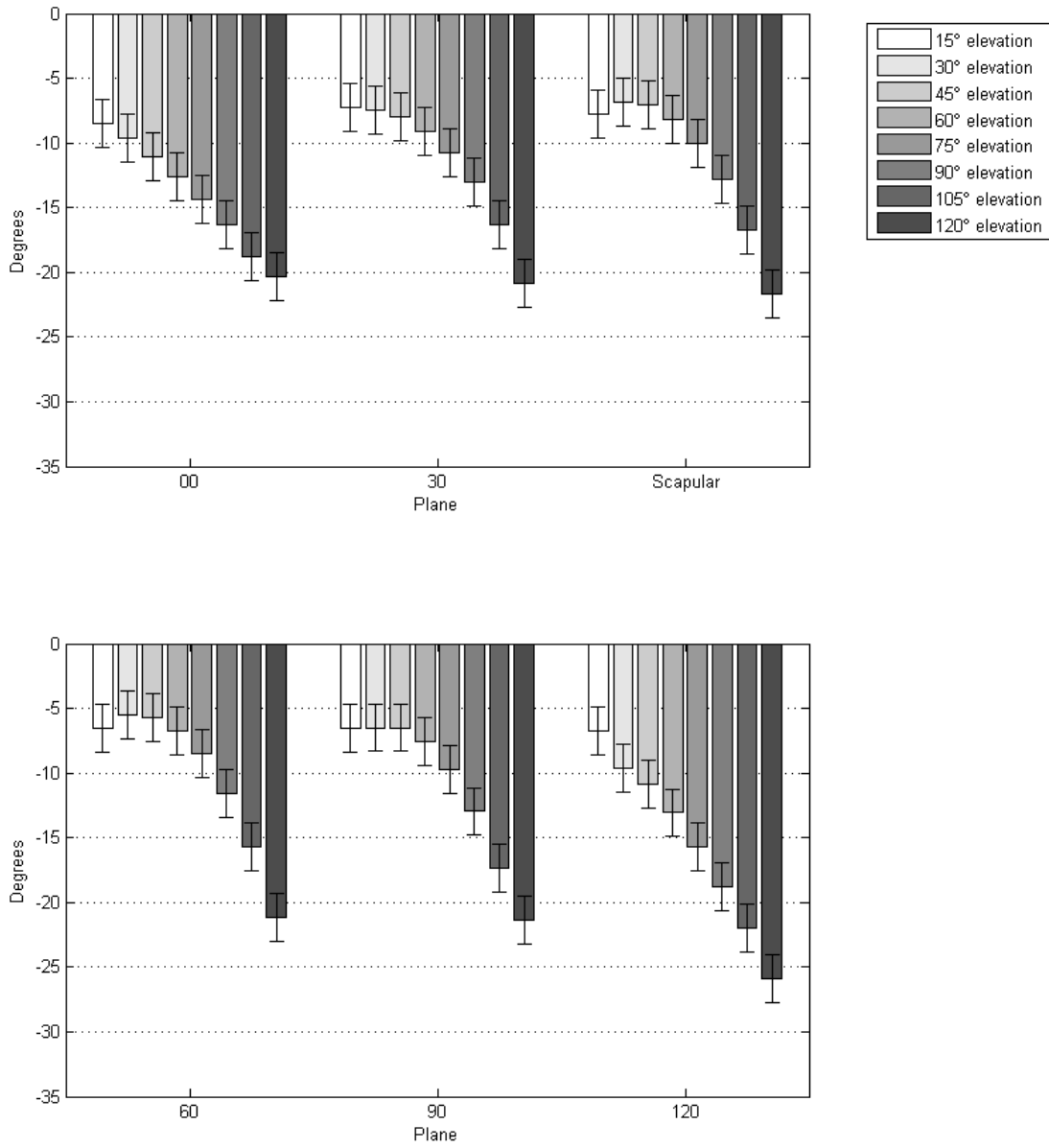


Figure 67: Effects of humeral movement plane and elevation angle on LSM right acromioclavicular depression +/-elevation (AED)

Table 12: Interaction effects of movement plane and humeral elevation angle on least squares mean (LSM) acromioclavicular elevation. Levels not connected by same letter are significantly different (*p*-value: 0.05)

| Level | LSM |
|-------|-----------------------|
| 4,30 | A -5.49 |
| 4,45 | A B -5.68 |
| 5,30 | A B C -6.49 |
| 5,45 | A B C -6.49 |
| 5,15 | A B C -6.58 |
| 4,15 | A B C -6.58 |
| 6,15 | A B C -6.71 |
| 4,60 | A B C -6.75 |
| 3,30 | A B C D -6.88 |
| 3,45 | A B C D E -7.06 |
| 2,15 | A B C D E F -7.24 |
| 2,30 | A B C D E F -7.43 |
| 5,60 | A B C D E F -7.59 |
| 3,15 | A B C D E F G -7.79 |
| 2,45 | A B C D E F G -8.01 |
| 3,60 | A B C D E F G -8.17 |
| 1,15 | A B C D E F G -8.53 |
| 4,75 | A B C D E F G -8.53 |
| 2,60 | A B C D E F G H -9.10 |
| 6,30 | B C D E F G H I -9.60 |
| 1,30 | C D E F G H I -9.65 |
| 5,75 | C D E F G H I -9.75 |
| 3,75 | C D E F G H I -10.00 |
| 2,75 | D E F G H I J -10.79 |
| 6,45 | E F G H I J -10.84 |
| 1,45 | F G H I J -11.05 |
| 4,90 | G H I J -11.57 |
| 1,60 | H I J K -12.65 |
| 3,90 | H I J K L -12.85 |
| 5,90 | H I J K L -12.97 |
| 2,90 | H I J K L -13.01 |
| 6,60 | I J K L -13.07 |
| 1,75 | J K L M -14.35 |
| 4,105 | K L M N -15.66 |
| 6,75 | K L M N -15.73 |
| 1,90 | K L M N -16.33 |
| 2,105 | K L M N -16.33 |
| 3,105 | L M N O -16.75 |
| 5,105 | M N O P -17.33 |
| 6,90 | N O P Q -18.76 |
| 1,105 | N O P Q -18.79 |
| 1,120 | O P Q -20.31 |
| 2,120 | P Q -20.84 |
| 4,120 | P Q -21.12 |
| 5,120 | Q -21.32 |
| 3,120 | Q -21.68 |
| 6,105 | Q -21.94 |
| 6,120 | R -25.92 |

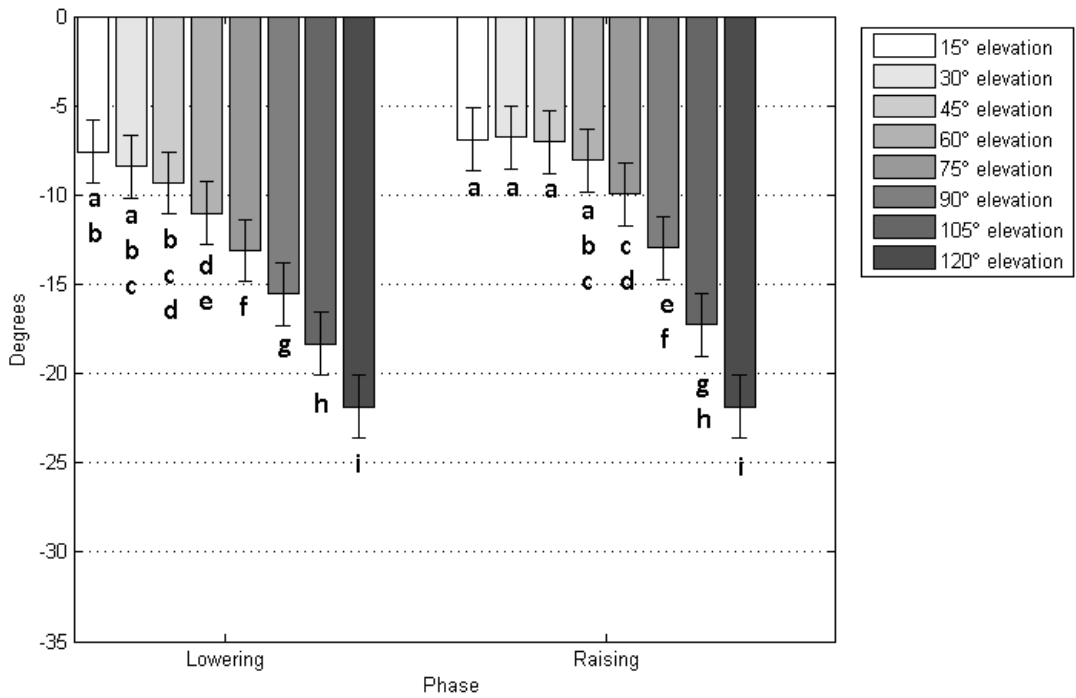


Figure 68: Effects of humeral elevation phase and elevation angle on LSM right acromioclavicular –elevation/+depression (AED). Levels not connected by same letter are significantly different (p-value: 0.05)

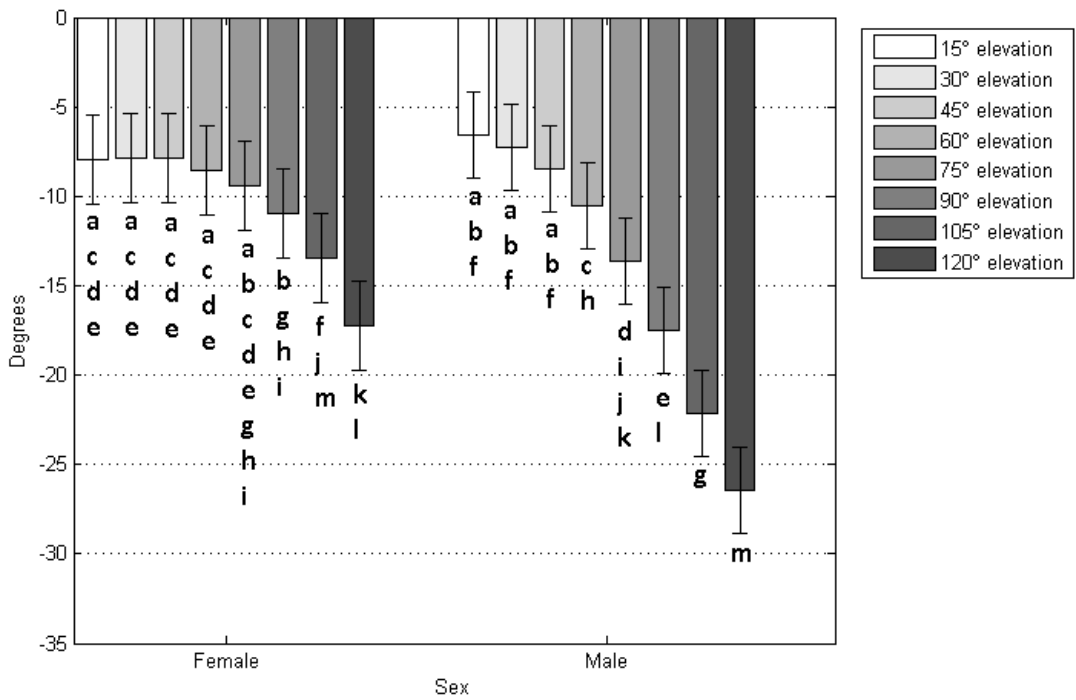


Figure 69: Effects of sex and humeral elevation angle on LSM right acromioclavicular –elevation/+depression (AED). Levels not connected by same letter are significantly different (p-value: 0.05)

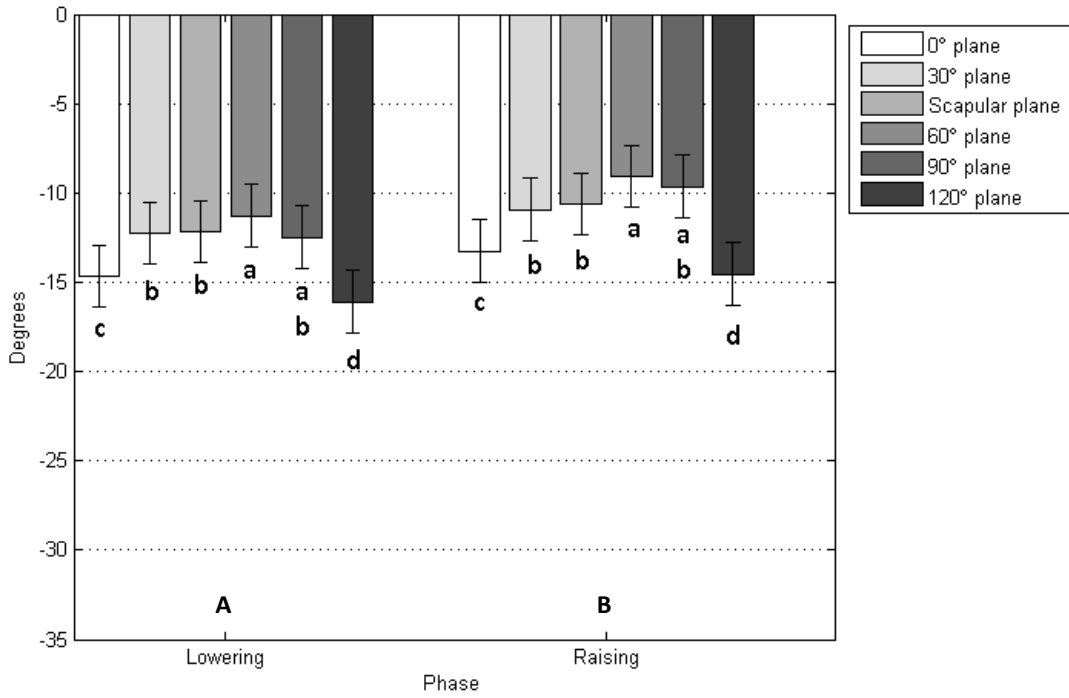


Figure 70: Effects of humeral elevation phase and movement plane on LSM right acromioclavicular – elevation/+depression (AED). Levels not connected by same letter are significantly different (p-value: 0.05)

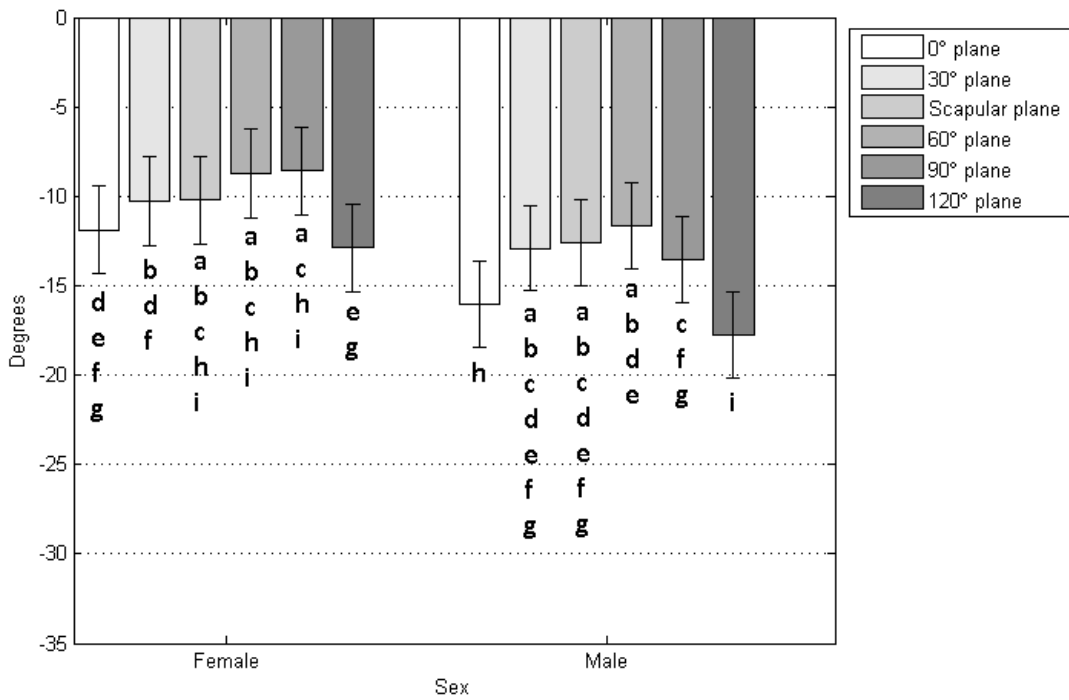


Figure 71: Effects of sex and humeral movement plane on LSM right acromioclavicular – elevation/+depression (AED). Levels not connected by same letter are significantly different (p-value: 0.05)

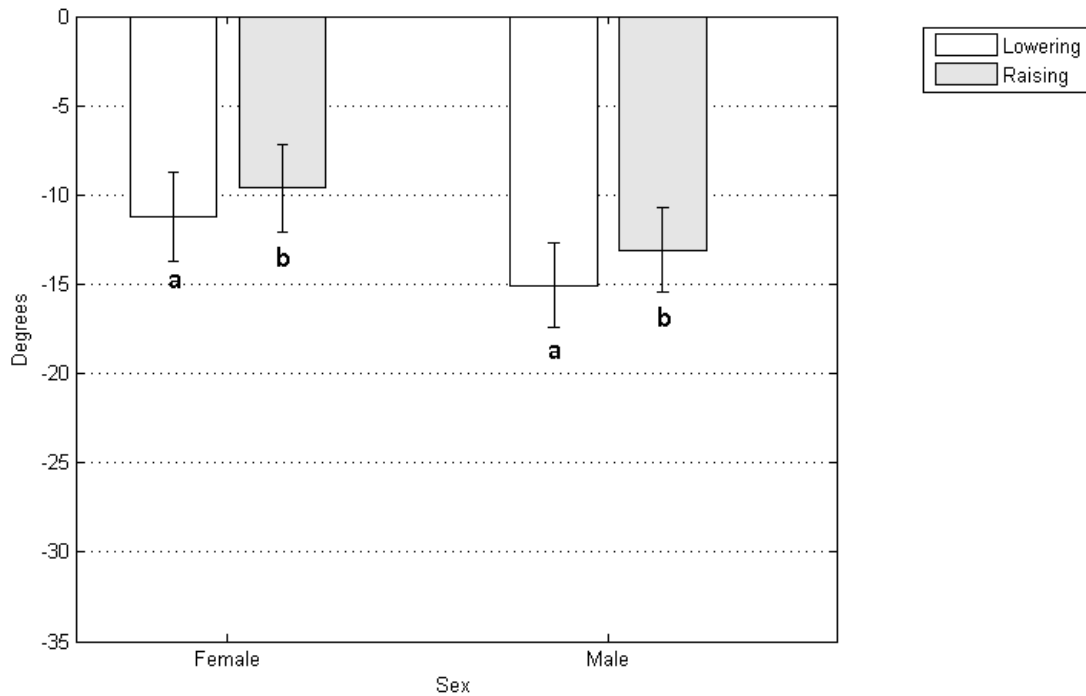


Figure 72: Effects of sex and humeral elevation phase on LSM right acromioclavicular – elevation/+depression (AED). Levels not connected by same letter are significantly different (p-value: 0.05)

Humeral elevation within 0P resulted in significantly more AC protraction than any other plane (45.56° of protraction). 60P and 90P were statistically the same (39.36° and 38.58° of protraction respectively) and resulted in the least AC protraction. Protraction within 30P, SCAP, and 120P were also statistically equivalent (41.74°, 40.84° and 41.47° respectively). 120E demonstrated significantly more AC protraction than all other elevation angles (47.05°). 30E, 45E, 60E, and 75E were statistically identical and resulted in the lowest AC protraction (39.63°, 38.69°, 38.63°, and 39.57° of protraction respectively). 15E and 105E resulted in statistically equivalent AC protraction (41.36° and 41.25° respectively). Plots of interaction effects indicating the results of post-hoc Tukey HSD for acromioclavicular +protraction/-retraction (APR)

kinematics are provided in Figures 73 through 78, with the exception of APR sex-humeral elevation angle which are presented in Table 13.

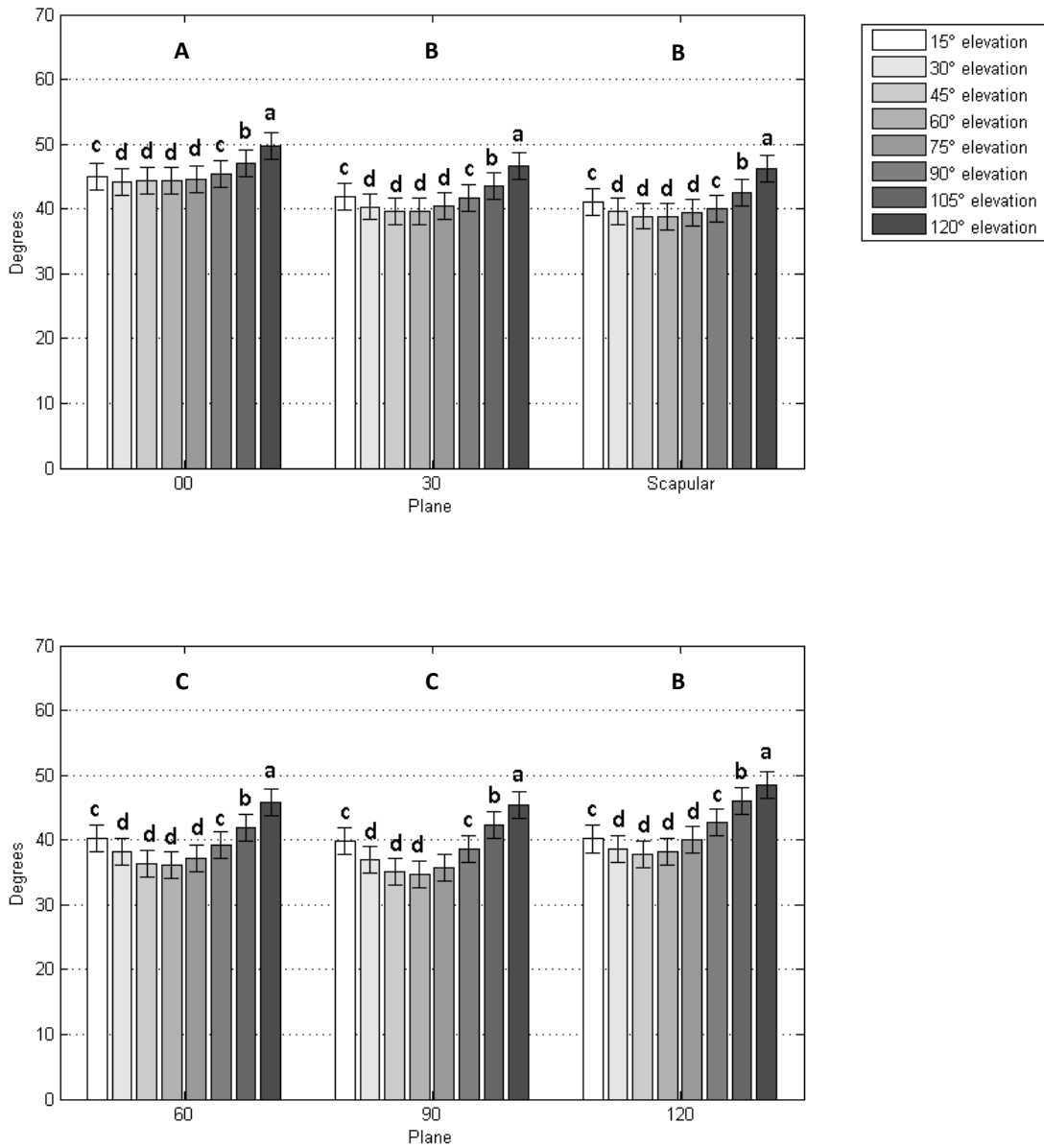


Figure 73: Effects of humeral movement plane and elevation angle on LSM right acromioclavicular +protraction/-retraction (APR). Levels not connected by same letter are significantly different (p-value: 0.05)

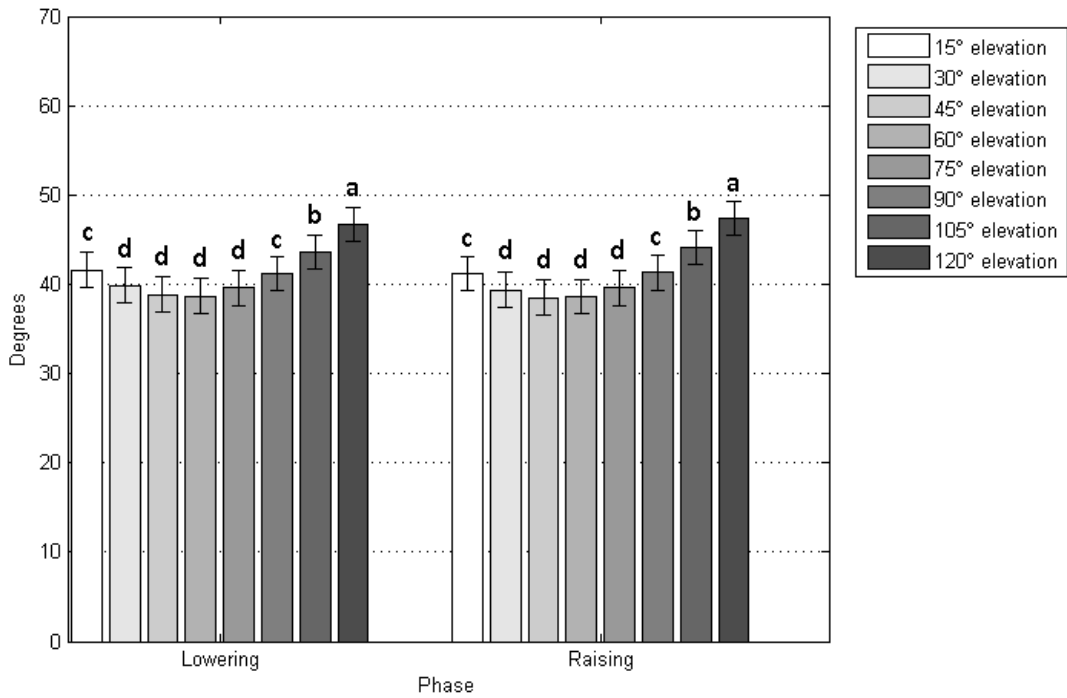


Figure 74: Effects of humeral elevation phase and elevation angle on LSM right acromioclavicular +protraction/-retraction (APR). Levels not connected by same letter are significantly different (p-value: 0.05)

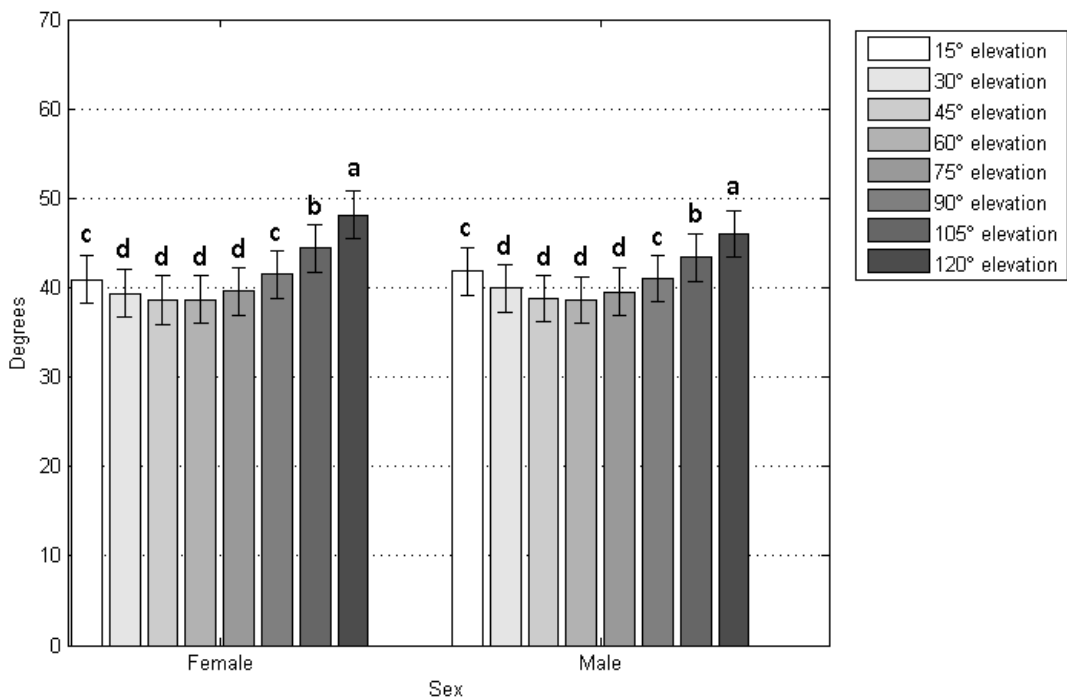


Figure 75: Effects of sex and humeral elevation angle on LSM right acromioclavicular +protraction/-retraction (APR). Levels not connected by same letter are significantly different (p-value: 0.05)

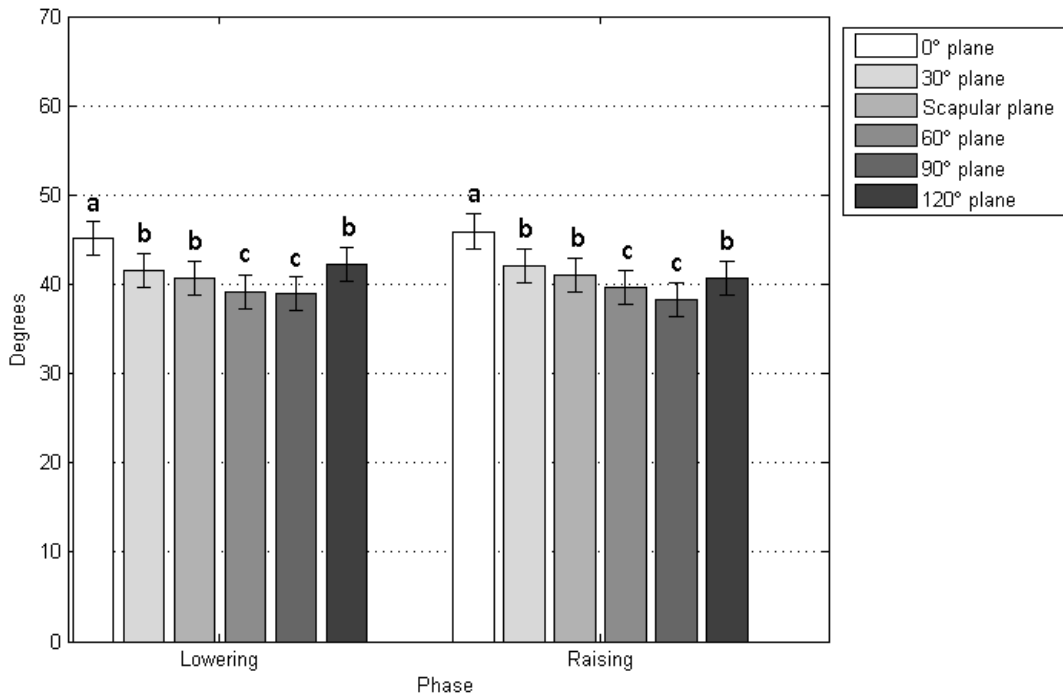


Figure 76: Effects of humeral elevation phase and movement plane on LSM right acromioclavicular +protraction/-retraction (APR). Levels not connected by same letter are significantly different (p-value: 0.05)

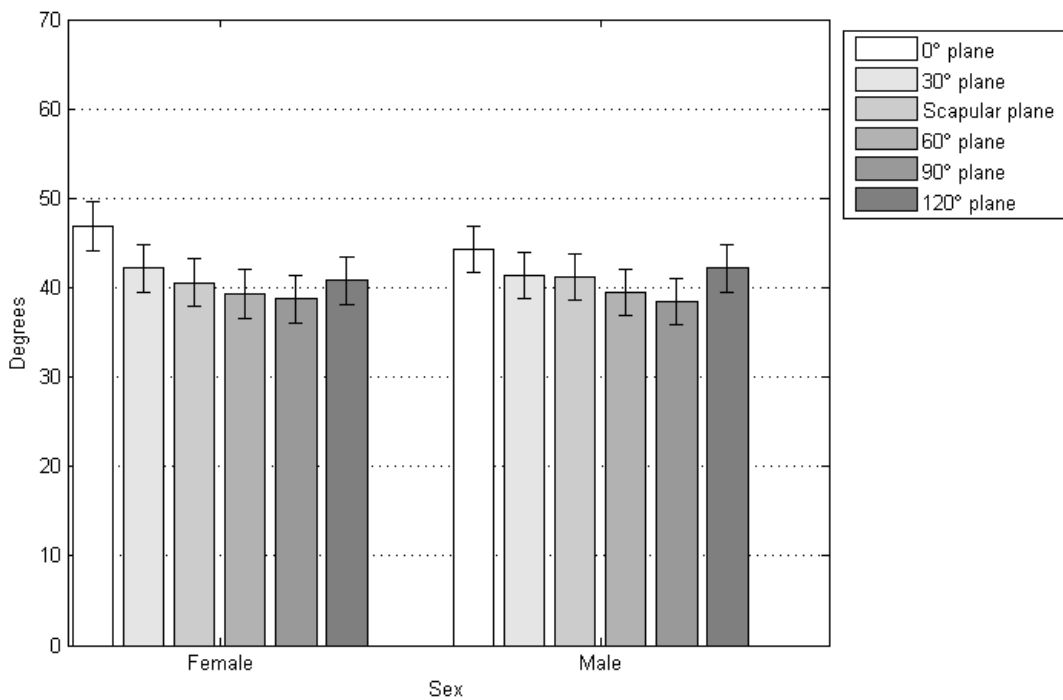


Figure 77: Effects of sex and humeral movement plane on LSM right acromioclavicular +protraction/-retraction (APR). Levels not connected by same letter are significantly different (p-value: 0.05)

Table 13: Interaction effects of sex and humeral movement plane on least squares mean (LSM) acromioclavicular +protraction/-retraction. Levels not connected by same letter are significantly different (p-value: 0.05)

| Level | | | | | | | | | LSM |
|-------|---|---|---|---|---|---|---|---|-------|
| 1,1 | A | | | | E | | | | 46.87 |
| 2,1 | A | B | | | | | | | 44.25 |
| 1,2 | | B | C | | | F | G | | 42.17 |
| 2,6 | | | C | D | | | | | 42.14 |
| 2,2 | | | C | D | E | F | | H | 41.31 |
| 2,3 | | | C | D | E | F | | H | 41.14 |
| 1,6 | B | C | D | | F | G | H | I | 40.79 |
| 1,3 | | B | C | D | | F | G | H | 40.55 |
| 2,4 | | | | | E | F | G | H | 39.42 |
| 1,4 | | | | D | | | | H | 39.30 |
| 1,5 | | | | D | | | | H | 38.71 |
| 2,5 | | | | | | G | | I | 38.46 |

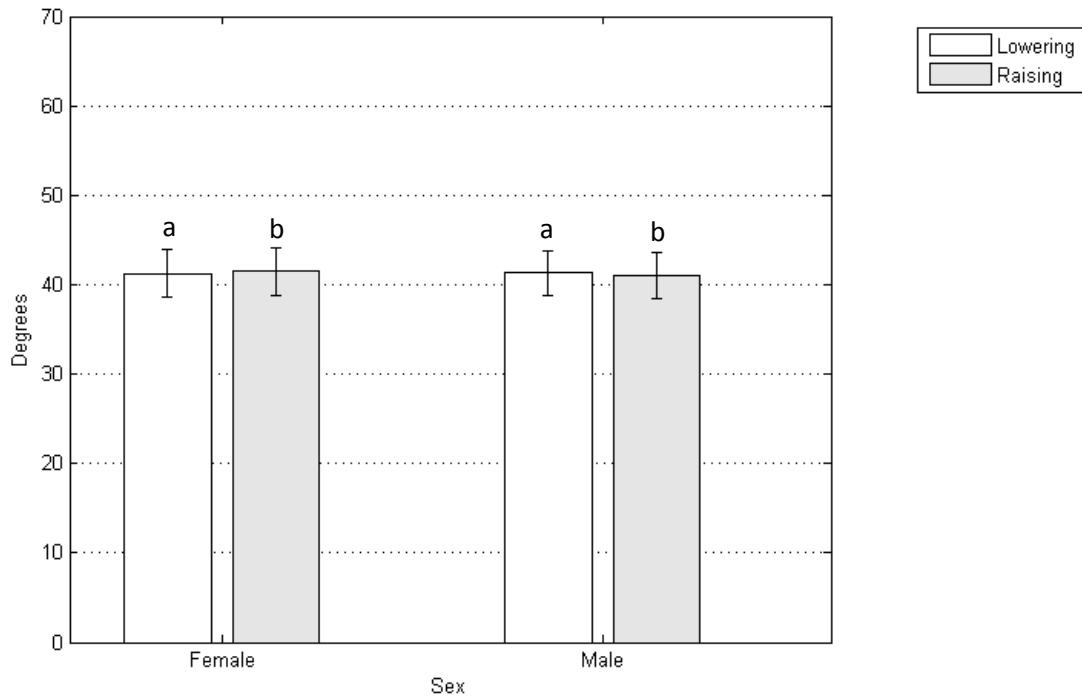


Figure 78: Effects of sex and humeral elevation phase on LSM right acromioclavicular +protraction/-retraction (APR). Levels not connected by same letter are significantly different (p-value: 0.05)

4.3.4 Sternoclavicular Kinematics

There was a main effect of humeral movement plane ($p < 0.0001$), angle ($p < 0.0001$), and phase ($p < 0.0001$) on right sternoclavicular (SC) +protraction/-retraction (CPR) and +depression/-elevation (CED). Sex-movement plane, sex-elevation angle, sex-phase, movement plane-elevation angle, movement plane-phase, and elevation angle-phase interaction effects were present for both CPR ($p < 0.0001$ for all significant interactions) and CED ($p < 0.0001$ for all significant interactions except for sex-movement plane where $p = 0.0124$). A summary of the main effects and interactions with F-statistics and p -values for SC kinematics is provided in Tables 9 in Appendix 10

As movement plane progressively changed across the body from 0P through to 120P, overall SC retraction decreased significantly (-32.31° to -24.92° respectively). However, significant increases of SC retraction occurred at each increment of elevation (-19.16° at 15E through to -39.91 at 120E). Also, more retraction occurred during the lowering phase (-30.17°) than the raising phase (-27.30°). Plots of interaction effects indicating the results of post-hoc Tukey HSD for SC retraction kinematics are provided in Figures 79 through 84, with the exception of SC retraction movement plane-elevation angle interactions which are displayed in Table 14.

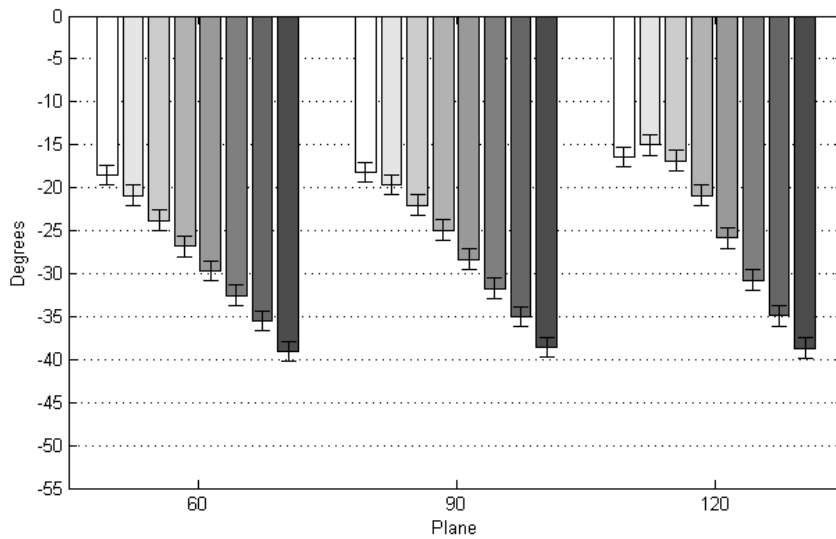
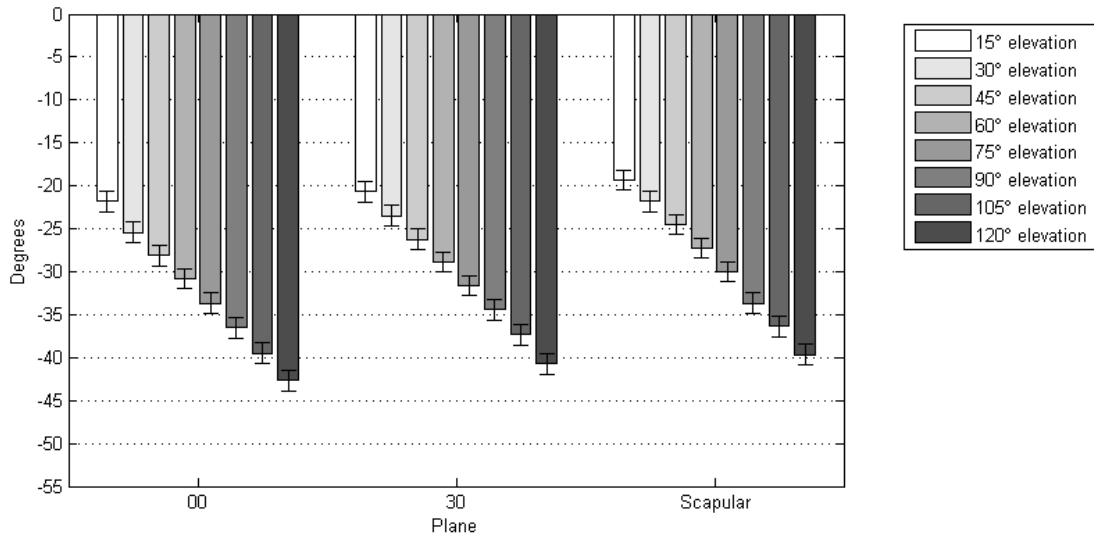


Figure 79: Effects of humeral movement plane and elevation angle on LSM right sternoclavicular +protraction/-retraction (CPR)

Table 14: Interaction effects of movement plane and humeral elevation angle on least squares mean (LSM) sternoclavicular +protraction/-retraction. Levels not connected by same letter are significantly different (*p*-value: 0.05)

| Level | | LSM |
|-------|-----------|--------|
| 6,30 | A | -15.03 |
| 6,15 | A B | -16.42 |
| 6,45 | A B | -16.83 |
| 5,15 | B C | -18.20 |
| 4,15 | B C D | -18.53 |
| 3,15 | C D E | -19.31 |
| 5,30 | C D E F | -19.66 |
| 2,15 | D E F G | -20.70 |
| 4,30 | E F G | -20.88 |
| 6,60 | E F G | -20.91 |
| 1,15 | F G H | -21.80 |
| 3,30 | F G H | -21.82 |
| 5,45 | G H | -22.01 |
| 2,30 | H I | -23.47 |
| 4,45 | H I J | -23.81 |
| 3,45 | I J K | -24.50 |
| 5,60 | I J K L | -24.96 |
| 1,30 | I J K L M | -25.44 |
| 6,75 | J K L M | -25.84 |
| 2,45 | K L M N | -26.22 |
| 4,60 | L M N O | -26.83 |
| 3,60 | M N O | -27.23 |
| 1,45 | N O P | -28.11 |
| 5,75 | N O P | -28.33 |
| 2,60 | O P Q | -28.89 |
| 4,75 | P Q R | -29.70 |
| 3,75 | P Q R | -29.99 |
| 6,90 | Q R S | -30.75 |
| 1,60 | Q R S | -30.80 |
| 2,75 | R S T | -31.65 |
| 5,90 | R S T | -31.72 |
| 4,90 | S T U | -32.55 |
| 1,75 | T U V | -33.65 |
| 3,90 | T U V | -33.70 |
| 2,90 | U V W | -34.45 |
| 6,105 | V W | -34.90 |
| 5,105 | V W | -35.04 |
| 4,105 | V W X | -35.51 |
| 3,105 | W X Y | -36.35 |
| 1,90 | W X Y Z | -36.51 |
| 2,105 | X Y Z [| -37.35 |
| 5,120 | Y Z [\ | -38.59 |
| 6,120 | Z [\ | -38.67 |
| 4,120 | [\ | -39.07 |
| 1,105 | [\ | -39.50 |
| 3,120 | \ | -39.68 |
| 2,120 | \] | -40.76 |
| 1,120 |] | -42.70 |

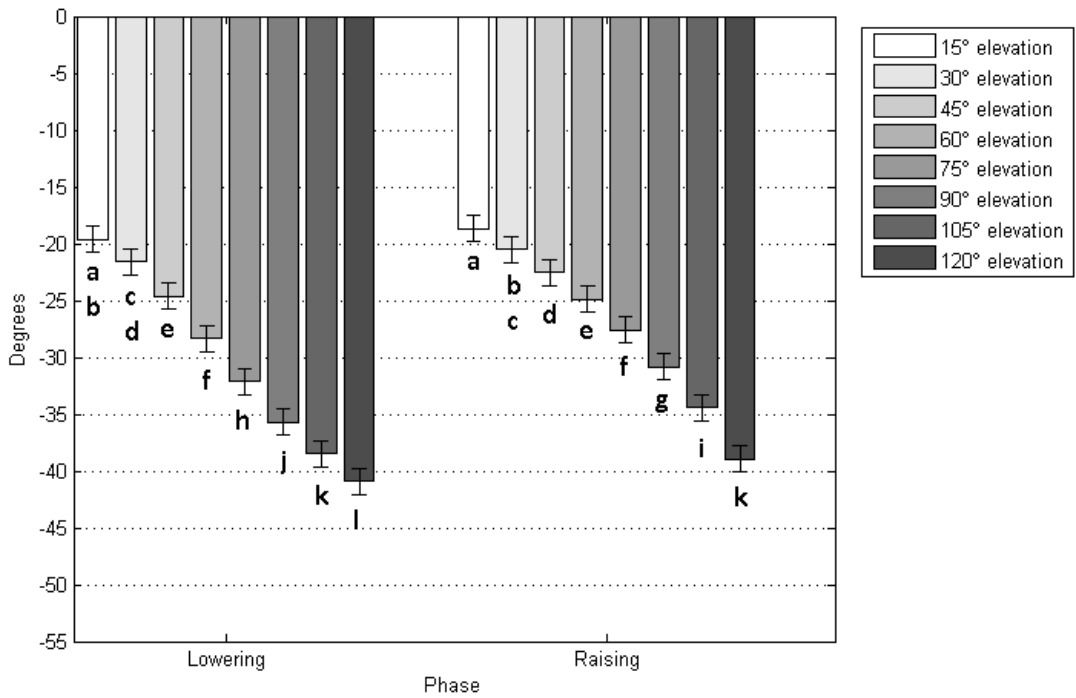


Figure 80: Effects of humeral elevation phase and elevation angle on LSM right sternoclavicular +protraction/-retraction (CPR). Levels not connected by same letter are significantly different (p-value: 0.05)

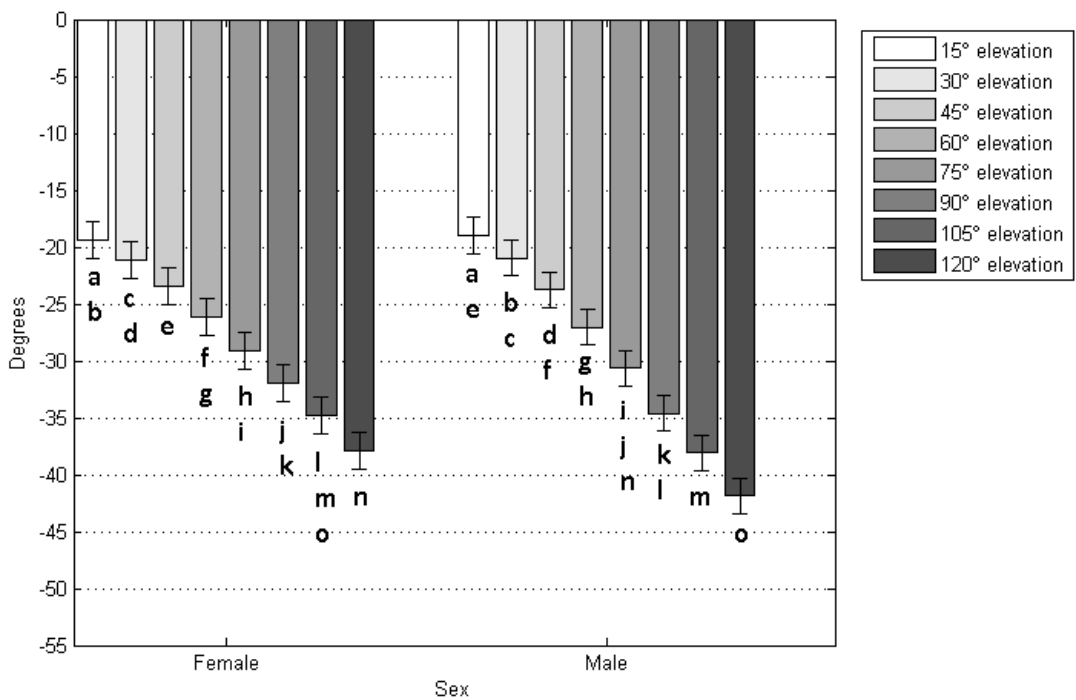


Figure 81: Effects of sex and humeral elevation angle on LSM right sternoclavicular +protraction/-retraction (CPR). Levels not connected by same letter are significantly different (p-value: 0.05)

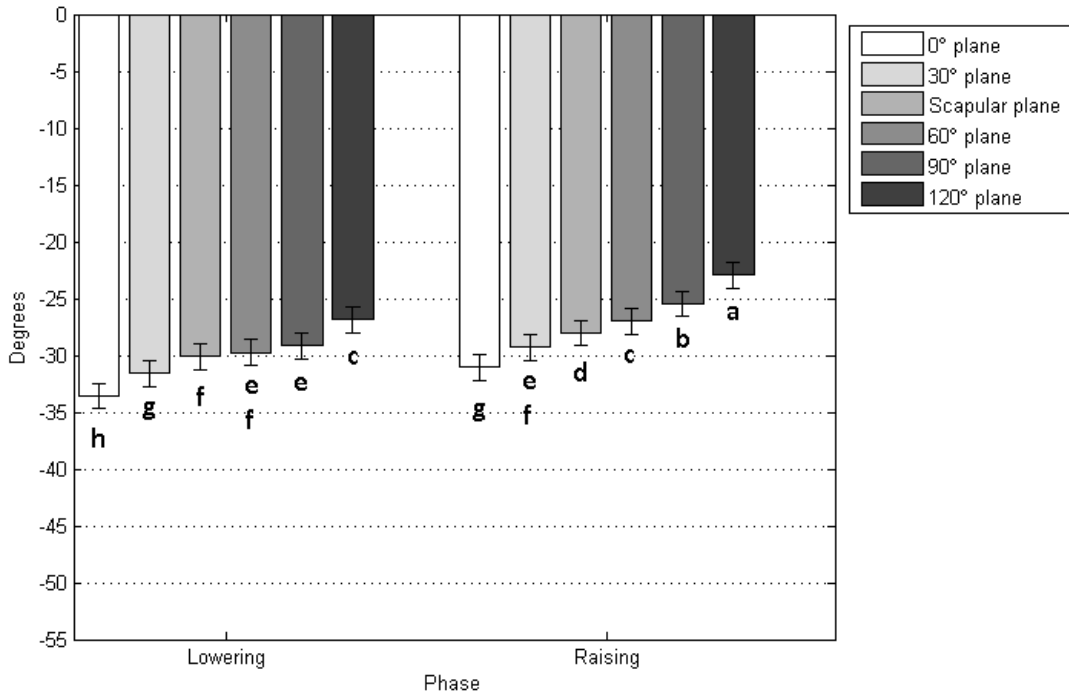


Figure 82: Effects of humeral elevation phase and movement plane on LSM right sternoclavicular +protraction/-retraction (CPR). Levels not connected by same letter are significantly different (p-value: 0.05)

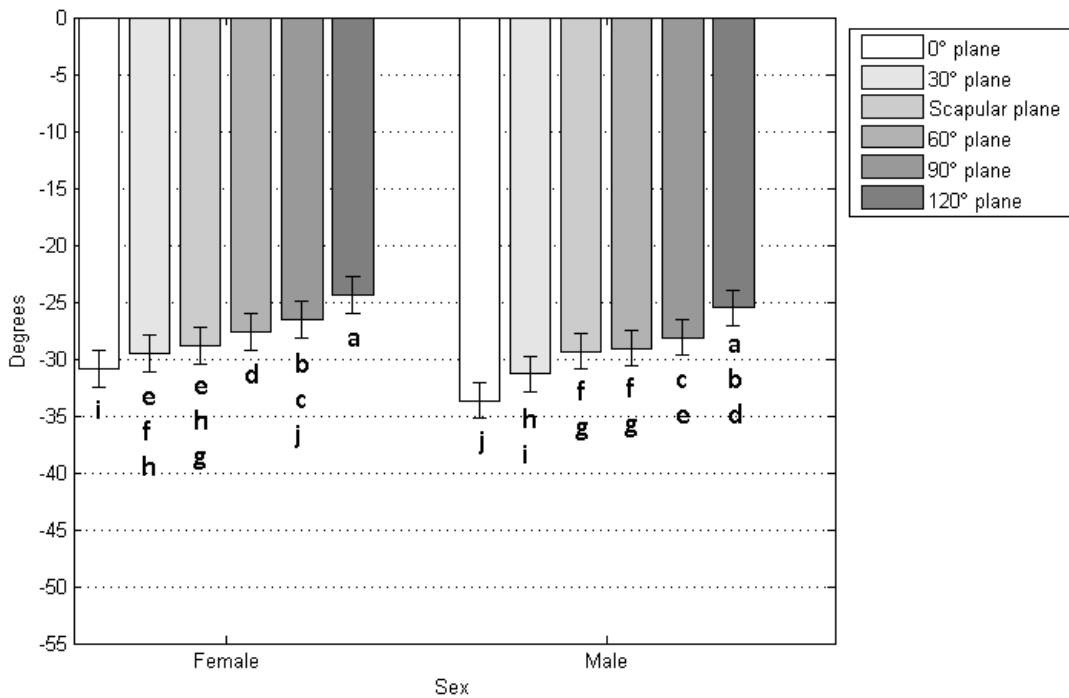


Figure 83: Effects of sex and humeral movement plane on LSM right sternoclavicular +protraction/-retraction (CPR). Levels not connected by same letter are significantly different (p-value: 0.05)

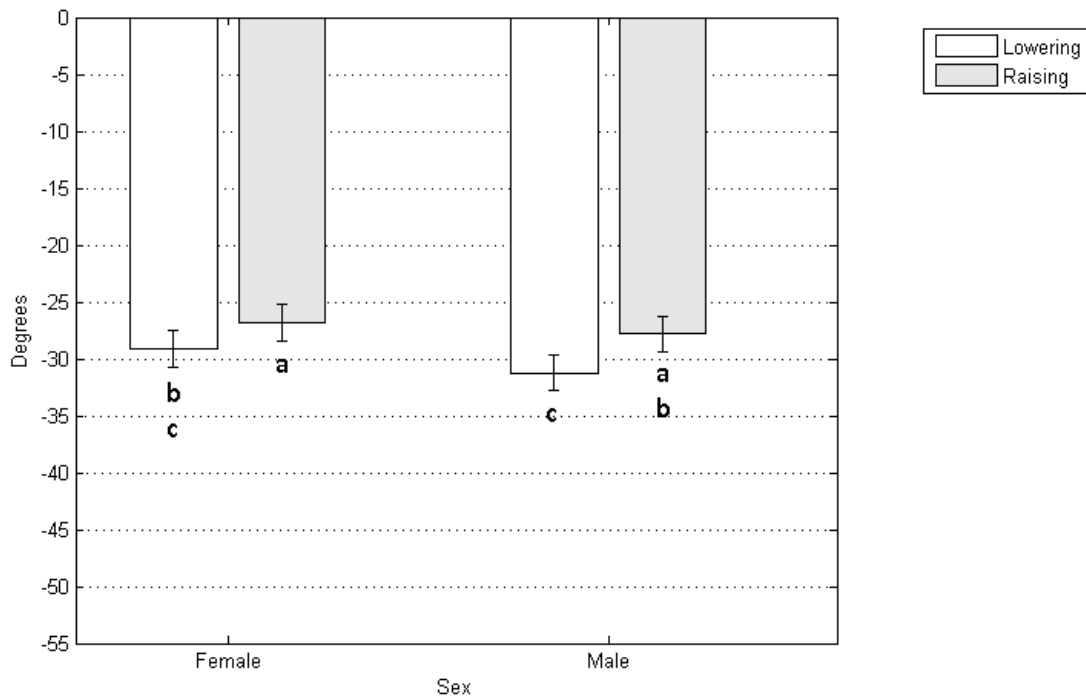


Figure 84: Effects of sex and humeral elevation phase on LSM right sternoclavicular +protraction/-retraction (CPR). Levels not connected by same letter are significantly different (p-value: 0.05)

The highest observed SC elevation occurred in 120P (-21.32°) while the lowest occurred in SCAP and 60P (-16.64° and -16.31° of elevation respectively). Significantly greater SC elevation occurred at each increment of elevation (-9.60° at 15E through to -25.80° at 120E). Lastly, significantly more elevation occurred during the lowering phase (-18.24°) than the raising phase (-17.57°). Plots of interaction effects indicating the results of post-hoc Tukey HSD for SC elevation kinematics are provided in Figures 85 through 90, with the exception of SC retraction movement plane-elevation angle interactions which are displayed in table for in Table 15.

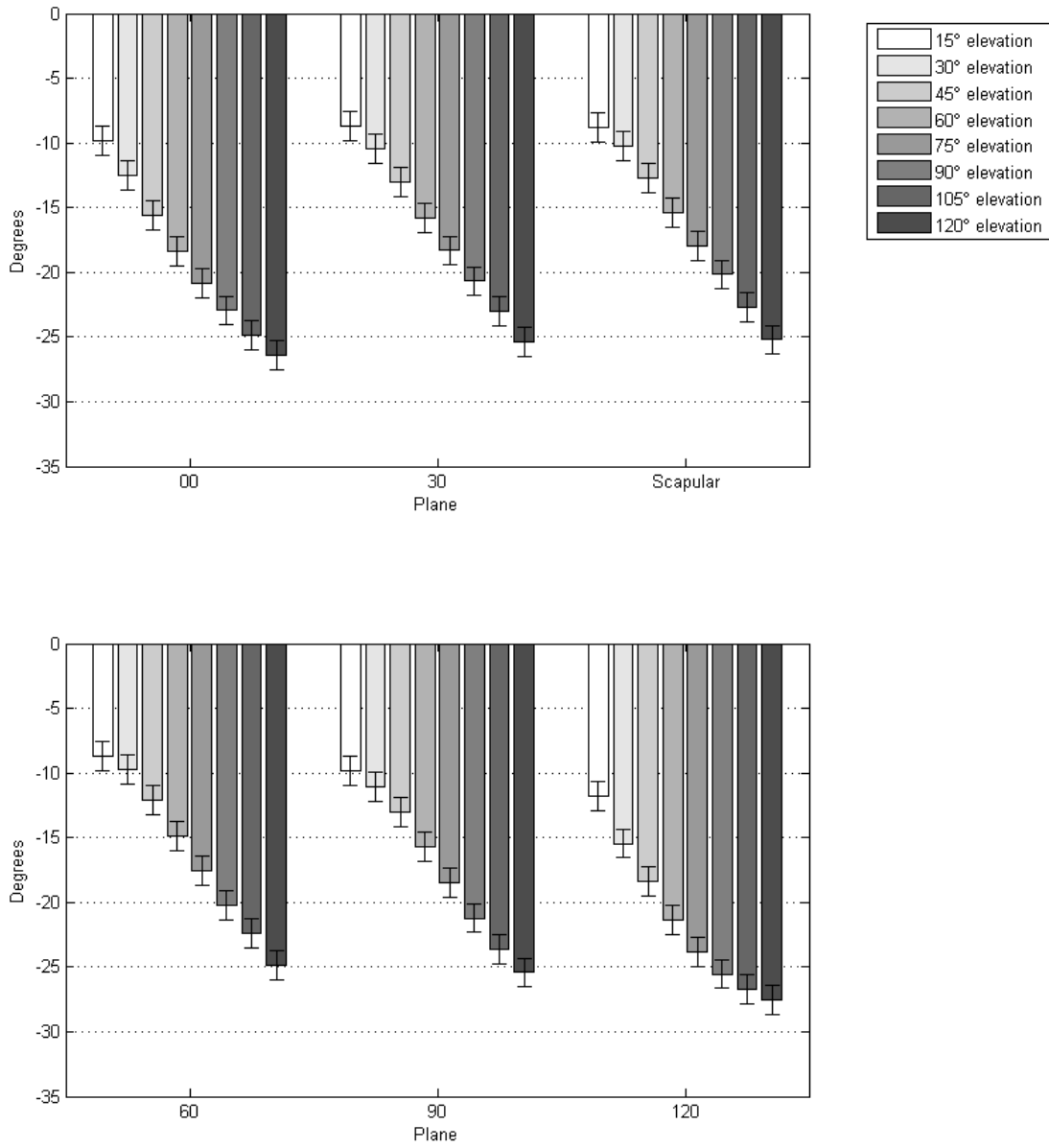


Figure 85: Effects of humeral movement plane and elevation angle on LSM right sternoclavicular - depression/+elevation (CED)

Table 15: Interaction effects of movement plane and humeral elevation angle on least squares mean (LSM) sternoclavicular +depression/-elevation. Levels not connected by same letter are significantly different (*p*-value: 0.05)

| Level | LSM |
|---------------|--------|
| 2,15 A | -8.66 |
| 4,15 A | -8.68 |
| 3,15 A | -8.80 |
| 4,30 A B | -9.74 |
| 5,15 A B | -9.83 |
| 1,15 A B | -9.83 |
| 3,30 A B C | -10.25 |
| 2,30 A B C D | -10.48 |
| 5,30 B C D E | -11.10 |
| 6,15 C D E F | -11.83 |
| 4,45 D E F | -12.10 |
| 1,30 E F | -12.52 |
| 3,45 E F | -12.68 |
| 5,45 F | -13.05 |
| 2,45 F | -13.05 |
| 4,60 G | -14.88 |
| 3,60 G | -15.36 |
| 6,30 G | -15.45 |
| 1,45 G | -15.61 |
| 5,60 G | -15.69 |
| 2,60 G H | -15.78 |
| 4,75 H I | -17.58 |
| 3,75 I | -17.95 |
| 2,75 I | -18.32 |
| 6,45 I J | -18.35 |
| 1,60 I J | -18.38 |
| 5,75 I J K | -18.47 |
| 3,90 J K L | -20.17 |
| 4,90 K L | -20.24 |
| 2,90 L M | -20.69 |
| 1,75 L M | -20.88 |
| 5,90 L M N | -21.22 |
| 6,60 L M N | -21.33 |
| 4,105 M N O | -22.40 |
| 3,105 N O | -22.72 |
| 1,90 N O | -22.94 |
| 2,105 N O P | -23.04 |
| 5,105 O P Q | -23.66 |
| 6,75 O P Q R | -23.84 |
| 4,120 P Q R S | -24.86 |
| 1,105 Q R S T | -24.89 |
| 3,120 Q R S T | -25.22 |
| 2,120 Q R S T | -25.36 |
| 5,120 Q R S T | -25.41 |
| 6,90 R S T | -25.53 |
| 1,120 S T U | -26.40 |
| 6,105 T U | -26.71 |
| 6,120 U | -27.54 |

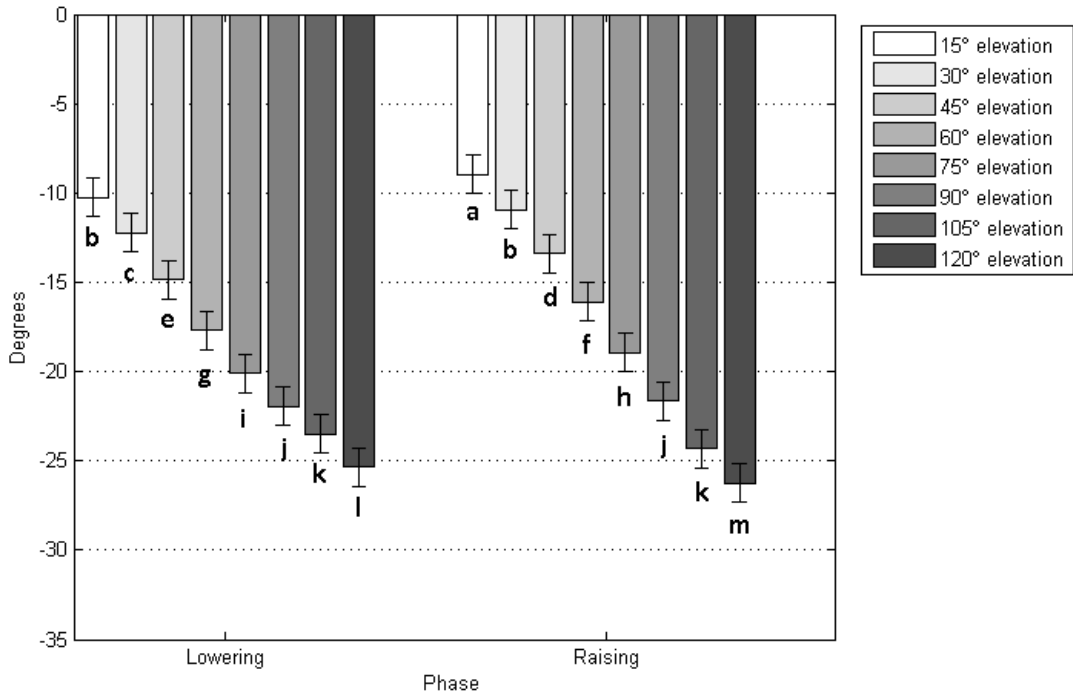


Figure 86: Effects of humeral elevation phase and elevation angle on LSM right sternoclavicular -depression/+elevation (CED). Levels not connected by same letter are significantly different (p-value: 0.05)

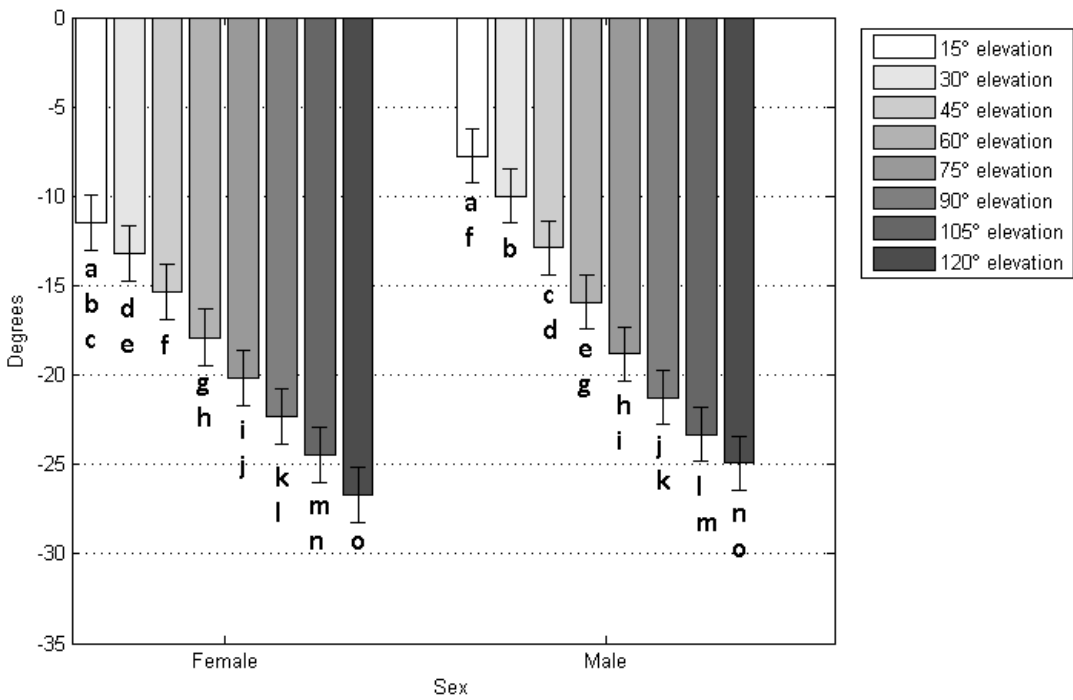


Figure 87: Effects of sex and humeral elevation angle on LSM right sternoclavicular -depression/+elevation (CED). Levels not connected by same letter are significantly different (p-value: 0.05)

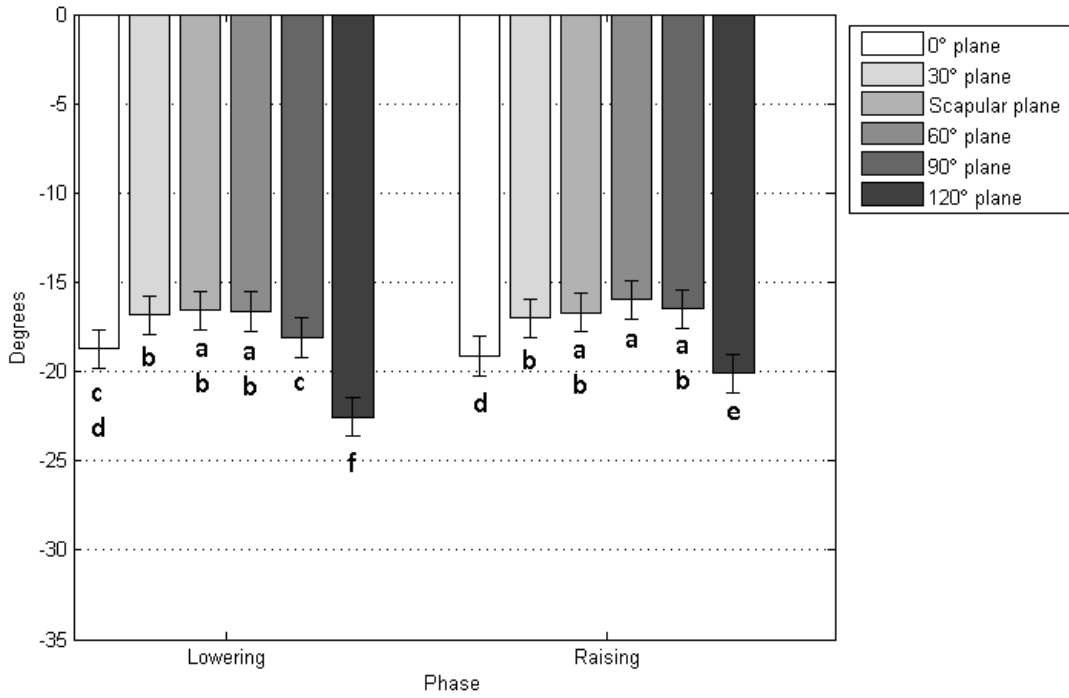


Figure 88: Effects of humeral elevation phase and movement plane on LSM right sternoclavicular -depression/+elevation (CED). Levels not connected by same letter are significantly different (p-value: 0.05)

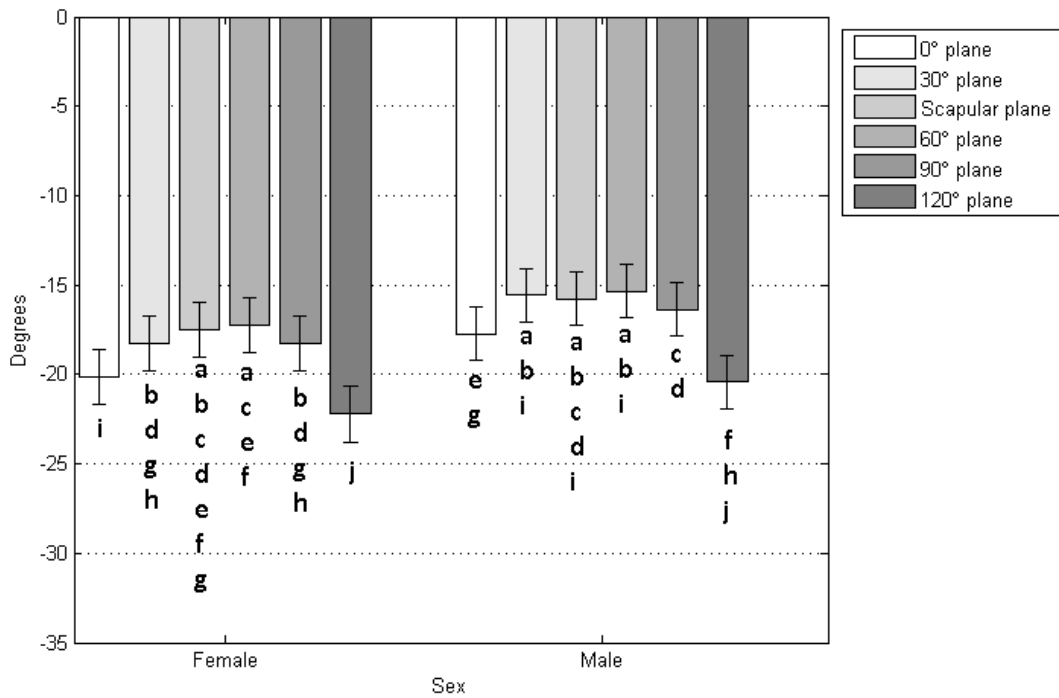


Figure 89: Effects of sex and humeral movement plane on LSM right sternoclavicular -depression/+elevation (CED). Levels not connected by same letter are significantly different (p-value: 0.05)

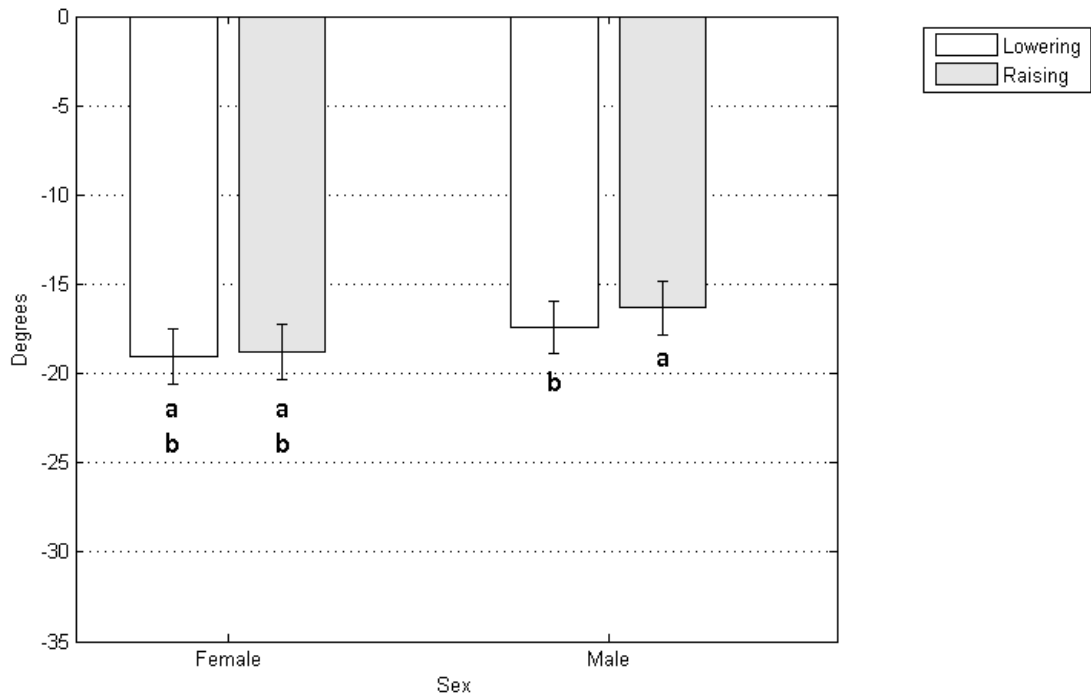


Figure 90: Effects of sex and humeral elevation phase on LSM right sternoclavicular -depression/+elevation (CED). Levels not connected by same letter are significantly different (p-value: 0.05)

4.4 Variability Summary

Figure 91 provides a graphical summary of the variability (standard deviation SD) observed for each measured joint rotation, averaged across all movement planes and movement phases, at each increment of humeral elevation. The total of each bar represents the total average SD observed at that humeral elevation angle. Each stacked bar represents the average SD observed for a given rotation (indicated in the legend) at a given humeral elevation angle. SD measures at given elevation angles and movement planes were taken from the kinematic profiles in Figures 21 through 30. The greatest total average kinematic SD was evident at the 10E elevation angle (223.74°), while 105E demonstrated the lowest total average SD (126.34°). Moreover, glenohumeral +internal/-external rotation or glenohumeral +anterior/-posterior plane of elevation demonstrated the highest individual average SD measures at a given elevation angle while clavicle rotations demonstrated the lowest.

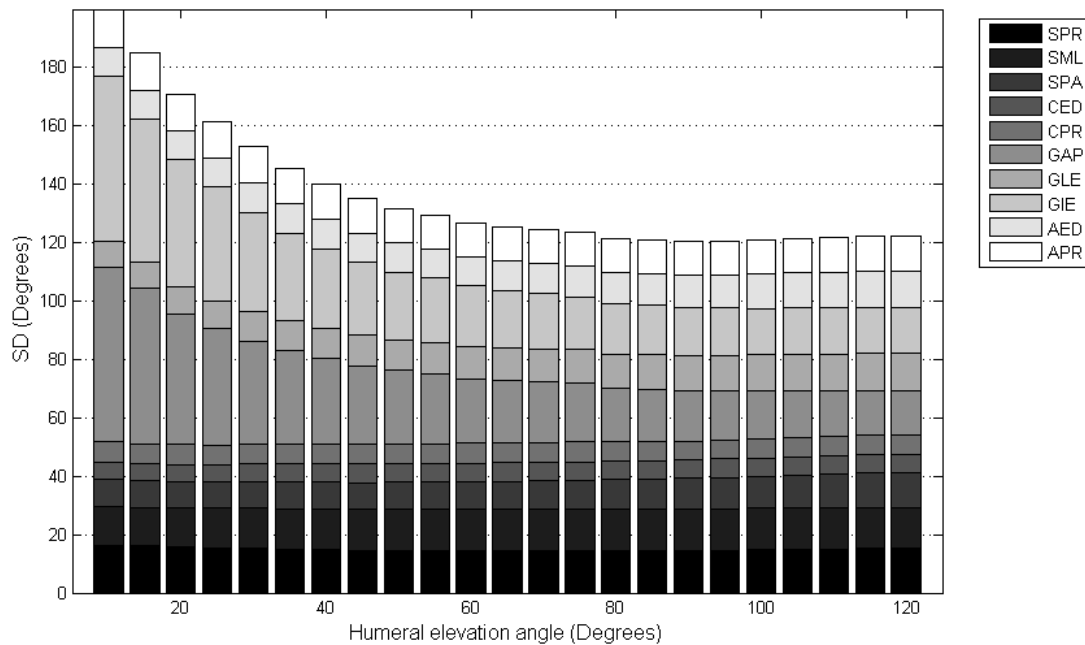


Figure 91: Total and individual joint rotation variation (standard deviation) at all measured humeral elevation angles averaged across planes

Figure 92 provides a graphical summary of the variability (SD) observed for each calculated joint rotation averaged within movement plane. The total of each bar represents the total average SD observed in a specific movement plane, averaged across the measured range of humeral elevation. Each stacked bar represents the average SD observed for a given rotation for a given movement plane. The greatest total average kinematic SD was seen in the 120P plane (171.62°). Likewise, the average SD observed in the 0P plane was similarly high (170.42°). However, the difference between the largest (120P, 171.62°) and smallest (60P, 151.82°) within plane total SD was 19.81°, representing an 11.54% difference. The rotations with the highest individual average SD within each plane were GIE and GAP, while HLE and the clavicle rotations demonstrated the lowest within plane average SD.

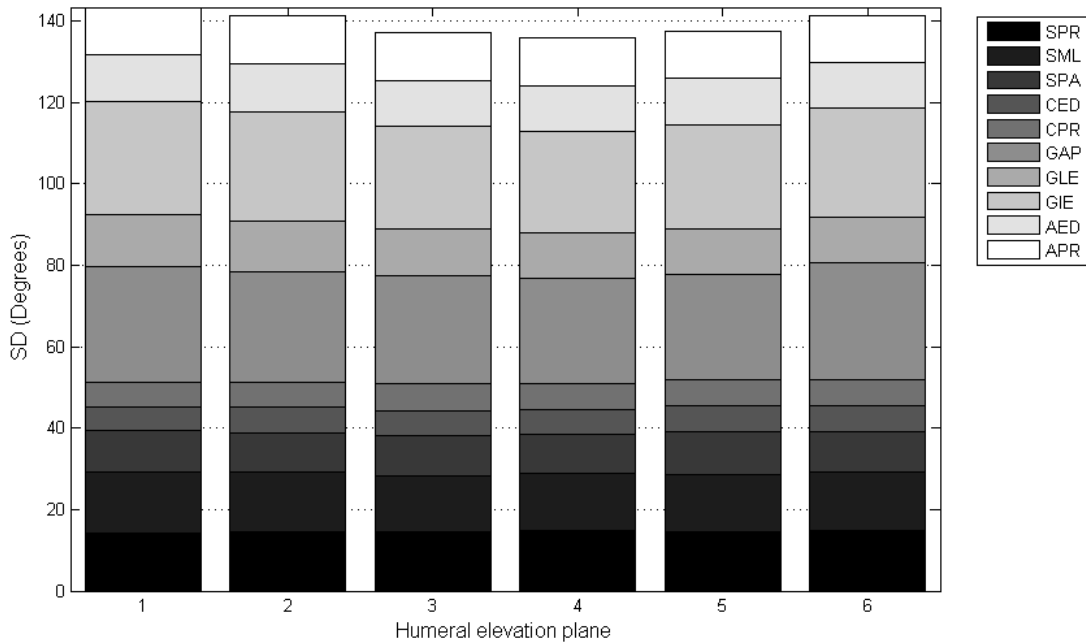


Figure 92: Total and individual joint rotation variation (standard deviation) for all measured humeral elevation angles averaged within planes

5. DISCUSSION

The purposes of this investigation were to produce a comprehensive description of typical shoulder kinematics during dynamic humeral elevation in six vertical movement planes, and to determine which factors influence shoulder kinematics. By offering detailed standards to compare results and quantifying the variability of typical shoulder motion, the findings benefit movement scientists and clinicians who attempt to indentify pathological shoulder motions. In terms of the factors hypothesized to influence typical shoulder kinematics, this study is innovative because it includes movement planes never before described. Also, the studied movements were dynamic, which allows movement phase to be investigated. Further, gender is rarely tested as a potential factor that could influence shoulder motion. Finally, all of these factors have yet to be tested on the same sample population to determine their relative influences on shoulder complex kinematics.

This discussion is organized into three sections. First, hypotheses are restated and addressed in the context of the specific results of the study. Next, the kinematic profiles are discussed and compared to previously reported data sets in terms of similarities in ranges of motion (ROM), trial-to-trial consistency, and variability. Statistical results are discussed in the context of factors known to affect shoulder kinematics and the implications of the study findings for future applications are discussed. Finally, study limitations will be summarized

5.1 Addressing the Hypotheses

Hypothesis 1

On page 18 it was hypothesized that as humeral movement plane was changed progressively across the body from frontal plane abduction (0P) through to 30° past flexion (120P), shoulder joint rotations occurring about a vertical axis (i.e. scapulothoracic (ST)

protraction, acromioclavicular (AC) protraction, and sternoclavicular (SC) protraction), as well as axial shoulder joint rotations (i.e. glenohumeral (GH) anterior plane of elevation and GH internal rotation) would be affected more than those rotations occurring about a horizontal axis (ST upward rotation, AC elevation, SC elevation, and GH elevation) and sagittal plane (ST posterior/anterior tilt) joint rotations. There was a main effect of plane ($p < 0.0001$) for every transverse plane rotation. However, SC protraction/retraction was more affected by humeral elevation angle than plane (elevation F -statistic = 2024.91; plane F -statistic = 317.24). In addition, AC protraction/retraction was equally affected by movement plane and humeral elevation angle (elevation F -statistic = 62.09; plane F -statistic = 58.17). Since movement plane's effects on shoulder transverse plane and humerus axial rotation were strong, Hypothesis 1 was **supported** by the study's findings. However, humeral elevations' significant effects on these rotations are important to note.

Hypothesis 2

It was further hypothesized on page 19 that humeral elevation angle would influence kinematics of those rotations occurring about a horizontal axis more than those occurring about a vertical axis. There was a main effect of humeral elevation angle on each these joint rotations ($p < 0.0001$). Moreover, the calculated elevation F -statistics for these joint rotations were always greater than that of the calculated elevation F -statistics of the transverse plane and axial rotations. Therefore, Hypothesis 2 was **supported** by the study's results.

Hypothesis 3

On page 19 it was further hypothesized that individual subjects would be able to perform the three repeated humeral movements within each plane consistently. Likewise, it was expected that all resulting shoulder joint rotations would be consistent as well. Since overall GH and ICCs

were high (0.999 (SD 0.013)), it can be concluded that the participants elevated their arms in a consistent manner. However, for the joint rotations that were less constrained such as humerus axial rotations and scapular lateral rotation, motions were less consistent. It was determined that when all joint rotation ICCs were averaged within each plane, overall ICCs for each plane were very similar (0.822 to 0.852 ICC range) and acceptable. However, since only eight of the thirteen calculated average joint rotation ICCs of each joint rotation were greater than 0.800, Hypothesis 3 was **partially supported** by the study's results.

Hypothesis 4

Earlier, on page 19 it was hypothesized that kinematic variability would be the highest at lower humeral elevation angles. When the standard deviations (SD) from kinematic profiles were separated by humeral elevation angle (Figure 91), averaged across phase and movement plane, and summed together, the highest cumulative SD existed at 15° humeral elevation (223.75°) and decreased gradually at each incremental elevation angle until 70° humeral elevation (127.71°). Beyond this point, a plateau in cumulative SD occurred through to the end of measured humeral elevation where the observed maximum change in SD was 1.74°. However, ST upward rotation and SC elevation variability did not change drastically (approximate 6% increase) over the span of the humeral elevation. Moreover, GH elevation and ST tilt SD increased with increasing elevation angle. Therefore, Hypothesis 4 was only **partially supported** by the study's results.

Hypothesis 5

On page 19 it was hypothesized that gender will have no effect on shoulder kinematics. Sex did not have a significant main effect on any of the thirteen measured joint rotations. ST tilt demonstrated the highest probability of a gender main effect ($P = 0.286$) but was not significant.

However, at least one significant interaction effect with gender as a factor was present for all kinematic results except for GH internal/external rotation and GH plane of elevation. Since significant gender interaction effects on shoulder were found, Hypothesis 5 was **not supported**.

Hypothesis 6

It was hypothesized that the phase of humeral motion (i.e. raising and lowering) would significantly affect shoulder kinematics. A significant main effect of movement phase was found for all shoulder joint rotations with the exception of GH elevation plane, GH elevation, and AC protraction. Moreover, each joint rotation except GH plane of elevation, GH internal/external rotation, and the AC rotations demonstrated at least one significant interaction effect involving movement phase. Therefore, Hypothesis 6 **supported**.

5.2 Kinematic profiles - Comparison to the literature

This section compares this investigation's typical kinematic profiles to past literature. Bone pin studies by McClure et al. (2001) and Ludewig et al. (2009) will be emphasized during comparisons, as this method directly measures scapula position and is considered the gold standard in kinematic measurement (Karduna et al., 2001; van Andel et al., 2009). However, general trends will be compared to skin-mounted techniques as well. Evaluation of scapular kinematics will be more detailed due to its prevalence in the literature. Important to note is that the profiles presented in this study display overall trends and any comparisons of these profiles to previous works are observational. An interpretation of statistical findings will be discussed. Also, a conscious effort was made to make note of the previous studies' tested humeral elevation ranges.

5.2.1 *Scapular Kinematics*

The typical motion profiles presented in Figures 21 through 23 demonstrate that the scapula laterally (i.e. upwardly) rotated and posteriorly tilted in a linear pattern as the humerus elevated in each movement plane regardless of phase. These trends have been observed in previous kinematic studies investigating only scapular plane abduction (de Groot et al., 1999; Ludewig and Cook, 2000; McClure et al., 2001; Borstad and Ludewig, 2002; Dayanidhi et al., 2005; Ludewig et al., 2009) and those limited to frontal and sagittal plane analyses (Meskers et al., 1998; Fayad et al., 2006, et al.; Bourne et al., 2007; van Andel et al., 2009; Ludewig et al., 2009). The combination of upward ST rotation and posterior tilt maintains the sub-acromial space during humeral elevation to prevent rotator cuff impingement (Cools et al., 2003). It is reasonable to expect that this motion pattern occurs in all planes as this investigation found.

There are notable similarities and differences in the magnitude of scapular upward rotation ROM in response to humeral elevation found in the literature. The current study demonstrated between 32.70° and 36.71° of upward rotation across all elevation planes and phases (Table C1; Figure 22). This ROM is very similar to the approximate 35° of rotation reported in the bone pin studies by McClure et al. (2001) and Ludewig et al. (2009) over the same tested humeral elevation levels, although their participants' scapulae were more upwardly rotated at the start of the movement. de Groot et al. (1999) also presented a comparable 39° ROM. The under estimation of upward rotation could be due to the acromion tracking technique applied in this investigation. Karduna et al (2001) stated that this method typically under estimated upward rotation. Moreover, the sample sizes of these bone pin studies were less than half of the sample size used in the current investigation. It is reasonable to suggest that their average trends would change somewhat if more participants were investigated.

This investigation's scapular posterior tilt ROM results agree in polarity to past works but dissimilar in magnitude. For the frontal, scapular and sagittal planes, findings of 11.92°, 10.58° and 7.98° (Table C1; Figure 23) were similar to Ludewig et al. (2009) findings of approximately 12° 10° and 13°, respectively; however, their participants were substantially more anterior tilted at rest. McClure et al. (2001) found subtly higher posterior tilt ROMs in the scapular and sagittal planes of approximately 16° and 13° respectively. Elsewhere, ROMs were found to be as high as 20° (de Groot et al., 1999) and as low as 3.5° (Dayanidhi et al., 2005) in the scapular plane. These tilt outcome discrepancies are most like due methodological differences. For example, the investigation by de Groot et al. (1999) was static, while the participants' humeral in the investigation by Dayanidhi et al., (2005) were more internally rotated, which has been shown to decrease posterior tilt (Koishi et al., 2011). Moreover, skin-mounted methods applied in the current study and Dayanidhi et al. (2005) are less accurate at measuring tilt at higher humeral elevation angles compared to bone pin studies (Karduna et al., 2001; van Andel et al., 2009). However, the most important finding from these studies is that the scapula always tilted posteriorly in typical populations during humeral elevation, which coincides with the current findings.

During humeral elevation in the frontal through scapular planes, the scapula retracted to the mid phase of elevation and then protracted as the movement was completed (Figure 21). This phasic trend, although slight, was also observed by Fayad et al. (2006) during frontal plane abduction. However, there is no consensus on the scapula protraction/retraction trends within these elevation planes. Borstad and Ludewig (2002) documented increasing protraction during scapular plane abduction while Dayanidhi et al. (2005) showed the opposite despite a similar experimental set-up. Drastic ST protraction/retraction trend differences exist in studies using

bone pins. Ludewig et al. (2009) found very little change in protraction (2° range) when the humerus was elevated in the frontal plane whereas increases in protraction greater than 15° were found by Bourne et al. (2007); however, the latter study's participants' motion planes were not physically constrained, possibly affecting results. Likewise, as with scapular tilt measures, the skin-mounted scapular protraction measurement technique applied in this study is error prone at higher humeral elevations. (Karduna et al., 2001; van Andel et al., 2009). This could partially influence the apparent scapulothoracic protraction kinematic profile changes observed at higher humeral elevation angles in Figure 23. Unfortunately, the directions of measurement errors are unknown.

Sagittal plane flexion (i.e. 90P) demonstrated scapular protraction/retraction kinematic trends comparable to past findings. As the humerus elevated to 90° progressive amounts of protraction occurred; beyond this point, the scapula retracted (Figure 21). This observable response has been demonstrated using bone pins (McClure et al., 2001; Ludewig et al., 2009) and skin-based acromion tracking techniques (Meskers et al, 1998; Fayad et al., 2006; van Andel et al., 2009). Humeral elevation within the 120P resulted in similar trends to sagittal plane flexion with the exception of increased protraction occurring in the mid to end range of humeral elevation. No previous study has investigated motions within this plane, but biomechanically it is feasible that the scapula must protract more to move the right humerus in a vertical plane angled 30° anterior (left) to the sagittal plane.

Likewise, when comparing measured ranges of scapula protraction/retraction to the literature, inconsistencies exist. For frontal plane (i.e. 0P) motions, 4.14° of scapula protraction/retraction occurred (Table C1). This result is similar to the 5° range found in van Andel et al. (2009), but is substantially greater than the approximate 1° of retraction presented in

Fayad et al. (2006) (Note: Fayad et al. averaged data over three elevation phases). In the scapular plane, the current study results show a ST protraction range of 3.62° . This is smaller than the 12° of retraction found in de Groot et al. (1999) and the approximately 7° range presented in Borstad and Ludewig (2002) and Dayanidhi et al. (2005). However, this 3.62° range is consistent with the findings from the bone pin investigation in Ludewig et al. (2009).

5.2.2 *Glenohumeral kinematics*

Typical frontal and sagittal plane GH motion plane profiles (Figure 24 through 26) align well with the literature; however ROM magnitudes do not. For frontal plane elevation between 10° and 40° , a progressive decrease in anterior plane motion was found, followed by an increase after this point. The opposite trend was found in 60P and 90P motions. This finding is comparable to Ludewig et al. (2009) mirror opposite frontal and sagittal plane profiles. ROMs they presented were approximately 16° for these planes, aligning with the current study's 0P (17.69°) ROM but almost 14° less than observed in 90P (29.78°). Also, Ludewig et al. showed very little ROM changes within the scapular plane as opposed to the 21.71° found in the current study

There were both similarities in motion trends but differences in magnitudes between the current study's typical GH external rotation profiles (Figure 26) and the GH profiles found in Ludewig et al (2009). Both studies demonstrated an initial period of external rotation at low elevation levels for 0P and SCAP followed by increasing internal rotation for the remainder of elevation. The current study also showed that trend for 90P. However, Ludewig et al. presented a linear trend of GH external rotation throughout the entire motion. The amount of GH external rotation seen at the end of elevation in the current study was nearly the same for each movement plane (approximately 55°), with the exception of 0P (48°). This is similar to Ludewig et al.,

(2009) whose GH external rotation profiles congregated at the same point. However, their end magnitude was higher (approximately 60°). Another discrepancy is that their roughly 45° of GH external rotation ROM in 90P was substantially higher than the current study's 25.46° . Differences between studies could be attributed to the humerus axial rotation not being constrained in the current study. Also, variability of both GH plane of elevation and internal/external rotation was quite high, particularly at lower elevations, and could further lead to differences. Fortunately, GH axial rotation at low humeral elevations is not often implicated as a contributing factor to shoulder injuries.

GH elevation kinematic profiles (Figure 25) and ranges (Table C3) were very similar to the bone pin results of Ludewig et al. (2009). The current investigation showed between 68.63° and 73.32° increases in GH elevation across all movement planes and phases. This trend and range is nearly identical to Ludewig et al.'s documented 70° (approximate), although their participants were slightly less elevated at the start of humeral elevation.

5.2.3 Acromioclavicular kinematics

In accordance with previous research, acromioclavicular (AC) elevation increased in all movement planes and phases as the humerus was elevated. There were little noticeable changes in the AC elevation kinematic profile between 10° and 50° of elevation within all movement planes except 120P (Figure 28). Beyond this point, the majority of AC elevation occurred. Ludewig et al. (2009) documented the opposite, with the majority of AC elevation occurring at the beginning movement. Another discrepancy was that they found a reduction in AC elevation ROM as plane was altered across the body (approximately 14° to 8° of elevation). The current study showed an increase in ROM (12.26° to 18.22° of elevation).

The typical AC protraction/retraction kinematic profiles shown in Figure 27 show trends that are different in magnitude than those documented in bone pin studies. An initial phase of retraction is visible in each elevation plane and phase between approximately 10° and 50° of elevation. After this point, the acromion protracts on the clavicle. In contrast, Ludewig et al. (2009) demonstrated a linear relationship between humeral elevation and AC protraction. Moreover, the AC retraction ROM reported for all movement planes (between 3° and 6° of retraction; Table C4) was half of that found in the current investigation (between 6.38° and 12.98°). The most likely cause for the AC joint rotation results not aligning well with previous studies is that the clavicle was only afforded 2 degrees of rotational freedom (no clavicle axial rotations were recorded). As a result, the International Biomechanics Society (ISB) (Wu et al., 2005) joint description recommendations could not be followed for AC joint motion. Therefore, analogous comparisons between the results of this study and investigations using bone pins cannot be confidently made.

5.2.4 *Sternoclavicular kinematics*

Typical sternoclavicular (SC) retraction profile motion trends found in this study (Figure 29 and 30) align well with bone pin studies found in the literature; however SC elevation ROM was substantially higher in the current investigation. The clavicle retracted on the sternum in a linear fashion during humeral elevation in all movement planes, with the exception of 120P (Figure 29), and had ROMs between 16.89° and 18.26° . McClure et al. (2001) and Ludewig et al. (2009) demonstrated similar linear trends but with SC retraction ROMs lower than 12° .

At the beginning of humeral elevation, there was little SC elevation (see Figure 30). Beyond 20° of humeral elevation, all of the clavicle elevation occurred. Ludewig et al. (2009) found a similar period of minimal clavicle elevation, but McClure et al (2001) did not. In

addition, SC elevation ROMs in this study was higher (between 20.24° and 22.79°) in comparison to both Ludewig et al. (2009) (no greater than 7°) and McClure et al (2001) (no more than 9°) across all planes.

Unfortunately, as with AC joint rotation, sternoclavicular (SC) anterior/posterior rotation (i.e. rotation about the long axis of the clavicle) could not be measured with skin-mounted motion capture techniques. However, SC retraction and elevation measurement outcomes do align with ISB recommendations provided found in Wu et al. (2005) because joint rotation description utilizes the thorax local coordinate system.

5.3 Kinematic profile application example

Three previously recorded 3D scapular kinematic profiles available in the literature obtained from participants free from shoulder injury symptoms were overlaid on top of the scapular kinematic profiles obtained in the current study to provide an example application of the curves. The scapular tracking methods used to collect the kinematics in Figures 93 through 95 include the gold standard bone pins (McClure et al., 2001; Ludewig et al., 2009) and an acromion tracking method similar to the current investigation (Dayanidhi et al., 2005). All other collection methodologies were the similar. For scapular protraction, the results from the literature fall with plus or minus one SD of the current studies profile. However, the studies using bone pins demonstrated retraction with increasing elevation while acromion tracking techniques presented a protracting scapula. On the contrary, none of the overlaid profiles of scapular lateral (i.e. upward) rotation fell within the current study's range. Conversely, all upward movement trends were very similar. Similar movement profiles were found for scapular tilting as well, although the ROM of Dayanidhi et al. (2005) was small. Lastly, only McClure et al (2001)

demonstrated scapular posterior tilt results outside of the typical range found in the current investigation.

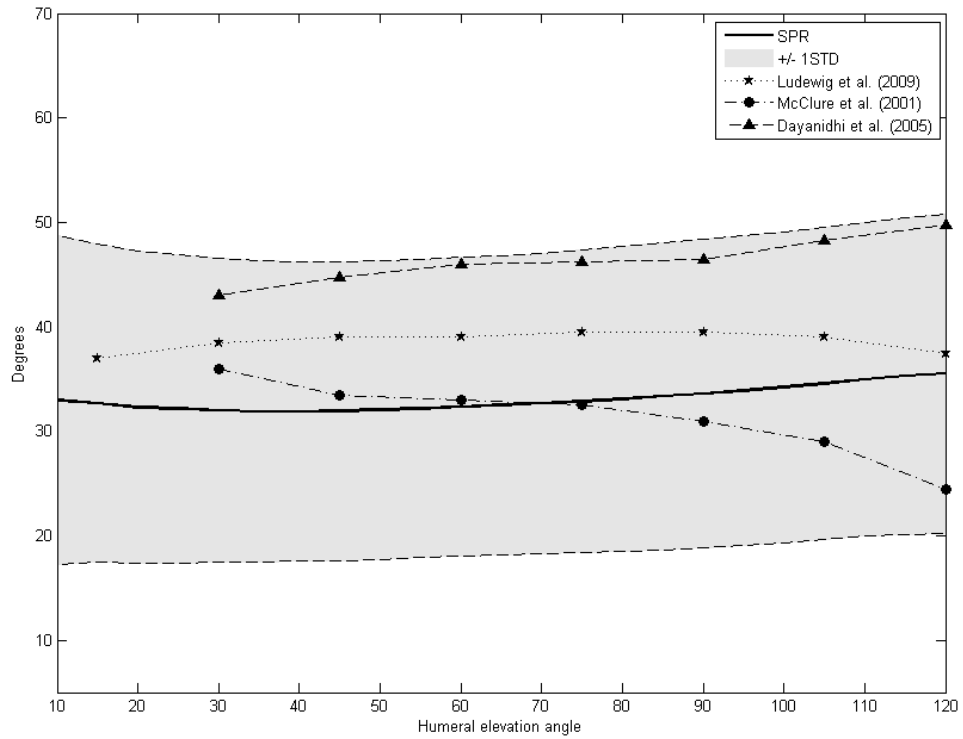


Figure 93: Comparison of ST protraction observed during humeral elevation (raising phase) in the scapular plane with select kinematic profiles available in the literature.

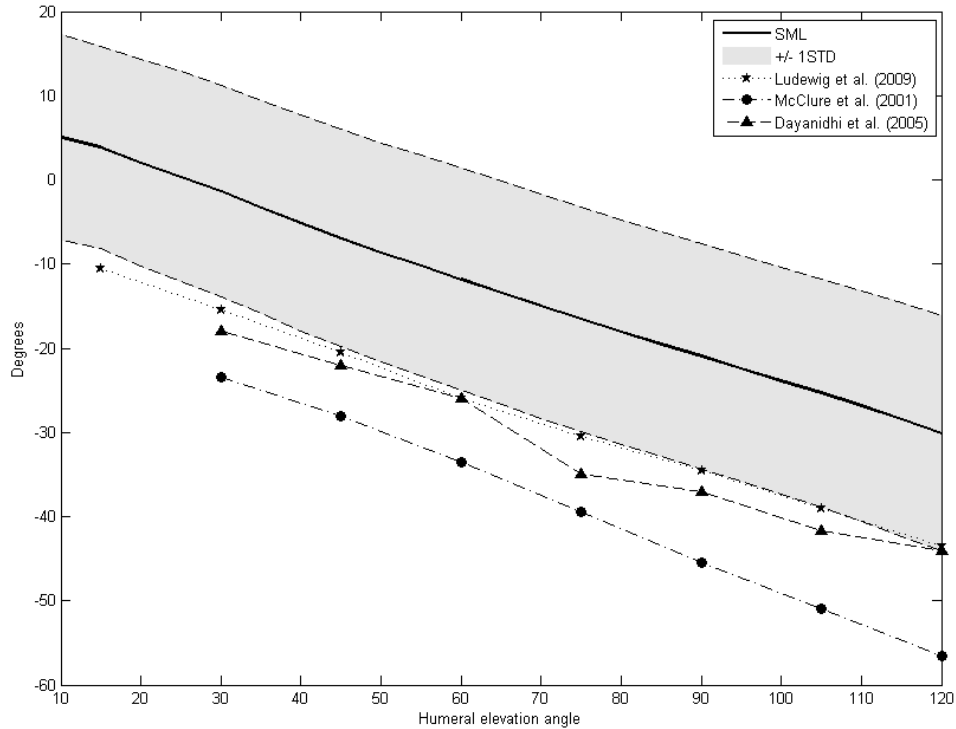


Figure 94: Comparison of ST upward rotation observed during humeral elevation (raising phase) in the scapular plane with select kinematic profiles available in the literature.

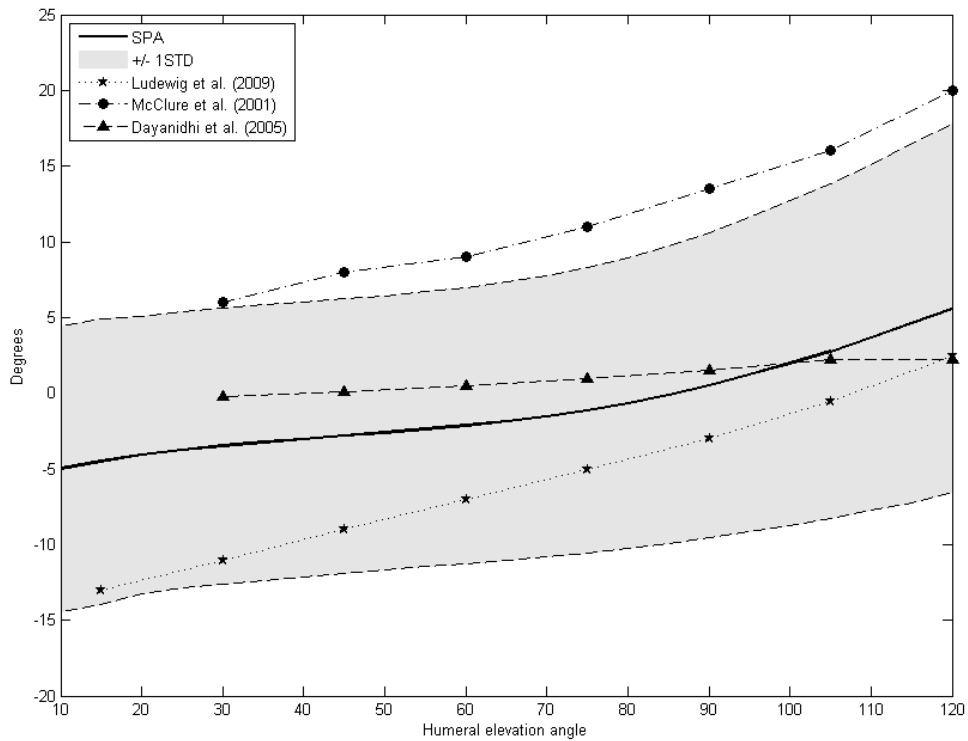


Figure 95: Comparison of ST posterior tilt observed during humeral elevation (raising phase) in the scapular plane with select kinematic profiles available in the literature.

5.4 The utility of kinematic profiles for identifying pathological shoulder motion

Typical normative shoulder kinematic data provide clinicians a means to identify pathological shoulder motion. To illustrate the utility of the profile curves to identify shoulder motion abnormalities, two hypothetical examples of pathological shoulder motion cited in the literature are contrasted against this study's typical profiles (Figures 96 and 97). The first example is the rapid upward scapular rotation reductions occurring during the end ranges of humeral lowering observable during some clinical evaluations of injured individuals (Kibler & McMullen, 2003), also known as the "shoulder dump" (McMullen & Uhl, 2000) (Figure 96). The second example is a reduction in posterior scapular tilt shown to occur at higher humeral elevation angles of those diagnosed with sub-acromial impingement syndrome (Ludewig & Cook, 2000) (Figure 97). In both cases, the trends of the hypothetical motion profiles do not agree with those presented in this thesis. In the first example, the phasic kinematic scapular upward rotation trend in response to humeral elevation angle is drastically different than the linear trend reported in this thesis (Figure 96). Likewise, the current results included increases in scapular posterior tilt at higher humeral elevation angles, rather than reductions in posterior tilt or increases in anterior tilt (Figure 97).

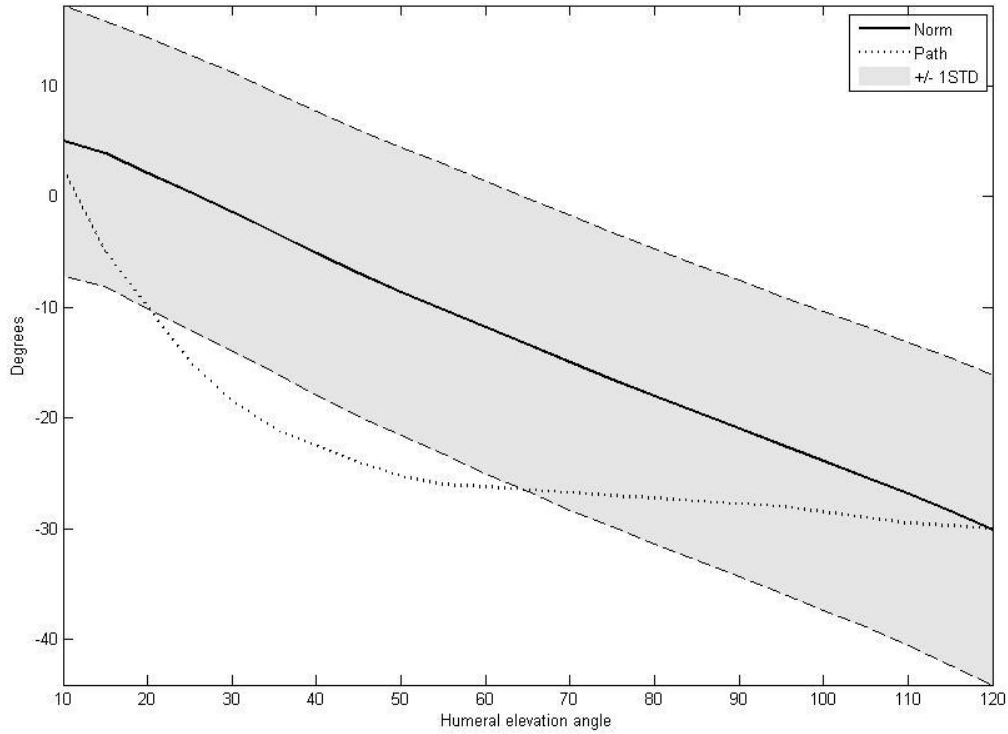


Figure 96: Hypothetical comparison of a pathological scapular upward rotation motion profile (Path) to the normative upward rotation profile generated in the current study (Norm) – Scapular plane, lowering phase

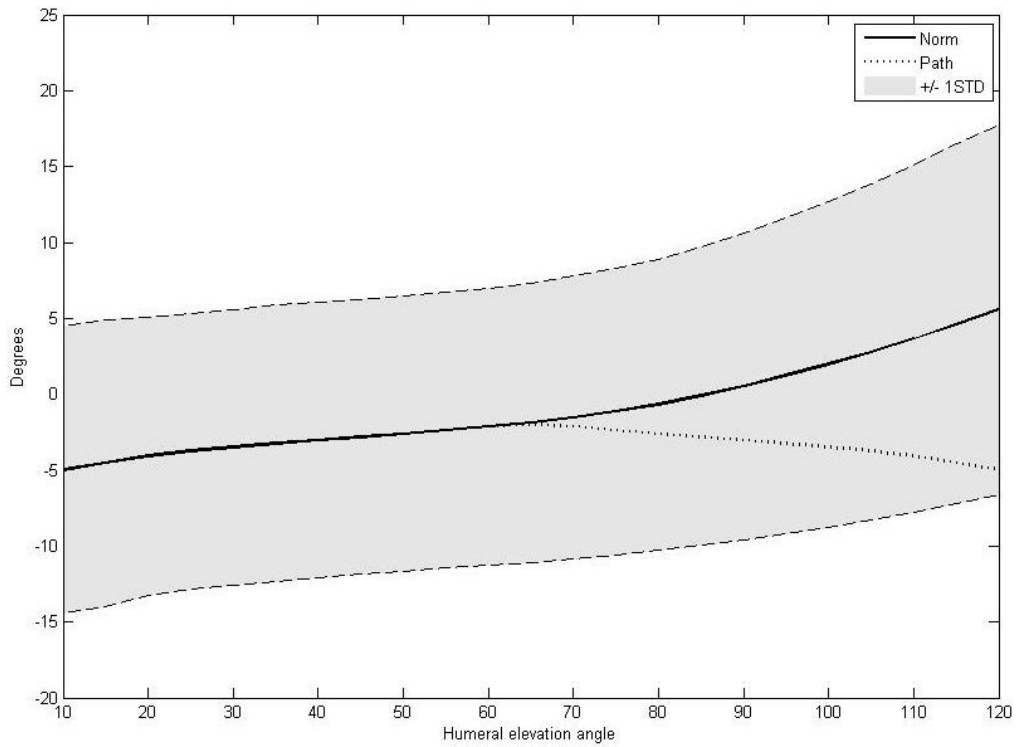


Figure 97: Hypothetical comparison of a pathological scapular tilt kinematic profile (Path) of an injured individual to the normative tilt curve generated in the current study (Norm) – Scapular plane abduction

5.5 Kinematic profile variability

There was considerably more variability overall, indicated by cumulative standard deviation (SD), observed during the first half of humeral elevation than the second half; however the majority of this variability was attributable to humeral axial rotations (see Figure 91). For GH plane of elevation and internal/external rotation, 171.05% and 170.48% reductions in respective SDs were observed when moving from 10° to 60° humeral elevation. However, ST and AC protraction were the only other rotations that experienced variability reductions greater than 3% over this range (12.34% and 8.82% respectively). This indicates that most rotations either had constant increasing variability during humeral elevation. The variability of these rotations at lower elevations was likely high due to protraction/retraction of the shoulder girdles or positioning upper arms to locate the vertical pole that guided their movement. Recent researchers have not commented on how rotational SDs change with respect to humeral elevation angle for GH rotations, other than that between subject variability is high (Ludewig et al., 2009).

The variability of several joint rotations increased with increasing humeral elevation despite a decline in cumulative variability. ST upward rotation, ST posterior tilt, SC elevation, GH elevation, and AC elevation increased in variability as the humerus was elevated from 10° to 120° (4.13%, 24.73%, 6.64%, 28.22%, and 19.92% increases respectively; Figure 91). Identifying that ST upward rotation variability was not highest at lower elevation angles disagrees with the findings of Braman et al., (2009) as well as the classical work of Inman et al. (1944). Interestingly, these joint rotations were most influenced by humeral elevation angle. Therefore, rotations affected by elevation angle are more variable at higher elevation angles. This influence will be addressed statistically in a subsequent section.

No visible differences in cumulative variability (SD) existed across movement planes when all joint rotations SD were averaged within a plane of elevation (Figure 92). This demonstrated that, on average, joint rotations measured within one humeral movement plane were no more or less variable than in any other plane. GH plane of elevation and internal/external rotation tended to be the most variable rotations measured, while the clavicle rotations were less variable. The influence of plane of movement on individual measured joint rotations as determined statistically is discussed later.

Important to consider is the variability of each rotation relative to its respective total range of motion. This consideration is similar to the coefficient of variability with the exception that the rotational SD is divided by the rotation's range of motion instead of the mean. The higher this relative variability is the less confident one is that the healthy curve represents the sample population. For example, ST protraction demonstrated the highest observed relative variability when averaged across all elevation angles, at 300.76% of ROM. This could explain why the movement profile observed for this rotation did not align well with both McClure et al. (2001) and Ludewig et al. (2009) protraction profiles. However, these researchers did state that ST protraction was the most variable of the ST rotations. Likewise, both GH plane of motion and internal/external rotation relative variability was substantially higher than that of GH elevation (106.86% and 158.02% respectively versus 15.76%). This could explain why their tracings did not align with Ludewig et al (2009) profiles as well as GH elevation did.

The high variability of the kinematic profiles presented in this study and in others is most likely due to different resting scapular orientations measured across participants rather than different motion trends. Ludewig et al (2009) found resting scapulothoracic orientation to be quite variable at rest. At the lowest humeral elevation angle measured in the current

investigation, scapular kinematic variability was also quite high. However, over the entire range of recorded humeral motion, scapulothoracic kinematic variability did not change drastically. This suggests the possibility that any offset in scapular kinematics at rest was maintained systematically throughout the range of tested humeral elevation. To demonstrate this suggestion, the raw kinematic profiles for each participant's scapula upward rotation during scapular plane elevation are presented in Figure 98. Any large differences existing between individuals' scapular upward rotation profiles can be attributed to participants' scapular orientations at lower elevation angles. Likewise, these large differences persisted until humeral elevation was complete. Some overlap in individual profile trends did occur. Fortunately these overlaps tended to be between individuals with very similar raw magnitudes of upward rotation. The finding of similar raw kinematic profile trends measured across participants further emphasizes the utility of the kinematic trends for future shoulder motion assessments, rather than the raw magnitudes of the profiles.

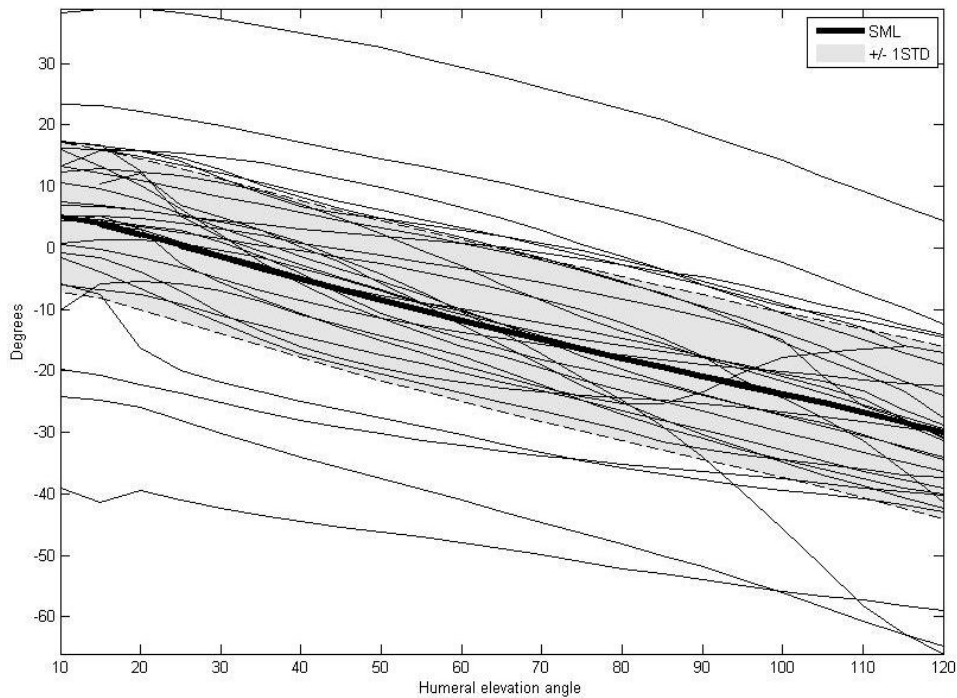


Figure 98: Participants' raw scapular upward rotation profiles overlaying the mean of these scores in bold with +/- one standard deviation shaded in grey – Raising phase of scapular plane elevation.

5.6 Intra-class correlation coefficient interpretation

All average joint rotation ICCs were greater 0.658, constituting comparable trial-to-trial movement consistency to previous research. Specifically, the 0.755 to 0.938 range of average ST rotational ICCs documented in Table C6 in Appendix C are similar to the 0.76 to 0.90 ICC range presented in Fayad et al. (2006) and the 0.63 to 0.96 range found in Brochard et al. (2011). Glenohumeral elevation was determined to be the most consistent of the rotations (ICC = 0.999). It is hypothesized that its ICC was higher than others because the movement plane and elevation angle were constrained. SC rotations were also consistent (0.814 for SC protraction; 0.959 for SC elevation), most likely because clavicle translation is tightly constrained at the SC and AC joints (McClure et al., 2001). Average ST upward rotation ICC was lower than anticipated (0.755). A reason for this could be that the upward scapula orientation is dependent of several other joint orientations. Perhaps the inconsistency occurring at the SC and AC joints manifest amplify the inconsistencies in ST upward rotation.

Movement plane ICCs ranged from 0.822 to 0.852 (Table 6) suggesting that the participants moved consistently trial-to-trial, regardless of plane. In the literature, ICCs are typically presented averaged across the tested planes and therefore individual movement plane consistencies are hard to determine. Ludewig et al. (2009) found average scapular rotation ICCs of 0.96, 0.94, and 0.92 for scapular, frontal, and sagittal planes respectively. The higher ICC values in their study could be attributed to a different type of ICC calculation used (Type 1,1), or the fact that bone pin readings may be more consistent.

According to previous research, the findings of this study support at least acceptable trial-to-trial movement consistency by participants. This is in light of the lack of consensus on how to rank ICC values in the movement sciences (Weir et al., 2005). For example, Brochard et al.

(2011) identified an ICC of 0.63 as “good” and 0.96 as “excellent” but offer no support for their explanations. Likewise, van Andel describe ICCs less than 0.60 as “poor,” between 0.60 and 0.80 as “acceptable,” and above 0.80 as “excellent”. The existence of multiple ICC calculation types further complicates comparisons. For example, Ludewig et al. ICC calculations, although high (greater than 0.92), were performed using a different ICC calculation (Type 1,1). Most scapular kinematic papers judging participant movement consistently utilize ICC calculation Type 3,1 because it emphasizes random error associated with participant movement.

5.7 Statistical Interpretations

5.7.1 Plane and elevation angle effects on shoulder kinematics

The scapula rotated upward and the clavicle and humerus elevated at statistically significant increments at each humeral elevation level. A main effect of plane on scapulothoracic (ST) upward rotation and glenohumeral (GH) elevation was present; however the largest relative difference for each of these rotations were modest, at only 5.86% and 3.66% of ROM (between the frontal and sagittal planes). Moreover, humeral elevation in 30P, scapular, 60P and 90P planes produced statistically equal amounts of clavicle elevation at each respective humeral elevation increment. Ludewig et al (2009) found that significantly more scapular upward rotation and clavicle and humeral elevation occurred in frontal plane abduction compared to scapular and sagittal plane movements, although these differences were also small. The largest difference reported was 3° more scapula upward rotation elevation levels above 90°. The current study demonstrates that frontal plane rotations (ST upward rotation, GH elevation, and SC elevation) work together to elevate the humerus in the same matter, regardless of plane.

ST and SC protraction/retraction and glenohumeral (GH) elevation plane interactions were highly coordinated and each contributed to the positioning of the humerus in the proper

movement plane. ST and GH relative contributions depended on humeral elevation angle and movement plane while SC retraction significantly increased throughout the entire humeral elevation range. Positioning the humerus in the frontal plane and elevating it from 15° to 45° required SC retraction (Figure 79), reduced ST protraction (Figure 31), and an increase in posterior GH elevation plane (Figure 49). For the 30P and scapular planes, this trend was repeated; however reductions in ST protraction were very small. Statistically, ST retraction did not change in these two planes throughout the full humeral elevation ROM while reductions in GH anterior plane were significant. For movements within 60P and sagittal planes, ST protraction increased throughout the range of humeral elevation, although a statistical plateau was reached at 60° humeral elevation. Beyond this point, SC retraction maintained movement plane as it was the only rotation of the three that steadily increased throughout the entire elevation range. This example of coordinated shoulder joint movements demonstrates the interdependency of upper limb joint rotations to move the humerus through space originally outlined by van der Helm & Pronk (1995).

Scapulothoracic posterior tilt decreased as movement plane became more sagittal (Figures 43, 46, and 47). However, due to the variability of the rotation relative to its small ROM, many of these changes were not significant. For example, no significant differences in posterior tilt were observed at 120° of humeral elevation across 30P through 90P planes despite a 53.18% reduction in tilt. This large relative change in posterior tilt, and the overall affect of plane, is likely meaningful. Ludewig et al. (2009) found no significant plane effect on tilt measures for same reasons mentioned above coupled with a smaller sample size ($n = 12$).

High amounts of posterior tilt measures observed in the frontal could have been due to the high glenohumeral external rotation observed in this plane (Figures 49, 52 and 53). The

humerus was significantly more externally rotated during frontal plane elevation than any other plane at all humeral elevation angles except for 120°. Koishi et al. (2011) reported that scapular anterior tilt increased (i.e. moved more anteriorly) as the humerus was internally rotated at 90° humeral elevation in frontal plane. It is speculated that different more anterior scapular tilt would occur if the current study was repeated with the thumb pointing perpendicular to the plane of motion, instead of in line with it. Another explanation for increased tilt could be increased deltoid muscle bulge occurring frontal plane elevation, which would affect measurement. However, this bulge was not explicitly measured.

Acromioclavicular (AC) elevation linearly increased during humeral elevation within the frontal plane; however in all other planes AC elevation occurred only after 45° of humeral elevation (Figure 67). A direct relationship between humeral and AC elevation was expected in all planes, particularly at lower elevations, as demonstrated by Ludewig et al. (2009). Also, because the clavicle and scapula linearly rotated upward, it is reasonable to expect that AC joint connecting them would elevate in a similar matter (Teece et al., 2008). Discrepancies in AC joint motion findings were most likely due to the inability to record clavicle axial rotation. ISB standards describes AC rotation utilizing a “floating axis” (Grood and Suntay, 1983) created with the vertical clavicle z-axis and the lateral scapular y-axis. Since a vertical clavicle axis could not be discerned, AC joint rotation was described using a floating axis created the scapula’s vertical z-axis and the long axis of the clavicle. This methodology potentially caused measurement error.

Further evidence of AC measurement inaccuracies existed in the AC protraction/retraction outcomes in response to elevation plane changes. As humeral elevation plane moved from 0P to 30P, a significant 3.82° decrease in protraction occurred, representing an 8.34% reduction (See Figure 76 for an example). This went against expectations and evidence

provided by Ludewig et al. (2009). Fortunately, no other planes demonstrated reductions greater than 1.5° , and an increase in AC protraction occurred in the 120P movement plane compared to sagittal plane elevation. Moreover, AC protraction did occur at higher humeral elevation angles in each movement plane in agreement with past findings (Ludewig et al. 2009). Therefore the AC elevation and protraction/retraction measurement approach applied in this study appeared to respond well to humeral elevation changes, but not movement plane changes.

5.7.2 *Gender effects on shoulder kinematics*

At least one gender interaction effect existed for every joint rotation, yet previous studies have routinely neglected gender as a possible factor. Often, the interaction effects found in this study were small in absolute magnitude. However, since rotations such as ST posterior tilt, ST protraction, AC protraction and AC elevation presented small ranges of motion (see Table C4), these small differences could be meaningful. Unfortunately, previous researchers who included females in their population samples did not treat gender as an effect (see Meskers et al., 1998; McClure et al., 2001; Ebaugh et al., 2005; van Andel et al., 2005; Ludewig et al., 2009). This limitation to shoulder kinematic research is remarkable, seeing that gender is known to affect other joints' kinematic outcomes such as in the hip (Cho et al., 2004) and knee (McKean et al., 2007; Boyer et al., 2008). It is recommended that gender be included a main factor in all subsequent shoulder kinematic research.

Males demonstrated observably more ST protraction than females. Males were only significantly more protracted at 60° of humeral elevation (2.40° more protracted). Similar differences were seen beyond this position, but were not significant (see Figure 45). For example, 2.88° more protraction occurred for males at 75° humeral elevation and 3.37° more protraction occurred at 90° humeral elevation. Considering that these ST protraction differences

represent over 50% of the participants average ROM, these differences are meaningful. Also, males were more protracted in every observed plane by 2.0° to 2.5° with the exception of 120P. A potential explanation for the increased protraction in males could be their higher amounts of SC retraction observed. Perhaps males have to protract their scapula more during humeral elevation to overcome this increased clavicle retraction, although this causal relationship is speculative since males' and females' acromioclavicular protraction amounts was very similar.

A second ST finding was that males demonstrated more ST posterior tilt than females in every plane and humeral elevation angle measured (see Figure 47). Again, the differences were not always statistically significant due to the relatively high variability of this rotation. Only in planes 30P and 120P were differences significant (3.09° and 4.53° more posterior tilt respectively); however larger gender-related differences were observed in plane 90P (4.72°). Males demonstrated substantially more posterior tilt at higher elevation angles. Only at 90° of humeral elevation were gender-elevation effects significant (4.82° more posterior tilt in males), yet the absolute differences between the sexes at 120° elevation were higher (8.62° more posterior tilt in males compared to females).

If these ST tilt findings truly represent gender-related tilt differences, they have considerable clinical importance. Posterior tilt at higher humeral elevation angles is typically characterized as a protective mechanism against sub-acromial impingement of the rotator cuff (Borstad and Ludewig, 2002; McClure et al., 2004; Cools et al., 2007). Our results suggest that females may be predisposed to a higher risk of rotator cuff injury due to these kinematics. The tissues at other joints are injured disproportionately in females, such knee anterior cruciate ligament tears (Moore and Dalley, 1999). However, these posterior tilt differences may be partially caused by the inaccuracy of the acromion marker cluster (AMC) at higher elevations.

Karduna et al. (2001) found an approximate 3.5° root mean square (RMS) error at higher elevations; although this error value was not higher than seen at lower elevations. It is reasonable to suggest that the higher tilt measures could be from the deltoid muscle bulging underneath the cluster at higher elevations (assuming that males possess larger deltoid muscle bulk than females) thereby tilting the cluster posteriorly (note: the scapular orientation is not indicative of AMC orientation. i.e. the scapula could be anteriorly tilted and the cluster posteriorly tilted). In light of these limitations, further investigation into gender related kinematic differences should be performed to determine if females are at an inherent increased risk for shoulder injury.

Gender appeared to have kinematic implications on AC elevation as well; however this difference could be attributed to artefact as well. At 75° , 90° and 105° , of humeral elevation, males had significantly more AC elevation than females (males presented up to 8.62° more AC elevation over these angles – see Figure 69). However, deltoid muscle bulk at higher elevations could be the source of gender-related differences. One would expect ST upward rotation to increase disproportionately in males as well if these changes in AC were true, yet this increase was not observed. Male scapulae were observably less upwardly rotated on average compared to females.

5.7.3 Movement phase effects on shoulder kinematics

Previous studies have cited both movement phase-movement plane (PH-PL) and PH-elevation angle (PH-E) interaction effects on ST rotations. This study found only significant PH-PL interaction effects on ST upward rotation and tilt (Figures 40 and 46). During sagittal plane movements, the raising phase had 1.67° less upward rotation than the lowering phase representing nearly 5% of upward rotation ROM and most likely is not meaningful. However, significantly less posterior tilt observed in the raising phase during frontal (2.49° less) and

scapular planes (1.57° less) are meaningful as they constitute 20.89% and 14.84% of ST posterior tilt ROM respectively. Similar tilt differences were found in other planes but were not significant. Ludewig et al. (2009) did not find a significant PL-PH interaction but found that in each elevation increment participants were on average 2° less posterior tilted in the raising phase. Borstad and Ludewig (2002) also documented a reduction in posterior tilt, but only at elevation angles above 80° .

The most likely cause of the lower posterior tilt during the raising phase is that participants actively moved differently during this phase. Since bone pin studies (McClure et al., 2001; Ludewig et al., 2009) demonstrated similar movement phase-related ST tilt effects, differences could not be attributed to the skin-mounted scapular tracking technique used in this study. Likewise, the higher scapular stabilizing muscle activity during the raising phase work together to encourage posterior tipping (Dvir et al., 1978; Johnson et al., 1994; Phadke et al., 2009), not reduce it. Most likely, lower posterior tilt occurred because participants were actively moving differently during the raising phase. Perhaps they were reaching excessively past the pole in the raising phase, as suggested by the documented significant 1.49° protraction increase in the raising phase. Increases in protraction in protraction could potentially result in reductions in posterior tilting as evident by the similar increases in ST protraction and ST anterior tilt as movement plane was altered across the body.

Clinicians have proposed that observable changes in scapular kinematics during the lowering phase constitute abnormal motion and are a cause of concern. They suggest that rapid reductions in ST upward rotation and observable scapular winging (increased ST protraction and anterior tilt) during humerus lowering compared to raising is indicative of “scapular dyskinesis” (Borstad and Ludewig, 2002; Kibler and McMullen, 2003). In this study, significant phase main

or interaction effect found were unlikely observable as the maximum change in scapular kinematics due to movement phase was less than 3° . Therefore this study's findings partially supported this clinical hypothesis. However, only an injury-free population sample was tested.

The finding that the raising phase had significantly less SC retraction (2.87° less) supports the notion that participants reached more forward in this phase compared to lowering. Participants' clavicles were significantly more protracted at every humeral elevation increment in the raising phase (maximum difference = 4.84°) except for at 15° and 30° of elevation. Both Ludewig et al. (2009) and Ebaugh & Spinelli (2010) demonstrated similar increases in SC protraction in the raising phase, however most of these changes were observed at higher elevations. Perhaps participants gave a more conscious effort to reach towards the pole when raising the humerus. For lowering, since participants knew where the pole was, they did not make the same effort.

PH-E and PH-PL interaction effects on GH internal/external (GIE) rotation (Figures 62 and 64) suggest that participants had difficulties locating the pole that constrained their elevation. Participants were approximately 6° less externally rotated at 15° and 30° humeral elevation during the raising phase. Moreover, participants were 5.68° less externally rotated in the OP plane during humerus raising. This difference represents 56.74% of GIE ROM in this plane. It is reasonable to suggest that participants had to position their humeri differently in this range of humeral elevation in the OP because they could not see the pole in their periphery.

When significant PH-gender interaction effects existed, phase interacted with gender the same for all rotations with the exception of three. In the raising phase, male scapulae were significantly less upwardly rotated by 1.67° , humeri 1.20° more elevated relative to the glenoid, and clavicles 1.08° less elevated compared to the lowering phase. On the contrary, no phase

effects were seen in females for these rotations. Since no past studies have tested for gender effects, these differences cannot be compared to the literature. Despite interaction effects being small, they support the inclusion of gender as a factor in future studies.

5.8 Study Limitations

In general, the study results are specific to the population sample tested: university-aged male and female volunteers. Investigating older and younger sample populations may have resulted in different findings. In a study by Dayanidhi et al. (2011), children (aged 4 – 9) had significantly more upward rotation than adult males during scapular plane elevation. Moreover, bone pin studies by Ludewig et al. (2009) and McClure et al. (2001) were performed on older population samples (29.3 ± 6.8 years and 27 to 37 year age range respectively) and therefore age could be the source of differences found between this study's kinematic profiles these previous works.

The movement planes tested were constrained to control movement variability and therefore did not define functional movement. Some researchers have suggested that more clinically relevant shoulder kinematic information can be attained by having participants perform goal orientated movements. For example, Braman et al. had their participants to “raise their arms as if reaching for an object on a high shelf” (2009). The reason behind this suggestion is that humans rarely move within tightly controlled vertical planes. However, since a goal of this paper was to determine if plane of humeral elevation dictated shoulder joint orientations, movement plane was treated as an independent variable that was modified by the researchers, rather than a dependent variable. Further, constrained tasks may be more straightforwardly instructed and interpreted in the context of clinical screening or evaluation. Verily, shoulder kinematic profiles of activities of daily living (ADL) are useful for workstation modifications and living

environment design for elderly or injured people, and evidence exists to support differences on the basis of factors such as age (Magermans et al., 2005; Hall et al., 2011). However, investigating ADL performance was outside the scope of the current investigation.

Skin-mounted scapular motion capture techniques possess documented measurement errors in comparison to direct scapular measurement techniques. The acromion marker cluster used in this investigation has been validated for humeral elevation angles below 120° and vertical humeral elevation planes including and between frontal through to sagittal (Karduna et al., 2001). However, the method was untested for other elevation planes. Therefore, the accuracy of the scapular kinematic measurements within the 120P is unknown. Moreover, Karduna et al. (2001) did not discuss the direction of the measurement error for scapular tilt and protraction measurements, nor provided error profiles for the sagittal and frontal planes. This makes discussing potential error in scapular measurement difficult because interpretation of whether tilt or protraction/retraction outcomes are over or underestimated is somewhat speculative.

Clavicle axial rotations were not measured and therefore robust descriptions of 3-dimensional sternoclavicular (SC) and acromioclavicular (AC) motion could not be determined. As a result, SC and AC joints were only afforded 2 rotational degrees of freedom. SC elevation and protraction/retraction were measured in accordance to ISB standards (Wu et al., 2005); however AC elevation and protraction/retraction rotations were not because no z (i.e. vertical) clavicle axis could be determined. Coupled with the notion that the skin-mounted acromion cluster use to measured scapula orientation possesses a level of inherent error, AC rotation outcomes are likely less accurate than other joint measurements.

Using invasive bone pins rigidly fixed to the clavicle is the only way to measure 3-dimension clavicle orientation directly. However, this method is very invasive and often limits

the study sample size (Ludewig et al., 2009), and may inhibit natural movement. An attempt to use a rigid cluster coordinate system secured to the skin overlying the clavicle was made, as suggested by Szucs et al. (2010). However, fixing the small cluster to a nearly cylindrical clavicle proved to be problematic and camera line of sight site issues arose. After attempting the method on 5 participants, the technique was abandoned. In a best case scenario, any clavicle orientation results using this method would have been suspect because the technique has only been validated thus far using 5 cadaveric specimens.

Finally, visual feedback of humeral movement plane was not provided to the participant during motion trials. This could potentially result in participants elevating the humerus in unintended movement planes. However participants remained seated through the duration of the study and both foot and torso positions were constrained to that the motion planes did not move relative to the defined approximate glenohumeral joint center. In addition, movement planes were verified throughout the investigation using the goniometer when the pole guiding motion was repositioned. Thus, the associated potential for movement error should be modest.

5.9 Future Research Directions

To investigate the potential clinical usefulness of the developed shoulder kinematic profiles, an identical study protocol should be repeated to study the movements of a diagnosed injured population. It is hypothesized that shoulder joint rotation trends, particularly scapulothoracic upward rotation and posterior tilt, would be different in injured populations (Ludewig and Cook, 2000). Perhaps most importantly, motion assessment should include multiple humeral elevation plane analyses, rather than the current standard of just scapular plane elevation. For example, the current results suggest that the plane in which kinematics is tested affects scapular tilt kinematics. In injured populations, this effect of plane is likely lessened or

heightened. Likewise, tilt and upward rotation measures might be present as “typical” in certain planes, but not others. Furthermore, certain shoulder pathologies (e.g. shoulder instability vs. sub-acromial impingement syndrome) may present different kinematic trends compared to typical populations, enabling more specific non-invasive diagnosis. For example, an unstable shoulder might have more posterior tilt during humeral elevation compared to the typical kinematic curve, while the impinged shoulder may present less tilt. The current results provide a robust basis for making these comparisons.

The discovery that males have more posterior scapular tilt than females, particularly at higher elevation angles, should be further investigated using direct scapular kinematic measurement techniques (i.e. bone pins). If this finding is confirmed, it strongly suggests that females may be more predisposed to sub-acromial impingement syndrome. Moreover, the discovery that gender interacts with other main effects such as movement plane and elevation angle suggests gender should be controlled for treated as an independent variable in future shoulder kinematic investigations and clinical evaluations.

The current investigation was performed in conjunction with an investigation by Grewal (2011) that attempted to develop regression equations that predict scapular and clavicle orientations based on externally measured humeral and thorax static positions. Twenty-eight participants from the current study also participated in the second study. Future work will input the humeral and thorax data from these participants into the regression equations found in Grewel (2011) and compare these to dynamic scapular motion profiles found in Figures 21 to 23. It is hypothesized that these profiles will closely align, as the equations were generated using the same sample population. To further test the feasibility of applying these equations to a general population, dynamic shoulder kinematics from a new sample of the university population should

be collected. Thorax and humeral measures from this sample should then be inputted into the regression equations, and outputs compared to dynamic measures.

Further work into the validation of the acromion marker cluster (AMC) skin-mounted scapular kinematic measurement technique is also warranted. The current investigation supports the notion that 3D scapular kinematics are highly variable across people. Therefore validating the AMC using only eight participants, as done by Karduna et al. (2001), may be inadequate. Presenting profiles detailing root mean square measurement error at each humeral increment level across multiple movement planes will benefit future biomechanists when considering their specific motion tracking instrumentation options.

5.10 Clinical applications of findings

Scapular upward rotation and posterior tilt kinematic profile trends and ranges presented in this study are useful for identifying shoulder motion abnormalities. For example, as the humerus was elevated beyond 30°, scapula upward rotation was directly related to humerus elevation. Failure to see this linear relationship or finding reductions in upward rotation at higher humeral elevation angles could indicate dyskinetic scapular motion. Likewise, if an individual presents a scapula that anteriorly tilts as the humerus is elevated, this could be deemed as abnormal as well. This combination of decreased upward rotation and increased anterior tilt at higher humeral elevation angles is often cited as one of the potential causes a reduction in sub-acromial space and rotator cuff tears (Ludewig & Cook, 2000; Borstad & Ludewig, 2002; McClure et al., 2004). The utility of scapular kinematic profiles to detect kinematic differences between uninjured and pathological shoulder motion was presented in Section 5.4 and shown graphically in Figures 96 and 97.

Due to the high variability of shoulder rotational outcomes found in Figures 21 through 30, the magnitudes of kinematic profiles will most likely not align precisely with the shoulder kinematic outcomes of all healthy individuals. This was exemplified for the scapular rotations in Figures 93 through 95, where the mean scapulothoracic protraction, upward rotation and tilt profiles obtained from typical individuals in four different studies, including this one, did not align perfectly with each other. However, overall trends persisted across raw individual kinematic profiles as shown for scapular upward rotation in Figure 98. Therefore, finding a discrepancy between the kinematic profile magnitudes presented in this study and raw kinematic magnitudes of an individual during a clinical assessment is not indicative of atypical motion.

This investigation adamantly supported moving away from singular scapular plane shoulder kinematic analyses in clinical settings. For example, movement plane did not meaningfully affect scapular upward rotation. Therefore any visible differences in scapular upward rotation in response to modifying movement plane should be classified as atypical and may indicate dysfunction. On the contrary, scapulothoracic posterior tilt and protraction were highly dependent on motion plane. If no changes are seen in these two scapular rotations in response to altering vertical humeral elevation plane, this response should be classified as atypical as well. Therefore, the identification of pathological scapular motion can be made possible if scapular motion is assessed during humeral elevation in multiple vertical movement planes.

Females presented less scapular posterior tilt than males at higher elevation angles, suggesting a predisposition to increased shoulder injury risk. Kinematic differences due to gender have been shown to occur at other joints such as the knee. Moreover, some of these differences have been linked to increased occurrences of anterior cruciate knee ligament tears in

females. The current investigation's findings hint at a similar connection between scapular kinematic differences in females and potential shoulder injury risk increases. Lower scapular posterior tilt, shown in females at higher elevation angles in the current investigation, is suggested to be a contributing factor to the development of shoulder impingement syndrome (Ludewig & Cook, 2000; McClure et al., 2004). However, this study was the first to test for gender effects on scapular kinematics. Therefore more clinical research into gender effects on scapular kinematics must be completed to validate the claim of increased shoulder injury risk in females.

Any significant effect of movement phase (i.e. raising or lowering of the humerus) on scapular upward rotation and anterior tilt would most likely not be perceptible by the eye in an assessment of motion in a clinical setting. This supports the notion that any visible change in scapular kinematics that occur in humeral lowering compared to raising should be classified as non-healthy (Borstad & Ludewig, 2000; Kibler, 2009). Moreover, findings suggest that this notion should be extended to the additional humeral elevation planes tested in this investigation. Therefore, if observable scapular kinematic changes do occur as a result of altering humeral elevation phase in a clinical assessment of shoulder motion, this should be classified as pathological. In addition, the absence of a visible motion phase effect in one movement plane does not guarantee that this absence persist across all movement planes.

6. CONCLUSIONS

The purposes of this investigation were to profile typical shoulder kinematics during dynamic humeral elevation and to determine statistically the potential factors that influence typical 3D shoulder kinematics. The following conclusions can be made pertaining to humeral elevation in six constrained vertical movement planes:

- Normal shoulder kinematics is highly variable across people. Several measures of variability, indicated by standard deviations, exceeded 100% of the recorded ROM (maximum 300.76% for scapulothoracic protraction).
- Most kinematic profile trends presented in this study agree with prior reports, when comparisons are possible. For example, the scapula presented upward rotation, increased posterior tilt, and range of scapular protraction/retraction occurring with increasing humeral elevation has been repeatedly documented in the past.
- Movement plane heavily influenced normal shoulder kinematics for all transverse plane rotations, as well some sagittal and frontal plane rotations such as scapulothoracic posterior tilt.
- Plane does not meaningfully affect normal typical scapular upward rotation.
- At least one significant gender interaction effect existed for all measured joint rotations excluding glenohumeral plane of elevation and internal/external rotation.
- Any significant motion phase main effect or interactions was most likely visually unobservable due to low magnitudes.

This investigation has produced the most comprehensive collection of typical 3D scapulothoracic, glenohumeral, and sternoclavicular kinematic profiles obtained using skin-mounted motion tracking techniques according to International Society of Biomechanics (ISB)

standards (Wu et al., 2005). The six motion planes assessed extend our knowledge of typical shoulder motion beyond the typically profiled scapular plane and humeral raising. Likewise, this study's inclusion of gender as a potential factor that influences shoulder kinematics was novel, and results showed that females might be predisposed to a higher risk of sub-acromial impingement than that of males. Most importantly, the dynamic profiles presented in this study provide researchers and clinicians a single reference for normative shoulder kinematic data that they can use to identify shoulder motion abnormalities. By testing for movement plane, elevation angle, motion phase, and gender effects on scapular kinematics specifically, clinicians gain insight into what observable scapular patterns during clinical assessments should be deemed typical or abnormal.

REFERENCES

- Ackland, D.C. Richardson, P.P., & Pandy, M.G. (2009). Moment arms of the muscles spanning the anatomical shoulder. *Journal of Anatomy*. 213, 383-390.
- Ackland, D.C. & Pandy, M.G. (2009). Lines of action and stabilizing potential of the shoulder musculature. *Journal of Anatomy*. 215, 184-197.
- Alpert, S.W., Pink, M.M., Jobe, F.W., McMahon, P.J., & Mathiyakom, W. (2000). Electromyographic analysis of deltoid and rotator cuff function under varying loads and speeds., *Journal of Shoulder and Elbow Surgery*. 9(1), 47-58.
- Anglin, C., & Wyss, U. P. (2000). Review of arm motion analyses. *Proceedings of the Institution of Mechanical Engineers, Part H: Journal of Engineering in Medicine*, 214(5), 541-555.
- Borstad, J.D. & Ludewig, P.M. (2002) Comparison of scapular kinematics between elevation and lowering of the arm in the scapular plane. *Clinical Biomechanics*. 17, 650-659.
- Bourne, D.A., Choo, A.M.T., Regan, W.D., MacIntyre, D.L., & Oxland., T.R. (2007). Three-dimensional rotation of the scapula during functional movements: An in vivo study in healthy volunteers. *Journal of Shoulder and Elbow Surgery*. 16, 150-162.
- Bovens, A. M. P., Van Baak, M. A., Vrencken, J. G. P. M., Wijnen, J. A. G., & Verstappen, F. T. J. (1990). Variability and reliability of joint measurements. *American Journal of Sports Medicine*, 18(1), 58-63.
- Boyer, K.A., Beaupre, G.S., & Andriacchi, T.P. (2008). Gender differences exist in the hip joint moments of healthy older walkers. *Journal of Biomechanics*, 41(16), 3360-3365.
- Braman, J.P., Engel, S.C., LaPrade, R.F., & Ludewig, P.M. (2009). In vivo assessment of scapulohumeral rhythm during unconstrained overhead reaching in asymptomatic subjects. *The Journal of Elbow and Joint Surgery*. 18, 960-970.

- Brochard, S., Lempereur, M., & Rémy-Néris, O. (2011). Double calibration: An accurate, reliable and easy-to-use method for 3D scapular motion analysis. *Journal of Biomechanics*, 44(4), 751-754.
- Brookham, R.L., Wong, J.M., & Dickerson, C.D. (2010). Upper limb posture and submaximal hand tasks influence shoulder muscle activity. *International Journal of Industrial Ergonomics*. 40(3), 337-344.
- Cho, S.H., Park, & J.M., Kwon, O.Y. (2004). Gender differences in three dimensional gait analysis data from 98 healthy Korean adults. *Clinical Biomechanics*, 19(2), 145-152.
- Codman, E.A., 1934. *The Shoulder: Rupture of the Supraspinatus Tendon and Other Lesions in or about the Sub-acromial Bursa*, second ed. T Todd Co., Boston.
- Cools, A.M., Witvrouw, E.E., Declercq, G.A., Danneels, L.A., & Cambier, D.C. (2003). Scapular Muscle Recruitment Patterns: Trapezius Muscle Latency with and without Impingement Symptoms *The American Journal of Sports Medicine*. 31(4), 542-549.
- Cools, A.M., Dewitte, V., Lanszweert, F., Notebaert, D., Roets, A., et al. (2007). Rehabilitation of scapular muscle balance: Which exercises to prescribe? *American Journal of Sports Medicine*, 35 (10), 1744-1751.
- Dayanidhi, S., Orlin, M., Kozin, S., Duff, S., & Karduna, A. (2005). Scapular kinematics during humeral elevation in adults and children. *Clinical Biomechanics*, 20(6), 600-606.
- De Luca, C.J. (1997) The use of surface electromyography in biomechanics. *Journal of Applied Biomechanics*. 13, 135-163.
- De Moraes Faria, C. D. C., Teixeira-Salmela, L. F., De Paula Goulart, F. R., & De Souza Moraes, G. F. (2008). Scapular muscular activity with shoulder impingement syndrome during lowering of the arms. *Clinical Journal of Sport Medicine*, 18(2), 130-136.

- de Groot, J.H. (1999). The scapulo-humeral rhythm: effects of 2-D roentgen projection. *Clinical Biomechanics*. 14(1), 63-68.
- de Groot, J.H., & Valstar, E.R. (1998). Velocity effects on the scapula-humeral rhythm. *Clinical Biomechanics*. 13, 593-602.
- Doody, S.G., Freedman, L., & Waterland, J.C. (1970). Doody SG, Freedman L, Waterland JC. Shoulder movements during abduction in the scapular plane. *Archives of Physical Medicine and Rehabilitation*. 51, 595-604.
- Dvir, Z., & Berme, N. (1978). The shoulder complex in elevation of the arm: A mechanism approach. *Journal of Biomechanics*, 11(5), 219-225.
- Ebaugh, D.D., McClure, P.W., & Karduna, A.R. (2005). Three-dimensional scapulothoracic motion during active and passive arm elevation. *Clinical Biomechanics*, 20(7), 700-709.
- Ebaugh, D.D., & Spinelli, B.A. (2010). Scapulothoracic motion and muscle activity during the raising and lowering phases of an overhead reaching task. *Journal of Electromyography and Kinesiology*, 20(2), 199-205.
- Endo, K., Ikata, T., Katoh, S., & Takeda, Y. (2001). Radiographic assessment of scapular rotational tilt in chronic shoulder impingement syndrome. *Journal of Orthopaedic Science*, 6(1), 3-10.
- Engen, T. J., & Spencer, W. A. (1968). Method of kinematic study of normal upper extremity movements. *Archives of Physical Medicine and Rehabilitation*, 49(1), 9-12.
- Fayad, F., Roby-Brami, A., Yazbeck, C., Hanneon, S., Lefevre-Colau, et al. (2008). Three-dimensional scapular kinematics and scapulohumeral rhythm in patients with glenohumeral osteoarthritis or frozen shoulder. *Journal of Biomechanics*. 41, 326-32.
- Grewal, T. (2011). Quantifying the Shoulder Rhythm and Comparing Non-

- Invasive Methods of Scapular Tracking for Overhead and Axially Rotated Humeral Postures In UWSpace. Retrieved February 1, 2012, from http://uwspace.uwaterloo.ca/bitstream/10012/6373/1/Grewal_Tej-Jaskirat.pdf.
- Gozna, E.R. & Harris, W.R. 1979. Traumatic winging of the scapula. *The Journal of Bone & Joint Surgery*. 61, 1230-1233.
- Grood, E. S., & Suntay, W. J. (1983). A joint coordinate system for the clinical description of three-dimensional motions: Application to the knee. *Journal of Biomechanical Engineering*, 105(2), 136-144.
- Hagberg, M., & Wegman, D. H. (1987). Prevalence rates and odds ratios of shoulder-neck diseases in different occupational groups. *British Journal of Industrial Medicine*, 44(9), 602-610.
- Hall, L.C., Middlebrook, E.E., & Dickerson, C.R. (2011). Analysis of the influence of rotator cuff impingements on upper limb kinematics in an elderly population during activities of daily living. *Clinical Biomechanics*, 26(6), 579-584.
- Happee, R. & van der Helm, F.C.T. (1995). The control of shoulder muscles during goal directed movements, an inverse dynamic analysis. *Journal of Biomechanics*. 28(10), 1179-1191.
- Hewitt, D. (1928). The range of active motion of the wrist of women. *J Bone Joint Surg* 26, 775-787.
- Hill, A. M., Bull, A. M. J., Dallalana, R. J., Wallace, A. L., & Johnson, G. R. (2007). Glenohumeral motion: Review of measurement techniques. *Knee Surgery, Sports Traumatology, Arthroscopy*, 15(9), 1137-1143.

- Hill, A. M., Bull, A. M. J., Wallace, A. L., & Johnson, G. R. (2008). Qualitative and quantitative descriptions of glenohumeral motion. *Gait and Posture*, 27(2), 177-188.
- Hogfers, C., Karlsson, & Peterson, B. (1995) Structure and internal consistency of a shoulder model. *Journal of Biomechanics*. 28(7), 767-777.
- Inman, V.T., Saunders J.B., & Abbott, L.C. (1944). Observations on the function of the shoulder joint. *The Journal of Bone and Joint Surgery*. 26, 1-30.
- Johnson, G., Bogduk, N., Nowitzke, A., & House, D. (1994). Anatomy and actions of the trapezius muscle. *Clinical Biomechanics*, 9(1), 44-50.
- Johnson, M.P., McClure, P.W., & Karduna, A.R. (2001). New method to assess scapular upward rotation in subjects with shoulder pathology, *Journal of Orthopaedic Sports Physical Therapy*. 31, 81–89.
- Karduna, A.R., McClure, P.W., Michener, L.A., & Sennett, B. (2001). Dynamic measurements of three-dimensional scapular kinematics: A validation study. *Journal of Biomechanical Engineering*. 123, 184-190.
- Kibler, W. B., & McMullen, J. (2003). Scapular dyskinesis and its relation to shoulder pain. *The Journal of the American Academy of Orthopaedic Surgeons*, 11(2), 142-151.
- Koishi, H., Goto, A., Tanaka, M., Omori, Y., Futai, K., et al. (2011). In vivo three-dimensional motion analysis of the shoulder joint during internal and external rotation. *International Orthopaedics*, 35(10), 1503-1509.
- Langrana, N. A. (1981). Spatial kinematic analysis of the upper extremity using a biplanar videotaping method. *Journal of Biomechanical Engineering*, 103(1), 11-17.

- Ludewig, P. M., & Cook, T. M. (1996). The effect of head position on scapular orientation and muscle activity during shoulder elevation. *Journal of Occupational Rehabilitation*, 6(3), 147-158.
- Ludewig, P.M. & Cook, T.M. (2000). Alterations in shoulder kinematics and associated muscle activity in people with symptoms of shoulder impingement. 80(3), 276-291.
- Ludewig, P.M., Hoff, M.S., Osowski, E.E., Mescke, S.A., & Rundquist, P.J. (2004). Relative balance of serratus anterior and upper trapezius muscle activity during push-up exercises. *The American Journal of Sports Medicine*. 32, 484-493.
- Ludewig, P.M., Phadke, V., Braman, J.P., Hassett, D.R., Cieminski, C.J., & LaPrade, R.F. (2009). Motion of the shoulder complex during multiplanar humeral elevation. *The Journal of Bone and Joint Surgery*. 91, 378-389.
- Magermans, D.J., Chadwick, E.K.J., Veeger, H.E.J., & Van Der Helm, F.C.T. (2005). Requirements for upper extremity motions during activities of daily living. *Clinical Biomechanics*, 20(6), 591-599.
- Matias, R., & Pascoal, A. G. (2006). The unstable shoulder in arm elevation: A three-dimensional and electromyographic study in subjects with glenohumeral instability. *Clinical Biomechanics*, 21 (SUPPL. 1), S52-S58.
- McKean, K.A., Landry, S.C., Hubley-Kozey, C.L., Dunbar, M.J., Stanish, W.D., et al. (2007). Gender differences exist in osteoarthritic gait. *Clinical Biomechanics*, 22(4), 400-409.
- McLure, P.W., Bialker, J., Neff, N., Williams, G., & Karduna, A. (2004). Shoulder function and 3D kinematics in people with shoulder impingement syndrome before and after a 6-week exercise program. *Physical Therapy*. 84,832-848.

- McClure, P.W., Michener, L.A., & Karduna, A.R. (2006). Shoulder function and 3-dimensional scapular kinematics in people with and without shoulder impingement syndrome. *Physical Therapy*. 86(8), 1075-1090.
- McClure, P. W., Michener, L. A., Sennett, B. J., & Karduna, A. R. (2001). Direct 3D measurement of scapular kinematics during dynamic movements in vivo. *Journal of Shoulder and Elbow Surgery*, 10(3), 269-277.
- McLean, L., Chislett, M., Keith, M., Murphy, M., & Walton, P. (2003). The effect of head position, electrode site, movement and smoothing window in the determination of a reliable maximum voluntary activation of the upper trapezius muscle. *Journal of Electromyography and Kinesiology*, 13(2), 169-180.
- McMullen, J. & Uhl, T.L. (2000). A kinetic chain approach for shoulder rehabilitation. *Journal of Athletic Training*. 35(3), 329-337.
- McQuade, K. J., & Smidt, G. L. (1998). Dynamic scapulohumeral rhythm: The effects of external resistance during elevation of the arm in the scapular plane. *Journal of Orthopaedic and Sports Physical Therapy*, 27(2), 125-131.
- Meskers, C.G.M., Vermeulen, J.H., de Groot, F.C.T., van der Helm, & Razing, P.M. (1998). 3D shoulder position measurements using a six-degree-of-freedom electromagnetic tracking device. *Clinical Biomechanics*. 13, 280-292.
- Moore, K.L. & Dalley A. F. (1999). *Clinically Orientated Human Anatomy* (4th ed.). Baltimore: Lippincott Williams & Wilkins.
- Neer, C.S. (1972). Anterior acromioplasty for the chronic impingement syndrome in the shoulder. A preliminary report. *Journal of Bone and Joint Surgery*. 54(A), 41-50.
- Nixon, M.A., McCallum, B.C., Fright, W.R., & Price, N.B. (1998). The Effects of Metals and

- Interfering Fields on Electromagnetic Trackers. *Presence*. 7(2), 204-218.
- Paletta Jr., G. A., Warner, J. J. P., Warren, R. F., Deutsch, A., & Altchek, D. W. (1997). Shoulder kinematics with two-plane x-ray evaluation in patients with anterior instability or rotator cuff tearing. *Journal of Shoulder and Elbow Surgery*, 6(6), 516-527.
- Palmerud, G., Forsman, M., Sporrang, H., Herberts, P., & Kadefors, R. (2000). Intramuscular pressure of the infra- and supraspinatus muscles in relation to hand load and arm posture. *European Journal of Applied Physiology*, 83(2-3), 223-230.
- Park, H.B., Yokota, A., Gill, H.S., El Rassi, G., & McFarland, E.G. 2005. Diagnostic Accuracy of Clinical Tests for the Different Degrees of Sub-acromial Impingement Syndrome. *The Journal of Bone & Joint Surgery*. 87, 1446-1455.
- Pascoal, A. G., Van Der Helm, F. F. C. T., Pezarat Correia, P., & Carita, I. (2000). Effects of different arm external loads on the scapulo-humeral rhythm. *Clinical Biomechanics*, 15(SUPPL. 1), S21-S24.
- Phadke, V., Camargo, P.R., & Ludewig, P.M. (2009) Scapular and rotator cuff muscle activity during arm elevation: A review of normal function and alterations with shoulder impingement. *Rev Bras Fisioter*. 13(1), 1-9.
- Picco, B.R., Fischer, S. L., & Dickerson, C.R. (2010). Quantifying scapula orientation and its influence on maximal hand force capability and shoulder muscle activity. *Clinical Biomechanics*. 25, 29-36.
- Poppen, N.K. & Walker, P.S. (1976). Normal and abnormal motion of the shoulder. *Bone and Joint Surgery of America*. 58, 195-201.

- Pronk, C.M., & van der Helm, F.C.T. (1991). The palpator: an instrument for measuring the positions of bones in three dimensions. *Journal of Medical Engineering Technology*, 15(1),15-20.
- Rab, G., Petuskey, K., & Bagley, A. (2002). A method for determination of upper extremity kinematics. *Gait and Posture*, 15(2), 113-119.
- Robertson, D.G.E., Caldwell, G.E., Hamill, J., Kamen, G., & Whittlesey, S.N. (2004). *Research Methods in Biomechanics*. Windsor: Human Kinetics.
- Shrout, P.E. & Fleiss, J.L. (1979). Intraclass correlations: uses in assessing rater reliability. *Physiology Bulletin*. 2, 420-428.
- Szucs, K.A. & Borstad, J.D. (2010). Capturing 3D clavicle kinematics: validation of surface sensor. *International Shoulder Group Conference Proceedings*. 77-78.
- Szucs, K., Navalgund, A., & Borstad, J. D. (2009). Scapular muscle activation and co-activation following a fatigue task. *Medical and Biological Engineering and Computing*, 47(5 SPEC. ISS.), 487-495.
- Taylor, C. L., & Blaschke, A. C. (1951). A method for kinematic analysis of motions of the shoulder, arm, and hand complex. *Annals of the New York Academy of Sciences*, 51(7), 1251-1265.
- Teece, R. M., Lunden, J. B., Lloyd, A. S., Kaiser, A. P., Cieminski, C. J., & Ludewig, P. M. (2008). Three-dimensional acromioclavicular joint motions during elevation of the arm. *Journal of Orthopaedic and Sports Physical Therapy*, 38(4), 181-190.
- van der Helm, F. C. T., & Pronk, G. M. (1995). Three-dimensional recording and description of motions of the shoulder mechanism. *Journal of Biomechanical Engineering*, 117(1), 27-40.

- van Andel, C., van Hutten, K., Eversdijk, M., Veeger, D.J., & Harlaar, J. (2008). Recording scapular motion using an acromion marker cluster. *Gait and Posture*. 29,123-128.
- Vaughan, C.L., Davis, B.L., and O'Connor, J.C. (1999). *Dynamics of Human Gait*, 2nd Edition. Champaign, IL: Human Kinetics.
- Weir, J.P. (2005). Quantifying test-retest reliability using the intraclass correlation coefficient and the SEM. *Journal of Strength and Conditioning Research*, 19 (1), 231-240.
- Wiedenbauer, M.M., & Mortensen, O.A. (1952). An electromyographic study of the trapezius muscle. *American Journal of Physical Medicine*. 31(5), 363-72.
- Winter, D.A. (2009). *Biomechanics and motor control of human movement*. (4th ed.). Toronto: Wiley and Sons, Inc.
- Woltring, H. J., & Huiskes, R. (1994). 3-D attitude representation of human joints: A standardization proposal. *Journal of Biomechanics*, 27(12), 1399-1414.
- Wu, G., van Der Helm F.C., Veeger, H.E., Makhsous, M., Van, R.P., Anglin, C., et al. (2005). ISB recommendation on definitions of joint coordinate systems of various joints for the reporting of human joint motion—Part II: shoulder, elbow, wrist and hand. *Journal of Biomechanics*. 38(5), 981–92.
- Yamaguchi, K., Sher, J. S., Andersen, W. K., Garretson, R., Uribe, J. W., Hechtman, K., et al. (2000). Glenohumeral motion in patients with rotator cuff tears: A comparison of asymptomatic and symptomatic shoulders. *Journal of Shoulder and Elbow Surgery*, 9(1), 6-11.
- Youdas, J. W., Carey, J. R., Garrett, T. R., & Suman, V. J. (1994). Reliability of goniometric measurements of active arm elevation in the scapular plane obtained in a clinical setting. *Archives of Physical Medicine and Rehabilitation*, 75(10), 1137-1144.

Yoshizaki, K., Hamada, J., Tamai, K., Sahara, R., Fujiwara, T., et al. (2009). Analysis of the scapulohumeral rhythm and electromyography of the shoulder muscles during elevation and lowering: Comparison of dominant and non-dominant shoulders

APPENDIX A: Link segment and local coordinate system descriptions

Table A1: Link segment definitions anatomical landmarks (Wu et al., 2005)

| Segment | Definition |
|---------|---|
| Thorax | Plane created by the C7, T8, XP, and SSN |
| Scapula | Plane created by the AA, IA, and RS |
| Humerus | Link connecting the midpoint between LE and ME and the approximate GH joint center |
| Forearm | Link connecting the midpoint between LE and ME and the midpoint between the US and RS |

Table A2: Segment-based orthogonal coordinate system definitions (Wu et al., 2005)

| System | Definition |
|--|--|
| Thorax coordinate system (Figure A1) | <p><i>Origin:</i> Coincident with the suprasternal notch</p> <p><i>x-axis (Tx):</i> Line normal to the plane formed by XP, SSN, C7, and T8, directed laterally</p> <p><i>y-axis (Ty):</i> Line normal to the x and z-axis directed forward</p> <p><i>z-axis (Tz):</i> Line connecting the midpoint between the SSN and C7, and the midpoint between the XP and T8 directed upward.</p> |
| Clavicle coordinate system (Figure A2) | <p><i>Origin:</i> Coincident with SC</p> <p><i>x-axis (Cx):</i> Line connecting SC and AC directed laterally</p> <p><i>y-axis (Cy):</i> Line normal to the clavicle x-axis and the thorax z-axis directed forward</p> <p><i>z-axis (Cz):</i> Line normal to the y-axis and x-axis directed superiorly</p> |
| Scapula coordinate system (Figure A3) | <p><i>Origin:</i> Coincident with AA</p> <p><i>x-axis (Sx):</i> Line connecting SR and AA directed at AA</p> <p><i>y-axis (Sy):</i> Line normal to the plane created by AA, IA, and SR directed forward</p> <p><i>z-axis (Sz):</i> Line normal to the y-axis and x-axis directed superiorly</p> |
| Humerus coordinate system (Figure A4) | <p><i>Origin:</i> Coincident with the GH</p> <p><i>x-axis (Hx):</i> Line normal to the z- and y-axis directed laterally</p> <p><i>y-axis (Hy):</i> Line normal to the plane formed by the LE, ME, and GH directed forward</p> <p><i>z-axis (Hz):</i> Line connecting the midpoint between the LE and ME and the GH directed at GH</p> |

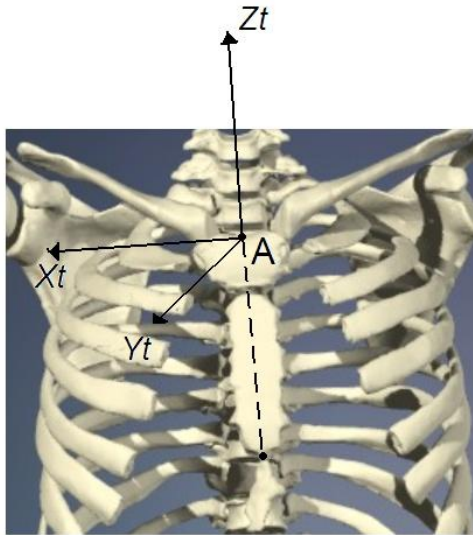


Figure A1: Orthogonal thorax system with the origin at the suprasternal notch (SSN) at A. Y_t is directed perpendicular to the plane created by XP, SSN, C7, and T8 directed forward (Image from Primal Pictures)

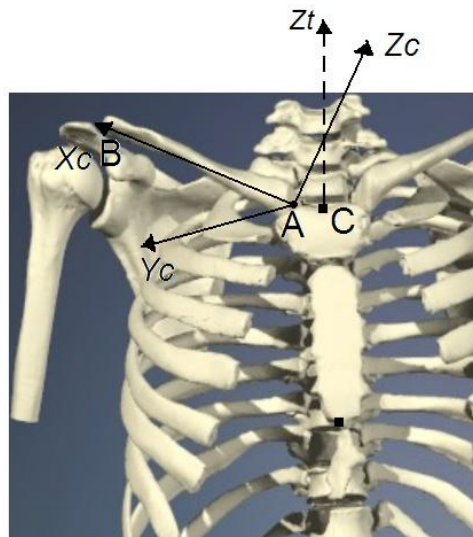


Figure A2: Orthogonal clavicle system with the origin at the sternoclavicular joint at point A. Y_c is directed perpendicular to the plane created by Z_t and X_c directed forward (Image from Primal Pictures)

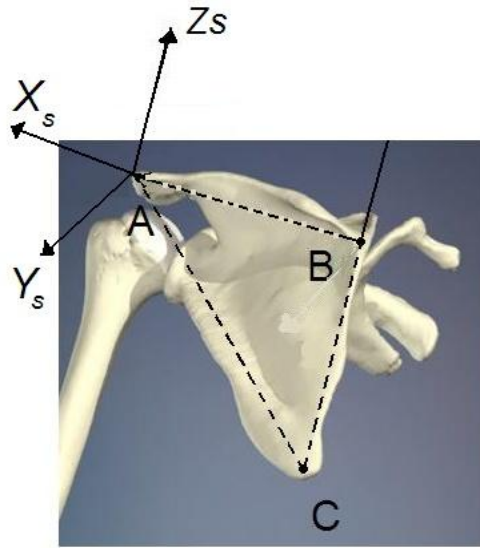


Figure A3: Orthogonal scapula system with the origin at the acromion angle AA at point A. Y_s is directed perpendicular to the plane created by the AA, inferior angle (IA) at C, and scapular spine root (SR) at C directed forward (Image from Primal Pictures)



Figure A4: Orthogonal humerus system with the origin at the glenohumeral joint (GH) at point A. Y_h is directed perpendicular to the plane created by the medial epicondyle (ME), lateral epicondyle (LE), and GH directed forward (Image from Primal Pictures)

Table A3: Marker cluster orthogonal coordinate system definitions

| System | Definition |
|-------------------------------------|---|
| Acromion marker cluster (Figure A5) | <p><i>Origin:</i> AMC3</p> <p><i>x-axis:</i> Line connecting AMC3 and AMC2 directed laterally</p> <p><i>y-axis:</i> Line normal to the plane created by AMC1, AMC2, directed forward</p> <p><i>z-axis:</i> Line orthogonal to the x- and y-axis directed superiorly</p> |
| Digitizing stylus (Figure A6) | <p><i>Origin:</i> STY3</p> <p><i>x-axis:</i> Line connecting STY3 and STY2 directed laterally</p> <p><i>y-axis:</i> Line normal to the plane created by AMC1, AMC2, directed forward</p> <p><i>z-axis:</i> Line orthogonal to the x- and y-axis directed superiorly</p> |
| Humerus cluster | <p><i>Origin:</i> HUM3</p> <p><i>x-axis:</i> Line connecting HUM3 and HUM2 directed laterally</p> <p><i>y-axis:</i> Line normal to the plane created by HUM1, HUM2, directed forward</p> <p><i>z-axis:</i> Line orthogonal to the x- and y-axis directed superiorly</p> |

Table A4: Joint coordinate system (JCS) (Grood and Suntay, 1983) definitions of the SC and AC joints; ST and TH segments. Each JCS floating axis is defined as the common perpendicular of the stationary and moving system's fixed axes, with the exception of the

| Joint or segment | Definition |
|------------------|--|
| SC | <p><i>Stationary system/fixed axis:</i> Thorax coordinate system/z-axis</p> <p><i>Moving system/fixed axis:</i> Clavicle coordinate system/x-axis</p> |
| AC | <p><i>Stationary system/fixed axis:</i> Clavicle coordinate system/x-axis</p> <p><i>Moving system/fixed axis:</i> Scapula coordinate system/z-axis</p> |
| ST | <p><i>Stationary system/fixed axis:</i> Thorax coordinate system/z-axis</p> <p><i>Moving system/fixed axis:</i> Scapula coordinate system/x-axis</p> |

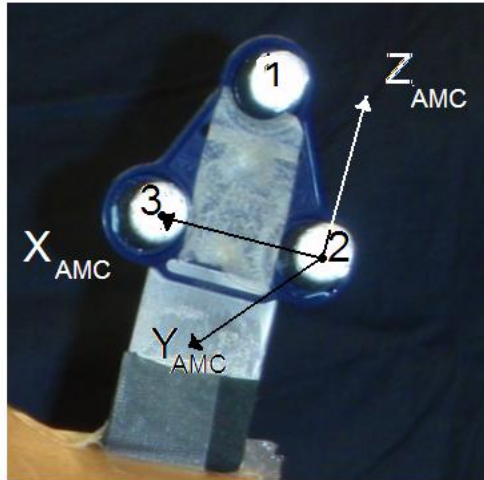


Figure A5: Orthogonal acromion marker cluster (AMC) coordinate system with the origin at AMC2 at point A. Y_{AMC} is perpendicular to the plane created by AMC1, AMC2, and AMC3 directed forward.

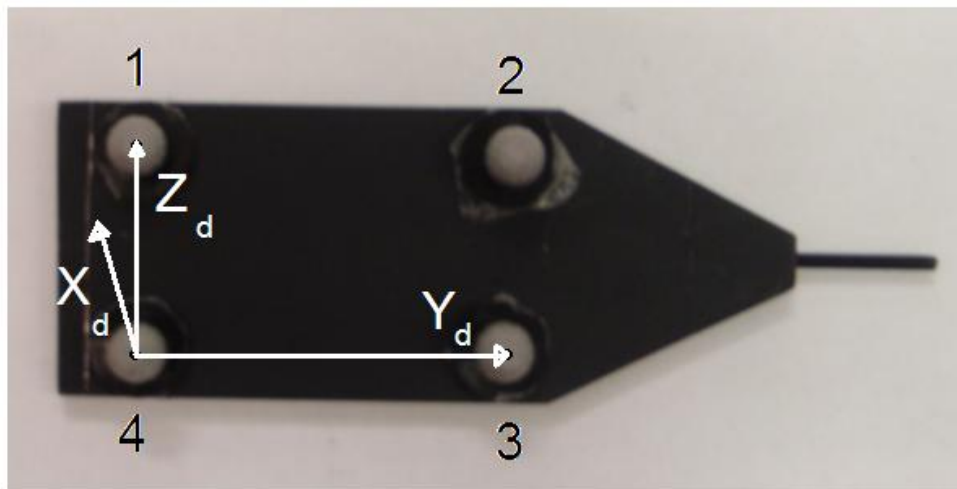


Figure A6: Orthogonal digitizing stylus system with the origin at STY4. S_d is perpendicular to the plane created by STY1, STY2, STY3, and STY4 directed forward.

APPENDIX B: Decomposition and rotational transformation matrices

- 1) **Decomposition rotation matrix [R] (order: Z-Y-Z) construction used to determine Euler angles that describe 3D GH joint rotation:**

$$[R] = [R_z] [R_y] [R_z] \quad \text{B1.0}$$

Where: B1.1

$$[R_z] = \begin{bmatrix} \cos \alpha & \sin \alpha & 0 \\ -\sin \alpha & \cos \alpha & 0 \\ 0 & 0 & 1 \end{bmatrix} \quad [R_y] = \begin{bmatrix} \cos \beta & 0 & -\sin \beta \\ 0 & 1 & 0 \\ \sin \beta & 0 & \cos \beta \end{bmatrix} \quad [R_z] = \begin{bmatrix} \cos \gamma & \sin \gamma & 0 \\ -\sin \gamma & \cos \gamma & 0 \\ 0 & 0 & 1 \end{bmatrix}$$

Therefore: B1.2

$$[R] = \begin{bmatrix} \cos \alpha \cdot \cos \beta \cdot \cos \gamma - \sin \alpha \cdot \sin \gamma & \cos \gamma \cdot \sin \alpha + \sin \gamma \cdot \cos \beta \cdot \cos \alpha & -\sin \beta \cdot \cos \alpha \\ -\cos \gamma \cdot \cos \beta \cdot \sin \alpha + \sin \beta \cdot \cos \alpha & \cos \alpha \cdot \cos \gamma - \sin \gamma \cdot \cos \beta \cdot \sin \alpha & \sin \beta \cdot \sin \alpha \\ \cos \gamma \cdot \sin \beta & \sin \gamma \cdot \sin \beta & \cos \beta \end{bmatrix}$$

- 2) **Rotational transformation matrix [TR] used to determine the projection of the humerus coordinate system (unit vectors i, j, k) on to the scapular coordinate system (unit vectors I,J,K)**

$$[R]_{hum}^{scap} = \begin{bmatrix} \mathbf{i} & \mathbf{j} & \mathbf{k} \end{bmatrix}_{hum} \begin{bmatrix} \mathbf{I} & \mathbf{J} & \mathbf{K} \end{bmatrix}_{scap}^{-1} \quad \text{B2.0}$$

Where: B2.1

$$[T]_{hum} = \begin{bmatrix} ix & iy & iz \\ jx & jy & jz \\ kx & ky & kz \end{bmatrix} \quad [T]_{scap} = \begin{bmatrix} Ix & Iy & Iz \\ Jx & Jy & Jz \\ Kx & Ky & Kz \end{bmatrix}$$

Therefore: B2.2

$$[R]_{hum}^{scap} = \begin{bmatrix} I \bullet i & I \bullet j & I \bullet k \\ J \bullet i & J \bullet j & J \bullet k \\ K \bullet i & K \bullet j & K \bullet k \end{bmatrix}$$

- 3) **Rotational transformation matrix used to determine the projection of the digitizing stylus or acromion marker cluster (“cluster”) coordinate systems (unit vectors i, j, k) on to the global coordinate system (unit vectors I,J,K)**

$$[R]_{cluster}^{GLOBAL} = \mathbf{T}_{cluster} \mathbf{T}_{GLOBAL}^T \quad \text{B3.0}$$

Where:

$$[T_{cluster}] = \begin{bmatrix} ix & iy & iz \\ jx & jy & jz \\ kx & ky & kz \end{bmatrix} \quad [T_{GLOBAL}] = \begin{bmatrix} Ix & Iy & Iz \\ Jx & Jy & Jz \\ Kx & Ky & Kz \end{bmatrix} = \begin{bmatrix} 1 & 0 & 0 \\ 0 & 1 & 0 \\ 0 & 0 & 1 \end{bmatrix} \quad \text{B3.1}$$

APPENDIX C: Descriptive statistics and intra-class correlation

Table C1: Three-dimensional scapulothoracic kinematics descriptive statistics for the examined humeral elevation planes organized by elevation phase (SPR = scapulothoracic +protraction/-retraction; SML = scapulothoracic +medial/-lateral rotation; SPA = scapulothoracic +posterior/-anterior tilt). All values are in degrees (°)

| Rotation | Plane | Raising Phase | | | Lowering Phase | | |
|----------|----------|---------------|-------|--------|----------------|-------|--------|
| | | Range | Max | Min | Range | Max | Min |
| SPR | 0° | 4.14 | 26.75 | 22.61 | 3.93 | 25.49 | 21.56 |
| | 30° | 2.44 | 32.35 | 29.91 | 3.28 | 31.22 | 27.93 |
| | Scapular | 3.62 | 35.52 | 31.90 | 3.56 | 33.38 | 29.82 |
| | 60° | 4.65 | 38.92 | 34.28 | 5.57 | 37.83 | 32.26 |
| | 90° | 12.03 | 46.10 | 34.07 | 13.29 | 44.25 | 30.95 |
| | 120° | 18.87 | 54.92 | 36.05 | 16.24 | 52.03 | 35.80 |
| SML | 0° | 36.71 | 4.35 | -32.37 | 33.12 | 1.96 | -31.16 |
| | 30° | 33.71 | 4.16 | -29.56 | 31.85 | 2.13 | -29.72 |
| | Scapular | 35.15 | 5.04 | -30.11 | 32.51 | 3.21 | -29.30 |
| | 60° | 35.14 | 3.93 | -31.21 | 33.11 | 2.61 | -30.50 |
| | 90° | 34.32 | 2.80 | -31.51 | 33.17 | 1.28 | -31.89 |
| | 120° | 32.70 | 0.07 | -32.63 | 36.15 | 3.36 | -32.79 |
| SPA | 0° | 11.92 | 7.61 | -4.31 | 13.77 | 9.27 | -4.50 |
| | 30° | 11.43 | 6.43 | -4.99 | 12.26 | 6.75 | -5.51 |
| | Scapular | 10.58 | 5.60 | -4.97 | 12.65 | 7.50 | -5.15 |
| | 60° | 10.16 | 4.54 | -5.62 | 9.51 | 4.48 | -5.02 |
| | 90° | 7.98 | 3.11 | -4.87 | 7.66 | 2.70 | -4.96 |
| | 120° | 7.62 | 2.09 | -5.53 | 6.03 | -0.11 | -6.14 |

Table C2: Scapulothoracic rhythm for the examined humeral elevation planes organized by elevation phase

| Plane | Raising Phase | | Lowering Phase | |
|----------|---------------|------|----------------|------|
| | Rhythm | SD | Rhythm | SD |
| 0° | -2.86 | 0.27 | -3.23 | 0.30 |
| 30° | -3.09 | 0.29 | -3.35 | 0.63 |
| Scapular | -3.18 | 0.35 | -3.25 | 0.19 |
| 60° | -3.13 | 0.26 | -3.24 | 0.33 |
| 90° | -3.08 | 0.31 | -3.10 | 0.32 |
| 120° | -3.45 | 0.50 | -3.65 | 0.90 |
| OVERALL | -3.13 | 0.37 | -3.30 | 0.52 |

Table C3: Three-dimensional glenohumeral kinematics descriptive statistics for the examined humeral elevation planes organized by elevation phase (GAP = glenohumeral +anterior/-posterior plane; GLE = glenohumeral –elevation; GIE glenohumeral +interior/-exterior rotation). All values are in degrees (°)

| Rotation | Plane | Raising Phase | | | Lowering Phase | | | |
|----------|----------|---------------|--------|--------|----------------|--------|--------|--------|
| | | Range | Max | Min | Range | Max | Min | |
| GAP | 0° | 18.07 | 1.51 | -16.56 | 21.95 | 8.47 | -13.48 | |
| | 30° | 21.71 | 27.04 | 5.33 | 23.91 | 31.58 | 7.67 | |
| | Scapular | 60° | 17.69 | 25.45 | 7.76 | 21.84 | 32.37 | 10.53 |
| | | 90° | 25.71 | 42.02 | 16.31 | 23.48 | 40.42 | 16.95 |
| | 120° | 29.78 | 55.01 | 25.24 | 29.71 | 54.89 | 25.18 | |
| | 120° | 35.16 | 60.59 | 25.43 | 41.54 | 65.07 | 23.53 | |
| GLE | 0° | 68.33 | -19.74 | -88.07 | 71.11 | -17.81 | -88.93 | |
| | 30° | 71.26 | -18.97 | -90.23 | 70.17 | -19.80 | -89.97 | |
| | Scapular | 60° | 69.69 | -20.02 | -89.72 | 70.56 | -19.51 | -90.07 |
| | | 90° | 68.64 | -20.06 | -88.70 | 70.49 | -19.50 | -89.99 |
| | 120° | 71.60 | -18.63 | -90.23 | 72.40 | -17.64 | -90.04 | |
| | 120° | 73.32 | -17.80 | -91.12 | 72.42 | -19.90 | -92.32 | |
| GIE | 0° | 10.01 | -40.31 | -50.32 | 6.94 | -49.03 | -55.97 | |
| | 30° | 11.60 | -53.46 | -65.05 | 19.15 | -54.38 | -73.52 | |
| | Scapular | 60° | 11.56 | -53.81 | -65.37 | 20.19 | -54.07 | -74.27 |
| | | 90° | 17.53 | -54.38 | -71.91 | 16.88 | -56.39 | -73.26 |
| | 120° | 25.46 | -45.20 | -70.66 | 35.20 | -36.73 | -71.94 | |
| | 120° | 37.06 | -29.76 | -66.82 | 43.56 | -23.73 | -67.29 | |

Table C4: Two-dimensional acromioclavicular kinematics descriptive statistics for the examined humeral elevation planes organized by elevation phase (APR = acromioclavicular +protraction/-retraction; ; AED = acromioclavicular –elevation). All values are in degrees (°)

| Rotation | Plane | Raising Phase | | | Lowering Phase | | | |
|----------|----------|---------------|-------|--------|----------------|-------|--------|--------|
| | | Range | Max | Min | Range | Max | Min | |
| APR | 0° | 6.38 | 50.77 | 44.39 | 6.29 | 49.69 | 43.40 | |
| | 30° | 7.23 | 46.94 | 39.71 | 7.17 | 46.42 | 39.26 | |
| | Scapular | 60° | 7.94 | 46.77 | 38.84 | 7.05 | 45.72 | 38.67 |
| | | 90° | 9.92 | 46.25 | 36.33 | 9.48 | 45.20 | 35.72 |
| | 120° | 11.95 | 45.99 | 34.04 | 10.86 | 46.01 | 35.16 | |
| | 120° | 12.98 | 49.32 | 36.34 | 9.66 | 48.68 | 39.02 | |
| AED | 0° | 12.26 | -8.39 | -20.65 | 14.03 | -7.75 | -21.78 | |
| | 30° | 13.65 | -7.35 | -21.00 | 14.39 | -6.58 | -20.97 | |
| | Scapular | 60° | 15.04 | -6.47 | -21.51 | 15.15 | -6.98 | -22.13 |
| | | 90° | 16.41 | -4.53 | -20.94 | 15.60 | -5.99 | -21.59 |
| | 120° | 18.22 | -4.25 | -22.47 | 13.94 | -8.12 | -22.06 | |
| | 120° | 21.13 | -5.91 | -27.05 | 16.41 | -8.73 | -25.14 | |

Table C5: Two-dimensional sternoclavicular kinematics descriptive statistics for the examined humeral elevation planes organized by elevation phase (CPR = sternoclavicular +protraction/-retraction; ; CED = sternoclavicular –elevation). All values are in degrees (°)

| Rotation | Plane | Raising Phase | | | Lowering Phase | | |
|----------|----------|---------------|--------|--------|----------------|--------|--------|
| | | Range | Max | Min | Range | Max | Min |
| CPR | 0° | 18.26 | -8.82 | -27.08 | 16.05 | -10.00 | -26.05 |
| | 30° | 17.57 | -8.34 | -25.92 | 15.88 | -8.84 | -24.72 |
| | Scapular | 17.81 | -7.95 | -25.77 | 15.06 | -9.56 | -24.62 |
| | 60° | 16.89 | -8.26 | -25.15 | 15.41 | -9.09 | -24.50 |
| | 90° | 17.43 | -8.51 | -25.94 | 14.71 | -10.50 | -25.21 |
| CED | 120° | 18.25 | -9.83 | -28.08 | 16.12 | -11.20 | -27.32 |
| | 0° | 21.48 | -20.74 | -42.22 | 20.66 | -22.74 | -43.39 |
| | 30° | 20.77 | -19.14 | -39.91 | 21.19 | -20.56 | -41.75 |
| | Scapular | 20.86 | -18.02 | -38.87 | 21.30 | -19.29 | -40.59 |
| | 60° | 20.37 | -17.45 | -37.81 | 21.95 | -18.50 | -40.46 |
| | 90° | 20.24 | -17.31 | -37.55 | 21.69 | -18.16 | -39.85 |
| | 120° | 22.79 | -14.94 | -37.73 | 25.02 | -14.83 | -39.84 |

Table C6: Mean intra-class correlation coefficients (ICCs) of all measured joint rotations for each plane of humeral elevation. ICCs are sorted from largest to smallest

| Plane | Rotation | Mean | Max | Min | STD | Plane | Rotation | Mean | Max | Min | STD |
|----------------|----------|-------|-------|-------|-------|------------|----------|-------|-------|-------|-------|
| 0° plane | GLE | 0.998 | 0.986 | 0.924 | 0.011 | 30° plane | GLE | 0.999 | 0.998 | 0.987 | 0.002 |
| | SPR | 0.968 | 0.994 | 0.673 | 0.057 | | CED | 0.969 | 0.999 | 0.603 | 0.058 |
| | CED | 0.958 | 0.999 | 0.489 | 0.071 | | SPR | 0.961 | 0.998 | 0.659 | 0.063 |
| | SPA | 0.941 | 0.999 | 0.200 | 0.142 | | SPA | 0.960 | 0.998 | 0.659 | 0.064 |
| | GIE | 0.937 | 0.998 | 0.628 | 0.076 | | GIE | 0.930 | 0.998 | 0.637 | 0.087 |
| | AED | 0.815 | 0.997 | 0.035 | 0.261 | | AED | 0.864 | 0.997 | 0.070 | 0.207 |
| | CPR | 0.794 | 0.996 | 0.001 | 0.240 | | CPR | 0.782 | 0.994 | 0.060 | 0.230 |
| | APR | 0.723 | 0.988 | 0.040 | 0.252 | | SML | 0.765 | 0.997 | 0.018 | 0.249 |
| | SML | 0.683 | 0.995 | 0.027 | 0.268 | | APR | 0.634 | 0.992 | 0.014 | 0.305 |
| | GAP | 0.668 | 0.995 | 0.030 | 0.318 | | GAP | 0.627 | 0.988 | 0.017 | 0.299 |
| Scapular plane | GLE | 0.999 | 0.999 | 0.980 | 0.003 | 60° plane | GLE | 1.000 | 0.992 | 0.987 | 0.002 |
| | CED | 0.955 | 0.999 | 0.319 | 0.127 | | CED | 0.942 | 0.987 | 0.166 | 0.148 |
| | SPA | 0.951 | 0.997 | 0.288 | 0.125 | | GIE | 0.941 | 0.997 | 0.209 | 0.116 |
| | SPR | 0.950 | 0.997 | 0.288 | 0.125 | | SPR | 0.939 | 0.998 | 0.342 | 0.121 |
| | GIE | 0.947 | 0.997 | 0.821 | 0.044 | | SPA | 0.844 | 0.998 | 0.007 | 0.277 |
| | AED | 0.887 | 0.990 | 0.274 | 0.151 | | CPR | 0.829 | 0.998 | 0.160 | 0.217 |
| | CPR | 0.836 | 0.996 | 0.219 | 0.194 | | AED | 0.813 | 0.996 | 0.060 | 0.239 |
| | SML | 0.755 | 0.995 | 0.010 | 0.270 | | SML | 0.755 | 0.995 | 0.010 | 0.268 |
| | APR | 0.628 | 0.975 | 0.040 | 0.321 | | APR | 0.683 | 0.988 | 0.028 | 0.267 |
| | GAP | 0.627 | 0.989 | 0.023 | 0.284 | | GAP | 0.623 | 0.992 | 0.080 | 0.301 |
| 90° plane | GLE | 0.999 | 0.986 | 0.990 | 0.002 | 120° plane | GLE | 0.999 | 0.998 | 0.986 | 0.002 |
| | CED | 0.967 | 0.986 | 0.752 | 0.040 | | CED | 0.963 | 0.999 | 0.810 | 0.038 |
| | GIE | 0.935 | 0.995 | 0.547 | 0.078 | | SPA | 0.884 | 0.994 | 0.189 | 0.178 |
| | SPR | 0.929 | 0.998 | 0.264 | 0.131 | | SPR | 0.861 | 0.995 | 0.189 | 0.188 |
| | SPA | 0.927 | 0.998 | 0.264 | 0.133 | | GIE | 0.857 | 0.991 | 0.089 | 0.212 |
| | CPR | 0.825 | 0.997 | 0.051 | 0.222 | | CPR | 0.816 | 0.995 | 0.160 | 0.246 |
| | SML | 0.798 | 0.990 | 0.059 | 0.222 | | AED | 0.717 | 0.981 | 0.000 | 0.243 |
| | APR | 0.784 | 0.985 | 0.120 | 0.201 | | SML | 0.711 | 0.988 | 0.016 | 0.264 |
| | AED | 0.749 | 0.989 | 0.045 | 0.260 | | APR | 0.706 | 0.984 | 0.075 | 0.248 |
| | GAP | 0.704 | 0.986 | 0.011 | 0.255 | | GAP | 0.700 | 0.995 | 0.046 | 0.294 |

APPENDIX D: Kinematic profiles for the lowering phase

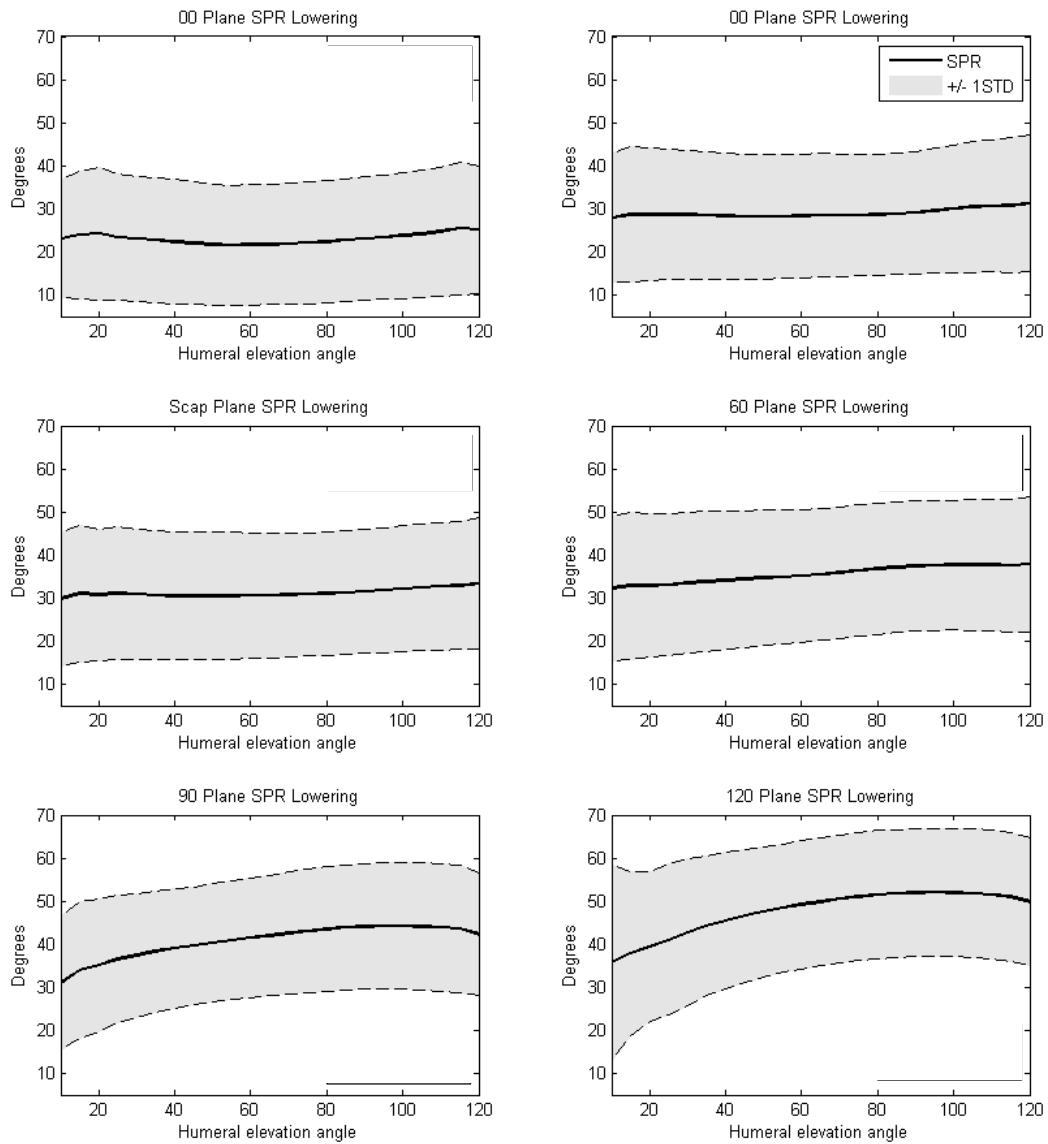


Figure D1: Mean scapulothoracic +protraction/-retraction (SPR) kinematic profiles, with +/- one standard deviation, for the six tested vertical planes – lowering phase

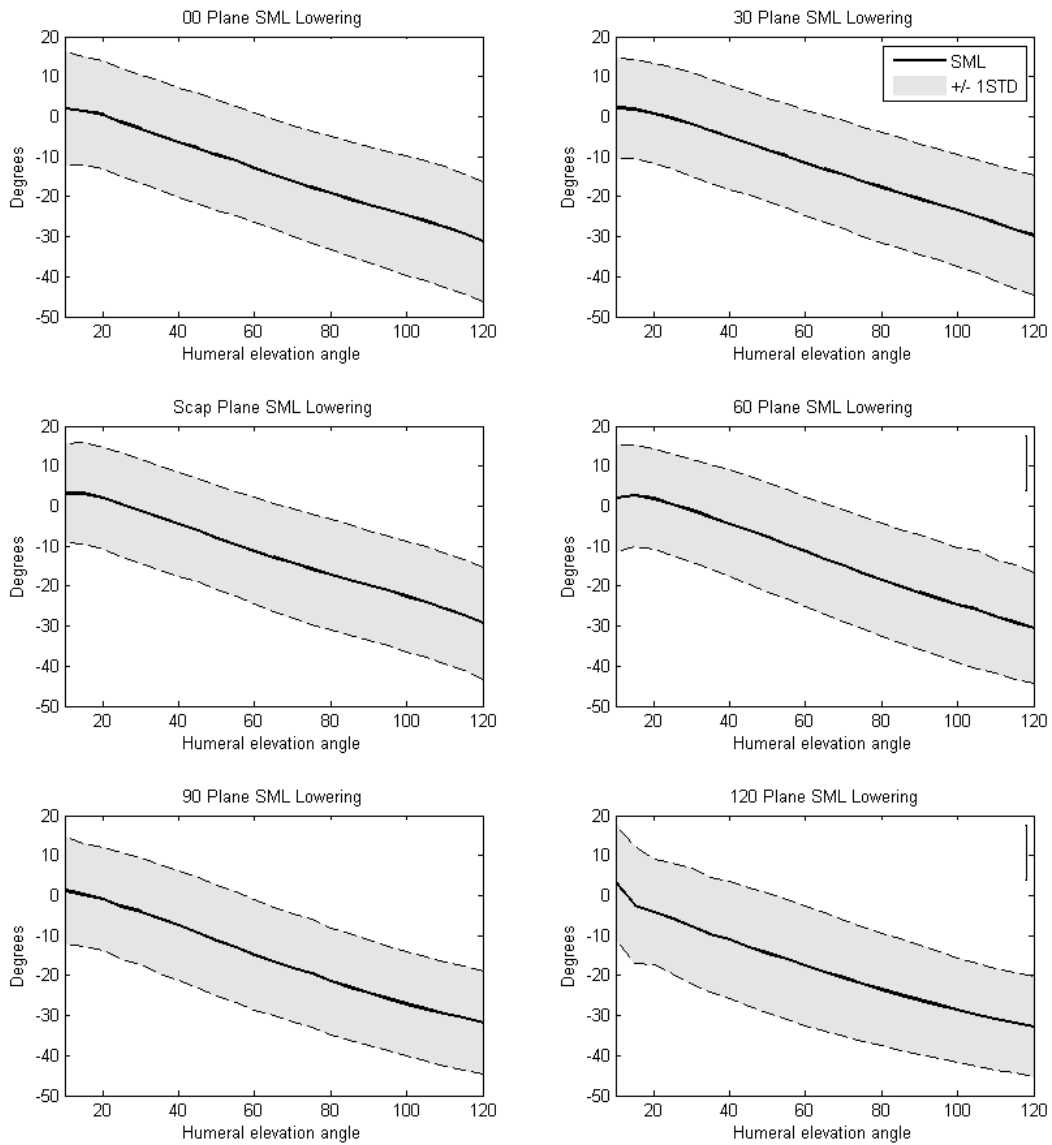


Figure D2: Mean scapulothoracic +medial/-lateral rotation (SML) kinematic profiles, with +/- one standard deviation, for the six tested vertical planes – lowering phase

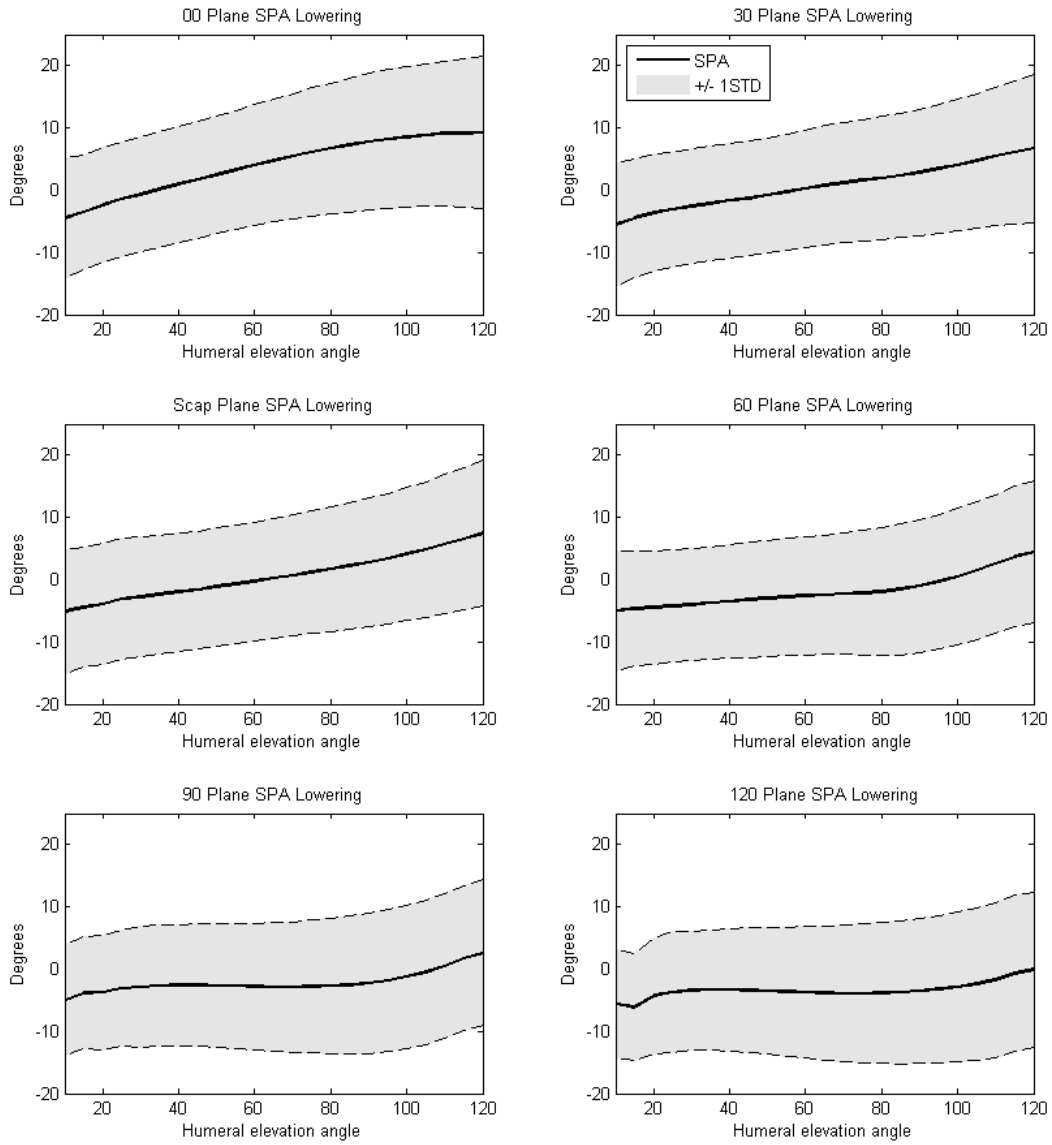


Figure D3: Mean scapulothoracic +positive/-retraction (SPA) kinematic profiles, with +/- one standard deviation, for the six tested vertical planes – lowering phase

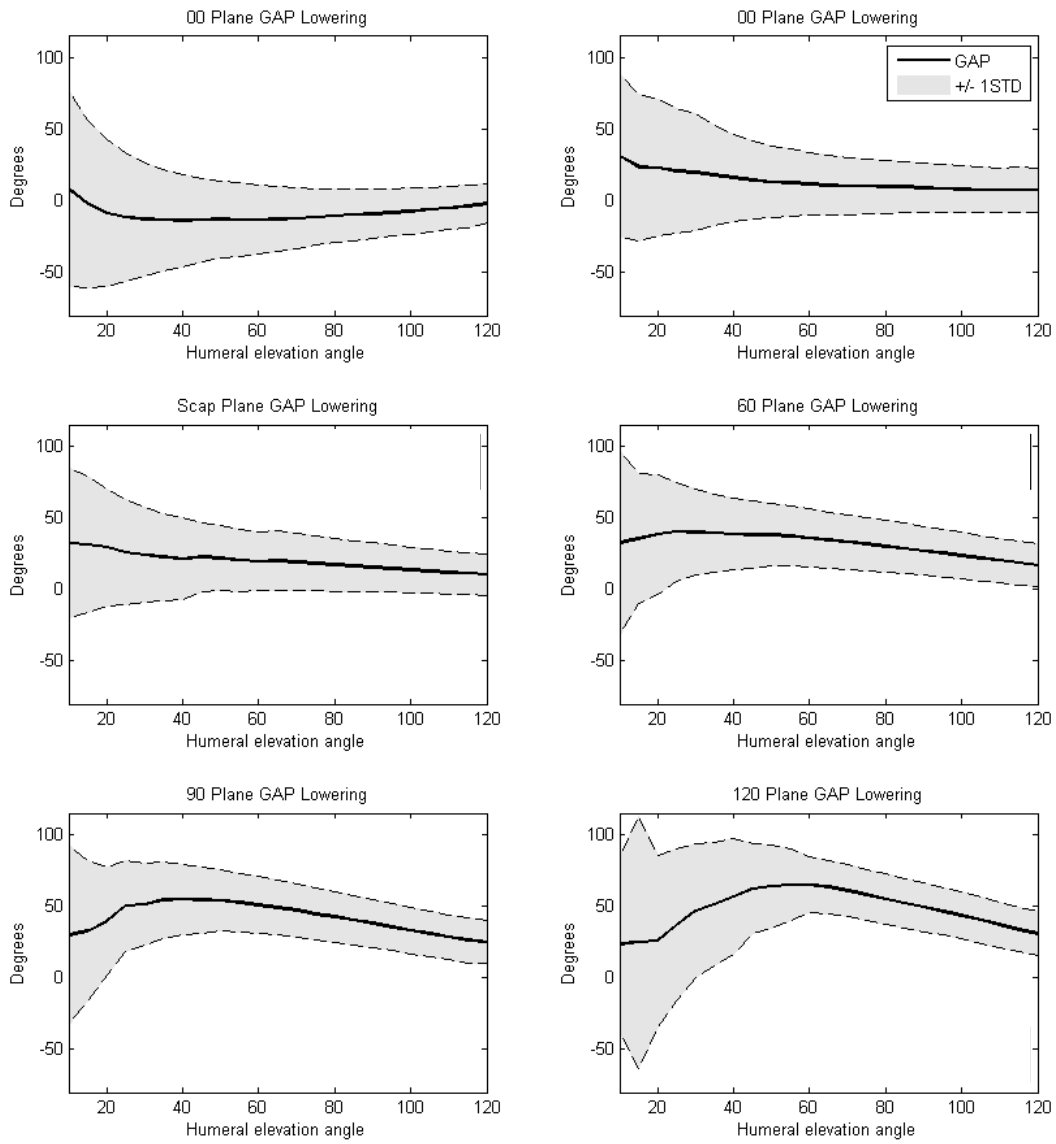


Figure D4: Mean glenohumeral +anterior/-posterior elevation plane (GAP) kinematic profiles, with +/- one standard deviation, for the six tested vertical planes – lowering phase

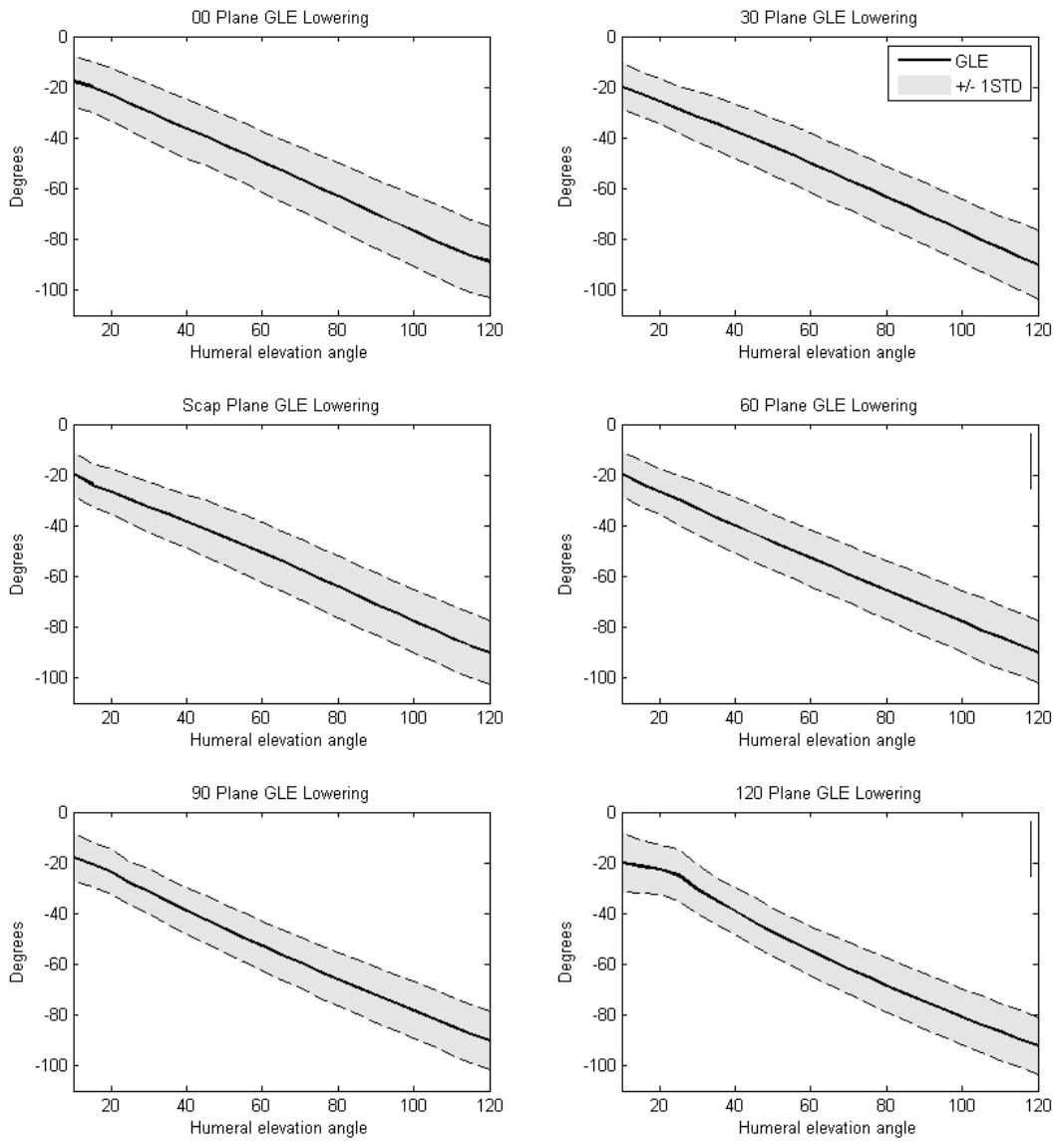


Figure D5: Mean glenohumeral -elevation (GLE) kinematic profiles, with +/- one standard deviation, for the six tested vertical planes – lowering phase

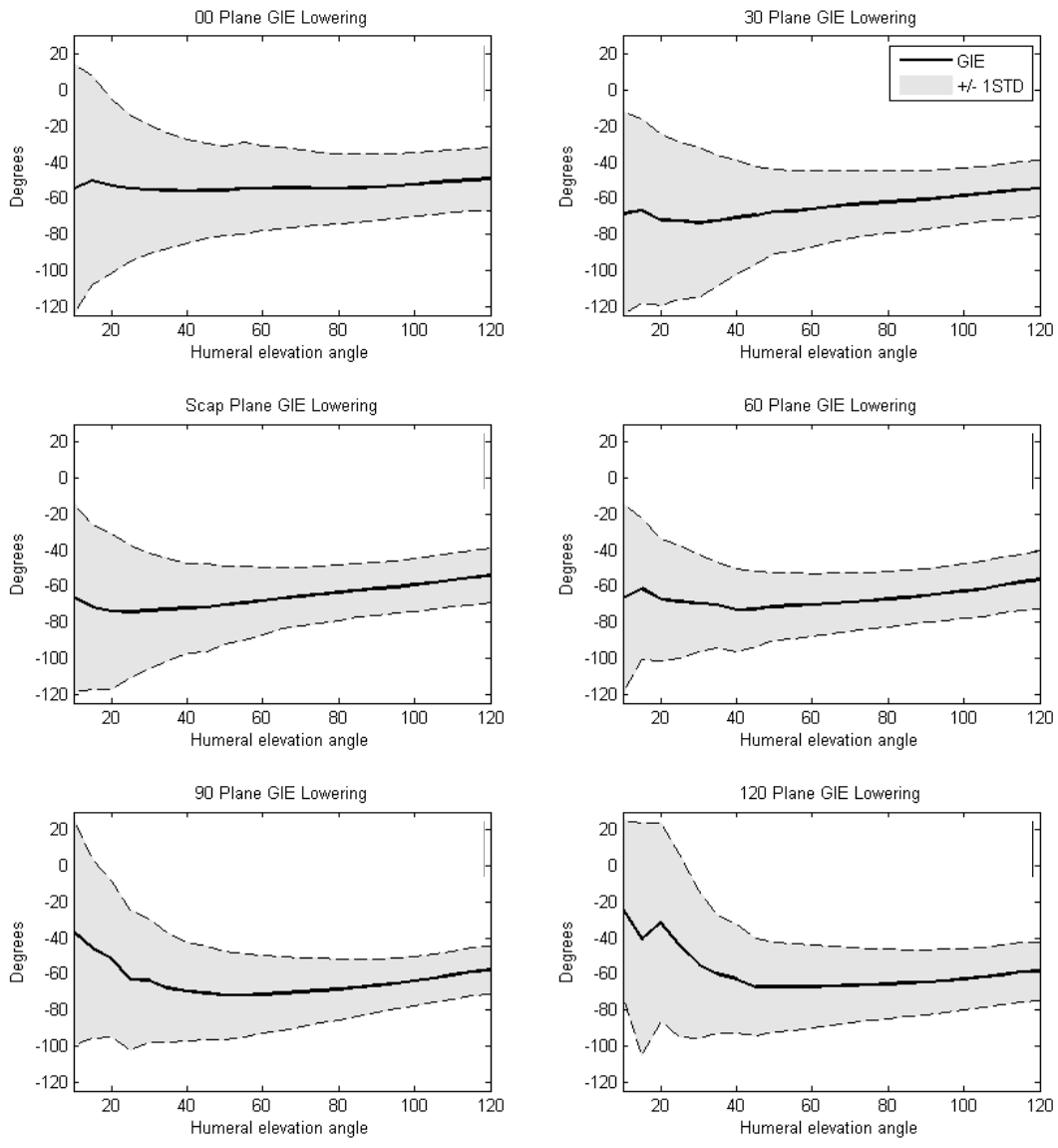


Figure D6: Mean glenohumeral +internal/-external rotation (GIE) kinematic profiles, with +/- one standard deviation, for the six tested vertical planes – lowering phase

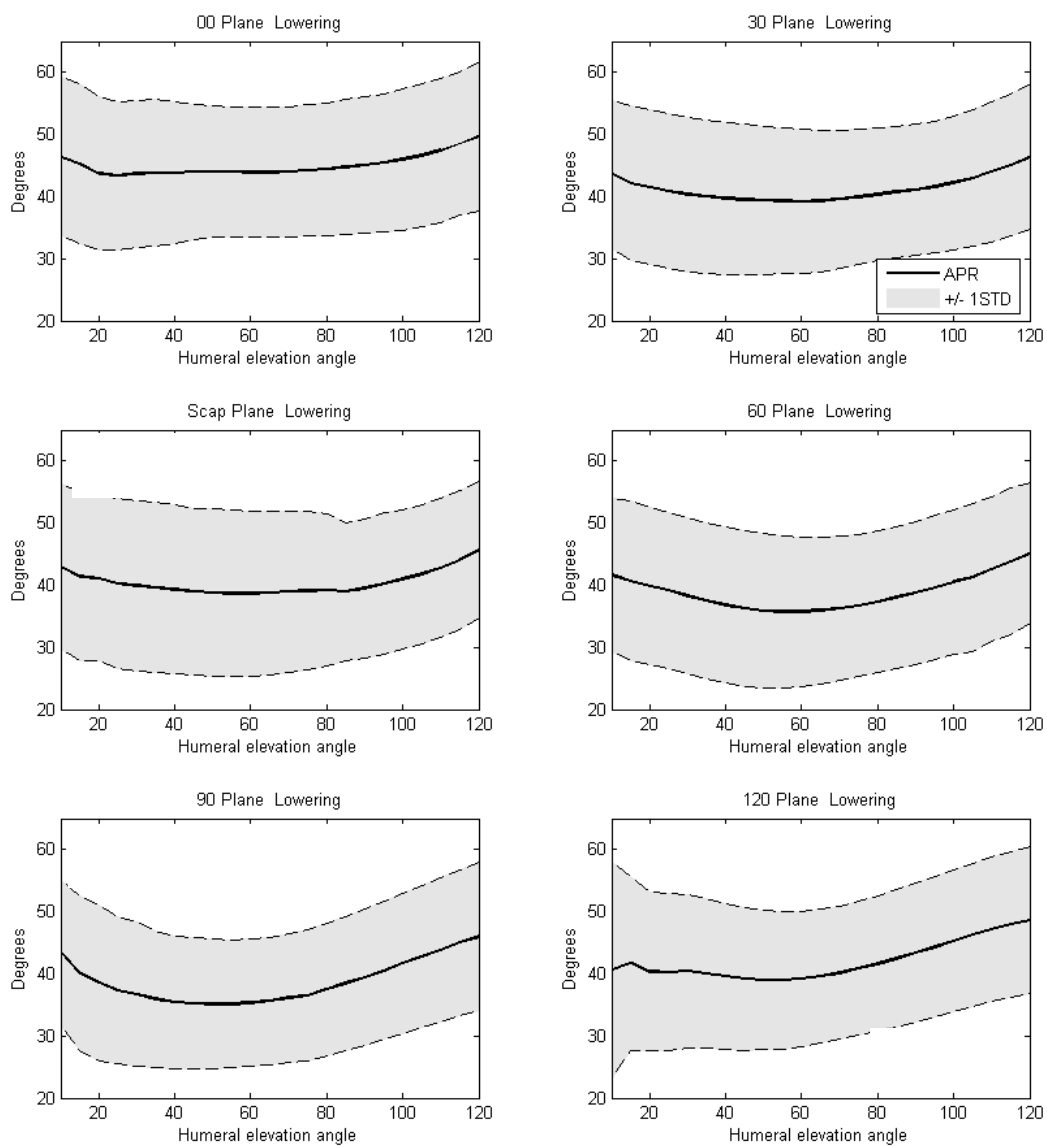


Figure D7: Mean acromioclavicular +protraction/-retraction (APR) kinematic profiles, with +/- one standard deviation, for the six tested vertical planes – lowering phase.

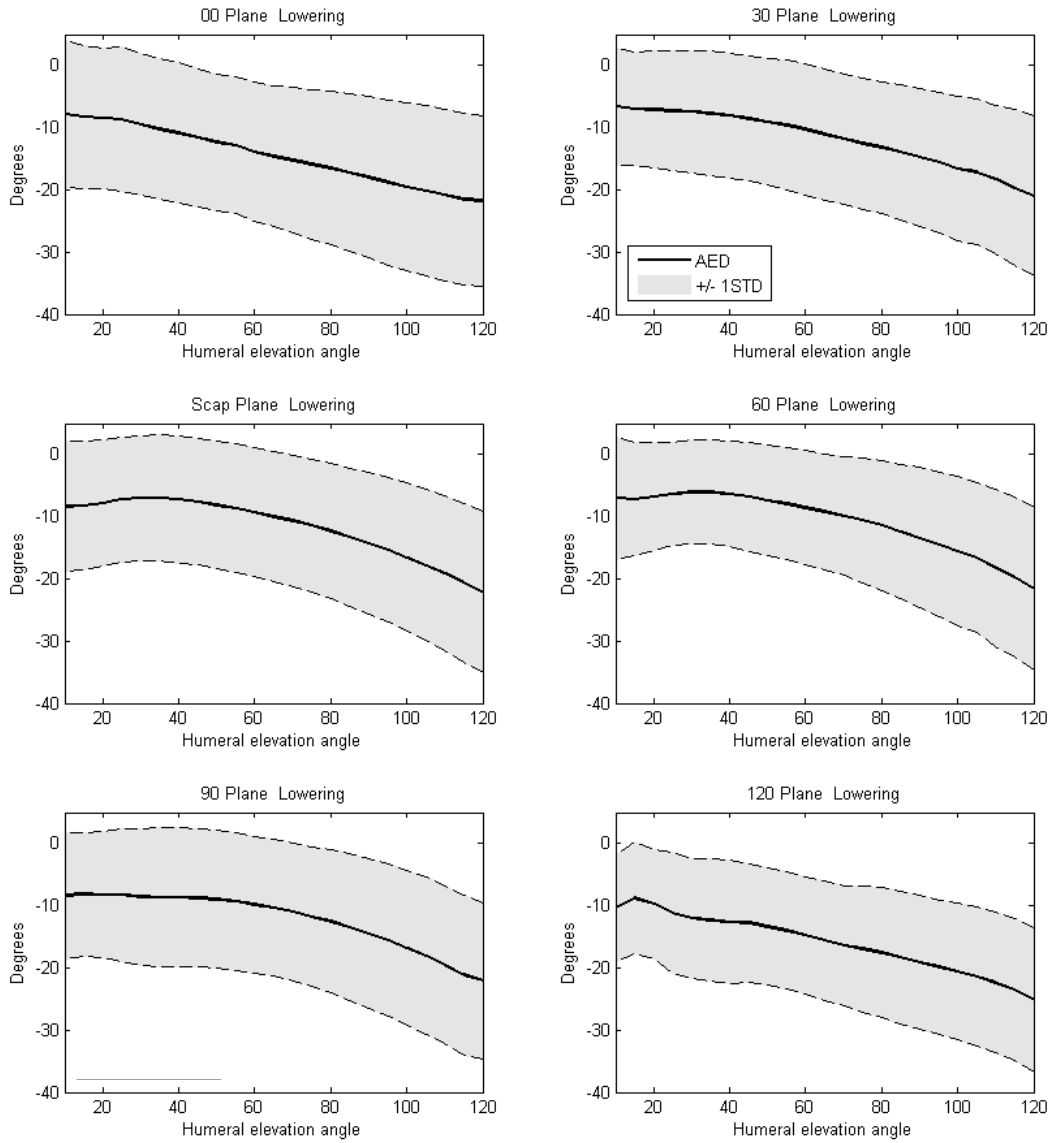


Figure D8: Mean acromioclavicular -elevation/+depression (AED) kinematic profiles, with \pm one standard deviation, for the six tested vertical planes – lowering phase.

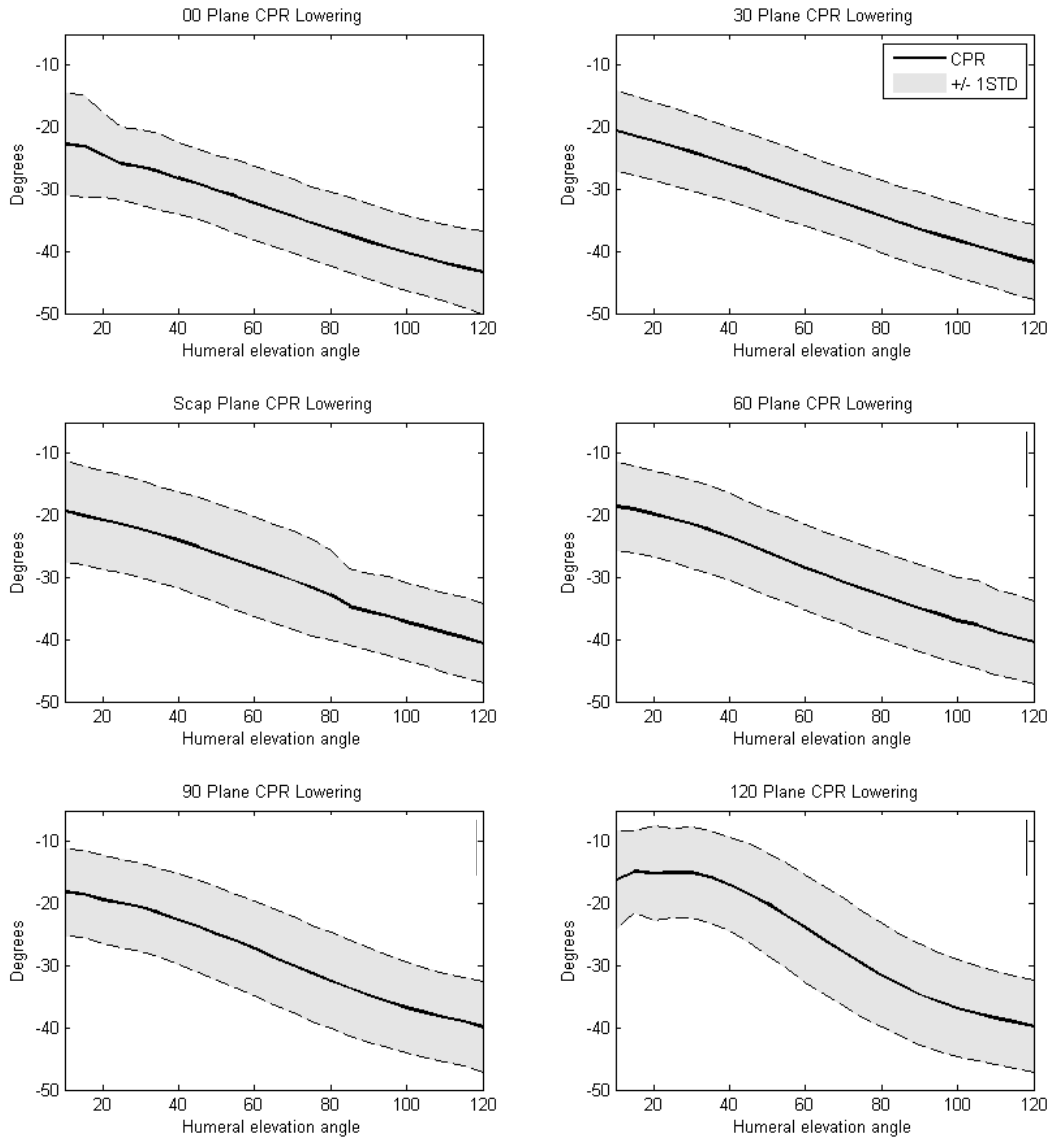


Figure D9: Mean sternoclavicular +protraction/-retraction (CPR) kinematic profiles, with +/- one standard deviation, for the six tested vertical planes – lowering phase

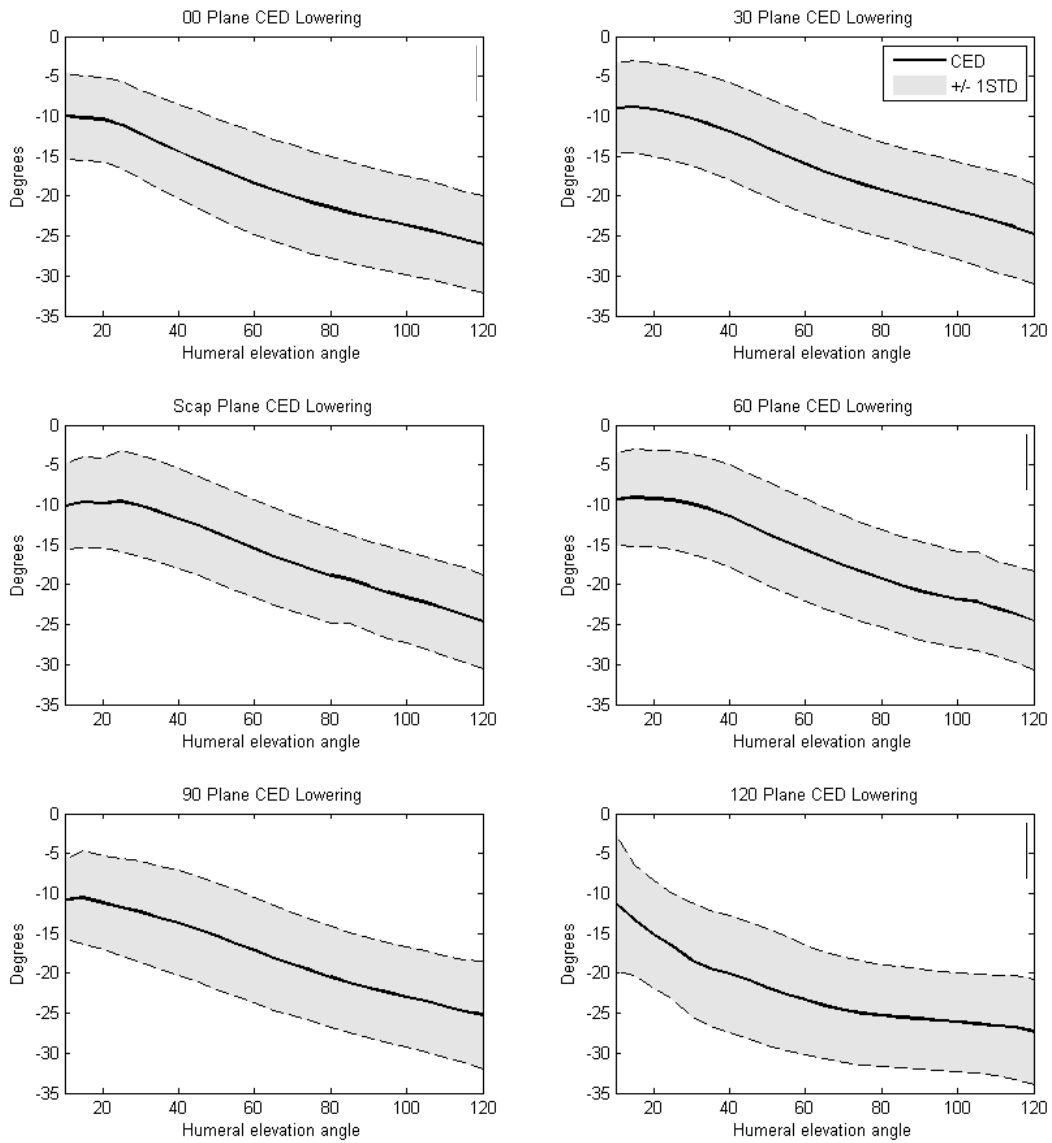


Figure D10: Mean sternoclavicular –elevation/+depression (CED) kinematic profiles, with +/- one standard deviation, for the six tested vertical planes – lowering phase.

APPENDIX E: Kinematic profiles' average standard deviation by elevation angle

Table E: Standard deviation measurements used in Figure 91 and 92. ELE = elevation angle

| ELE | SPR | SML | SPA | CED | CPR | GAP | GLE | GIE | AED | APR |
|------------|------------|------------|------------|------------|------------|------------|------------|------------|------------|------------|
| 10 | 13.73 | 14.20 | 9.68 | 5.45 | 8.16 | 68.28 | 9.92 | 69.68 | 11.87 | 12.79 |
| 15 | 14.91 | 13.61 | 9.25 | 5.27 | 8.26 | 58.53 | 10.08 | 58.12 | 11.48 | 12.89 |
| 20 | 15.45 | 13.48 | 9.15 | 5.29 | 6.80 | 51.12 | 10.52 | 48.09 | 11.28 | 12.33 |
| 25 | 14.75 | 13.43 | 9.23 | 5.46 | 5.86 | 45.05 | 10.79 | 40.72 | 11.57 | 11.91 |
| 30 | 14.62 | 13.51 | 9.26 | 5.53 | 5.99 | 39.52 | 11.17 | 35.62 | 11.41 | 11.88 |
| 35 | 14.48 | 13.56 | 9.32 | 5.73 | 6.12 | 35.32 | 11.46 | 31.99 | 11.32 | 11.77 |
| 40 | 14.40 | 13.65 | 9.34 | 5.91 | 5.77 | 32.10 | 11.57 | 28.80 | 11.25 | 11.39 |
| 45 | 14.22 | 13.75 | 9.39 | 6.12 | 5.62 | 29.31 | 11.52 | 26.39 | 11.08 | 10.95 |
| 50 | 14.07 | 13.73 | 9.45 | 6.25 | 5.65 | 27.04 | 11.62 | 24.73 | 11.02 | 10.61 |
| 55 | 13.88 | 13.61 | 9.56 | 6.35 | 5.95 | 26.07 | 11.84 | 25.46 | 10.98 | 10.47 |
| 60 | 13.93 | 13.62 | 9.71 | 6.37 | 5.93 | 23.84 | 12.01 | 23.59 | 11.16 | 10.43 |
| 65 | 14.01 | 13.71 | 9.90 | 6.40 | 5.94 | 22.62 | 12.18 | 22.61 | 11.32 | 10.42 |
| 70 | 14.07 | 13.90 | 10.11 | 6.41 | 5.94 | 21.23 | 12.42 | 21.50 | 11.63 | 10.48 |
| 75 | 14.12 | 14.08 | 10.33 | 6.39 | 5.95 | 19.55 | 12.77 | 20.15 | 12.00 | 10.59 |
| 80 | 14.12 | 14.23 | 10.54 | 6.35 | 6.01 | 18.64 | 13.15 | 19.54 | 12.34 | 10.74 |
| 85 | 14.18 | 14.38 | 10.77 | 6.29 | 6.08 | 17.87 | 13.41 | 19.00 | 12.72 | 10.88 |
| 90 | 14.32 | 14.51 | 10.99 | 6.23 | 6.09 | 17.18 | 13.71 | 18.51 | 13.00 | 11.00 |
| 95 | 14.49 | 14.68 | 11.19 | 6.20 | 6.07 | 16.63 | 13.96 | 18.14 | 13.26 | 11.17 |
| 100 | 14.67 | 14.89 | 11.30 | 6.18 | 6.06 | 16.11 | 14.13 | 17.80 | 13.49 | 11.38 |
| 105 | 14.84 | 15.00 | 11.41 | 6.16 | 6.10 | 15.64 | 14.37 | 17.47 | 13.66 | 11.53 |
| 110 | 15.01 | 15.10 | 11.56 | 6.11 | 6.21 | 15.18 | 14.39 | 17.38 | 13.75 | 11.64 |
| 115 | 15.37 | 14.94 | 11.87 | 6.03 | 6.42 | 14.81 | 14.34 | 17.40 | 13.83 | 11.55 |
| 120 | 14.85 | 15.01 | 12.31 | 6.14 | 6.73 | 13.91 | 14.04 | 17.58 | 13.80 | 11.96 |

APPENDIX F: Analysis of variance (anova) summaries

Table F1: Scapulothoracic protract/retraction ANOVA summary table. * indicates significance (*P*-value: 0.05)

| Source | DF | F Ratio | Prob > F |
|-------------|----|---------|----------|
| SEX | 1 | 0.16 | 0.694 |
| PLANE | 5 | 2020.09 | <.0001* |
| ELE | 7 | 80.55 | <.0001* |
| PHASE | 1 | 87.23 | <.0001* |
| SEX*PLANE | 5 | 2.39 | 0.0355* |
| SEX*ELE | 7 | 4.57 | <.0001* |
| SEX*PHASE | 1 | 4.85 | 0.0277* |
| PLANE*ELE | 35 | 18.29 | <.0001* |
| PLANE*PHASE | 5 | 0.98 | 0.4271 |
| ELE*PHASE | 7 | 0.12 | 0.997 |

Table F2: Scapulothoracic medial/lateral rotation ANOVA summary table. * indicates significance (*P*-value: 0.05)

| Source | DF | F Ratio | Prob > F |
|-------------|----|---------|----------|
| SEX | 1 | 0.04 | 0.8489 |
| PLANE | 5 | 35.37 | <.0001* |
| ELE | 7 | 1112.24 | <.0001* |
| PHASE | 1 | 6.74 | 0.0095* |
| SEX*PLANE | 5 | 5.01 | 0.0001* |
| SEX*ELE | 7 | 0.70 | 0.6756 |
| SEX*PHASE | 1 | 17.98 | <.0001* |
| PLANE*ELE | 35 | 0.46 | 0.997 |
| PLANE*PHASE | 5 | 4.02 | 0.0012* |
| ELE*PHASE | 7 | 0.57 | 0.781 |

Table F3: Scapulothoracic posterior/anterior tilt ANOVA summary table. * indicates significance (*P*-value: 0.05)

| Source | DF | F Ratio | Prob > F |
|-------------|----|---------|----------|
| SEX | 1 | 1.19 | 0.2858 |
| PLANE | 5 | 93.63 | <.0001* |
| ELE | 7 | 150.30 | <.0001* |
| PHASE | 1 | 17.86 | <.0001* |
| SEX*PLANE | 5 | 5.04 | 0.0001* |
| SEX*ELE | 7 | 33.36 | <.0001* |
| SEX*PHASE | 1 | 3.03 | 0.082 |
| PLANE*ELE | 35 | 3.48 | <.0001* |
| PLANE*PHASE | 5 | 7.76 | <.0001* |
| ELE*PHASE | 7 | 0.73 | 0.6484 |

Table F4: Glenohumeral anterior/posterior plane ANOVA summary table. * indicates significance (P-value: 0.05)

| Source | DF | F Ratio | Prob > F |
|-------------|----|---------|----------|
| SEX | 1 | 0.01 | 0.9421 |
| PLANE | 5 | 505.77 | <.0001* |
| ELE | 7 | 29.18 | <.0001* |
| PHASE | 1 | 1.05 | 0.305 |
| SEX*PLANE | 5 | 1.44 | 0.2058 |
| SEX*ELE | 7 | 0.24 | 0.9764 |
| SEX*PHASE | 1 | 0.18 | 0.675 |
| PLANE*ELE | 35 | 7.67 | <.0001* |
| PLANE*PHASE | 5 | 0.82 | 0.5378 |
| ELE*PHASE | 7 | 0.23 | 0.978 |

Table F5: Glenohumeral elevation ANOVA summary table. * indicates significance (P-value: 0.05)

| Source | DF | F Ratio | Prob > F |
|-------------|----|---------|----------|
| SEX | 1 | 0.00 | 0.9608 |
| PLANE | 5 | 11.95 | <.0001* |
| ELE | 7 | 3771.28 | <.0001* |
| PHASE | 1 | 1.81 | 0.179 |
| SEX*PLANE | 5 | 25.85 | <.0001* |
| SEX*ELE | 7 | 9.41 | <.0001* |
| SEX*PHASE | 1 | 9.23 | 0.0024* |
| PLANE*ELE | 35 | 1.29 | 0.1159 |
| PLANE*PHASE | 5 | 1.94 | 0.0843 |
| ELE*PHASE | 7 | 0.51 | 0.8243 |

Table F6: Glenohumeral internal/external rotation ANOVA summary table. * indicates significance (P-value: 0.05)

| Source | DF | F Ratio | Prob > F |
|-------------|----|---------|----------|
| SEX | 1 | 0.29 | 0.5916 |
| PLANE | 5 | 39.50 | <.0001* |
| ELE | 7 | 22.26 | <.0001* |
| PHASE | 1 | 11.28 | 0.0008* |
| SEX*PLANE | 5 | 1.11 | 0.3536 |
| SEX*ELE | 7 | 0.89 | 0.5126 |
| SEX*PHASE | 1 | 0.44 | 0.5093 |
| PLANE*ELE | 35 | 3.61 | <.0001* |
| PLANE*PHASE | 5 | 1.94 | 0.0843 |
| ELE*PHASE | 7 | 1.56 | 0.1434 |

Table F7: Acromioclavicular protraction/retraction ANOVA summary table. * indicates significance (P-value: 0.05)

| Source | DF | F Ratio | Prob > F |
|-------------|----|---------|----------|
| SEX | 1 | 0.01 | 0.9405 |
| PLANE | 5 | 58.17 | <.0001* |
| ELE | 7 | 62.09 | <.0001* |
| PHASE | 1 | 0.01 | 0.9229 |
| SEX*PLANE | 5 | 4.56 | 0.0004* |
| SEX*ELE | 7 | 1.63 | 0.123 |
| SEX*PHASE | 1 | 1.28 | 0.2584 |
| PLANE*ELE | 35 | 1.23 | 0.1647 |
| PLANE*PHASE | 5 | 2.15 | 0.0571 |
| ELE*PHASE | 7 | 0.34 | 0.9337 |

Table F8: Acromioclavicular elevation ANOVA summary table. * indicates significance (P-value: 0.05)

| Source | DF | F Ratio | Prob > F |
|-------------|----|---------|----------|
| SEX | 1 | 1.13 | 0.2974 |
| PLANE | 5 | 63.06 | <.0001* |
| ELE | 7 | 348.45 | <.0001* |
| PHASE | 1 | 80.20 | <.0001* |
| SEX*PLANE | 5 | 5.47 | <.0001* |
| SEX*ELE | 7 | 52.71 | <.0001* |
| SEX*PHASE | 1 | 0.89 | 0.3448 |
| PLANE*ELE | 35 | 2.92 | <.0001* |
| PLANE*PHASE | 5 | 1.42 | 0.2135 |
| ELE*PHASE | 7 | 3.98 | 0.0002* |

Table F9: Sternoclavicular protraction/retraction ANOVA summary table. * indicates significance (P-value: 0.05)

| Source | DF | F Ratio | Prob > F |
|-------------|----|---------|----------|
| SEX | 1 | 0.48 | 0.4953 |
| PLANE | 5 | 317.24 | <.0001* |
| ELE | 7 | 2024.91 | <.0001* |
| PHASE | 1 | 608.21 | <.0001* |
| SEX*PLANE | 5 | 6.52 | <.0001* |
| SEX*ELE | 7 | 24.15 | <.0001* |
| SEX*PHASE | 1 | 24.28 | <.0001* |
| PLANE*ELE | 35 | 7.34 | <.0001* |
| PLANE*PHASE | 5 | 6.95 | <.0001* |
| ELE*PHASE | 7 | 22.14 | <.0001* |

Table F10: Sternoclavicular elevation ANOVA summary table. * indicates significance (*P*-value: 0.05)

| Source | DF | F Ratio | Prob > F |
|---------------|-----------|----------------|--------------------|
| SEX | 1 | 0.94 | 0.3406 |
| PLANE | 5 | 271.76 | <.0001* |
| ELE | 7 | 1921.63 | <.0001* |
| PHASE | 1 | 50.80 | <.0001* |
| SEX*PLANE | 5 | 2.92 | 0.0124* |
| SEX*ELE | 7 | 13.15 | <.0001* |
| SEX*PHASE | 1 | 18.79 | <.0001* |
| PLANE*ELE | 35 | 3.52 | <.0001* |
| PLANE*PHASE | 5 | 24.20 | <.0001* |
| ELE*PHASE | 7 | 14.91 | <.0001* |